Průhled do nitra protonu v obraze strukturních funkcí

Petr Závada, CSc.

Disertační práce k získání vědeckého titulu „doktor věd“
ve skupině věd fyzikálně-matematických

Fyzikální ústav
Akademie věd ČR, v.v.i.

Praha, duben 2010

Poděkování

Na tomto místě chci poděkovat všem svým kolegům, kteří různými způsoby přispěli ke vzniku této disertační práce. Chci poděkovat kolegům a spoluautorům z experimentálního týmu BCDMS za skvělé společně vytvořené výsledky. Za jejich delší řadu jmenovitě uvádím vedoucího týmu Dr. Rüdigera Vosse a své kolegy z Fyzikálního ústavu, s nimiž jsem měl možnost pravidelně diskutovat o řešení našich úkolů a přejímat jejich cenné zkušenosti: Jaroslava Cvacha, Petra Reimera a Stanislava Němečka. Chci poděkovat svým kolegům, spoluautorům teoretické části disertace. Jsou to Anatoly Efremov, Oleg Teryaev a Peter Schweitzer; spolupráce s nimi pro mne byla a je vynikající školou i skvělým zážitkem. Poděkovat chci i všem svým kolegyním a kolegům ve Fyzikálním ústavu za mnohé formy každodenních inspirujících podnětů.

Obsah

Kapitola 1

Úvod

1.1 Historie a motivace

Dnešní představy a poznatky o vnitřní struktuře protonu se začaly postupně rýsovat v šedesátých a sedmdesátých letech minulého století. Na konci šedesátých let byla ve SLACu (Stanford Linear Accelerator Center, USA) získána experimentální data vztahující se ke srážkám vysokoenergetických elektronů (20 GeV) s protony. Princip experimentu je schematicky znázorněn na obrázku 1.1. Soubor experimentálních dat v podstatě spočíval v tom, že se u každého rozptýleného elektronu současně určila energie, kterou při srážce ztratil, a úhel, o který byl srážkou odchýlen. Z těchto dat se stanovil příslušný diferenciální účinný průřez procesu a z něj následně i tzv. strukturní funkce. Jsou to invariantní veličiny, které mají pro diskusi o vnitřní struktuře protonu (i dalších hadronů) zcela fundamentální význam. Ze strukturních funkcí lze do určité míry rekonstruovat vnitřní obraz protonu. Jejich teoretická analýza ukázala, že elektron se uvnitř protonu nechová jako při průchodu homogenním prostředím, nýbrž tak, jakoby v nitru protonu narážel na jakési tvrdé částečky. Ze strukturních funkcí se dalo vyčíst i to, že tyto částečky mají s největší pravděpodobností spin 1/2.

K návrhu modelu protonu (a neutronu), v němž jsou přítomny diracovské částice, které stojí v cestě procházejícím elektronům, přispěl především americký fyzik R. Feynman [1]. Ukázalo se, že tyto částice − Feynman je pracovně nazval partony − vlastně odpovídají kvarkům, jejichž reálná existence byla do té doby spojena s velikým otazníkem. Analýza strukturních funkcí dále ukázala, že uvnitř nukleonu jsou společně s kvarky i gluony − částice zprostředkovávající vzájemnou interakci a vazbu kvarků (glue=lepidlo). Kvarková struktura byla teoreticky předpovězena zhruba již o pět let dříve, v roce 1964 (nezávisle na sobě M. Gell-Mannem a G. Zweigem). Hypotéza kvarků, která se do té doby opírala především o abstraktní a estetické argumenty, se proměnila v realitu. Zmíněný experiment ve SLACu tak otevřel novou kapitolu ve fyzice. Jednalo se o objev, za který byla v roce 1990 udělena Nobelova cena (R. Taylor, H. Kendall, J. Friedman) [5].

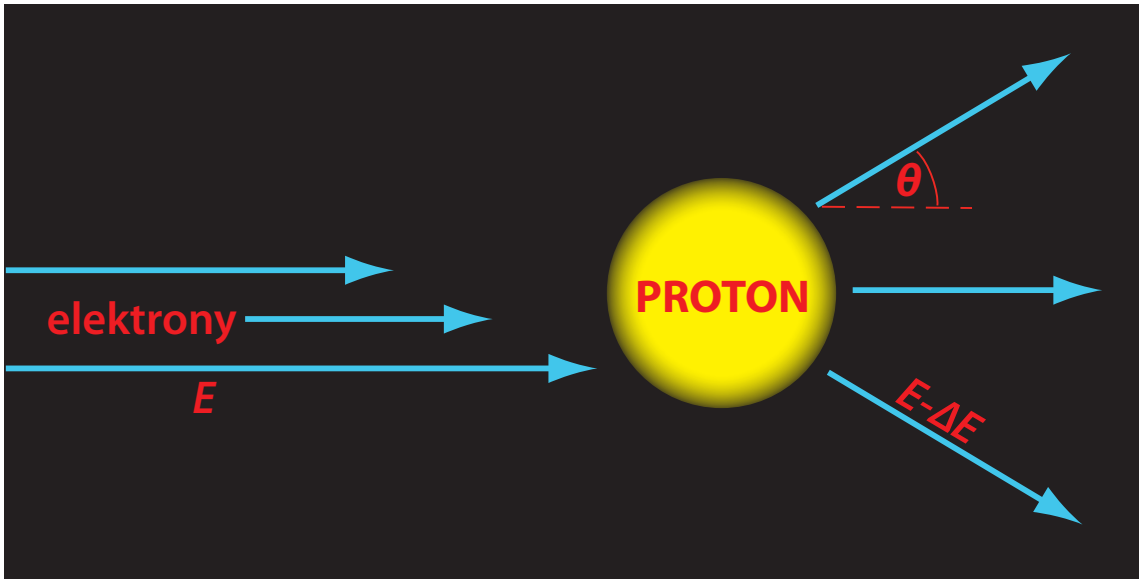

Obrázek 1.1: Svazek vysokoenergetických elektronů prostupuje terčíkem. Při srážce s protonem se elektron vychýlí z původního směru letu o úhel θ a ztratí část své původní energie (ΔE).

Na obrázku 1.2 je znázorněn proces srážky elektronu s protonem ve zjednodušeném obrazu kvark-partonového modelu (QPM) navrženém Feynmanem. V tomto zjednodušení se vlastně jedná spíše o srážku s jedním kvarkem uvnitř protonu než s protonem jako takovým. S tímto detailem souvisí několik velmi důležitých momentů:

1) Elektron i kvark mají elektrický náboj, proto na sebe působí elektromagnetickými silami. V jazyce kvantové teorie to znamená, že mezi nimi dochází k předání fotonu, který je na obrázku znázorněn vlnovkou. Elektromagnetické procesy obecně umíme v kvantové teorii vypočítat s neobyčejnou přesností. Pro získání obrazu uvnitř protonu je v této souvislosti důležité především to, že umíme velmi přesně vypočítat, co se stane s elektronem, který se prostřednictvím fotonu střetne s kvarkem.

2) Proč vlastně bylo třeba mít pro experiment ve SLACu elektrony s tak vysokou energií? Důvod je jednoduchý, stačí si připomenout, za jakých okolností přestává fungovat obyčejný optický mikroskop. Nelze jím věrně zobrazit objekty, jejichž rozměry jsou srovnatelné či ještě menší než je vlnová délka viditelného světla. I když je náš obraz vnitřku protonu získáván trochu jinou technikou, pro vlnovou délku fotonu platí stejné pravidlo: Chceme-li obraz protonu získat v dostatečném rozlišení, musí být jeho vlnová délka podstatně menší než je jeho rozměr. A protože respektujeme kvantovou mechaniku, musíme dodat, že vlnová délka fotonu λ je nepřímo úměrná jeho energii $E, \lambda = h/E$, kde h je Planckova konstanta. S pomocí tohoto vztahu si můžeme vypočítat, že k tomu, aby vlnová délka fotonů byla několikrát kratší než je rozměr protonu t.j. řádově 10^{-13} cm, je žádoucí, aby jejich energie byla alespoň několik GeV. Protože energie fotonů jde ve zmíněném experimentu na úkor energie elektronu, potřebujeme

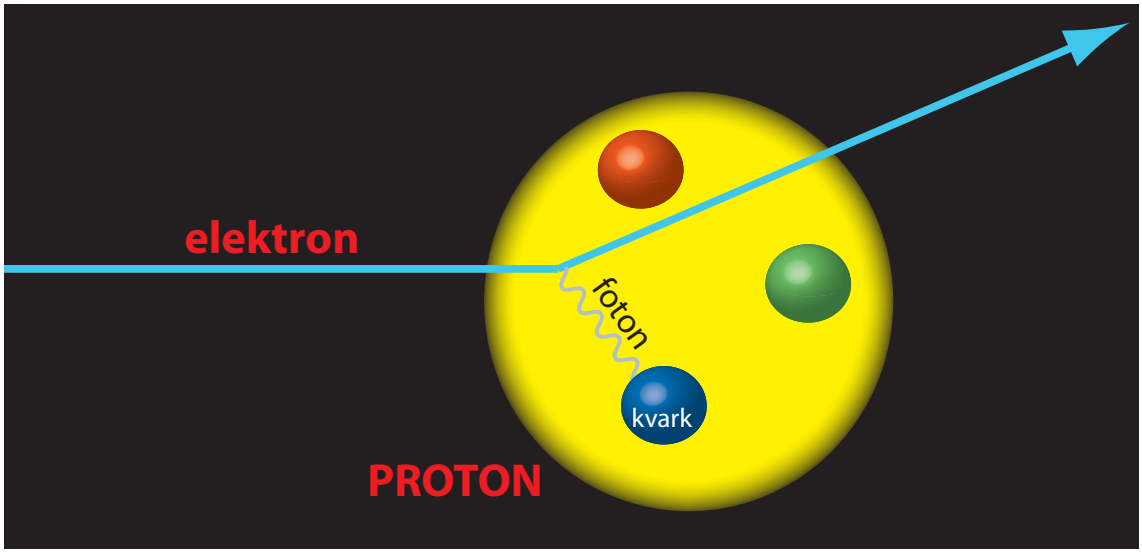

Obrázek 1.2: Vysokoenergetický elektron proniká do elektromagnetického pole kvarků uvnitř protonu. Dochází k výměně fotonu mezi elektronem a některým z kvarků.

svazek elektronů s energií ještě vyšší. A takovou energii elektrony ve SLACu spolehlivě měly, proto podmínka nutná k tomu, abychom kvarky uvnitř protonu „viděli“ byla splněna. A obráceně, při snižování energie elektronů kouzlo s kvarky zmizí a obraz protonu se scvrkne na pouhou tečku bez jakékoli další struktury „uvnitř“. Z těchto důvodů režim rozptylu elektronů (a dalších leptonů, mionů či neutrin) na nukleonech, při němž se projevuje jejich kvarková struktura, dostal název ‘Deep inelastic scattering’ (DIS). Jde vlastně o proces, v jehož prvním kroku dojde k pružné srážce leptonu s kvarkem jak naznačuje obrázek 1.2. V druhém kroku odražený kvark „fragmentuje“ na hadrony, zatímco stav leptonu se od srážky s kvarkem již nemění.

3) Proton i elektron mohou mít projekci spinu do zvoleného směru $\pm 1/2$, tím se definuje jejich polarizace. Zvláště důležité jsou přitom dva směry; jednak směr, ve kterém svazek elektronů míří k terči s protony (tzv. podélná polarizace), a jednak směr v některé kolmici ke svazku (příčná polarizace). V obou těchto směrech elektron a proton mohou být polarizovány souhlasně nebo opačně. Křivky rozdělení rozptýlených elektronů se v těchto případech liší a jejich rozdíly, tzv. spinové asymetrie, jsou velmi důležitým klíčem. Z těchto asymetrií lze totiž stanovit spinové strukturní funkce, které obsahují informaci o tom, jak spin protonu souvisí se spiny kvarků, jimiž je tvořen.

Součástí obrazu nukleonu je i vzájemné působení kvarků prostřednictvím gluonů v souladu s teorií silných interakcí, kvantovou chromodynamikou (QCD). Podrobnější úvod do problematiky zahrnující zmíněné pojmy jako partonový model, DIS, strukturní a distribuční funkce lze najít například v klasických učebnicích [1]– [3] nebo v učebním textu [4]. Rigorózní přístup k partonovému modelu s QCD korekcemi a k pojmům nepolarizovaných a polarizovaných strukturních funkcí lze nalézt v [6]. S nejnovějšími

experimentálními a teoretickými poznatky se lze seznámit ve sbornících pravidelných konferencí, např. [7, 8].

S nastíněnou problematikou souvisí i téma předložené disertační práce, jejímž základem jsou dvě části:

A. Experimentální část: Měření strukturních funkcí v experimentu BCDMS

Tato část pojednává o experimentálních výsledcích, na jejichž zpracování jsem se podílel v experimentálním týmu BCDMS během svého jednoročního pobytu v CERN v roce 1986 a v následujícím období i v Praze nebo během krátkodobějších pobytů v CERN. Konkrétně se jedná především o přesné stanovení nepolarizovaných strukturních funkcí $F_2(x, Q^2)$ měřených na terčích naplněných kapalným vodíkem nebo deuteriem a umístěných ve svazku vysokoenergetických mionů. V dalším kroku je provedena analýza strukturní funkce protonu z hlediska narušení škálování a srovnáním s předpovědí poruchové QCD je stanoven fundamentální parametr Λ_{QCD}. Důležitým výsledkem je rovněž získání strukturní funkce nukleonu měřené na terči Fe. Tato strukturní funkce v kombinaci se strukturní funkcí změřenou na deuteriu umožňuje stanovit efekt prostředí jádra na rozdělení kvarků v nukleonu (tzv. EMC efekt). Podkladem pro tuto první část disertační práce jsou publikace [A1]– [A4].

B. Teoretická část: Polarizované a nepolarizované strukturní funkce v kovariantním QPM

V této části je rozpracována kovariantní verze partonového modelu. Základním východiskem našeho přístupu jsou požadavky symetrie:

i) relativistická kovariance

ii) sférická symetrie nukleonu (3D hybnosti kvarků jsou v klidovém systému nukleonu popsány rotačně symetrickým pravděpodobnostním rozdělením)

Tyto požadavky se neuplatňují ve standardní formulaci partonového modelu, v tom spočívá hlavní rozdíl mezi obvyklým a naším přístupem. Zatímco v případě nepolarizovaných strukturních funkcí tento rozdíl nemá příliš podstatné důsledky, v případě spinových strukturních funkcí jsou důsledky zcela zásadní. Podkladem pro tuto část disertační práce jsou publikace [A5]− [A13]. V článcích [A5]− [A9] je postupně formulována konstrukce modelu a jsou demonstrovány vlastnosti strukturních funkcí F_1, F_2, g_1 a g_2, které z modelu vyplývají. Důležitou součástí této konstrukce je korektní započtení vnitřního pohybu kvarků. Ve spolupráci se spoluautory článků [A10]− [A13] byl model dále rozšířen o popis dalších strukturních (distribučních) funkcí, které jsou v současnosti v různých teoretických a experimentálních přístupech předmětem intenzivního výzkumu. Přibývají totiž experimentální data, jejichž interpretace se neobejde bez předpokladu o vnitřním pohybu kvarků. Jde například o asymetrii v produkci hadronů, která je vztažena ke směru polarizace terčového nukleonu [9]− [15]. Předpoklad o vnitřním pohybu je rovněž nevyhnutelný pro vyjasnění role orbitálního momentu kvarků. Jde o poznatky, které zásadním způsobem přispívají k hlubšímu pochopení 3D struktury nukleonů.

1.2 Notace a základní veličiny

V práci užíváme standardní notaci kinematických veličin. Symboly

$$P \equiv (P_0, P_1, P_2, P_3), \quad S \equiv (S_0, S_1, S_2, S_3), \quad M = \sqrt{P^2} \tag{1.1}$$

reprezentují čtyřimpuls, spinový vektor a hmotnost nukleonu. Symboly

$$p \equiv (p_0, p_1, p_2, p_3), \quad q \equiv (q_0, q_1, q_2, q_3), \quad m = \sqrt{p^2} \tag{1.2}$$

reprezentují čtyřimpulsy kvarku a fotonu, m je hmotnost kvarku. Při interakci elektronu (nebo mionu) s kvarkem v nukleonu se předpokládá přiblížení jednofotonové výměny. Velmi důležitou roli hrají invariantní veličiny

$$x \equiv \frac{Q^2}{2Pq}, \quad Q^2 \equiv -q^2. \tag{1.3}$$

Oba invarianty lze pro každou událost DIS určit z kinematiky rozptýleného leptonu. Po zanedbání hmoty leptonu platí

$$Q^2 \simeq 4EE' \sin^2 \frac{\theta}{2}, \quad x = \frac{2EE'}{M(E-E')} \sin^2 \frac{\theta}{2}, \tag{1.4}$$

kde $E(E')$ je energie leptonu před a po rozptylu, θ je úhel rozptylu. Tyto veličiny se vztahují ke klidové soustavě nukleonu. Z jejich rozdělení se stanoví diferenciální účinný průřez a z něj lze pak extrahovat strukturní funkce:

$$\frac{d^2\sigma}{dxdQ^2} \to F_1, F_2, g_1, g_2, \tag{1.5}$$

které jsou skalárními funkcemi obou invariantních proměnných. Poznamenejme, že pro získání polarizovaných funkcí g_1, g_2 je třeba provést dvojí měření účinného průřezu, v konfiguracích se souhlasnými a opačnými spinovými polarizacemi leptonu a nukleonu.

Veličinu x (tzv. Bjorkenova proměnná) lze v kinematické oblasti

$$Q^2 \gg 4M^2x^2 \tag{1.6}$$

nahradit zlomkem

$$x \to \frac{p_0 + p_1}{P_0 + P_1}, \tag{1.7}$$

který lze interpretovat jako podíl impulsu daného kvarku na impulsu nukleonu − v soustavě v níž je impuls protonu velký (užívá se termín 'infinite momentum frame', IMF) a ve schematu, v němž se příčná hybnost kvarku zanedbává. Proměnná (1.7) se obvykle nazývá 'light-cone fraction' a hraje důležitou úlohu v teorii a fenomenologii DIS. Přibližná rovnost parametru x vyjádřeného vztahy (1.3) nebo (1.7) hraje zcela klíčovou roli při formulaci QPM. Tato rovnost dává jednoduché propojení mezi kinematikou elektronu po rozptylu (Brojkenovo x se vypočte z úhlu θ a energie E') a kinematikou kvarku před rozptylem (proměnná x je dána výrazem, který závisí na komponentách hybnosti kvarku). Podmínka (1.6) není nikterak extrémním požadavkem, v dalších úvahách předpokládáme její splnění.

Kapitola 2

Měření strukturních funkcí v experimentu BCDMS

2.1 Experiment

Po experimentech ve SLAC přirozeně následoval mimořádný zájem poznatky o DIS dále experimentálně i teoreticky prohlubovat. Jedním z experimentů, které následovaly, byl experiment BCDMS ('BCDMS Collaboration' − název je zkratka zúčastněných laboratoří Bologna, CERN, Dubna, Mnichov, Saclay). Společný projekt se uskutečnil na mionovém svazku urychlovače SPS v CERN a byl též znám jako experiment NA4, zkratka souvisí s umístěním příslušné experimentální haly: NA=North Area. Návrh se zrodil v roce 1974, ke schválení experimentu v CERN došlo v roce 1975, konstrukce probíhala v letech 1976–1978 a data se pak nabírala do roku 1985. V následujících letech dále probíhala jejich fyzikální analýza. Detailní popis aparatury je uveden v samostatných článcích [17].

Základem aparatury byly toroidální magnetické segmenty na bázi železa ve stavu blízkém k magnetickému nasycení, mezi nimiž byly rozmístěny scintilační detektory a souřadnicové proporcionální komory s rozlišením 4 mm. Průměr magnetických segmentů byl 2.75 m a celková délka spektrometru dosáhla 40 m. Terč s náplní (H_2, D_2, Fe) byl umístěn na ose spektrometru v jeho přední části. V tomto uspořádání dochází k pohlcení většiny sekundárních hadronů v železných segmentech, které jsou však průchodné pro rozptýlené miony. Z údajů v detektorech bylo možné rekonstruovat jejich trajektorie, zejména úhel θ a energii E' a z nich dále určit odpovídající invarianty x, Q^2. Pro stanovení odpovídajícího diferenciálního průřezu bylo třeba přesně stanovit akceptanci celé aparatury jako funkci obou invariantů. Tato úloha byla řešena metodou Monte-Carlo, při níž probíhala detailní simulace průchodu mionů celou aparaturou. Jednalo se o úlohu, která na tehdejší výkon počítačů kladla mimořádné nároky.

2.2 Strukturní funkce protonu a deuteronu

Podrobné výsledky protonových strukturních funkcí F_2 a F_1 měřených s vysokou statistikou ve svazcích mionů μ^+ s energiemi 100, 120, 200 a 280 GeV jsou uvedeny v práci [A1], viz část 2.2.1. Poznamenejme, že v této práci se uvádějí hodnoty funkcí F_2 a R, tento pár je však ekvivalentní páru funkcí F_2 a F_1. Funkce R vlastně vyjadřuje odchylku od relace Callan-Gross $F_2/F_1 = 2x$, která platí v partonovém modelu a o níž se ještě zmíníme v části 3.2. Tato odchylka není nijak dramatická a roli hraje jen v oblasti menších x. Posloupnost energií svazku má dvojí cíl, jednak umožňuje stanovení dvojice strukturních funkcí (jedna energie by vedla k jedné rovnici o dvou neznámých) a jednak rozšiřuje kinematickou oblast definovanou proměnnými x, Q^2. Strukturní funkce získané s vysokou přesností tak pokrývají širokou oblast,

$$0.06 \leq x \leq 0.80, \qquad 7 \text{ GeV}^2 \leq Q^2 \leq 260 \text{ GeV}^2,$$

která byla zásluhou dalších experimentů dále postupně rozšiřována.

U změřené strukturní funkce F_2 lze na první pohled pozorovat velmi důležitou vlastnost, tzv. narušení škálování. Tím je míněna skutečnost, že funkce slabě závisí na proměnné Q^2. Tato závislost je příznakem toho, že kvarky nejsou volnými částicemi, ale že jejich chování uvnitř protonu je řízeno zákony QCD. Současně však poznamenejme, že úplnou závislost experimentálně změřených strukturních funkcí na obou proměnných x, Q^2 dosud neumíme v rámci QCD počítat. Umíme ale s pomocí *pertubative* QCD (pQCD) velmi dobře interpretovat a analyzovat závislost strukturní funkce F_2 na proměnné Q^2. Takovou analýzu jsme provedli s naší protonovou strukturní funkcí v práci [A2], viz část 2.2.2, jejímž výsledkem bylo především stanovení QCD parametru Λ_{QCD}.

Dalším velmi důležitým výsledkem experimentu BCDMS bylo změření strukturních funkcí F_2 a $F_1(R)$ s terčem naplněným kapalným deuteriem, výsledek tedy odpovídal součtu nebo průměru ze strukturních funkcí protonu a neutronu [A3], viz část 2.2.3. Je podstatné, že toto měření bylo provedeno v identických podmínkách jako měření na vodíkovém terči, výsledky lze proto kombinovat a určit z nich strukturní funkce neutronu. Pro globální QCD analýzu založenou na partonovém modelu, jejímž cílem je stanovení distribučních funkcí kvarků u a d a jejich antikvarků v protonu (a neutronu), je nutná znalost strukturních funkcí *obou* nukleonů. Při separování distribučních funkcí se předpokládá izotopická invariance mezi protonem a neutronem, což znamená, že záměna $p \rightleftarrows n$ je provázena záměnou $u^p \rightleftarrows d^n$ a $d^p \rightleftarrows u^n$, což znamená, že distribuce kvarku u, d a jejich antikvarků v protonu je shodná s distribucemi d, u a jejich antikvarků v neutronu. Protože distribuční funkce vstupují do strukturních funkcí s vahami danými kvadráty nábojů odpovídajících kvarků, lze z kombinace strukturních funkcí protonu a neutronu určit uvedené distribuční funkce, které do nich vstupují. Kvarky u a d jsou v protonu a neutronu valentními kvarky, proto jejich distribuční funkce dominují. Jejich antikvarky vystupují pouze mezi „mořskými“ kvarky (sea quarks). V obecném případě

je třeba vzít do úvahy, že mezi mořskými kvarky nukleonů vystupují i virtuální páry dalších, těžších kvarků, především $s\bar{s}$. Narušení škálovaní pro deuteron rovněž odpovídá předpovědi pQCD. Výsledkem analýzy tohoto narušení byl opět parametr Λ_{QCD}, jehož hodnota velmi dobře souhlasí s hodnotou získanou v předchozí práci z protonové strukturní funkce.

Změřené hodnoty strukturních funkcí $F_2(x, Q^2)$ protonu a deuteronu ve výše uvedené kinematické oblasti představují pravděpodobně nejvýznamnější výsledky experimentu BCDMS. Tvoří součást našeho dnešního obrazu protonu a deuteronu zprostředkovaného strukturními funkcemi, na obrázcích 2.1 a 2.2 jsou uvedeny s navazujícími hodnotami naměřenými v pozdějších experimentech. Oba obrázky jsou převzaty z *Review of Particle Physics* [16], v prvém jsme BCDMS hodnoty pro lepší viditelnost barevně zvýraznili.

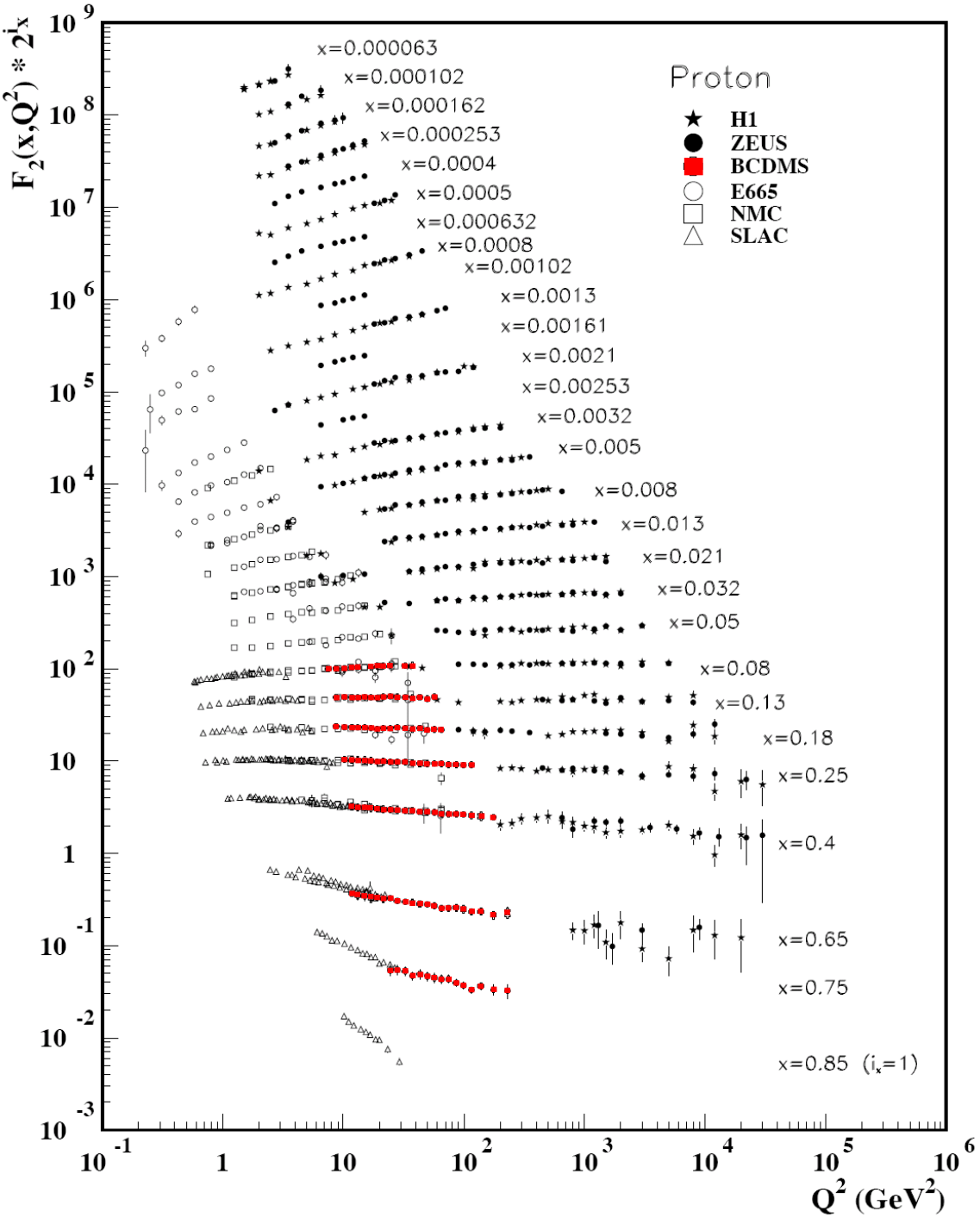

Obrázek 2.1: Strukturní funkce protonu F_2 změřená v experimentech H1 [19], ZEUS [20], BCDMS [A1], NMC [22], E665 [21] a SLAC [23].

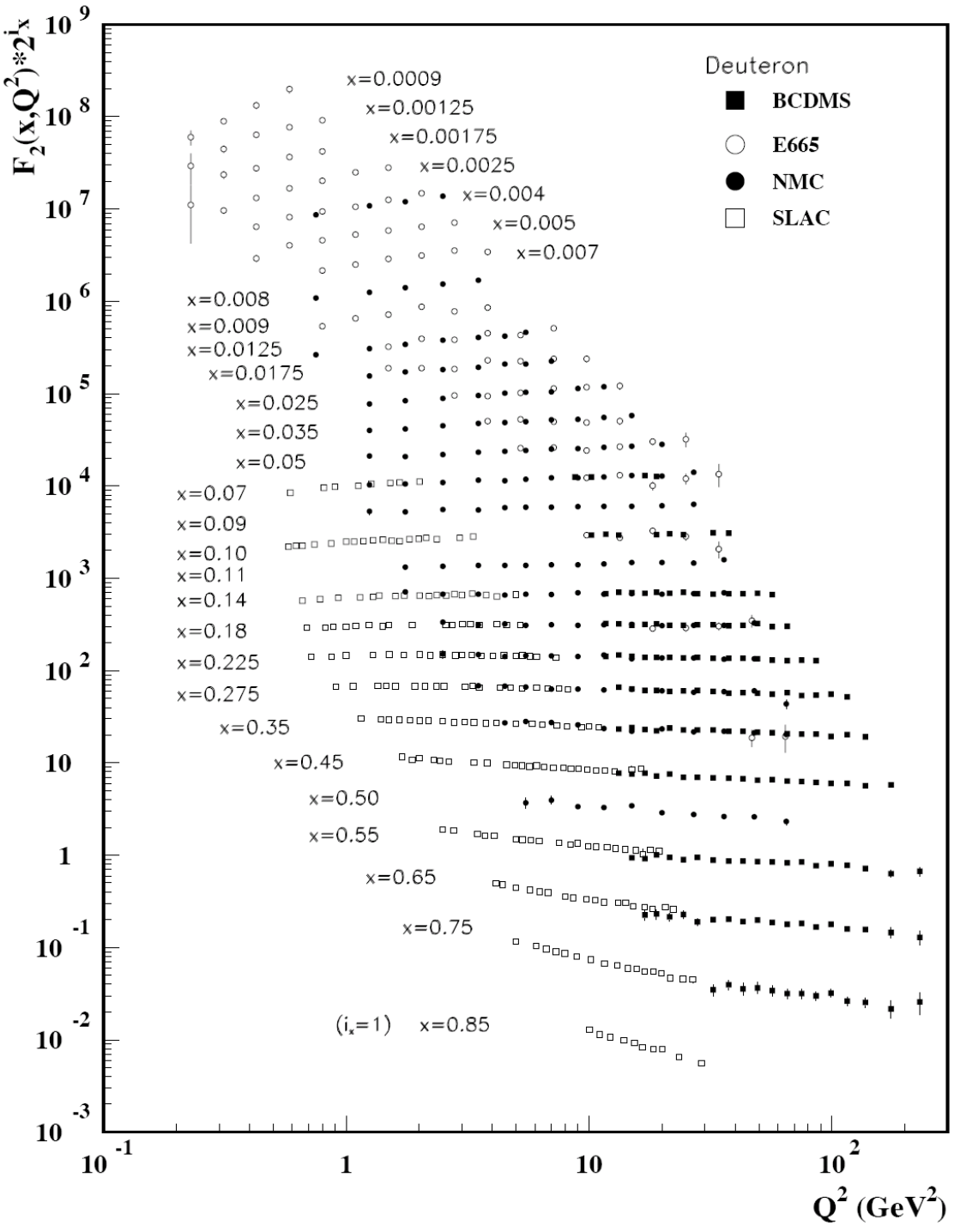

Obrázek 2.2: Strukturní funkce deuteronu F_2 změřená v experimentech BCDMS [A3], NMC [22], E665 [21], SLAC [23].

Article copy

Volume 223, number 3,4 PHYSICS LETTERS B 15 June 1989

A HIGH STATISTICS MEASUREMENT OF THE PROTON STRUCTURE FUNCTIONS $F_2(x, Q^2)$ AND R FROM DEEP INELASTIC MUON SCATTERING AT HIGH Q^2

BCDMS Collaboration

A.C. BENVENUTI, D. BOLLINI, G. BRUNI, T. CAMPORESI, L. MONARI [1], F.L. NAVARRIA
Dipartimento di Fisica dell'Università and INFN, I-40126 Bologna, Italy

A. ARGENTO [2], J. CVACH [3], W. LOHMANN [4], L. PIEMONTESE [5], P. ZAVADA [3]
CERN, CH-1211 Geneva 23, Switzerland

A.A. AKHUNDOV, V.I. GENCHEV, I.A. GOLUTVIN, Yu.T. KIRYUSHIN, V.G. KRIVOKHIZHIN, V.V. KUKHTIN, R. LEDNICKY, S. NEMECEK, P. REIMER, I.A. SAVIN, G.I. SMIRNOV, J. STRACHOTA [3], G. SULTANOV [6], P. TODOROV [6], A.G. VOLODKO
Joint Institute for Nuclear Research, Dubna, 101 000 Moscow, USSR

D. JAMNIK [7], R. KOPP [8], U. MEYER-BERKHOUT, A. STAUDE, K.-M. TEICHERT, R. TIRLER [9], R. VOSS [10], Č. ZUPANČIČ
Sektion Physik der Universität, D-8000 Munich, Fed. Rep. Germany [11]

M. CRIBIER, J. FELTESSE, A. MILSZTAJN, A. OURAOU, P. RICH-HENNION, Y. SACQUIN, G. SMADJA and M. VIRCHAUX
DPhPE, CEN Saclay, F-91191 Gif-sur-Yvette Cedex, France

Received 8 March 1989

We present results on a high statistics study of the proton structure functions $F_2(x, Q^2)$ and $R=\sigma_L/\sigma_T$ measured in deep inelastic scattering of muons on a hydrogen target. The analysis is based on 1.8×10^6 events after all cuts, recorded at beam energies of 100, 120, 200 and 280 GeV and covering a kinematic range $0.06 \leqslant x \leqslant 0.80$ and $7\ \text{GeV}^2 \leqslant Q^2 \leqslant 260\ \text{GeV}^2$. At small x, we find R to be different from zero in agreement with predictions of perturbative QCD.

We present results on the structure functions of the proton measured with high statistics in deep inelastic scattering of muons on a hydrogen target. In the one-photon exchange approximation, the deep inelastic muon–proton cross section can be written as

[1] Deceased
[2] Present address: Digital Equipment, Turin, Italy.
[3] On leave from Institute of Physics, CSAV, CS-18040 Prague, Czechoslovakia.
[4] On leave from the Institut für Hochenergiephysik der AdW der DDR, DDR-1615 Berlin-Zeuthen, GDR.
[5] Present address: INFN, I-34100 Ferrara, Italy.
[6] Present address: Institute of Nuclear Research and Nuclear Energy, Bulgarian Academy of Sciences, 1784 Sofia, Bulgaria.
[7] On leave from E. Kardelj University and the J. Stefan Institute, 61111 Ljubljana, Yugoslavia.
[8] Present address: Siemens AG, Munich, Fed. Rep. Germany.
[9] Present address: DPhPE, CEN Saclay, F-91191 Gif-sur-Yvette Cedex, France.
[10] Present address: CERN, CH-1211 Geneva 23, Switzerland.
[11] Funded in part by the German Federal Minister for Research and Technology (BMFT) under contract number 054MU12P6.

Volume 223, number 3,4 PHYSICS LETTERS B 15 June 1989

$$\frac{d^2\sigma}{dQ^2dx}=\frac{4\pi\alpha^2}{Q^4x}\left(1-y-\frac{Q^2}{4E^2}+\frac{y^2E^2+Q^2}{2E^2[R(x,Q^2)+1]}\right)$$

$$\times F_2(x, Q^2)\,, \qquad (1)$$

where E is the energy of the incident beam, Q^2 the squared four-momentum transfer between the muon and the proton, and x and y are the Bjorken scaling variables. This cross section depends on two structure functions F_2 and R, where $R=\sigma_L/\sigma_T$ is the ration of absorption cross sections for virtual photons of longitudinal and transverse polarization. R is related to F_2 and to the longitudinal structure function F_L by

$$R(x, Q^2) = \frac{F_L(x, Q^2)}{(1+4M^2x^2/Q^2)F_2(x, Q^2)-F_L(x, Q^2)}\,, \qquad (2)$$

where M is the mass of the proton.

The data were collected at the CERN SPS muon beam with a high-luminosity spectrometer which is described in more detail elsewhere [1]. It consists of a 40 m long segmented toroidal iron magnet which is magnetized close to saturation and surrounds a 30 m long "internal" liquid hydrogen target. The iron absorbs the hadronic shower after a few meters and the surviving scattered muon is focused towards the spectrometer axis. The toroids are instrumented with scintillation trigger counters and multiwire proportional chambers. A 10 m long "external"target in front of the spectrometer magnet extends the acceptance of the apparatus to smaller angles, i.e. to smaller values of x and Q^2, than are accessible with the internal target. Four hodoscopes along the spectrometer axis detect the incoming muons and measure their trajectories. The momentum of the incident muon is measured with a spectrometer consisting of an air-gap magnet and another four scintillator hodoscopes upstream of the apparatus.

The results presented here are based on 1.8×10^6 reconstructed events after all cuts, recorded with positive muon beams of 100, 120, 200 and 280 GeV energy. The kinematic ranges and data samples are summarized in table 1. The data analysis is similar to the one performed by our Collaboration in an earlier experiment using a carbon target [2–4]. A more detailed account of this analysis can be found in ref. [5]. The principal difference between this and the carbon target experiment is due to the additional external target. For events originating from the internal target, the geometrical acceptance is greater than 65% and is rather flat in the kinematic region $x>0.25$ and $Q^2/2ME>0.10$. For events from the external target, the acceptance depends on the position of the interaction vertex along the beam direction; only data points with an acceptance larger than 50% were retained for the analysis. The structure functions were evaluated separately for the two target regions. The background from target–wall interactions was determined from special empty target runs and was subtracted from the data. At all beam energies, the data from external and internal target were found to be in statistical agreement and were combined for the subsequent analysis. Radiative corrections were applied using the calculations of ref. [6]. The error on $F_2(x, Q^2)$ from uncertainties on these corrections is estimated to be smaller than 1%.

Table 1
Kinematic ranges and number of events after all cuts at the four beam energies.

Beam energy (GeV)	Q^2 range (GeV^2)	x range	Number of events
100	7– 80	0.06–0.80	530 000
120	8–106	0.06–0.80	330 000
200	16–150	0.06–0.80	770 000
280	30–260	0.08–0.80	180 000

The principal sources of systematic errors in the data are uncertainties in
- the calibration of the incident beam energy ($\Delta E/E<0.15\%$),
- the calibration of the spectrometer magnetic field ($\Delta B/B<0.15\%$),
- corrections for the energy loss ε of muons in iron [7] ($\Delta\varepsilon/\varepsilon<1\%$),
- corrections for the finite resolution Σ of the spectrometer ($\Delta\Sigma/\Sigma<5\%$),
- the relative cross section normalization of data taken at different beam energies (1%),
- the absolute cross section normalization (3%).

Most of the results presented in this and a following paper [8], especially those on R and on the comparison of scaling violations to QCD predictions, are affected by the uncertainty on the relative but not on the absolute cross section normalization. Systematic

Volume 223, number 3,4 PHYSICS LETTERS B 15 June 1989

errors originating from uncertainties in the detector efficiencies (0.5%) are small due to the redundancy in the experimental apparatus. A detailed discussion of the Monte Carlo simulation used to compute the acceptance and the resolution of the apparatus, of the treatment of the systematic errors, and of the calibrations undertaken to minimize them can be found in refs. [2,5].

According to eq. (1) the measured cross section depends on the two functions $R=\sigma_L/\sigma_T$ and F_2. Both functions can be separated by comparing cross sections at the same value of x and Q^2, measured at different beam energies. In this analysis we have chosen to compare the values of four test F_2's, called $F_2^*(R)$, obtained at the four beam energies assuming trial values for R. The experimental value of R was then obtained together with the parameters of a common phenomenological parametrization of F_2 by minimizing the χ^2 of the four $F_2^*(R)$ with respect to this parametrization. This was done separately in each bin of x under the assumption that R, eq. (2), is independent of Q^2 in our kinematic range, as suggested by QCD calculations which predict only a weak (logarithmic) variation of the longitudinal structure function F_L with Q^2 [9]:

$$F_L(x,Q^2)=\frac{\alpha_s(Q^2)}{2\pi}x^2\int_x^1\left[\tfrac{8}{3}F_2(z,Q^2)+\frac{40}{9}\left(1-\frac{x}{z}\right)zG(z,Q^2)\right]\frac{dz}{z^3}, \quad (3)$$

where $\alpha_s(Q^2)$ is the running coupling constant of QCD. The theoretical prediction R_{QCD} was computed from eqs. (2) and (3) assuming a gluon momentum distribution $xG(x,Q_0^2)=4.5(1-x)^8$ at $Q_0^2=5$ GeV^2 and a QCD mass scale parameter $\Lambda=220$ MeV [8]. In the kinematic range of our experiment, this prediction does not depend strongly on the gluon distribution assumed. Eq. (3) does not account for effects of the charm quark mass and for target mass corrections which were included following ref. [10] and ref. [11], respectively. The experimental results for R are given in table 2 and are compared to the QCD prediction in fig. 1 together with earlier hydrogen data in a similar kinematical range by the European Muon Collaboration (EMC) [12]. At $x>0.20$, the measured values are compatible with zero in agreement with our carbon target measurement [2]. At smaller x, the data show a rise which is consistent with the QCD prediction.

Table 2
Results for $R=\sigma_L/\sigma_T$ as a function of x. R is assumed to be independent of Q^2 in each bin of x.

x	$\langle Q^2\rangle$ (GeV^2)	R	Statistical error	Systematic error
0.07	15	0.167	0.134	0.074
0.10	20	0.122	0.078	0.062
0.14	20	0.163	0.055	0.040
0.18	25	0.121	0.051	0.031
0.225	30	0.046	0.032	0.028
0.275	35	0.025	0.027	0.022
0.35	40	0.023	0.025	0.022
0.45	45	−0.011	0.035	0.027
0.55	50	0.005	0.056	0.039
0.65	50	−0.057	0.092	0.071

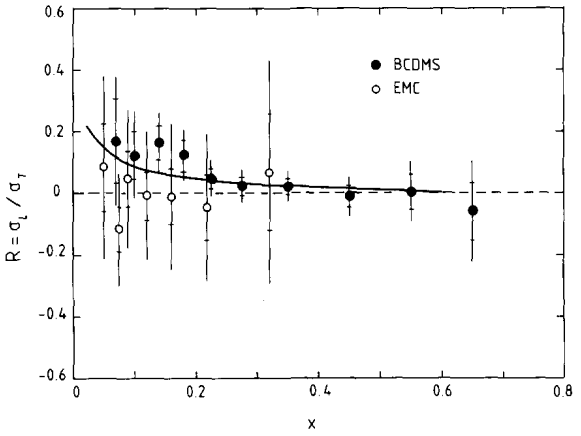

Fig. 1. $R=\sigma_L/\sigma_T$ measured in this experiment (BCDMS) as a function of x. Also shown is the measurement by the EMC on a hydrogen target [12]. Inner error bars are statistical only, outer error bars are statistical and systematic errors combined linearly. The solid line is the next-to-leading order QCD prediction using $\Lambda_{\overline{MS}}=220$ MeV and a gluon distribution $xG(x,Q_0^2)=4.5(1-x)^8$ at $Q_0^2=5$ GeV^2.

R_{QCD} was used to compute the final structure functions at the four different beam energies which are shown [#1] in fig. 2. The agreement between the different data sets in the region of large x allows to set stringent limits on most of the systematic errors as is

[#1] A version of this paper containing detailed tables of $F_2(x,Q^2)$ with statistical and systematic errors is available [13].

Volume 223, number 3,4 PHYSICS LETTERS B 15 June 1989

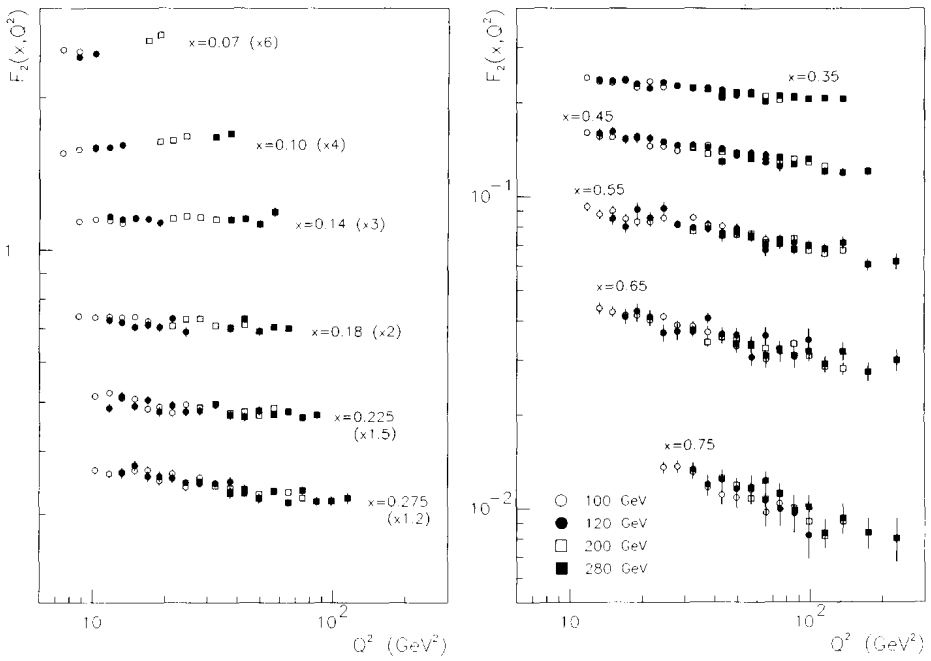

Fig. 2. The proton structure function $F_2(x, Q^2)$ measured at the four beam energies 100, 120, 200 and 280 GeV, using $R=R_{QCD}$. At $x \leqslant 0.275$, $F_2(x, Q^2)$ has been multiplied by the factors shown in the figure. Only statistical errors are shown.

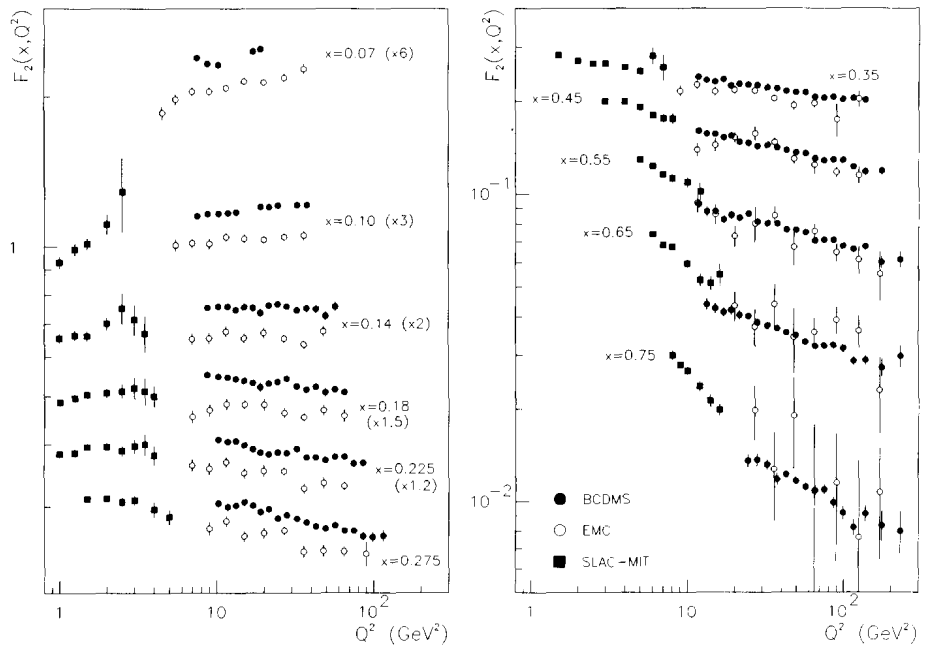

Fig. 3. The structure function $F_2(x, Q^2)$ from this experiment for all beam energies combined, using $R=R_{QCD}$. Also shown are data from the EMC [12] and SLAC–MIT [14] experiments. Where necessary, the EMC and SLAC data were interpolated to the x bins of this experiment at each value of Q^2 using a third order polynomial. Note that there are no SLAC data in the lowest x bin. The relative normalizations between the experiments have not been adjusted. At $x \leqslant 0.225$, all data have been multiplied by the factors indicated in the figure. Only statistical errors are shown.

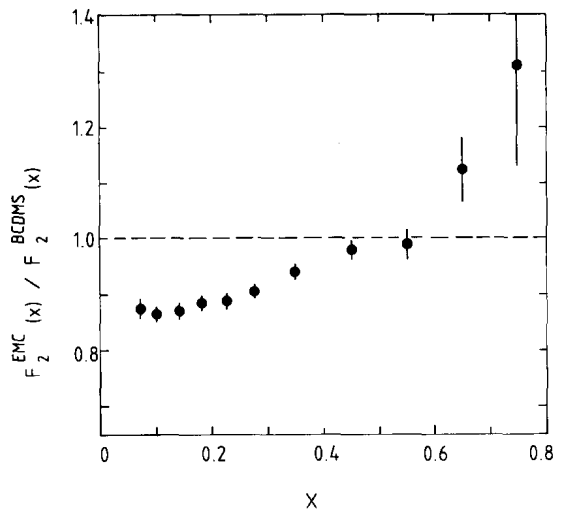

Fig. 4. The ratio of the proton structure functions $F_2(x)$ from this and from the EMC experiment [12]. In each bin of x, the data are averaged over the Q^2 range common to both measurements. Only statistical errors are shown. Systematic errors are difficult to visualize because of correlation effects but can be found in detail in refs. [12,13]. The systematic errors estimated for this experiment do not explain the observed discrepancy.

discussed in more detail in ref. [2]. The final $F_2(x, Q^2)$ from the combined data sets is shown in fig. 3. The scaling violations which are observed in these data are compared to predictions from perturbative QCD in a separate paper [8].

Also shown in fig. 3 are the earlier EMC data from muon–hydrogen scattering [12] and the SLAC–MIT results from electron–hydrogen scattering at lower Q^2 [14]. The x dependence of F_2 from this experiment is compared to the EMC result in fig. 4 where the data are averaged over the Q^2 range common to both measurements. The agreement is poor, especially at small x where F_2 measured in the present experiment is larger by up to 15%. In the lowest bin of x, about 4% of this difference is due to the fact that the EMC result was obtained using $R=0$. A similar behaviour was observed in our measurement on a carbon target [2] which indicated a steeper x dependence of F_2 than measured in earlier experiments. A quantitative comparison to the SLAC data is difficult at small x where the experiments cover disjoint ranges of Q^2. At large x, the two experiments agree within the systematic errors.

In conclusion, we have presented a high statistics measurement of the proton structure functions F_2 and R from deep inelastic scattering of muons at high Q^2 on a hydrogen target. The systematic uncertainties are comparable to the statistical accuracy of the results. $R=\sigma_L/\sigma_T$ is found to be in good agreement with the perturbative QCD prediction.

References

[1] BCDMS Collab., D. Bollini et al., Nucl. Instrum. Methods 204 (1983) 333;
BCDMS Collab., A.C. Benvenuti et al., Nucl. Instrum. Methods 226 (1984) 330.
[2] BCDMS Collab., A.C. Benvenuti et al., Phys. Lett. B 195 (1987) 91.
[3] BCDMS Collab., A.C. Benvenuti et al., Phys. Lett. B 195 (1987) 97.
[4] M. Virchaux, Thèse, Université Paris VII (1988).
[5] A. Ouraou, Thèse, Université Paris XI (1988).
[6] A.A. Akhundov et al., Sov. J. Nucl. Phys. 26 (1977) 660; 44 (1986) 988; JINR Communication E2-86-104 (Dubna 1986);
D.Yu. Bardin and N.M. Shumeiko, Sov. J. Nucl. Phys. 29 (1979) 499;
[7] BCDMS Collab., R. Kopp et al., Z. Phys. C 28 (1985) 171; W. Lohmann, R. Kopp and R. Voss, CERN Yellow Report CERN 85-03.
[8] BCDMS Collab., A.C. Benvenuti et al., Phys. Lett. B 223 (1989) 490.
[9] G. Altarelli and G. Martinelli, Phys. Lett. B 76 (1978) 89.
[10] M. Glück, E. Hoffmann and E. Reya, Z. Phys. C 13 (1982) 119.
[11] H. Georgi and D. Politzer, Phys. Rev. D 14 (1976) 1829.
[12] EM Collab., J.J. Aubert et al., Nucl. Phys. B 259 (1985) 189.
[13] BCDMS Collab., A.C. Benvenuti et al., preprint CERN-EP/89-06.
[14] A. Bodek et al., Phys. Rev. D 20 (1979) 1471.

Article copy

Volume 223, number 3,4 PHYSICS LETTERS B 15 June 1989

TEST OF QCD AND A MEASUREMENT OF Λ FROM SCALING VIOLATIONS IN THE PROTON STRUCTURE FUNCTION $F_2(x, Q^2)$ AT HIGH Q^2

BCDMS Collaboration

A.C. BENVENUTI, D. BOLLINI, G. BRUNI, L. MONARI [1], F.L. NAVARRIA
Dipartimento di Fisica dell'Università and INFN, I-40126 Bologna, Italy

A. ARGENTO [2], J. CVACH [3], W. LOHMANN [4], L. PIEMONTESE [5], G. TODOROVA [6], P. ZAVADA [3]
CERN, CH-1211 Geneva 23, Switzerland

A.A. AKHUNDOV, V.I. GENCHEV, V.G. KRIVOKHIZHIN, V.V. KUKHTIN, R. LEDNICKY, S. NEMECEK, P. REIMER, I.A. SAVIN, N.B. SKACHKOV, A.V. SIDOROV, G.I. SMIRNOV, J. STRACHOTA [3], G. SULTANOV [7], P. TODOROV [7], A.G. VOLODKO
Joint Institute for Nuclear Research, Dubna, P.O. Box 79, Head Post Office, 101000 Moscow, USSR

D. JAMNIK [8], R. KOPP [9], U. MEYER-BERKHOUT, A. STAUDE, K.-M. TEICHERT, R. TIRLER [10], R. VOSS [11], Č. ZUPANČIČ
Sektion Physik der Universität, D-8000 Munich, Fed. Rep. Germany[12]

M. CRIBIER, J. FELTESSE, A. MILSZTAJN, A. OURAOU, Y. SACQUIN, G. SMADJA and M. VIRCHAUX
DPhPE, CEN Saclay, F-91191 Gif-sur-Yvette Cedex, France

Received 8 March 1989

Scaling violations in the proton structure function $F_2(x, Q^2)$ measured with high statistics in deep inelastic scattering of muons on a hydrogen target are compared to predictions of perturbative QCD. Excellent agreement is observed with numerical solutions of the evolution equations in leading and next-to-leading order. The QCD mass scale parameter Λ is determined from these data both in a flavour nonsinglet approximation and with a complete flavour singlet and nonsinglet treatment. An estimate of the gluon distribution in the proton is given.

[1] Deceased.
[2] Present address: Digital Equipment, Turin, Italy.
[3] On leave from Institute of Physics, CSAV, CS-18040 Prague, Czechoslovakia.
[4] On leave from Institut für Hochenergiephysik der AdW der DDR, DDR-1615 Berlin-Zeuthen, GDR.
[5] Present address: INFN, I-34100 Ferrara, Italy.
[6] Present address: Institute of Mathematics, Bulgarian Academy of Sciences, Sofia, Bulgaria.
[7] Present address: Institute of Nuclear Research and Nuclear Energy, Bulgarian Academy of Sciences, 1784 Sofia, Bulgaria.
[8] On leave from E. Kardelj University and the J. Stefan Institute, YU-61111 Ljubljana, Yugoslavia.
[9] Present address: Siemens AG, Munich, Fed. Rep. Germany.
[10] Present address: DPhPE, CEN Saclay, F-91191 Gif-sur-Yvette Cedex, France.
[11] Present address: CERN, CH-1211 Geneva 23, Switzerland.
[12] Funded in part by the German Federal Minister for Research and technology (BMFT) under contract number 054MU12P6.

Volume 223, number 3,4 PHYSICS LETTERS B 15 June 1989

In a previous letter [1], we have reported on a high statistics measurement of the proton structure function $F_2(x, Q^2)$ at large four-momentum transfer Q^2 in deep inelastic scattering of muons on a hydrogen target. These data exhibit clear deviations from Bjorken scaling. Here we compare the measured scaling violations to predictions from perturbative quantum chromodynamics (QCD). The results of a similar analysis of the nucleon structure function measured with a carbon target have been reported earlier [2–4]. Tests of QCD from earlier high statistics muon and neutrino experiments are reported on in refs. [5–12].

In the framework of perturbative QCD [#1], scaling violations are due to the Q^2 evolution of quark and gluon distributions which can be described by the Altarelli–Parisi equations [14] or, alternatively, by the Q^2 dependence of their moments [#2]. Higher twist contributions to F_2, which are not described by these equations, vary like power series in $1/Q^2$ [16] and are expected to be small over most of the Q^2 range of our data. Furthermore, the data extend up to $x=0.75$, thus requiring only little extrapolation to calculate the evolution integrals. Our measurement is therefore well suited to a precise test of perturbative QCD.

Several numerical methods have been proposed to fit the QCD predictions to experimental data. We have mainly employed two methods [4,17–19] which have been developed within our Collaboration. They allow to fit the flavour singlet and nonsinglet evolution equations both in a leading order (LO) perturbation expansion and in a next-to-leading order expansion in the $\overline{\text{MS}}$ renormalization scheme. Four quark flavours were assumed throughout the QCD analysis.

The experimental data shown in fig. 2 of ref. [1] were used for the fits. Data points with $y<0.20$ at $x=0.75$, $y<0.16$ at $x=0.65$ and $y<0.14$ in all other bins of x were excluded to reduce the sensitivity of the fits to systematic uncertainties. Points with $Q^2<8$ GeV^2 at $x<0.16$, $Q^2<14$ GeV^2 at $0.16<x<0.25$, and with $Q^2<20$ GeV^2 at $x>0.25$ were excluded to suppress possible higher twist effects. The combined data after these cuts are shown in fig. 1.

[#1] For extensive reviews of perturbative QCD and further references, see ref. [13].

[#2] For a review see ref. [15].

In the nonsinglet approximation, the gluon contribution is neglected in the evolution equations. Estimates of the gluon distribution from muon [3,5,6] and neutrino scattering experiments [8,9] have shown that this approximation is valid at high values of the scaling variable x. Therefore, in the non-singlet analysis of the data reported here, only the kinematic region with $x\geqslant 0.275$ was considered. The cut at $Q^2<20$ GeV^2 further reduces the contribution of the gluon distribution which becomes softer with increasing Q^2 due to its QCD evolution. The results of these fits are summarized in table 1. We find good agreement between the values of Λ obtained with the different programs. The average result for the QCD mass scale parameter in next-to-leading order is

$$\Lambda_{\overline{\text{MS}}}=205\pm 22\ (\text{stat.})\pm 60\ (\text{syst.})\ \text{MeV}\,,$$

corresponding to a strong coupling constant of

$$\alpha_s(Q^2=100\ \text{GeV}^2)$$
$$=0.156\pm 0.004\ (\text{stat.})\pm 0.011\ (\text{syst.})\,.$$

To evaluate the systematic errors on Λ and α_s, the individual systematic uncertainties on F_2 were added to the data and the fits repeated. This was done for each contribution to the systematic error in turn and the resulting changes in Λ were combined in quadrature. The final systematic error $\Delta\Lambda=60$ MeV is dominated by the 1% uncertainty on the relative normalization between data taken at the four different beam energies. We have checked that all numerical results on Λ and α_s presented in this paper are insensitive to the choice of the Q_0^2 at which the QCD evolution is started.

Global QCD fits as they are conventionally used to determine Λ do not, however, constitute a sensitive test of quantum chromodynamics. In general, the χ^2's of such fits describe mainly their agreement with the x dependence of the structure functions which is not predicted by the theory, and the fits can be biased by a priori assumptions on the functional form of $F_2(x, Q_0^2)$. A more stringent test is obtained by comparing directly the x dependence of the measured scaling violations, averaged over Q^2, to the one expected from the QCD evolution. Within the accuracy of the present measurements, this is the only specific prediction of perturbative QCD for deep inelastic scattering which can be tested experimentally. In the nonsinglet

Volume 223, number 3,4 PHYSICS LETTERS B 15 June 1989

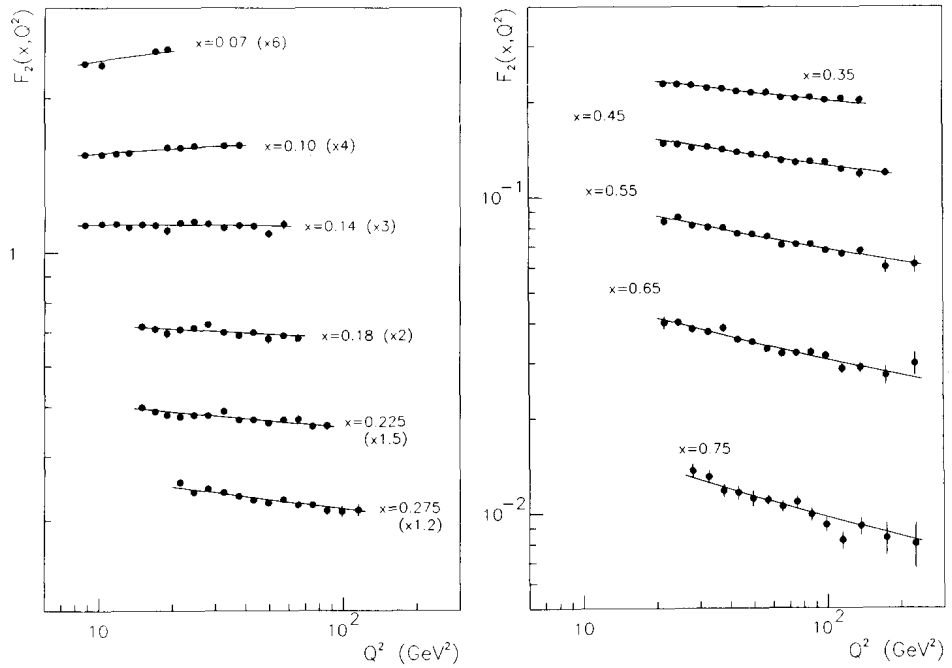

Fig. 1. The structure function $F_2(x, Q^2)$ using $R=R_{QCD}$ for all beam energies combined. The solid lines represent the singlet+nonsinglet QCD fit discussed in the text. Only statistical errors are shown.

approximation, this comparison depends on Λ as the sole free parameter whereas in a singlet analysis over the full x range it is also sensitive to the gluon distribution.

The nonsinglet case is shown in fig. 2a where the logarithmic derivatives $\mathrm{d}\ln F_2(x, Q^2)/\mathrm{d}\ln Q^2$ are compared to the next-to-leading order prediction for $\Lambda_{\overline{\mathrm{MS}}}=205$ MeV. The logarithmic derivatives in this figure are the slope parameters of straight line fits $\ln F_2 = a\ln Q^2 + b$ to the data. To calculate in a consistent way the theoretical predictions shown in the same figure, the result of the QCD fit, F_2^*, was assigned at each (x, Q^2) point the statistical error of the corresponding experimental F_2. The logarithmic derivatives $\mathrm{d}\ln F_2^*/\mathrm{d}\ln Q^2$ were then obtained by the same straight line fit as for the experimental data. Within the errors, this linear representation is an excellent approximation of both the experimental and the predicted Q^2 evolution. The measured x dependence of the scaling violations in fig. 2a is in agreement with the predicted one within statistical errors.

We have searched for higher twist effects in our data

Table 1
Results of nonsinglet QCD fits to $F_2(x, Q^2)$ in leading order (LO) and next-to-leading order in the $\overline{\mathrm{MS}}$ renormalisation scheme. The data are fitted in the kinematic range $x\geq 0.275$ and $Q^2\geq 20$ GeV^2; additional cuts on y are discussed in the text. Four quark flavours are assumed in the QCD analysis. χ_s^2 is the χ^2 of the direct comparison between measured and predicted scaling violations (fig. 2a). Only statistical errors are given.

Method	Λ_{LO} (MeV)	χ^2/DOF	χ_s^2/DOF	$\Lambda_{\overline{\mathrm{MS}}}$ (MeV)	χ^2/DOF	χ_s^2/DOF
ref. [18]	178±22	180/198	7.8/5	208±22	177/198	6.1/5
ref. [19]	181±21	180/198	7.9/5	198±21	177/198	4.7/5
carbon target [3]	210±20			230±20		

Volume 223, number 3,4 PHYSICS LETTERS B 15 June 1989

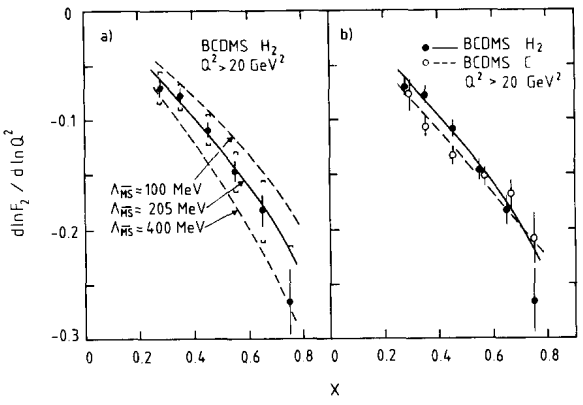

Fig. 2. (a) The logarithmic derivatives $\mathrm{d}\ln F_2(x, Q^2)/\mathrm{d}\ln Q^2$ observed in this experiment at $Q^2 > 20$ GeV^2 and $x \geq 0.275$. The inner error bars are statistical, the outer error bars show statistical and systematic errors added linearly. The systematic errors are strongly correlated. The lines show nonsinglet QCD predictions for $\Lambda_{\overline{MS}} = 205$ MeV and for two other values of Λ. (b) As (a), compared to carbon target results obtained with the same apparatus [3]. The QCD predictions are shown for a common value of $\Lambda_{\overline{MS}} = 220$ MeV. Only statistical errors are shown. The systematic errors of the carbon data are very similar to those of the hydrogen data shown in (a).

in the region $x > 0.25$ in several ways. We first do an explicit fit on higher twist terms, parametrizing $F_2(x, Q^2)$ as [16]

$$F_2(x, Q^2) = F_2^{\mathrm{LT}}(x, Q^2)[1 + H(x)/Q^2],$$

where $F_2^{\mathrm{LT}}(x, Q^2)$ follows the leading twist QCD evolution equations. We fix Λ to the value obtained in the nonsinglet fit (table 1). The higher twist term $H(x)$ is fitted as a set of parameters $H_i = H(x_i)$ and is found to be compatible with zero at all x_i. The same result is found, albeit with larger errors, when Λ is treated as a free parameter in the fit. We have also made pure nonsinglet QCD fits with different lower cut-offs in Q^2. Cutting at $Q^2 = 30$ GeV^2 and $Q^2 = 40$ GeV^2 changes Λ by $+15$ MeV and -10 MeV, respectively. There is thus no evidence for higher twist effects in the kinematic range of the nonsinglet fit.

For the QCD analysis over the full x range of the data, the proton structure function is decomposed into a singlet (S) and a nonsinglet (NS) part as $F_2 = F_2^{\mathrm{S}} + F_2^{\mathrm{NS}}$, where F_2^{NS} and F_2^{S} follow different Q^2 evolutions, the evolution of F_2^{S} being coupled to the gluon distribution. We have checked using the method of ref. [20] that the effect of the charm threshold is negligible in the kinematic range of this analysis.

The usual method to determine the gluon momentum distribution is to parametrize it at a given Q_0^2 and to evolve it with Q^2. We have chosen the parametrization $xG(x, Q_0^2) = A(\eta+1)(1-x)^\eta$ at $Q_0^2 = 5$ GeV^2. A more complicated parametrization is not justified by the accuracy of our measurement. The parameters A and η have been fitted together with Λ and with parametrizations of F_2^{NS} and F_2^{S}. The results obtained with our two fitting programs are in good agreement and are given in table 2. The results for Λ agree with those of the nonsinglet fits. In next-to-leading order, we find a soft gluon distribution which justifies the nonsinglet fits of $\Lambda_{\overline{MS}}$ discussed above. Systematic errors on A and η have been evaluated as for the nonsinglet case.

Assuming the parametrization of $xG(x, Q_0^2)$ to be valid over the full x range, A equals the fraction of the proton momentum carried by the gluons. When it is treated as a free parameter in the fits, we find $A \approx 0.5$. This is compatible with what is expected from the momentum sum rule which we have therefore imposed in the following analysis in order to constrain A. The results from such fits are given in table 3 and are in good agreement with those quoted in table 2. We have also used the program of ref. [18] to calculate for fixed values of η the χ^2 of the comparison of measured and predicted logarithmic derivatives of F_2 in the same way as for the nonsinglet fits. These χ^2's are shown in fig. 3a and exhibit different minima for the leading and next-to-leading order fits. Λ and η corresponding to these minima coincide with the results given in table 3. The correlation between η and Λ is shown in fig. 3b and is weaker than observed in previous experiments. This is a consequence of the softness of the gluon distribution and of the high accuracy of the data at large x where the effect of the gluons becomes negligible. The measured scaling violations are compared in fig. 3c to next-to-leading order fits for different values of η and show again very good agreement with the theoretical prediction for $\eta = 8.3$.

The gluon distributions in leading and next-to-leading order which correspond to the fits of table 2 are shown in fig. 4. They are valid only in the range $0.06 \leqslant x \leqslant 0.30$ since there are no F_2 data at smaller x, and at large x the gluon distribution is too small to have a noticeable effect on the scaling violations. Also

Volume 223, number 3,4 PHYSICS LETTERS B 15 June 1989

Table 2
Results of singlet+nonsinglet QCD fits to $F_2(x, Q^2)$ over the full x range of the data, in leading order (LO) and next-to-leading order in the $\overline{\text{MS}}$ renormalisation scheme, without imposing the momentum sum rule. Kinematic cuts are discussed in the text. A and η are the parameters of the gluon momentum distribution which is chosen as $xG(x)=A(\eta+1)(1-x)^{\eta}$. Four quark flavours are assumed in the QCD analysis. Only statistical errors are given.

Method	Λ_{LO} (MeV)	A_{LO} ($Q^2=5$ GeV^2)	η_{LO} ($Q^2=5$ GeV^2)	χ^2/DOF	χ_s^2/DOF	$\Lambda_{\overline{\text{MS}}}$ (MeV)	$A_{\overline{\text{MS}}}$ ($Q^2=5$ GeV^2)	$\eta_{\overline{\text{MS}}}$ ($Q^2=5$ GeV^2)	χ^2/DOF	χ_s^2/DOF
ref. [18]	200±30	0.61±0.12	5.8±2.5	254/268	11.7/8	214±22	0.62±0.20	11.6±3.0	256/268	8.6/8
ref. [19]	210±35	0.59±0.10	4.8±2.2	257/269	12.5/8	207±23	0.58±0.10	8.5±2.3	256/269	10.7/8

Table 3
As table 2, but imposing the momentum sum rule.

Method	Λ_{LO} (MeV)	η_{LO} ($Q^2=5$ GeV^2)	χ^2/DOF	χ_s^2/DOF	$\Lambda_{\overline{\text{MS}}}$ (MeV)	$\eta_{\overline{\text{MS}}}$ ($Q^2=5$ GeV^2)	χ^2/DOF	χ_s^2/DOF
ref. [18]	215±27	3.7±1.2	257/269	15.2/9	224±21	8.3±1.5	258/269	11.4/9
ref. [19]	216±30	4.2±1.5	257/270	13.4/9	212±21	7.8±1.5	256/270	11.5/9

shown in the same figure is the earlier EMC result [5] obtained in leading order for a fixed value of $\Lambda=90$ MeV.

A complementary method to determine the gluon momentum distribution consists in evaluating it from the measured scaling violation in each bin of x separately. When the QCD mass scale parameter is fixed, the gluon distribution is the only unknown function in the QCD evolution equation. It is estimated at each bin center x_i individually by assuming a parametrization for $xG(x, Q_0^2)$ at $x \geq x_i$, which we take to be

$$xG_i(x, Q_0^2)=C_i[(1-x)/(1-x_i)]^{\zeta} \quad (x \geq x_i),$$

using only the scaling violations measured at $x=x_i$ and assuming $\Lambda_{\overline{\text{MS}}}=220$ MeV (see below). The coefficients $C_i=x_iG_i(x_i, Q_0^2)$ are fitted separately using the same value for ζ. This parameter is determined iteratively such that the x dependence of the fitted C_i is well described by a parametrization proportional

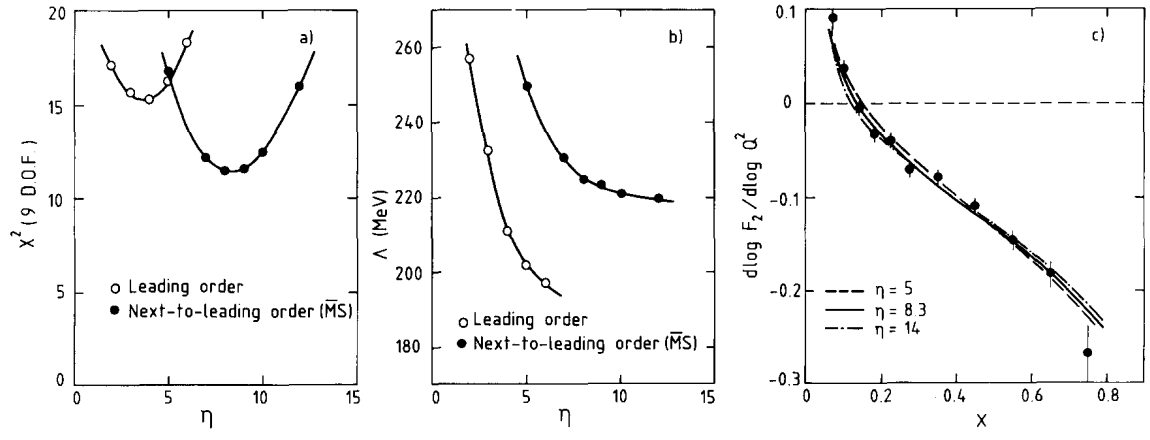

Fig. 3. (a) The χ^2 of the comparison of measured and predicted scaling violations as a function of the exponent η of a gluon distribution $xG(x, Q_0^2)=A(\eta+1)(1-x)^{\eta}$ at $Q_0^2=5$ GeV^2 from flavour singlet+nonsinglet fits at leading and next-to-leading order. (b) The dependence of the QCD mass scale parameter Λ on the exponent η of the gluon distribution from the same fits as in (a). (c) The same as fig. 2a, but for the full kinematical range of the data. The singlet+nonsinglet prediction in next-to-leading order QCD is also shown for different exponents η.

Volume 223, number 3,4 PHYSICS LETTERS B 15 June 1989

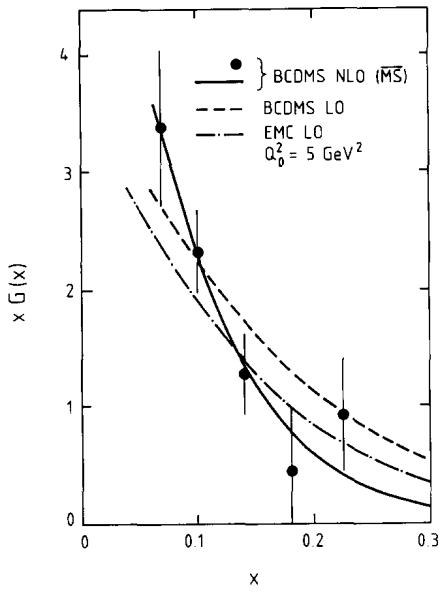

Fig. 4. The gluon momentum distribution $xG(x, Q_0^2)$ in the proton at $Q_0^2 = 5$ GeV^2. The parametrizations shown correspond to the results of the QCD fits in leading and next-to-leading order from table 2 and are compared to the earlier leading order analysis from the EMC experiment [5]. Also shown is the gluon distribution determined in bins of x as discussed in the text. No systematic errors are shown.

to $(1-x)^{\zeta}$. In next-to-leading order, the best agreement is observed for $\zeta = 11$ as expected from the previous method. Assuming $\zeta = 9$ ($\zeta = 13$) decreases (increases) all C_i by approximately 8%. The principal interest of this method lies in the reliable estimate of statistical errors. The coefficients C_i for $\zeta = 11$ are shown in fig. 4 together with the fits of $xG(x, Q_0^2)$ given in table 2. The dominant systematic error is due to the relative normalisation uncertainty, whereas the uncertainty on $\Lambda_{\overline{\rm MS}}$ has only a negligible effect. The total systematic errors, including the uncertainty on ζ, are typically half the statistical ones.

The QCD analysis presented in this paper can be compared to the one performed on our earlier measurement with a carbon target [3]. The kinematical domains used for the nonsinglet fits are almost identical and the results for Λ are in agreement within statistical errors. They can be combined to give

$$\Lambda_{\overline{\rm MS}} = 220 \pm 15 \text{ (stat.)} \pm 50 \text{ (syst.) MeV}$$

corresponding to a strong coupling constant

$$\alpha_s(Q^2 = 100 \text{ GeV}^2) = 0.1585 \pm 0.0025 \text{ (stat.)} \pm 0.0090 \text{ (syst.)} .$$

The largest contributions to the systematic errors on the two measurements of $\Lambda_{\overline{\rm MS}}$ come from the normalization uncertainties between data taken at different beam energies. These uncertainties are to a large extent uncorrelated between the carbon and hydrogen experiments, thus allowing to reduce the systematic error from this contribution for the combined result. The scaling violations measured with the two different targets are compared in fig. 2b to their respective QCD prediction for the same value of $\Lambda_{\overline{\rm MS}} = 220$ MeV. Different scaling violations in hydrogen and carbon are predicted by the evolution equation from the different x dependence of F_2 measured on proton and isoscalar targets. Such a difference is observed in the data with a good statistical significance: the probability $P(\chi^2)$ of the carbon and hydrogen data to agree with their respective QCD prediction is 40%, whereas the combined probability of the carbon data to agree with the hydrogen prediction and of the hydrogen data to agree with the carbon prediction is less than 0.3%. We estimate the latter probability to increase to a few percent when systematic errors are taken into account. The fact that different patterns of scaling violation are compatible with a common value of $\Lambda_{\overline{\rm MS}}$ is an additional confirmation of the remarkable consistency between our data and the QCD predictions.

In conclusion, we find that scaling violations observed in our high statistics measurement of the proton structure function $F_2(x, Q^2)$ at high Q^2 are in quantitative agreement with predictions from perturbative QCD. Nonperturbative effects are not required to explain scaling violations in the kinematic range of this experiment. The nonsinglet approximation and the complete singlet and nonsinglet fits to the data give consistent results for $\Lambda_{\overline{\rm MS}}$ which are in agreement with our earlier result from a carbon target. Combining these measurements, we obtain a value of $\Lambda_{\overline{\rm MS}} = 220 \pm 15 \pm 50$ MeV. The gluon distribution of the proton has been determined from singlet + nonsinglet fits in next-to-leading order QCD in the range $0.06 \leqslant x \leqslant 0.30$.

Volume 223, number 3,4 PHYSICS LETTERS B 15 June 1989

References

[1] BCDMS Collab., A.C. Benvenuti et al., Phys. Lett. B 223 (1989) 485.
[2] BCDMS Collab., A.C. Benvenuti et al., Phys. Lett. B 195 (1987) 91.
[3] BCDMS Collab., A.C. Benvenuti et al., Phys. Lett. B 195 (1987) 97.
[4] M. Virchaux, Thèse, Université Paris VII (1988).
[5] EM Collab., J.J. Aubert et al., Nucl. Phys. B 259 (1985) 189.
[6] EM Collab., J.J. Aubert et al., Nucl. Phys. B 272 (1986) 158.
[7] BFP Collab., P.D. Meyers et al., Phys. Rev. D 34 (1986) 1265.
[8] CDHS Collab., H. Abramowicz et al., Z. Phys. C 17 (1983) 283.
[9] CHARM Collab., F. Bergsma et al., Phys. Lett. B 123 (1983) 269; B 153 (1985) 111.
[10] CCFRR Collab., D.B. MacFarlane et al., Z. Phys. C 26 (1984) 1.
[11] BEBC-WA25 Collab., D. Allasia et al., Phys. Lett. B 135 (1984) 231; Z. Phys. C 28 (1985) 321.
[12] BEBC-WA59 Collab., K. Varvell et al., Z. Phys. C 36 (1987) 1.
[13] A. Buras, Rev. Mod. Phys. 52 (1980) 199;
G. Altarelli, Phys. Rep. 81 (1982) 1.
[14] G. Altarelli and G. Parisi, Nucl. Phys. B 126 (1977) 298.
[15] D.W. Duke and R.G. Roberts, Phys. Rep. 120 (1985) 275.
[16] See e.g. R.K. Ellis, W. Furmanski and R. Petronzio, Nucl. Phys. B 212 (1983) 29.
[17] A. Ouraou, Thèse, Université Paris XI (1988).
[18] M. Virchaux and A. Ouraou, preprint DPhPE 89-07, in preparation.
[19] V.G. Krivokhizhin et al., Z. Phys. C 36 (1987) 51.
[20] M. Glück, E. Hoffmann and E. Reya, Z. Phys. C 13 (1982) 119;
S.P. Luttrell and S. Wada, Nucl. Phys. B 182 (1981) 381.

Article copy

Volume 237, number 3,4 PHYSICS LETTERS B 22 March 1990

A HIGH STATISTICS MEASUREMENT OF THE DEUTERON STRUCTURE FUNCTIONS $F_2(x, Q^2)$ AND R FROM DEEP INELASTIC MUON SCATTERING AT HIGH Q^2

BCDMS Collaboration

A.C. BENVENUTI, D. BOLLINI, G. BRUNI, F.L. NAVARRIA
Dipartimento di Fisica dell' Università and INFN, I-40126 Bologna, Italy

A. ARGENTO [1], W. LOHMANN [2], L. PIEMONTESE [3], J. STRACHOTA [4], P. ZAVADA [4]
CERN, CH-1211 Geneva 23, Switzerland

S. BARANOV, V.I. GENCHEV [5], I.A. GOLUTVIN, Yu.T. KIRYUSHIN, V.G. KRIVOKHIZHIN, V.V. KUKHTIN, R. LEDNICKY, S. NEMECEK, P. REIMER [4], I.A. SAVIN, E. TELYUKOV, G.I. SMIRNOV, G. SULTANOV [5], P. TODOROV [5], A.G. VOLODKO
Joint Institute for Nuclear Research, Dubna, SU 101 000 Moscow, USSR

D. JAMNIK [6], R. KOPP [7], U. MEYER-BERKHOUT, A. STAUDE, K.-M. TEICHERT, R. TIRLER [8], R. VOSS [9], C. ZUPANCIC
Sektion Physik der Universität, D-8000 Munich, FRG [10]

M. CRIBIER, J. FELTESSE, A. MILSZTAJN, A. OURAOU, Y. SACQUIN, G. SMADJA and M. VIRCHAUX
DPhPE, CEN Saclay, F-91191 Gif-sur-Yvette Cedex, France

Received 22 December 1989

We present results on a high statistics study of the nucleon structure functions $F_2(x, Q^2)$ and $R=\sigma_L/\sigma_T$ measured in deep inelastic scattering of muons on a deuterium target. The analysis is based on 8×10^5 events after all cuts, recorded at beam energies of 120, 200 and 280 GeV in the kinematic range $0.06\leqslant x\leqslant 0.80$ and $8\ \text{GeV}^2\leqslant Q^2\leqslant 260\ \text{GeV}^2$. Scaling violations observed in the data are in agreement with predictions of perturbative QCD and allow to determine the QCD mass scale parameter Λ.

We present results on the structure functions of the nucleon measured with high statistics in deep inelastic scattering of muons on a deuterium target. In the one-photon exchange approximation, the deep inelastic muon–nucleon cross section can be written as

[1] Present address: Digital Equipment, Turin, Italy.
[2] On leave from the Institut für Hochenergiephysik der AdW der DDR, DDR-1615 Berlin-Zeuthen, GDR.
[3] Present address: INFN, I-34100 Ferrara, Italy.
[4] On Leave from Institute of Physics, CSAV, CS-18040 Prague, Czechoslovakia.
[5] Present address: Institute of Nuclear Research and Nuclear Energy, Bulgarian Academy of Sciences, 1784 Sofia, Bulgaria.
[6] On leave from E. Kardelj University and the J. Stefan Institute, YU-61111 Ljubljana, Yugoslavia.
[7] Present address: Siemens AG, Munich, FRG.
[8] Present address: DPhPE, CEN Saclay, F-91191 Gif-sur-Yvette Cedex, France.
[9] Present address: CERN, CH-1211 Geneva 23, Switzerland.
[10] Funded in part by the German Federal Minister for Research and Technology (BMFT) under contract number 054MU12P6.

Volume 237, number 3,4 PHYSICS LETTERS B 22 March 1990

$$\frac{d^2\sigma}{dQ^2\,dx} = \frac{4\pi\alpha^2}{Q^4 x}\left(1-y-\frac{Q^2}{4E^2}+\frac{y^2E^2+Q^2}{2E^2[R(x,Q^2)+1]}\right) \times F_2(x,Q^2)\,, \quad (1)$$

where E is the energy of the incident muon, Q^2 the squared four-momentum transfer between the muon and the nucleon, and x and y are the Bjorken scaling variables. This cross section depends on two structure functions F_2 and R, where $R=\sigma_L/\sigma_T$ is the ratio of absorption cross sections for virtual photons of longitudinal and transverse polarization.

The measurement which we describe here is similar to an earlier one with a hydrogen target [1–3]. The data were collected at the CERN SPS muon beam with a high-luminosity spectrometer which is described in detail elsewhere [4]. The results presented here are based on 8×10^5 reconstructed events after all cuts, recorded with positive muon beams of 120, 200 and 280 GeV energy. The kinematic ranges and data samples are summarized in table 1. A part of these data has been used earlier in a study of nuclear effects [5]. The analysis of the data proceeds in exactly the same way as for the measurement with the hydrogen target and is also very similar to the analysis of our earlier carbon target data [6–8]. We therefore do not describe it here. Radiative corrections were calculated following ref. [9]. In comparison to the hydrogen data, the only additional contribution is due to coherent scattering on the deuteron.

The experimental results for R are given in table 2 and are shown in fig. 1 together with a perturbative QCD prediction R_{QCD} which is calculated from

$$R(x,Q^2)=\frac{F_L(x,Q^2)+(4M^2x^2/Q^2)F_2(x,Q^2)}{F_2(x,Q^2)-F_L(x,Q^2)}\,, \quad (2)$$

Table 1
Kinematic ranges and number of events after all cuts at the three different beam energies.

Beam energy (GeV)	Q^2 range (GeV^2)	x range	Number of events
120	8–106	0.06–0.80	311 000
200	16–150	0.06–0.80	385 000
280	30–260	0.08–0.80	77 000

Table 2
Results for $R=\sigma_L/\sigma_T$ as a function of x. R is averaged over Q^2 in each bin of x.

x	$\langle Q^2\rangle$ (GeV^2)	R	ΔR (stat.)	ΔR (syst.)
0.10	20.0	0.190	0.120	0.072
0.14	25.0	0.114	0.076	0.046
0.18	35.0	0.160	0.077	0.038
0.225	45.0	0.222	0.069	0.041
0.275	50.0	0.061	0.049	0.036
0.35	65.0	0.077	0.042	0.034
0.45	75.0	0.060	0.062	0.036
0.55	85.0	0.165	0.120	0.056
0.65	85.0	0.043	0.181	0.107

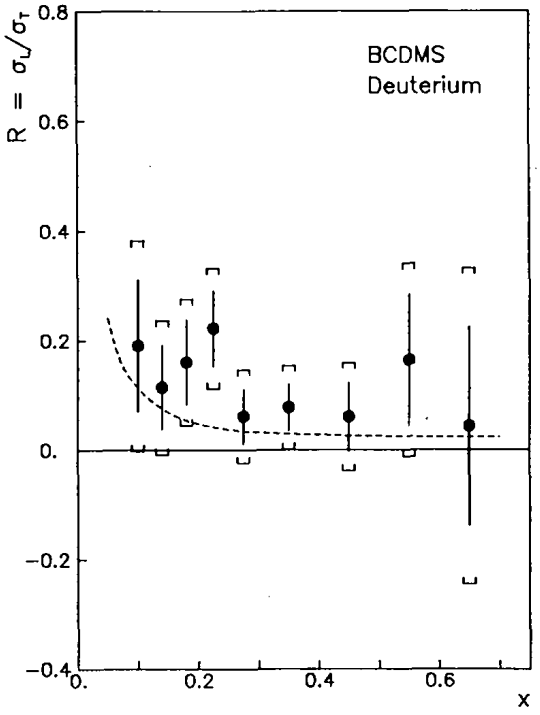

Fig. 1. $R=\sigma_L/\sigma_T$ measured in this experiment as a function of x. Inner error bars are statistical only, outer error bars are statistical and systematic errors combined linearly. The systematic errors are dominated by the relative normalization uncertainty between data taken at different beam energies and are thus strongly correlated. The solid line is the next-to-leading order QCD prediction using $\Lambda_{\overline{MS}}=220$ MeV and a gluon distribution $xG(x,Q_0^2)=4.5(1-x)^8$ at $Q_0^2=5$ GeV^2 [2].

Volume 237, number 3,4 PHYSICS LETTERS B 22 March 1990

where F_L is the longitudinal structure function and M is the mass of the nucleon [#1]. In perturbative QCD, F_L is given by

$$F_L(x, Q^2) = \frac{\alpha_s(Q^2)}{2\pi} x^2 \int_x^1 \left[\tfrac{8}{3} F_2(z, Q^2) + \frac{40}{9}\left(1 - \frac{x}{z}\right) zG(z, Q^2) \right] \frac{dz}{z^3} \quad (3)$$

[10], where $\alpha_s(Q^2)$ is the running coupling constant of QCD. To compute F_L, we assume a QCD mass scale parameter $\Lambda = 220$ MeV and a gluon momentum distribution $xG(x, Q_0^2) = 4.5(1-x)^8$ at $Q_0^2 = 5$ GeV^2 [2]. In the kinematic range of our data, R_{QCD} does not depend strongly on the gluon distribution assumed. The data lie above this prediction but there is no disagreement within the errors.

R_{QCD} was used to compute the structure function $F_2(x, Q^2)$ which is shown [#2] in fig. 2 for the three different beam energies. The principal sources of systematic errors in the data are uncertainties in

- the calibration of the incident beam energy ($\Delta E/E < 0.15\%$),
- the calibration of the spectrometer magnetic field B ($\Delta B/B < 0.15\%$),
- corrections for the energy loss ε of muons in iron [11] ($\Delta\varepsilon/\varepsilon < 1\%$),
- corrections for the finite resolution Σ of the spectrometer ($\Delta\Sigma/\Sigma < 5\%$),
- the relative cross section normalization of data taken at different beam energies (1% between the 120

[#1] In refs. [1,6], we have used a relation between R and F_L which is not consistent with the expression for F_L of eq. (3). This increases slightly the QCD prediction for R but does not affect the measured values. Since we used the perturbative QCD prediction for F_L in the computation of F_2, the latter decreases by approximately 1‰ over the entire kinematic range of the data. This is completely negligible when compared to the errors.

[#2] A version of this paper containing detailed tables of $F_2(x, Q^2)$ with statistical and systematic errors is available as preprint CERN-EP/89-170.

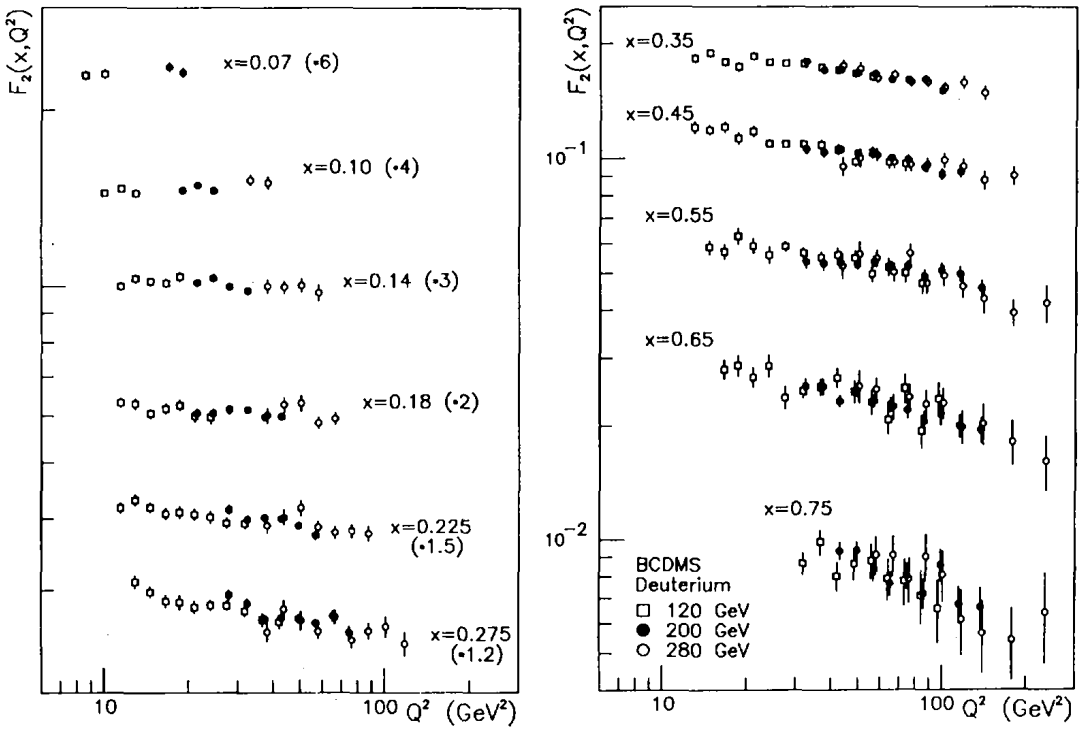

Fig. 2. The deuteron structure function $F_2(x, Q^2)$ measured at the three beam energies 120, 200 and 280 GeV, using $R = R_{QCD}$. At $x < 0.275$, $F_2(x, Q^2)$ has been multiplied by the factors shown in the figure. Only statistical errors are shown.

Volume 237, number 3,4 PHYSICS LETTERS B 22 March 1990

GeV and 200 GeV data, 1.5% between the 280 GeV and 200 GeV data),
- the absolute cross section normalization (3%).

Most of the results presented in this paper, especially those on R and on the comparison of scaling violations to QCD predictions, are affected by the uncertainty on the relative but not on the absolute cross section normalization. Systematic errors originating from uncertainties in the detector efficiencies (0.5%) are small due to the redundancy in the experimental apparatus. The agreement between the different data sets in the region of large x confirms our estimate of most of the systematic errors as we have discussed in more detail in ref. [6].

The final $F_2(x, Q^2)$ from the combined data sets is shown in fig. 3. Shown in the same figure are earlier EMC data from muon–deuterium scattering [12]. In comparison to these data we find a poor agreement, especially at small x, which is similar to the one observed in the hydrogen data [1]. Also shown in this figure are results from a recent analysis of SLAC data on electron–deuterium scattering at lower Q^2 [13]. In the region of $x \leqslant 0.35$ where the experiments cover disjoint ranges of Q^2, the SLAC data extrapolate to our results within the errors. At larger x and in the Q^2 region of overlap the errors of our data are dominated by the systematic uncertainties, which are strongly correlated. Within these errors, both data sets are compatible with a smooth Q^2 evolution of a common F_2.

Clear deviations from Bjorken scaling are observed in the structure function F_2 (fig. 2). We compare these scaling violations to predictions of QCD using the same methods which we have applied previously to our carbon [7,8] and hydrogen [2,3] data. In the framework of perturbative QCD [14] scaling violations are due to the Q^2 evolution of quark and gluon distributions and can be described by the Altarelli–Parisi equations [15] or, alternatively, by the Q^2 dependence of their moments [16]. The data extend up to $x=0.75$, thus requiring only little extrapolation to calculate the evolution integrals. Higher

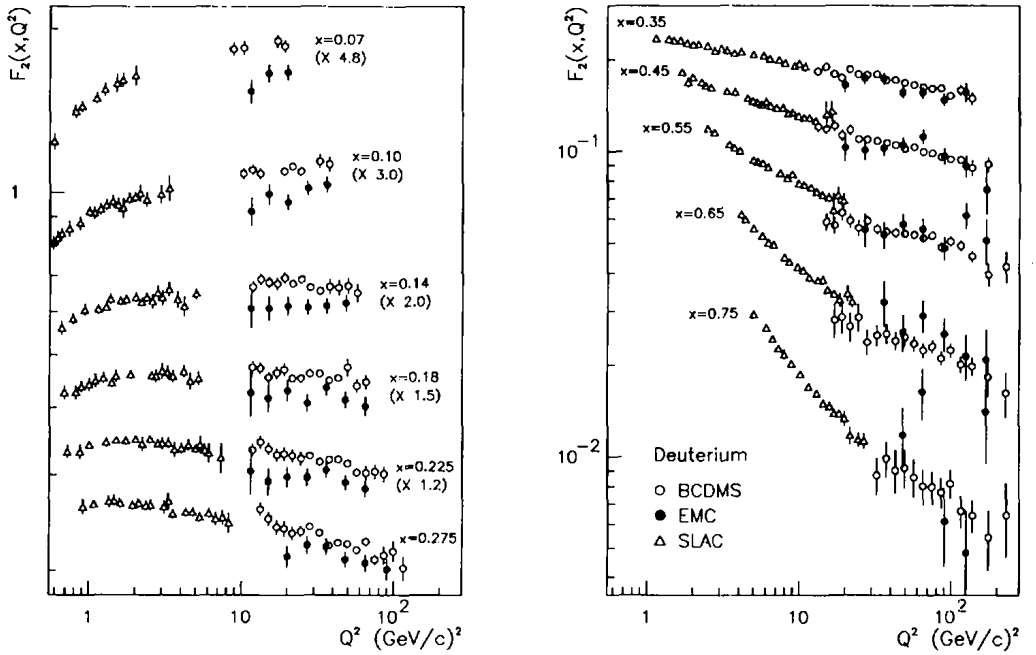

Fig. 3. The structure function $F_2(x, Q^2)$ from this experiment for all beam energies combined, using $R=R_{QCD}$. Also shown are data from the EMC [12] and SLAC [13] experiments. Where necessary, the EMC data were interpolated to the x bins of this experiment at each value of Q^2 using a third order polynomial. The relative normalizations between the experiments have not been adjusted; the normalization uncertainties are 3%, 5% and 2% for the BCDMS, EMC and SLAC data, respectively. At $x \leqslant 0.225$, all data have been multiplied by the factors indicated in the figure. The error bars are statistical and systematic errors combined in quadrature and are thus partially correlated.

Volume 237, number 3,4 PHYSICS LETTERS B 22 March 1990

twist contributions to F_2, which are not described by these equations, vary like power series in $1/Q^2$ [17] and are expected to be small over most of the Q^2 range of our data.

Several numerical methods have been proposed to fit the QCD predictions to experimental data. We have mainly employed two methods [3,8,18] which have been developed within our collaboration. They allow to fit the flavour singlet and nonsinglet evolution equations both in a leading order (LO) perturbation expansion and in a next-to-leading order expansion in the $\overline{\text{MS}}$ renormalization scheme. Four quark flavours were assumed throughout the QCD analysis.

The experimental data shown in fig. 2 were used for the fits. Data points with $y<0.20$ at $x=0.75$, $y<0.16$ at $x=0.65$ and $y<0.14$ in all other bins of x were excluded to reduce the sensitivity of the fits to systematic uncertainties. Points with $Q^2<14$ GeV^2 at $0.16<x<0.25$ and with $Q^2<20$ GeV^2 at $x>0.25$ were excluded to suppress possible higher twist effects. These cuts are the same as in the analysis of the hydrogen data.

In the nonsinglet approximation, the gluon contribution is neglected in the evolution equations. Estimates of the gluon distribution from muon [2,7,19,20] and neutrino scattering experiments [21,22] have shown that this approximation is valid at high values of x. Therefore, in the nonsinglet analysis of the data reported here, only the kinematic region $x\geqslant 0.275$ was used. The cut at $Q^2=20$ GeV^2 further reduces the contribution of the gluon distribution which becomes softer with increasing Q^2 due to its QCD evolution. The results of these fits are summarized in table 3. We find good agreement between the values of Λ obtained with the different programs. The average result for the QCD mass scale parameter in next-to-leading order is

$$\Lambda_{\overline{\text{MS}}}=230\pm40\ (\text{stat.})\pm70\ (\text{syst.})\ \text{MeV},$$

corresponding to a strong coupling constant of

$$\alpha_s(Q^2=100\ \text{GeV}^2)=0.160\pm0.006\ (\text{stat.})\pm0.011\ (\text{syst.}).$$

This is in good agreement with the results of our earlier measurements on carbon and hydrogen targets, $\Lambda_{\overline{\text{MS}}}=220\pm15$ (stat.) ±50 (syst.) MeV [2,7]. To evaluate the systematic errors on Λ and α_s, the individual systematic uncertainties on F_2 were added to the data and the fits repeated. This was done for each contribution to the systematic error in turn and the resulting changes in Λ were combined in quadrature. The final systematic error $\Delta\Lambda=70$ MeV is dominated by the uncertainty on the relative normalization between data taken at three different beam energies.

As we have discussed in more detail in refs. [2,7], the agreement between data and QCD fit, which is prerequisite for a meaningful determination of α_s, is best verified by comparing the x dependence of measured and predicted scaling violations. This is shown for the nonsinglet case in fig. 4a where the average logarithmic derivatives $\mathrm{d}\ln F_2(x, Q^2)/\mathrm{d}\ln Q^2$ are compared to the next-to-leading order prediction for $\Lambda_{\overline{\text{MS}}}=230$ MeV. The measured x dependence of the scaling violations is in agreement with the predicted one.

In the QCD analysis over the full x range of the data, the Q^2 evolution of the deuteron structure function, which is an almost pure flavour singlet, is sensitive to the gluon distribution at small x. We use the gluon distribution $xG(x)\propto(1-x)^8$ at $Q_0^2=5$ GeV^2 determined in next-to-leading order from our hydrogen data [2] and fit Λ over the full kinematic range of the data. This fit yields $\Lambda_{\overline{\text{MS}}}=250\pm35$ (stat.) MeV in agreement with the result of the nonsinglet fit. The measured logarithmic derivatives and the corre-

Table 3
Results of nonsinglet QCD fits to $F_2(x, Q^2)$ in leading order (LO) and next-to-leading order in the $\overline{\text{MS}}$ renormalisation scheme. The data are fitted in the kinematic range $x\geqslant0.275$ and $Q^2\geqslant20$ GeV^2; additional cuts on y are discussed in the text. Four quark flavours are assumed in the QCD analysis. χ_s^2 is the χ^2 of the direct comparison between measured and predicted scaling violations (fig. 4a). Only statistical errors are given; systematic errors are discussed in the text.

Method	Λ_{LO} (MeV)	χ^2/DOF	χ_s^2/DOF	$\Lambda_{\overline{\text{MS}}}$ (MeV)	χ^2/DOF	χ_s^2/DOF
refs. [3,8]	210 ± 37	123/155	6.5/5	236 ± 39	126/155	9.2/5
ref. [22]	206 ± 35	135/154	5.9/5	220 ± 34	140/154	8.2/5

Volume 237, number 3,4 PHYSICS LETTERS B 22 March 1990

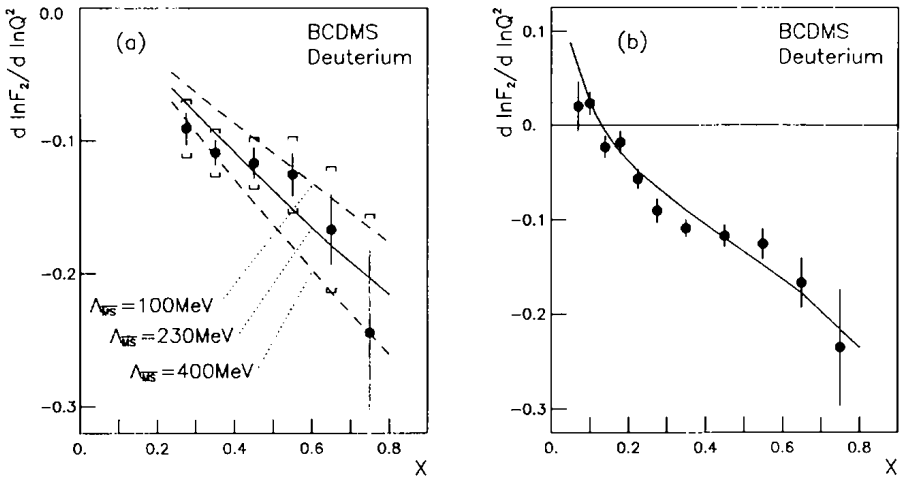

Fig. 4. (a) The logarithmic derivatives $d \ln F_2(x, Q^2)/d \ln Q^2$ observed in this experiment, averaged over Q^2, for $Q^2 > 20$ GeV^2 and $x \geq 0.275$. The inner error bars are statistical, the outer error bars show statistical and systematic errors added linearly. The systematic errors are strongly correlated. The lines show nonsinglet QCD predictions for $\Lambda_{\overline{MS}} = 230$ MeV and for two other values of Λ. (b) The same as (a) but for the full x range of the data. The line shows a singlet QCD prediction for $\Lambda_{\overline{MS}} = 250$ MeV, assuming a gluon momentum distribution $xG(x, Q_0^2) = 4.5(1-x)^8$ at $Q_0^2 = 5$ GeV^2 [2]. The QCD prediction fits the data with a $\chi_s^2/\mathrm{DOF} = 19.0/10$. Only statistical errors are shown.

sponding QCD prediction for $\Lambda_{\overline{MS}} = 250$ MeV are shown in fig. 4b. Treating the power of the gluon distribution as a free parameter in the fit gives compatible results within large errors.

In conclusion, we have presented a high statistics measurement of the deuteron structure functions F_2 and R from deep inelastic scattering of muons at high Q^2 on a deuterium target. Scaling violations are observed in the data and are in agreement with predictions from perturbative QCD. We find $\Lambda_{\overline{MS}}$ to be in good agreement with our earlier result obtained with carbon and hydrogen targets.

References

[1] BCDMS Collab., A.C. Benvenuti et al., Phys. Lett B 223 (1989) 485.
[2] BCDMS Collab., A.C. Benvenuti et al., Phys. Lett. B 223 (1989) 490.
[3] A. Ouraou, Thèse, Université Paris XI (1988).
[4] BCDMS Collab., D. Bollini et al., Nucl. Instrum. Methods 204 (1983) 333;
BCDMS Collab., A.C. Benvenuti et al., Nucl. Instrum. Methods 226 (1984) 330.
[5] BCDMS Collab., G. Bari et al., Phys. Lett. B 163 (1985) 282;
BCDMS Collab., A.C. Benvenuti et al., Phys. Lett. B 189 (1987) 483;
A. Milsztajn, Thèse Université Paris XI (1989).
[6] BCDMS Collab., A.C. Benvenuti et al., Phys. Lett. B 195 (1987) 91.
[7] BCDMS Collab., A.C. Benvenuti et al., Phys. Lett. B 195 (1987) 97.
[8] M. Virchaux, Thèse, Université Paris VII (1988).
[9] A.A. Akhundov et al., Sov. J. Nucl. Phys. 26 (1977) 660; 44 (1986) 988; JINR Communication E2-86-104 (Dubna, 1986);
D.Yu Bardin and N.M. Shumeiko, Sov. J. Nucl. Phys. 29 (1979) 499.
[10] G. Altarelli and G. Martinelli, Phys. Lett. B 76 (1978) 89.
[11] BCDMS Collab., R. Kopp et al., Z. Phys. C 28 (1985) 171; W. Lohmann, R. Kopp and R. Voss, CERN Yellow Report, CERN 85-03.
[12] European Collab., J.J. Aubert et al., Nucl. Phys. B 293 (1987) 740.
[13] L.W. Whitlow et al., University of Rochester preprint UR-1119 (ER-13065-586), in: Proc. Europhys. Conf. on High energy physics (Madrid, 1989), to be published.
[14] For extensive reviews of perturbative QCD and further references, see A. Buras, Rev. Mod. Phys. 52 (1980) 199; G. Altarelli, Phys. Rep. 81 (1982) 1.
[15] G. Altarelli and G. Parisi, Nucl. Phys. B 126 (1977) 298.
[16] For a review, see D.W. Duke and R.G. Roberts, Phys. Rep. 120 (1985) 275.
[17] See e.g. R.K. Ellis, W. Furmanski and R. Petronzio, Nucl. Phys. B 212 (1983) 29.

[18] V.G. Krivokhizhin et al., Z. Phys. C 36 (1987) 51.
[19] European Muon Collab., J.J. Aubert et al., Nucl. Phys. B 259 (1985) 189.
[20] European Muon Collab., J.J. Aubert et al., Nucl. Phys. B 272 (1986) 158.
[21] CDHS Collab., H. Abramowicz et al., Z. Phys. C 17 (1983) 283;
CDHSW Collab., P. Berge et al., CERN preprint CERN-EP/89-103, submitted to Z. Phys. C.
[22] CHARM Collab., F. Bergsma et al., Phys. Lett. B 123 (1983) 269; B 153 (1985) 111.

2.3 Studium EMC efektu

Na počátku osmdesátých let vyvolal ve světě značnou pozornost výsledek experimentu *European Muon Collaboration*, který se rovněž uskutečnil v CERN. Podstatou tohoto výsledku, pro který se brzy ujal název *EMC efekt*, bylo zjištění, že strukturní funkce nukleonu vázaného v jádře se poněkud liší od strukturní funkce volného nukleonu. Tento výsledek přirozeně vyvolal zajímavé hypotézy a spekulace o chování kvarků v nukleonech vázaných v jádrech, o vlivu této vazby na vnitřní strukturu nukleonu. Do vazby mezi nukleony například významně přispívá výměna mezonů, tj. i tyto částice mohou efektivně přispívat do strukturní funkce měřené na jádře.

EMC efekt lze dobře a čistě demonstrovat na poměru strukturních funkcí měřených na jádře s hmotovým číslem A a na jádře deuteria:

$$F_2^A(x,Q^2)/F_2^D(x,Q^2).$$

Tento poměr se podařilo spolehlivě změřit i v experimentu BCDMS pro jádro $^{56}_{26}$Fe [A4], viz část 2.3.1. Analýza ukázala, že v kinematické oblasti experimentu BCDMS tento poměr nezávisí na Q^2 a v oblasti $x > 0.25$ velmi dobře souhlasí s existujícími daty jiných experimentů. V oblasti $0.06 < x < 0.25$ byl v BCDMS naměřen efekt méně výrazný, než ukazovala původní EMC data [25], avšak pozdější a přesnější EMC data [26] jsou v dobré shodě s daty BCDMS, viz obrázek 2.3. Poznamenejme, že EMC efekt zůstává aktuálním problémem i v současnosti, jak o tom svědčí například nedávné práce [28]− [30] i další práce v nich citované.

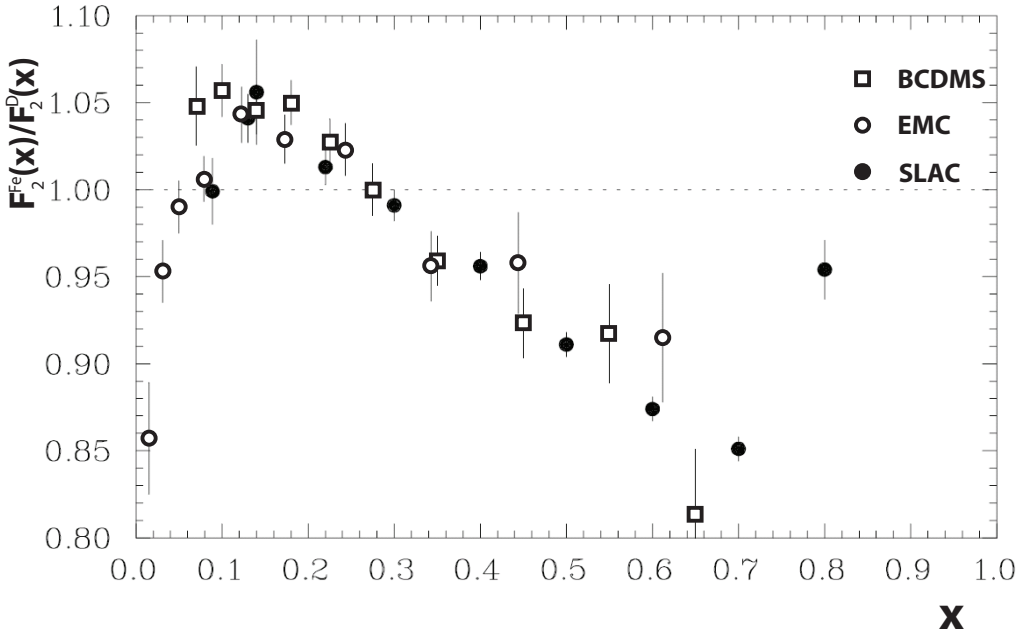

Obrázek 2.3: EMC efekt změřený v experimentech BCDMS [A4], EMC [26] a SLAC [27]

Article copy

Volume 189, number 4 PHYSICS LETTERS B 14 May 1987

NUCLEAR EFFECTS IN DEEP INELASTIC MUON SCATTERING ON DEUTERIUM AND IRON TARGETS

BCDMS Collaboration

A.C. BENVENUTI, D. BOLLINI, G. BRUNI, F.L. NAVARRIA
Dipartimento di Fisica dell'Università and INFN, I-40126 Bologna, Italy

A. ARGENTO [1], J. CVACH [2], K. DIETERS [3], L. PIEMONTESE [4], I. VERESS [5], P. ZAVADA [2]
CERN, CH-1211 Geneva 23, Switzerland

N.G. FADEEV, I.A. GOLUTVIN, M.Yu. KAZARINOV, Yu.T. KIRYUSHIN, V.G. KRIVOKHIZHIN, V.V. KUKHTIN, W. LOHMANN [3], S. NEMECEK, P. REIMER, I.A. SAVIN, G.I. SMIRNOV, J. STRACHOTA [2], G. SULTANOV [6], P. TODOROV, A.G. VOLODKO
Joint Institute for Nuclear Research, Dubna, 101000 Moscow, USSR

D. JAMNIK [7], R. KOPP [8], U. MEYER-BERKHOUT, A. STAUDE, K.-M. TEICHERT, R. TIRLER [9], R. VOSS, C. ZUPANCIC
Sektion Physik der Universität, D-8000 Munich, Fed. Rep. Germany [10]

M. CRIBIER, J. FELTESSE, A. MILSZTAJN, A. OURAOU, P. RICH-HENNION, Y. SACQUIN, G. SMADJA and M. VIRCHAUX
DPhPE, CEN Saclay, F-91191 Gif-sur-Yvette Cedex, France

Received 17 March 1987

New results are presented on nuclear effects in deep inelastic muon scattering on deuterium and iron targets at large Q^2. The ratio $F_2^{Fe}(x)/F_2^{D_2}(x)$ measured in the kinematic range $0.06 \leqslant x \leqslant 0.70$, $14\ \text{GeV}^2 \leqslant Q^2 \leqslant 70\ \text{GeV}^2$ is in good agreement with earlier measurements in the region of $x > 0.25$. At lower x, the structure function ratio exhibits an enhancement of $\approx 5\%$.

Several muon and electron scattering experiments at CERN and SLAC have investigated the effect that a nucleon embedded in a nucleus has a quark distribution different from that of a free nucleon. In deep inelastic scattering, the "EMC effect" is studied by comparing the nucleon structure function $F_2^A(x)$ measured on a heavy nucleus of mass A to the deuterium structure function $F_2^{D_2}(x)$, where x is the Bjorken scaling variable. While all experiments agree on the pattern of the nuclear effect in the valence-quark region $x > 0.3$, namely a softening of the structure function when measured on a heavy target, the experimental situation in the low-x region is controversial. The EM Collaboration. in their original

[1] Present address: Digital Equipment, I-10125 Turin, Italy.
[2] On leave from Institute of Physics, CSAV, CS-18040 Prague, Czechoslovakia.
[3] On leave from the Institut für Hochenergiephysik der AdW der DDR, DDR-1615 Berlin-Zeuthen, GDR.
[4] Present address: INFN, I-34100 Trieste, Italy
[5] On leave from Central Research Institute for Physics, H-1525 Budapest, Hungary.
[6] Present address: Institute of Nuclear Research and Nuclear Energy, Sofia 1784, Bulgaria.
[7] On leave from E. Kardelj University and the J. Stefan Institute, 61111 Ljubljana, Yugoslavia.
[8] Present address: Siemens AG, D-8000 Munich, Germany.
[9] Present address: DPhPE, CEN Saclay, F-91191 Gif-sur-Yvette Cedex, France.
[10] Funded in part by the German Federal Minister for Research and Technology (BMFT) under contract number 054MU12P6.

0370-2693/87/$ 03.50

Volume 189, number 4 PHYSICS LETTERS B 14 May 1987

measurement [1] observed the ratio $F_2^{Fe}(x)/F_2^{D_2}(x)$ to increase linearly towards small x. On the contrary, the SLAC E139 experiment [2] which measured cross section ratios σ^A/σ^D for a variety of nuclei found no significant effect in the region of $x<0.3$, independent of the target mass. An earlier SLAC experiment [3] at small four-momentum transfers $Q^2\approx 1$ GeV^2 had observed an enhancement around $x\simeq 0.15$ and a turnover at very small $x\simeq 0.05$.

In a previous paper [4] we have presented data on the structure function ratios $F_2^A(x)/F_2^{D_2}(x)$ for nitrogen ($A=14$) and iron ($A=56$) measured at a beam energy of 280 GeV. The N_2 data covered the range $0.08\leqslant x\leqslant 0.70$ and exhibited no significant enhancement at small x in agreement with the SLAC E139 data. The Fe data extended over the range $0.20\leqslant x\leqslant 0.70$ only and allowed no conclusion on the behaviour of the effect at low x. In this letter, we report on a new experiment with deuterium and iron targets which was specifically designed to study the ratio $F_2^{Fe}(x)/F_2^{D_2}(x)$ in this kinematic domain with good statistical and systematic accuracy.

The experiment was performed at the CERN SPS muon beam with a high-luminosity spectrometer which is described in detail elsewhere [5]. A schematic view of the experimental set-up is shown in fig. 1. The apparatus consists of a 40 m long magnetized iron toroid which is subdivided into 8 modules and instrumented with scintillation trigger counters and multiwire proportional chambers. The central bores of the first six modules contain target vessels ("internal" targets) filled with liquid deuterium. Two external targets in front of the magnet, followed by a set of MWPC with three-coordinate readout, extend the acceptance of the spectrometer to small angles, i.e., to smaller Q^2 and x than are accessible with the internal targets. For a part of the data taking, the first of the external targets was replaced by a 45 cm long iron target. The data were recorded with a beam of 200 GeV positive muons of 2×10^7 μ/s average intensity. The total beam flux was 17.2×10^{11} μ for the "all D_2" target arrangement and 6.0×10^{11} μ with the iron target installed.

Due to the vertex resolution of the spectrometer, the deuterium data are strongly contaminated by iron events when both target materials are exposed to the beam simultaneously. The deuterium events from this period of data taking are therefore not included

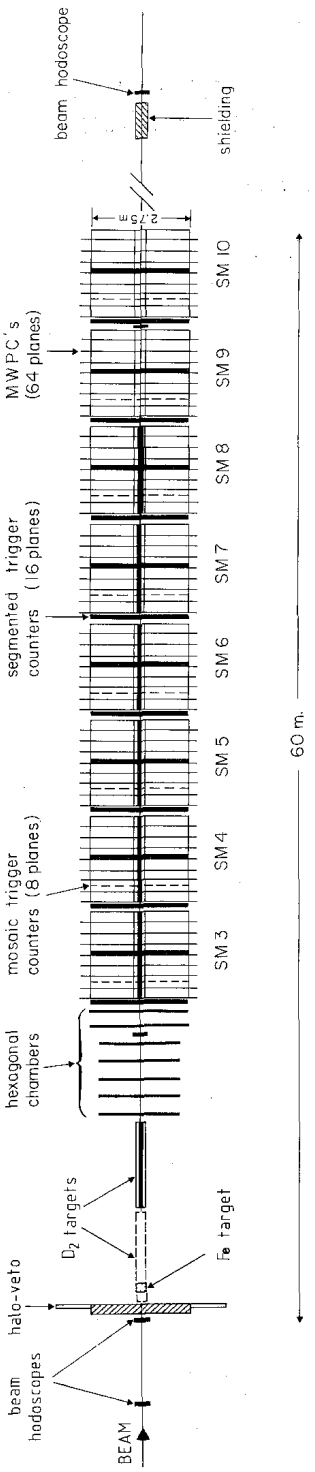

Fig. 1. Schematic view of the apparatus.

Volume 189, number 4 PHYSICS LETTERS B 14 May 1987

in the present analysis. For the second half of the iron data taking the deuterium targets were emptied. The inverse contamination of the iron data by events from the neighbouring D_2 target is much smaller due to the strongly different target densities. This background was determined both by a Monte Carlo study of the vertex resolution and by a direct comparison of the iron samples taken with and without D_2 in the second target. With both methods we find a contamination of 1.3% for which the data are corrected. A background from target wall interactions which amounts to 0.7% for the external and 2.5% for the internal targets is subtracted from the D_2 data.

The structure functions are obtained from the experimental data in a way which is very similar to the one described in ref. [4]. The experimental distributions are converted to cross sections, correcting for acceptance and resolution of the spectrometer by a detailed Monte Carlo simulation of the experiment. To evaluate the structure functions $F_2(x,Q^2)$ we assume a constant value $R=\sigma_L/\sigma_T=0$. Although this is an approximation in the region of small x, it does not affect the F_2 ratio provided that R is independent of atomic mass. The deuterium structure function is computed separately for events from internal and external targets for which the acceptance of the spectrometer is different. In the kinematical region of overlap, the structure functions are in agreement within statistical errors and were combined for the subsequent analysis. The iron data are corrected for the non-isoscalarity of ^{56}Fe assuming a neutron/proton structure function ratio $F_2^n/F_2^p=1-0.75x$. No corrections are applied for the Fermi motion of nucleons inside the nucleus. The results presented here are based on 4.1×10^5 reconstructed events originating from the deuterium and 2.8×10^5 events from the iron targets.

The sources of systematic errors in the F_2 ratio are largely the same as in our earlier experiment [4]. They are mainly due to the resolution of the spectrometer, small uncertainties on the energy loss in the different target materials, hadronic shower punchthrough into the proportional chambers, and the reproducibility of the spectrometer magnetic field settings. The uncertainty from spectrometer resolution is larger than in our previous data because the acceptance of the apparatus for events from the external targets decreases along the beam direction and is therefore different for the two target materials. Errors on the acceptance correction due to this effect were calculated by varying the vertex resolution in the Monte Carlo simulation of the experiment. The uncertainty on the relative luminosity calibration of the Fe and D_2 data is estimated to be 1.5%.

The $F_2^{Fe}/F_2^{D_2}$ ratio is shown as a function of x and Q^2 in fig. 2 and does not exhibit a significant Q^2 dependence. It is therefore averaged over Q^2 and is shown as a function of x in fig. 3 together with our previously published data [4]. Good agreement is observed between the two measurements and the structure function ratio $F_2^{Fe}(x)/F_2^{D_2}(x)$ from the combined data sets is given in table 1.

The results from this and from other charged lepton experiments are shown in fig. 4. The comparison to the EMC iron data [1] shows good agreement for $x>0.15$, apart from a 3% shift in the relative nor-

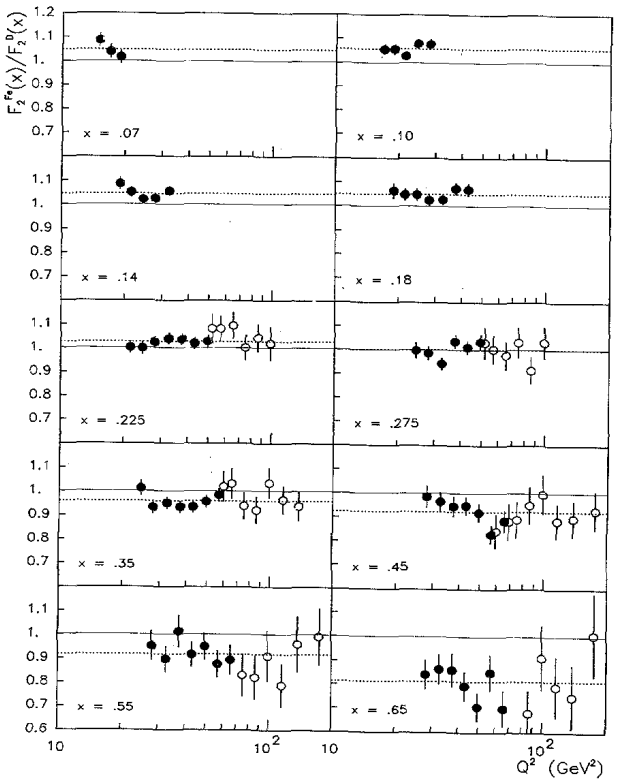

Fig. 2. The structure function ratio $F_2^{Fe}/F_2^{D_2}$ in bins of x and Q^2 from this experiment at 200 GeV beam energy (closed points) and from an earlier experiment at 280 GeV [4] (open points). Only statistical errors are shown. The dotted lines indicate the average over the respective x bin.

Volume 189, number 4 PHYSICS LETTERS B 14 May 1987

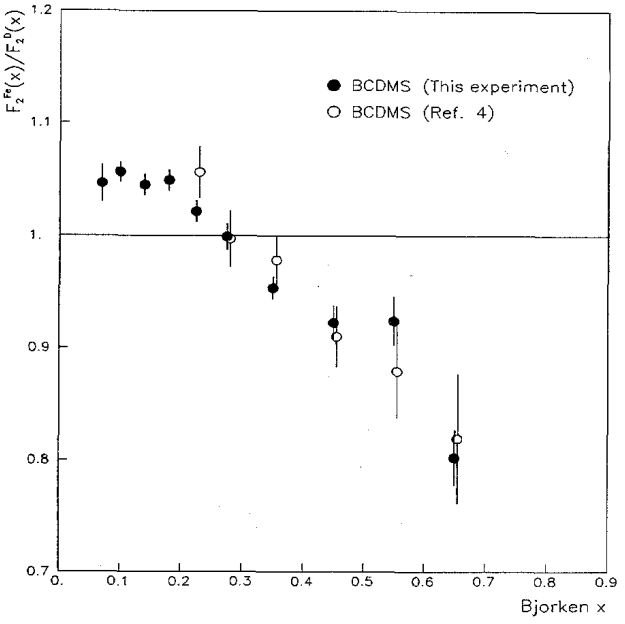

Fig. 3. The structure function ratio $F_2^{Fe}(x)/F_2^{D_2}(x)$ measured in this and in a previous [4] experiment. Only statistical errors are shown.

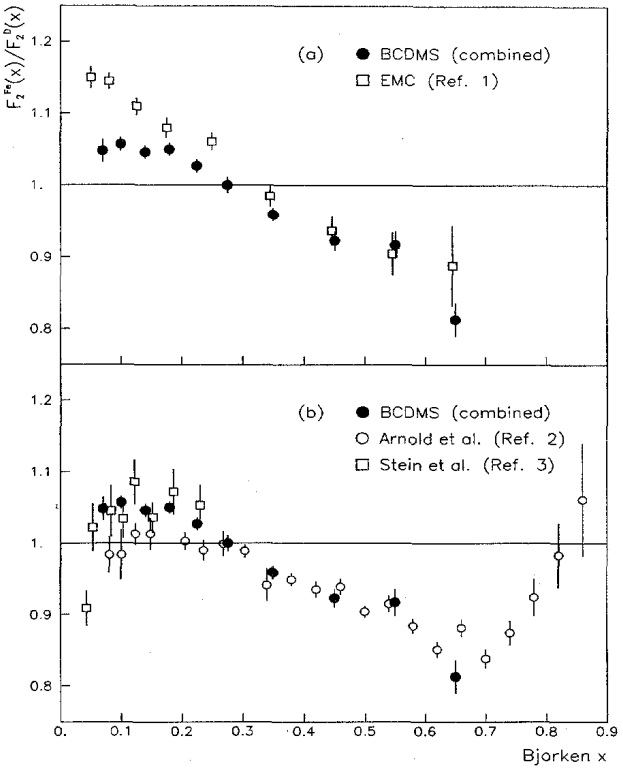

Fig. 4. The structure function ratio $F_2^{Fe}(x)/F_2^{D_2}(x)$ from this and from a previous measurement [4] combined, compared to other muon (a) and electron (b) scattering experiments. The data from ref. [3] were taken with a copper target. Only statistical errors are shown.

malization. For $x<0.15$, the two measurements are marginally compatible within the quoted systematic errors. Preliminary data from the EM Collaboration on a copper target show a less pronounced effect at small x in good agreement with our result [6]. The agreement with the SLAC E139 data [2] is excellent for $x>0.25$ but rather poor at small x. In this region, we observe, however, a very good agreement with the earlier SLAC experiment on a copper target [3] at small $Q^2 \approx 1$ GeV^2.

In summary, we have complemented our earlier measurement of the structure function ratio $F_2^{Fe}(x,Q^2)/F_2^{D_2}(x,Q^2)$ by new data covering the region of small x ($0.06 \leqslant x \leqslant 0.20$) and improving the

Table 1
Results for $R(x)=F_2^{Fe}(x)/F_2^{D_2}(x)$ from this experiment and ref. [4] combined. The systematic errors do not include the 1.5% uncertainty on the relative normalization of Fe and D_2 data.

x	Q^2 range (GeV^2)	$R(x)$	Statistical error	Systematic error
0.07	14– 20	1.048	0.016	0.016
0.10	16– 30	1.057	0.009	0.012
0.14	18– 35	1.046	0.009	0.011
0.18	18– 46	1.050	0.009	0.009
0.225	20–106	1.027	0.009	0.010
0.275	23–106	1.000	0.011	0.010
0.35	23–150	0.959	0.009	0.011
0.45	26–200	0.923	0.013	0.015
0.55	26–200	0.917	0.019	0.021
0.65	26–200	0.813	0.023	0.030

Volume 189, number 4 PHYSICS LETTERS B 14 May 1987

statistical accuracy at larger x. No Q^2 dependence of the nuclear effect is observed over the kinematic range of the experiment. In the region $x>0.25$, we find good agreement with all other charged lepton experiments [1,2,4,6]. For $x<0.25$, we observe an enhancement of the structure function ratio of $4.5\% \pm 0.5\%$ (stat.) $\pm 2.0\%$ (syst.) where the systematic error includes the uncertainty on the relative normalization of iron and deuterium data.

References

[1] EM Collab., J.J. Aubert et al., Phys. Lett. B 123 (1983) 275.
[2] R.G. Arnold et al., Phys. Rev. Lett. 52 (1984) 722, SLAC-PUB-3257.
[3] S. Stein et al., Phys. Rev. D 12 (1975) 1884.
[4] BCDMS Collab., G. Bari et al., Phys. Lett. B 163 (1985) 282.
[5] BCDMS Collab., D. Bollini et al., Nucl. Instrum. Methods 204 (1983) 333;
BCDMS Collab., A.C. Benvenuti et al., Nucl. Instrum. Methods 226 (1984) 330.
[6] P.R. Norton, Proc. XXIII Intern. Conf. on High energy physics (Berkeley, 1986), to be published.

Kapitola 3

Strukturní a distribuční funkce v kovariantním QPM

Partonový model je nepostradatelným nástrojem pro analýzu a interpretaci strukturních funkcí nukleonů, které se měří v experimentech DIS. Tyto funkce lze v současnosti získat pouze z experimentálního měření. Při analýze jsou strukturní funkce uvedeny *modelově závislým způsobem* do vztahu s distribučními funkcemi kvarků, které již obsahují o přítomnosti kvarků v nukleonu přímou a detailní informaci. K měření strukturních funkcí slouží dva typy experimentů:

i) nepolarizovaný DIS

V příslušném experimentálním uspořádání jsou terč i svazek leptonů nepolarizované. Jak jsme ukázali v předchozí části, nepolarizované strukturní funkce nukleonů jsou v současnosti s vysokou přesností zmapovány v široké kinematické oblasti. Analýza těchto dat pomocí obvyklého, tj. *nekovariantního* QPM se započtením korekcí pQCD dává konsistentní obraz nukleonů v jazyce partonových distribučních funkcí (PDF). Široký soubor experimentálních dat je v skvělém souladu s pQCD, což je pozitivní výsledek, který nevyvolává potřebu na metodě analýzy (nekovariantní QPM + pQCD) cokoliv měnit.

ii) polarizovaný DIS

Experimenty tohoto typu jsou metodicky nesrovnatelně náročnější. Vyžadují polarizované terče i svazky, přesnou kontrolu stupně polarizace a možnost měnit její orientaci (podélná/příčná). Z těchto důvodů se polarizované strukturní funkce g_1, g_2 podařilo měřit až později a jejich přesnější hodnoty byly získány až v poměrně nedávné době [31]− [37]. Rovněž kinematická oblast x, Q^2, v níž jsou tyto funkce změřeny, je podstatně menší, než v případě nepolarizovaných funkcí. Je však důležité, že metoda analýzy založená na *nekovariantním* QPM + pQCD se v případě analýzy polarizovaných strukturních funkcí střetává s některými vážnými problémy, o nichž se zmíníme níže.

Dále je tato kapitola členěna následovně. V části 3.1 je popsána konstrukce *kovariantního* QPM. V částech 3.2 a 3.3 následuje detailnější diskuse o rozdílech mezi

nekovariantním a kovariantním QPM. V další části 3.4 je uvedena diskuse o roli orbitálního momentu kvarků v kontextu kovariantního QPM. Diskusi o dalších aspektech kovariantního QPM je věnována část 3.5.

3.1 Konstrukce kovariantního QPM

Obecným základem QPM je předpoklad, že kvarky lze při jejich interakci s procházejícím leptonem považovat za (téměř) volné. Tato podmínka může být splněna pouze při interakcích s velkým přenosem impulsu Q^2 (t.j. při DIS), které se odehrávají v malém prostoročasovém intervalu, kdy pro kvarky platí tzv. asymptotická volnost. Dále předpokládáme, že rozdělení hybností kvarků má v klidovém systému nukleonu rotační symetrii, závisí tedy pouze na absolutní hodnotě hybnosti $|\mathbf{p}|$, nebo na energii p_0, což je ekvivalentní, protože $p_0 = \sqrt{m^2 + \mathbf{p}^2}$. Přítomnost kvarků tedy lze popsat sadou rozdělovacích funkcí $G_k^{\pm}(p_0)d^3p$, které vyjadřují pravděpodobnost, že kvark (index k vyjadřuje *flavour* kvarků a antikvarků) lze nalézt ve stavu

$$u\left(\mathbf{p},\lambda\mathbf{n}\right)=\frac{1}{\sqrt{N}}\left(\begin{array}{c}\phi_{\lambda\mathbf{n}}\\ \frac{\mathbf{p}\sigma}{p_0+m}\phi_{\lambda\mathbf{n}}\end{array}\right);\qquad \frac{1}{2}\mathbf{n}\sigma\phi_{\lambda\mathbf{n}}=\lambda\phi_{\lambda\mathbf{n}},\qquad N=\frac{2p_0}{p_0+m} \tag{3.1}$$

s polarizací $\lambda = \pm 1/2$, $\phi^{\dagger}_{\lambda\mathbf{n}}\phi_{\lambda\mathbf{n}} = 1$ ve směru $\mathbf{n}$, který je určen směrem polarizace nukleonu. Poznamenejme však, že uvedená pravděpodobnostní rozdělení obecně závisí i předávaném čtyřimpulsu Q^2. Jinými slovy, obraz nukleonu závisí na dosaženém rozlišení. Dále nahradíme energii kvarku v klidovém systému nukleonu invariantním výrazem Pp/M a předpokládáme jednofotonovou výměnu. Následný výpočet strukturních funkcí odpovídajících tomuto zjednodušenému obrazu je pak v podstatě již jen technickou úlohou. Vývoj řešení této úlohy pro nepolarizované a polarizované strukturní funkce je dokumentován v pracech [A5]− [A9], viz části 3.1.1–3.1.5. Součástí poslední z nich je i shrnutí jednotlivých kroků a výsledků.

Article copy

PHYSICAL REVIEW D VOLUME 55, NUMBER 7 1 APRIL 1997

Structure functions and parton momenta distribution in the hadron rest system

Petr Závada*
Institute of Physics, Academy of Sciences of Czech Republic, Na Slovance 2, CZ-180 40 Prague 8
(Received 25 September 1996; revised manuscript received 6 December 1996)

The alternative to the standard formulation of the quark-parton model (QPM) in the infinite momentum frame is suggested. The proposed approach does not require any extra assumptions in addition, consistently takes into account the parton transversal momenta, and does not prefer any special reference system. The standard approach is involved as a limiting case. As a result, the modified relations between the structure and distribution functions are obtained together with some constraint on their shape. The comparison with experimental data offers speculation about the values of the effective masses of quarks, which emerge as a free parameter in the approach. [S0556-2821(97)02707-0]

PACS number(s): 13.60.−r, 12.15.Ff, 14.65.−q

I. INTRODUCTION

The deep inelastic scattering (DIS) of leptons on the nucleons and nuclei has been, since the early 1970s a powerful tool for the investigation of the nucleon internal structure and simultaneously has served as a crucial test of the related theory—QCD. For recent results in this field see, e.g., [1] and citations therein.

The quark-parton model (QPM), motivated by the experimental data, is extraordinarily simple if formulated in the reference system in which the nucleon is fast moving [the infinite momentum frame (IMF)]. Namely, in this system the Bjorken scaling variable x_B can be approximately identified with the momentum fraction of the nucleon carried by a parton and experimentally measured structure functions can be easily related to the combinations of distribution functions expressed in terms of x_B. The distribution functions extracted from the experimental data by the global analysis (see, e.g., [13]) relying on QPM+QCD represent basic elements of the present picture of nucleons and other hadrons.

In this paper we attempt to cope with the not only aesthetic drawback of the QPM which in the standard formulation has a good sense only in the *preferred* reference system—the IMF. The idea of alternatives to the QPM postulated in the IMF is not new; the possibility to obtain in some approximation the structure and distribution functions from a definite parton model formulated in the nucleon rest frame has been shown, e.g., in [2,3,5] and recently in [4,6]. We suggest rather a consistent modification of the general standard formulation which does not adhere necessarily to the IMF and simultaneously does not require any special assumptions in addition. The bases of our considerations are only kinematics and mathematics.

The paper is organized as follows. In the following section, the basic kinematic quantities related to the DIS are introduced and particularly the meaning of the variable x_B is discussed. In Sec. III we formally apply the standard assumptions of the QPM to the nucleon in its rest system (lab) and compare the results with those normally related to the IMF. Section IV is devoted to the discussion from a more physical point of view together with a glance at the experimental data on proton structure function F_2. The last section shortly summarizes the possible conclusions.

II. KINEMATICS

First of all let us recall some basic notions used in the description of DIS and the interpretation of the experimental data on the basis of QPM. The process is usually described (see Fig. 1) by the variables

$$q^2 \equiv -Q^2 = (k-k')^2, \quad x_B = \frac{Q^2}{2Pq}. \tag{2.1}$$

As a rule, lepton mass is neglected, i.e., $k^2 = k'^2 = 0$. An important assumption of QPM is that the struck parton remains on-shell, which implies

$$q^2 + 2pq = 0. \tag{2.2}$$

Bjorken scaling variable x_B can be interpreted as the fraction of the nucleon momentum carried by the parton in the IMF. The motivation of this statement can be explained as follows. Let us denote

$$p(\text{lab}) \equiv (p_0, p_1, p_2, p_3), \quad P(\text{lab}) \equiv (M, 0, 0, 0),$$
$$q(\text{lab}) \equiv (q_0, q_1, q_2, q_3), \tag{2.3}$$

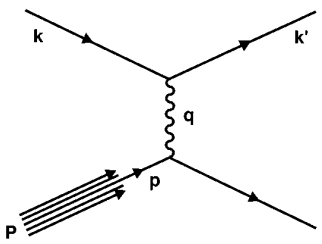

FIG. 1. Diagram describing DIS as a one photon exchange between the charged lepton and parton.

*Electronic address: zavada@fzu.cz

the four-momenta of the parton, nucleon, and exchanged photon in the nucleon rest system (lab). The Lorentz boost to the IMF (in the direction of the collision axis) gives

$$p(\mathrm{inf})\equiv(p_0',p_1',p_2,p_3),\quad P(\mathrm{inf})\equiv(P_0',P_1',0,0),$$
$$q(\mathrm{inf})\equiv(q_0',q_1',q_2,q_3), \tag{2.4}$$

where, for $\beta\to-1$,

$$p_0'=p_1'=\gamma(p_0+p_1),\ \ P_0'=P_1'=\gamma M,\quad \gamma=1/\sqrt{1-\beta^2}. \tag{2.5}$$

If we denote

$$x\equiv\frac{p_0'}{P_0'}=\frac{p_1'}{P_1'}=\frac{p_0+p_1}{M}, \tag{2.6}$$

then one can write

$$p(\mathrm{inf})=xP(\mathrm{inf})+(0,0,p_2,p_3). \tag{2.7}$$

Now let the lepton have initial momentum $k(\mathrm{lab})\equiv(k_0,-k_0,0,0)$. If we denote $\nu\equiv k_0-k_0'$ and $q_L\equiv q_1$, then $q_L<0$ and from Eqs. (2.1), (2.2), it follows

$$x_B=\frac{pq}{Pq}=\frac{p_0\nu+|q_L|p_1}{M\nu}-\frac{\vec{p_T}\vec{q_T}}{M\nu}, \tag{2.8}$$

where $\vec{p_T}$, $\vec{q_T}$ are the parton and photon transversal momenta. Obviously,

$$k'^2=(k-q)^2=k^2+q^2-2k_0\nu+2k_0|q_L|=0,$$
$$\frac{|q_L|}{\nu}=1+\frac{Q^2}{2k_0\nu}=1+\frac{M}{k_0}x_B. \tag{2.9}$$

Using this relation Eq. (2.8) can be modified:

$$x_B=\frac{p_0+p_1}{M}+\frac{p_1}{k_0}x_B-\frac{\vec{p_T}\vec{q_T}}{M\nu}; \tag{2.10}$$

therefore, if the lepton energy is sufficiently high, so $p_1/k_0\approx0$, one can write

$$x_B=x-\frac{p_T\ \ q_T}{M\nu}\cos\varphi, \tag{2.11}$$

where φ is the angle between the parton and photon momenta in the transversal plane.

So, if parton transversal momenta are neglected, x_B really represents the fraction of momentum (2.6). In a higher approximation the experimentally measured x_B, being an integral over φ is effectively smeared with respect to the fraction x—which is not correlated with φ. An estimation of the second term in the last equation can be done as follows. Because

$$q^2=\nu^2-|\vec{q}|^2,\quad \left(\frac{\vec{q}}{\nu}\right)^2=1+\frac{Q^2}{\nu^2}=1+\frac{4M^2}{Q^2}x_B^2, \tag{2.12}$$

then Eqs. (2.9), (2.12) give

$$\frac{q_T}{\nu}=\sqrt{\left(\frac{\vec{q}}{\nu}\right)^2-\left(\frac{q_L}{\nu}\right)^2}=\sqrt{\left(\frac{4M^2}{Q^2}-\frac{M^2}{k_0^2}\right)x_B^2-\frac{2M}{k_0}x_B}$$
$$<\frac{2Mx_B}{\sqrt{Q^2}}; \tag{2.13}$$

therefore, for $M/k_0\approx0$ we obtain

$$\frac{pq}{M\nu}=\frac{p_0+p_1}{M}-\frac{2p_Tx_B}{\sqrt{Q^2}}\cos\varphi \tag{2.14}$$

and

$$x_B=x-\frac{2p_Tx_B}{\sqrt{Q^2}}\cos\varphi. \tag{2.15}$$

Therefore x_B can be at sufficiently high Q^2 considered as a good approximation of x (and vice versa). At the end of the next section, we shall suggest how to treat this correction more accurately.

Let us note, the parameter x [Eq. (2.6)] can be expressed also as

$$x\equiv\frac{p_0+p_1}{P_0+P_1} \tag{2.16}$$

and identified with the light cone variable, which can be expressed also in terms of rapidity and transversal mass:

$$x\equiv\frac{m_T}{M}\exp(y-y_0),\quad m_T\equiv\sqrt{p_T^2+m^2},\quad y\equiv\frac{1}{2}\ln\frac{p_0+p_1}{p_0-p_1}, \tag{2.17}$$

where y_0 denotes the proton rapidity. In this form the parameter x is invariant with respect to any Lorentz boost along the collision axis.

Now, if we assume parton phase space is spherical (in lab) and a rather idealized scenario in which the parton has a mass $m^2=p_0^2-p_1^2-p_2^2-p_3^2$, then further relations can be obtained.

(1) *variable x*. From Eq. (2.6) and the condition $x\leqslant1$, it can be shown that

$$x\geqslant\frac{m^2}{M^2}, \tag{2.18}$$

$$\sqrt{p_1^2+p_2^2+p_3^2}\leqslant p_m\equiv\frac{M^2-m^2}{2M},$$

$$p_T^2\leqslant M^2\left(x-\frac{m^2}{M^2}\right)(1-x). \tag{2.19}$$

Obviously, the highest value of p_1 is reached if $p_T=0$ and

$$x=\frac{\sqrt{p_1^2+m^2}+p_1}{M}=1 \tag{2.20}$$

which gives

$$p_{1\max}=p_m\equiv\frac{M^2-m^2}{2M}. \tag{2.21}$$

Then spherical symmetry implies

$$\sqrt{p_1^2+p_2^2+p_3^2}\leqslant p_m, \tag{2.22}$$

i.e., the first relation in Eq. (2.19) is proved. Apparently, the minimal value of x is reached for $p_1=-p_m$ and $p_T=0$. After inserting Eq. (2.6), one gets Eq. (2.18). Finally, the relation (2.6) implies

$$p_1=\frac{M^2x^2-m^2-p_T^2}{2Mx} \tag{2.23}$$

which, inserted to the modified relation (2.22),

$$p_1^2+p_T^2\leqslant\left(\frac{M^2-m^2}{2M}\right)^2 \tag{2.24}$$

after some computation gives the second relation in Eq. (2.19).

(2) *variable* x_B. Let us express x_B in the lab

$$x_B=\frac{pq}{Pq}=\frac{p_0\nu-\vec{p}\vec{q}}{M\nu}=\frac{1}{M}\left(\sqrt{m^2+|\vec{p}|^2}-\frac{\vec{p}\vec{q}}{\nu}\right) \tag{2.25}$$

and estimate its minimal value. With the use of Eq. (2.12), we obtain

$$x_B\geqslant\frac{1}{M}\left(\sqrt{m^2+p_m^2}-p_m\sqrt{1+\frac{4M^2}{Q^2}x_B^2}\right). \tag{2.26}$$

Since

$$\sqrt{1+\frac{4M^2}{Q^2}x_B^2}\leqslant 1+\frac{2M^2}{Q^2}x_B^2 \tag{2.27}$$

and

$$\frac{1}{M}(\sqrt{m^2+p_m^2}-p_m)=\frac{m^2}{M^2}, \tag{2.28}$$

relation (2.26) can be rewritten

$$x_B\geqslant\frac{m^2}{M^2}-\frac{2Mp_m}{Q^2}x_B^2\geqslant\frac{m^2}{M^2}-\frac{2Mp_m}{Q^2}\frac{m^4}{M^4}$$
$$=\frac{m^2}{M^2}\left(1-\frac{2p_m}{M}\frac{m^2}{Q^2}\right), \tag{2.29}$$

i.e., for $m^2\ll Q^2$ the lower limit of x_B coincides with the limit (2.18).

III. DISTRIBUTION OF PARTONS IN THE NUCLEON REST SYSTEM

In this section we imagine partons as a gas (or a mixture of gases) of quasifree particles filling up the nucleon volume. The prefix *quasi* means that partons bounded inside the nucleon behave at the interaction with an external photon probing the nucleon as free particles having the four-momenta on the mass shell. This is the standard assumption of the QPM, but whereas in the IMF parton masses are ''hidden,'' in the description related to the lab, the masses will be present. In the next section we shall discuss to what extent the results obtained for this idealized picture could be applied for a more realistic scenario.

A. Deconvolution of the distribution function

Let us suppose $F(x)$ is the distribution function of some sort of parton given in terms of variable x [Eq. (2.6)] and these partons are assumed to have the mass m. If the spherical symmetry is assumed in the hadron rest system and $G(p_0)d^3p$ is the number of partons in the element of the phase space, then the distribution function $F(x)$ can be expressed as the convolution

$$F(x)=\int\delta\left(\frac{p_0+p_1}{M}-x\right)G(p_0)d^3p,$$
$$p_0=\sqrt{m^2+p_1^2+p_2^2+p_3^2}. \tag{3.1}$$

Using the set of integral variables h,p_0,φ instead of p_1,p_2,p_3,

$$p_1=h,\quad p_2=\sqrt{p_0^2-m^2-h^2}\sin\varphi,$$
$$p_3=\sqrt{p_0^2-m^2-h^2}\cos\varphi, \tag{3.2}$$

the integral (3.1) can be rewritten

$$F(x)=2\pi\int_m^{E_{\max}}\int_{-H}^{+H}\delta\left(\frac{p_0+h}{M}-x\right)G(p_0)p_0dhdp_0,$$
$$H=\sqrt{p_0^2-m^2}. \tag{3.3}$$

First of all, we calculate the inner integral within limits $\pm H$ depending on p_0. For given x and p_0 there contributes only h, for which

$$p_0+h=Mx, \tag{3.4}$$

but simultaneously h must be inside the limits

$$-\sqrt{p_0^2-m^2}\leqslant h\leqslant\sqrt{p_0^2-m^2} \tag{3.5}$$

which means, that for

$$p_0+\sqrt{p_0^2-m^2}<Mx \tag{3.6}$$

or equivalently for

$$p_0<\xi\equiv\frac{Mx}{2}+\frac{m^2}{2Mx}, \tag{3.7}$$

the considered integral gives zero. For $p_0>\xi$, when both conditions (3.4), (3.5) are compatible for some value h, the integral can be evaluated

$$\int_{-H}^{+H}\delta\left(\frac{p_0+h}{M}-x\right)G(p_0)p_0dh=MG(p_0)p_0. \tag{3.8}$$

Therefore integral (3.3) can be expressed

$$F(x)=2\pi M\int_{\xi}^{E_{\max}}G(p_0)p_0dp_0. \tag{3.9}$$

Let us note, an equation similar to this appears already in [2], but with structure function $F_2(x)$ instead of the distribution one. We shall deal with the F_2 in the next subsection, where it will be shown that the corresponding equation is more complicated. For a comparison, see also [5], where on the place of $G(p_0)$ the statistical distribution characterized by some temperature and chemical potential is used.

Next, from relation (3.7) we can express x as a function ξ:

$$x_{\pm}=\frac{\xi\pm\sqrt{\xi^2-m^2}}{M}. \tag{3.10}$$

Using relations (2.18), (3.7), one can easily check

$$1\geqslant x_+\geqslant\frac{m}{M}\geqslant x_-\geqslant\frac{m^2}{M^2},\quad E_{\max}=\frac{M^2+m^2}{2M}\geqslant\xi\geqslant m. \tag{3.11}$$

First, let us insert x_+ into Eq. (3.9)

$$F\left(\frac{\xi+\sqrt{\xi^2-m^2}}{M}\right)=2\pi M\int_{\xi}^{E_{\max}}G(p_0)p_0dp_0. \tag{3.12}$$

Differentiation in respect to ξ, gives

$$G(\xi)=-\frac{1}{2\pi M^2}F'\left(\frac{\xi+\sqrt{\xi^2-m^2}}{M}\right)\left(\frac{1}{\xi}+\frac{1}{\sqrt{\xi^2-m^2}}\right). \tag{3.13}$$

Now we integrate the density $G(p_0)$ over angular variables obtaining

$$P(p_0)dp_0\equiv\int_{\Omega}G(p_0)d^3p=4\pi G(p_0)p_0\sqrt{p_0^2-m^2}dp_0 \tag{3.14}$$

and after inserting into Eq. (3.13), we get

$$P(p_0)dp_0=-2F'\left(\frac{p_0+\sqrt{p_0^2-m^2}}{M}\right)\frac{p_0+\sqrt{p_0^2-m^2}}{M}\frac{dp_0}{M}. \tag{3.15}$$

Second root x_- gives a very similar result

$$P(p_0)dp_0=+2F'\left(\frac{p_0-\sqrt{p_0^2-m^2}}{M}\right)\frac{p_0-\sqrt{p_0^2-m^2}}{M}\frac{dp_0}{M}. \tag{3.16}$$

From the definition

$$x_{\pm}\equiv\frac{p_0\pm\sqrt{p_0^2-m^2}}{M}, \tag{3.17}$$

the useful relations easily follow:

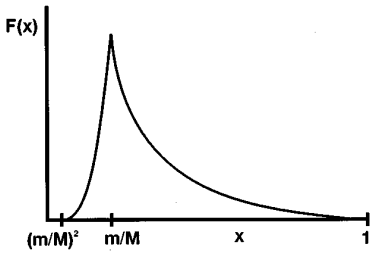

FIG. 2. Example of the function obeying Eqs. (3.23), (3.24).

$$x_+x_-=\frac{m^2}{M^2},\quad x_++x_-=\frac{2p_0}{M},\quad x_+-x_-=\frac{2\sqrt{p_0^2-m^2}}{M}, \tag{3.18}$$

$$\frac{dp_0}{M}=\frac{1}{2}\left(1-\frac{m^2}{M^2x_{\pm}^2}\right)dx_{\pm},\quad \frac{dx_+}{x_+}=-\frac{dx_-}{x_-}. \tag{3.19}$$

Now, Eqs. (3.15), (3.16) can be joined:

$$P(p_0)=\mp\frac{2}{M}F'(x_{\pm})x_{\pm}. \tag{3.20}$$

Why do the two different partial intervals (3.11) of x give independently the complete distribution $P(p_0)$ in Eq. (3.20)? It is due to the fact that, e.g., x_- represents in integral (3.1) the region

$$\frac{\sqrt{p_1^2+p_T^2+m^2}+p_1}{M}=x_-\leqslant\frac{m}{M}, \tag{3.21}$$

given by the paraboloid

$$p_T^2\leqslant 2m|p_1|,\quad p_1\leqslant 0, \tag{3.22}$$

containing complete information about $G(p_0)$ which is spherically symmetric. A similar argument is valid for x_+ representing the rest of sphere. Equations (3.15), (3.16) imply the similarity of $F(x)$ in both intervals,

$$\frac{F'(x_+)x_+}{F'(x_-)x_-}=-1, \tag{3.23}$$

which, with the use of the second relation in Eq. (3.19), can be easily shown to be equivalent to

$$F(x_+)=F(x_-). \tag{3.24}$$

The relation (3.20) implies the distribution function $F(x)$ should be increasing for $(m/M)^2<x<m/M$ and decreasing for $m/M<x<1$, e.g., as shown in Fig. 2. Now let us calculate the following integrals.

The total number N of partons:

$$N=\int_m^{E_{\max}}P(p_0)dp_0$$
$$=-\int_{m/M}^1 F'(x_+)\left(x_+-\frac{m^2}{M^2x_+}\right)dx_+$$
$$=-\int_{m/M}^1 F'(x_+)x_+dx_++\int_{m/M}^1 F'(x_+)x_-dx_+. \tag{3.25}$$

The last integral can be modified with the use of Eqs. (3.19), (3.23):

$$\int_{m/M}^1 F'(x_+)x_-dx_+=-\int_{m/M}^1 F'(x_-)x_-^2\frac{dx_+}{x_+}$$
$$=\int_{m/M}^{m^2/M^2}F'(x_-)x_-dx_-. \tag{3.26}$$

Then integration by parts gives

$$N=-\int_{m^2/M^2}^1 F'(x)xdx=\int_{m^2/M^2}^1 F(x)dx. \tag{3.27}$$

The total energy E of partons:

$$E=\int_m^{E_{\max}}P(p_0)p_0dp_0$$
$$=-\int_{m/M}^1 F'(x_+)\left(x_+-\frac{m^2}{M^2x_+}\right)\frac{M}{2}(x_++x_-)dx_+$$
$$=-\frac{M}{2}\int_{m/M}^1 F'(x_+)(x_+^2-x_-^2)dx_+. \tag{3.28}$$

A similar procedure as for N then gives the result

$$E=-\frac{M}{2}\int_{m^2/M^2}^1 F'(x)x^2dx=M\int_{m^2/M^2}^1 F(x)xdx. \tag{3.29}$$

Therefore, both descriptions based either on the IMF variable x or the parton energy p_0 in the lab give consistent results on the total number of partons and the fraction of energy carried by the partons.

B. The structure function

An important connection between the structure and distribution functions can be derived by a few (equivalent) ways, see, e.g., textbooks [7–9]. In this paper we confine ourself to the electromagnetic unpolarized structure functions assuming spin 1/2. The general form of the cross section for the scattering *electron + proton* and *electron + pointlike Dirac particle* can be written

$$d\sigma(e^-+p)=\frac{e^4}{q^4}\frac{1}{4\sqrt{(kP)^2-m_e^2M^2}}$$
$$\times K^{\alpha\beta}W_{\alpha\beta}4\pi M\frac{d^3k'}{2k_0'(2\pi)^3}, \tag{3.30}$$

$$d\sigma(e^-+l)=\frac{e^4}{q^4}\frac{1}{4\sqrt{(kp)^2-m_e^2m_l^2}}K^{\alpha\beta}L_{\alpha\beta}2\pi$$
$$\times\delta((p+q)^2-m^2)\frac{d^3k'}{2k_0'(2\pi)^3}, \tag{3.31}$$

where the electron tensor has the standard form

$$K^{\alpha\beta}=2\left(k^\alpha k'^\beta+k'^\alpha k^\beta+g^{\alpha\beta}\frac{q^2}{2}\right) \tag{3.32}$$

and the remaining hadron and lepton tensors $W_{\alpha\beta}$, $L_{\alpha\beta}$ can be written in the ''reduced'' shape

$$W_{\alpha\beta}=\frac{P_\alpha P_\beta}{M^2}W_2-g_{\alpha\beta}W_1, \tag{3.33}$$

$$L_{\alpha\beta}=4p_\alpha p_\beta-2g_{\alpha\beta}pq. \tag{3.34}$$

The general assumption that the scattering on the proton is realized via scattering on the partons implies

$$d\sigma(e^-+p)=\int F(\xi)d\sigma(e^-+l)d\xi, \tag{3.35}$$

where $F(\xi)$ is a function describing distribution of partons according to some parameter(s) ξ. Now, if $F(\xi)$ is substituted by the usual distribution function and we assume

$$p_\alpha\approx\xi P_\alpha, \tag{3.36}$$

then it is obvious, that Eq. (3.35) will be satisfied provided that

$$P_\alpha P_\beta\frac{W_2}{M^2}-g_{\alpha\beta}W_1=\frac{1}{M}\int\frac{F(\xi)}{\xi}(2\xi^2P_\alpha P_\beta$$
$$-g_{\alpha\beta}\,\xi Pq)\,\delta((\xi P+q)^2-m^2)d\xi. \tag{3.37}$$

For simplicity in this equation, and anywhere in the following, the weighting by the parton charges is omitted. In fact Eq. (3.37) is just a master equation in [7] [lesson 27, Eq. (27.4)], from which the known relations are derived:

$$2MW_1(q^2,\nu)=\frac{F_2(x)}{x},\quad xF(x)=F_2(x)\equiv\nu W_2(q^2,\nu),$$
$$x\equiv\frac{-q^2}{2M\nu}. \tag{3.38}$$

Here, let us point out, this result is based on the approximation (3.36), which is acceptable in the IMF, but only if *parton transversal momenta are neglected*. Actually, relation (3.36) would be exact only in the (unrealistic) case, when the partons are without any motion inside the nucleon, then the distribution function describes momenta fractions in *any* ref-

erence frame (including the IMF), therefore it also describes the distribution of parton masses $\xi=m/M$.

Before repeating the above procedure for our distribution $G(p_0)d^3p$ in lab, one has to account correctly for the flux factor corresponding to partons moving inside the proton volume. For $k\equiv(k_0,-k_0,0,0)$ the flux factor in Eq. (3.31),

$$4\sqrt{(kp)^2-m_e^2m_l^2}=4k_0(p_0+p_1)=4k_0p_0(1+v_1), \tag{3.39}$$

corresponds for some fixed p to the subset of partons moving with velocity $\vec{v}=\vec{p}/p_0$. If this velocity has the opposite direction to the probing electron, then after passing through the whole subset $G(p_0)d^3p$, the electron has still not reached the backward boundary of the proton, where, meanwhile, the new partons appeared. And on the contrary, if the velocity of the subset has the same direction as the electron, then not all of these partons have the same chance to meet this electron. Namely, the partons close to the backward boundary are excluded from the game sooner than the electron reaches them. Quantitatively, the number of partons limited by the proton volume and having a chance to meet the electron (with velocity ~ 1) will be

$$dN=(1+v_1)G(p_0)d^3p. \tag{3.40}$$

Including this correction to the flux factor (3.39), then instead of Eq. (3.37), we get the tensor equation

$$P_\alpha P_\beta\frac{W_2}{M^2}-g_{\alpha\beta}W_1+A(P_\alpha q_\beta+P_\beta q_\alpha)+Bq_\alpha q_\beta$$
$$=\frac{P_0}{M}\int\frac{G(p_0)}{p_0}(2p_\alpha p_\beta-g_{\alpha\beta}\,pq)\,\delta((p+q)^2-m^2)d^3p,$$
$$p_0=\sqrt{m^2+p_1^2+p_2^2+p_3^2} \tag{3.41}$$

for which Eq. (3.36) *is not required*. The terms with the functions A and B do not contribute to the cross section (since $q_\alpha K^{\alpha\beta}=q_\beta K^{\alpha\beta}=0$), but generally must be included to ensure the equation consistence if the tensors are not gauge invariant. Also let us note, a correction similar to Eq. (3.40) was not used in Eq. (3.37) since due to Eq. (3.36), all the partons in the applied approach have the same velocity as the proton.

Now the contracting of Eq. (3.41) with tensors $g^{\alpha\beta},q^\alpha q^\beta,P^\alpha P^\beta,P^\alpha q^\beta$ gives in the result set of four equations

$$W_2-4W_1+2M\nu(A-xB)=\frac{1}{M\nu}\int\frac{G(p_0)}{p_0}(m^2-2Mx\nu)\,\delta\left(\frac{pq}{M\nu}-x\right)d^3p, \tag{3.42}$$

$$\frac{\nu}{2Mx}W_2+W_1-2M\nu(A-xB)=\frac{1}{M\nu}\int\frac{G(p_0)}{p_0}(Mx\nu)\,\delta\left(\frac{pq}{M\nu}-x\right)d^3p, \tag{3.43}$$

$$W_2-W_1+\nu(2MA+\nu B)=\frac{1}{M\nu}\int\frac{G(p_0)}{p_0}\left(p_0^2-\frac{Mx\nu}{2}\right)\delta\left(\frac{pq}{M\nu}-x\right)d^3p, \tag{3.44}$$

$$W_2-W_1+(M\nu-2M^2x)A-2Mx\nu B=\frac{1}{M\nu}\int\frac{G(p_0)}{p_0}\left(p_0Mx-\frac{Mx\nu}{2}\right)\delta\left(\frac{pq}{M\nu}-x\right)d^3p \tag{3.45}$$

in which the δ function from the integral (3.41) is expressed

$$\delta((p+q)^2-m^2)=\delta(2pq+q^2)=\delta\left(2M\nu\left(\frac{pq}{M\nu}-\frac{Q^2}{2M\nu}\right)\right)=\frac{1}{2M\nu}\delta\left(\frac{pq}{M\nu}-x\right). \tag{3.46}$$

If we define

$$V_j(x)\equiv\int G(p_0)\left(\frac{p_0}{M}\right)^j\delta\left(\frac{pq}{M\nu}-x\right)d^3p,\quad j=-1,0,1, \tag{3.47}$$

then the solution of the set (3.42)–(3.45) reads

$$2MW_1=\frac{\nu}{2Mx+\nu}\left\{V_{-1}(x)\left[x-\frac{M}{\nu}\left(\frac{m^2}{M^2}-x^2\right)-2\frac{m^2x}{\nu^2}\right]+V_0(x)\frac{2Mx}{\nu}+V_1(x)\frac{2M^2x}{\nu^2}\right\}, \tag{3.48}$$

$$\nu W_2=x\left(\frac{\nu}{2Mx+\nu}\right)^2\left\{V_{-1}(x)\left[x-\frac{M}{\nu}\left(\frac{m^2}{M^2}+x^2\right)-2\frac{m^2x}{\nu^2}\right]+V_0(x)\frac{6Mx}{\nu}+V_1(x)\frac{6M^2x}{\nu^2}\right\}, \tag{3.49}$$

$$\nu^2MA=-\left(\frac{\nu}{2Mx+\nu}\right)^2\left\{V_{-1}(x)\left[\frac{1}{2}\left(\frac{m^2}{M^2}+3x^2\right)+\frac{m^2x}{M\nu}\right]-V_0(x)2x\left(1-\frac{Mx}{\nu}\right)-V_1(x)\frac{3Mx}{\nu}\right\}, \tag{3.50}$$

$$\nu^3B=\left(\frac{\nu}{2Mx+\nu}\right)^2\left\{V_{-1}(x)\left[\frac{1}{2}\left(\frac{m^2}{M^2}+3x^2\right)+\frac{m^2x}{M\nu}\right]-V_0(x)3x+V_1(x)\left(1-\frac{Mx}{\nu}\right)\right\}. \tag{3.51}$$

For the next discussion we assume $\nu\gg M$, then

$$\nu W_2\equiv F_2(x)=x^2V_{-1}(x),\quad MW_1\equiv F_1(x)=\frac{x}{2}V_{-1}(x), \tag{3.52}$$

so it is obvious the Callan-Gross relation $2xF_1=F_2$ holds in this approximation.

In the next step, following Eq. (2.14), we accept the approximation

$$\frac{pq}{M\nu}\approx\frac{p_0+p_1}{M} \tag{3.53}$$

then the integrals (3.47) can be expressed

$$V_j(x)=\int G(p_0)\left(\frac{p_0}{M}\right)^j\delta\left(\frac{p_0+p_1}{M}-x\right)d^3p,\quad j=-1,0,1. \tag{3.54}$$

This relation, with the use of Eqs. (3.1), (3.20) implies

$$\left(\frac{p_0}{M}\right)^j P(p_0)=\mp\frac{2}{M}V_j'(x_\pm)x_\pm,\quad j=-1,0,1, \tag{3.55}$$

where $x_\pm$ is defined in Eq. (3.17). The relations (3.55) and (3.18) give

$$\frac{V_j'(x)}{V_k'(x)}=\left(\frac{p_0}{M}\right)^{j-k}=\left(\frac{x_++x_-}{2}\right)^{j-k}=\left(\frac{x}{2}+\frac{x_0^2}{2x}\right)^{j-k},\quad x_0=\frac{m}{M}. \tag{3.56}$$

In the previous section we have shown such functions as Eq. (3.54) obey the relation (3.24), which means in particular, that the functions have a maximum at x_0 and vanish for $x\leqslant x_0^2$. Therefore the same statement is valid also for functions F_2/x^2 and F_1/x from Eq. (3.52):

$$\frac{F_2(x_+)}{x_+^2}=\frac{F_2(x_-)}{x_-^2},\quad \frac{F_1(x_+)}{x_+}=\frac{F_1(x_-)}{x_-}. \tag{3.57}$$

This means that the structure functions of our idealized hadron also have the maximum at x_0 or higher, if the peak of $V_{-1}(x)$ is not rather sharp. Obviously, the peak will be sharp if $P(p_0)\neq 0$ for $p_0=m$. At the same time, it should be kept in mind, that due to Eq. (2.15) any function expressed in ''real'' variable x_B will be slightly smeared in view of this function expressed in x. That is just the case of the integrals (3.47) approximated by Eq. (3.54). But this smearing should be quite negligible for very low x_B and high Q^2, see the end of Sec. II.

Further, our considerations have started to move in the previous section from the distribution function $F(x)$ for which we have obtained relation (3.20). The combination of this equation with Eqs. (3.52), (3.55), and (3.18) gives

$$P(p_0)=-\frac{1}{M}\left(\frac{F_2(x)}{x^2}\right)'(x^2+x_0^2),\quad x=\frac{p_0+\sqrt{p_0^2-m^2}}{M}, \tag{3.58}$$

$$F'(x)=\frac{1}{2}\left(\frac{F_2(x)}{x^2}\right)'\left(x+\frac{x_0^2}{x}\right). \tag{3.59}$$

How do we compare the last equation with the standard relation (3.38) for F and F_2? As we have already stated, the standard approach (3.37) is exact in the case when the partons are static with respect to the nucleon, i.e., when $x=m/M$. Equation (3.41) itself is more exact, but any further procedure with it requires the masses of all the partons in the considered subset being equal. Therefore for a comparison, let us consider first the extreme scenario when the parton distribution functions $F(x)$ and $P(p_0)$ are [see Eq. (3.20)] rather narrowly peaked around the points $x_0=m/M$ and $p_0=m$. Then for $x\approx x_0$ Eq. (3.59) gives

$$F'(x)=\frac{1}{2}\left(\frac{F_2(x)}{x^2}\right)'\left(x+\frac{x_0^2}{x}\right)\simeq\frac{1}{2}\frac{F_2'(x)}{x_0^2}(x_0+x_0)=\frac{F_2'(x)}{x_0} \tag{3.60}$$

from which the second relation (3.38) follows as a limiting case of Eq. (3.59):

$$x_0F(x_0)\approx F_2(x_0). \tag{3.61}$$

Now, in the realistic case when the distribution functions are broad, the exact validity of Eq. (3.37) again requires static partons, therefore the corresponding distribution function also represents a spectrum of masses. But then obviously, the above procedure for a single m can be repeated with spectrum of masses $F(x_0)$ giving in the result instead of Eq. (3.61) the relation

$$\int x_0F(x_0)\,\delta(x-x_0)dx_0=\int F_2(x_0)\,\delta(x-x_0)dx_0, \tag{3.62}$$

which implies

$$xF(x)=F_2(x). \tag{3.63}$$

In this sense the approach based on Eq. (3.37) can be understood as a limiting case of that based on Eq. (3.41).

C. The high-order corrections

The considerations of the previous subsection are based on the approximation (3.53) which in the result gives relations (3.58), (3.59). Actually, we had to calculate integrals (3.47) instead of (3.54) differing in the argument of the δ function according to Eq. (2.14). The integrals (3.47) cannot be solved analytically according to the recipe for Eq. (3.1), however, in principle their solution can be obtained by iterations. For example, Eq. (3.52) reads

$$F_2(x)=x^2\int G(p_0)\frac{M}{p_0}\delta\left(\frac{pq}{M\nu}-x\right)d^3p. \tag{3.64}$$

Let us have some F_2, then the algorithm of iterative procedure could be the following.

0 step: G_0 is given by Eq. (3.58), G is related to P by Eq. (3.14).

1 step: Insert G_0 into Eq. (3.64). The result of the integration is some function $f_1(x)$. Make the difference $\Delta_1F_2=F_2-f_1$ and insert Δ_1F_2 into Eq. (3.58); the relation gives the corresponding correction Δ_1G. The result of this iterative step is $G_1=G_0+\Delta_1G$. Then the next steps will follow by analogy. In the end, the corrected G should be obtained.

A more detailed discussion of the considered correction exceeds the scope of this paper and requires further study. The correction should be rather small, but let us remark that its evaluation requires some assumption about mass m (or the spectrum of masses). Also, let us note that this correction together with terms $O(1/\nu)$ in Eqs. (3.48), (3.49) introduces into the structure functions some Q^2 dependence having

purely kinematic origin (we still assume G being Q^2 independent). Obviously, all these corrections vanish for $Q^2 \to \infty$.

IV. DISCUSSION

Are the considerations suggested in the previous section compatible with the assumptions and philosophy of the QPM? Is it justifiable to speak about the distribution function in lab? First, let us shortly recall the standard interpretation of DIS in the framework of QPM.

In the classical experiment, e.g., BCDMS [10] muons scatter on the proton target at rest in the *laboratory system*. From measured angles and energies of the scattered muons, one determines the invariant cross section as the function of kinematic invariants x_B, Q^2. Next, from this cross section the electromagnetic structure function $F_2(x_B, Q^2)$ is evaluated. The fact that for sufficiently big Q^2, the structure function (approximately) scales $F_2(x_B, Q^2) \approx F_2(x_B)$, leads to the conclusion that in the experiment, the scattering of two *pointlike* particles takes place. This experimental fact is a basic motivation of the QPM in which it is postulated that the nucleon contains pointlike electromagnetically active particles (partons), which can be for sufficiently high Q^2 treated as effectively free and their interaction with the muon is described by the Feynman diagram with one photon exchange. That also means the struck partons remain on the mass shell. These assumptions should be fulfilled first of all in the system, where our experiment is done, i.e., in lab. Of course, another point is, that in this system the picture of partons is in some respect obscured by the fact that we do not know more about the kinematics of partons, their momenta, or energies. The picture is quite clarified when we change over from lab to the IMF. Then the masses of partons do not play any role and the energy is the same as the momentum. Simultaneously, the invariant parameter x_B obtains simple physical sense—the fraction of the proton energy that is carried by the parton. Only now are the quark-parton distribution functions introduced, and one can show their known connection with the structure function.

The difference between this standard approach and ours can be well seen by comparing Eqs. (3.37) and (3.41). The general philosophy according to which the scattering of charged lepton on a nucleon in DIS is realized via scattering on pointlike charged partons is common for both equations. The actual difference is rather only technical consisting in the choice of integration variables and approximations enabling to evaluate the integrals.

The practical consequence of a more simplifying approach based on Eq. (3.37) is that the resulting picture has good sense only in the IMF where also the problem of parton masses is completely separated, which can even be useful.

On the other hand, the approach based on Eq. (3.41), requiring in addition only an assumption about the nucleon spherical symmetry, takes consistently into account, parton transversal momenta and is not confined to some preferred system (even though our results are presented in lab). There is one important consequence, namely in this description the parton masses, or more exactly the ratio m/M appeared as a free parameter.

Any speculation about parton mass already goes beyond

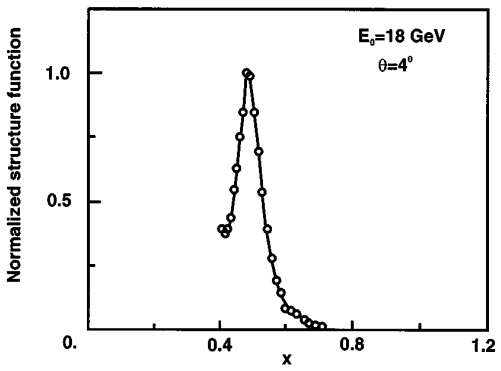

FIG. 3. The structure function for quasielastic $e^- d$ scattering, see text.

the postulates of QPM, nevertheless, look on some experimental data. Before coming to the proton structure function, let us look at Fig. 3, where the ''structure function'' of the deuteron measured in quasielastic $e^- d$ scattering [11] is shown, clearly proving the presence of two nucleons in the nucleus. The similarity with the general picture Fig. 2 is well seen. The kinematics of the two nucleons in the deuteron rest system implies

$$\sqrt{m^2+|\vec{p_1}|^2}+\sqrt{m^2+|\vec{p_2}|^2}=M_D, \quad \vec{p_1}=-\vec{p_2}, \quad (4.1)$$

where m should be understood as some *effective mass* which, due to binding is slightly less than $M_D/2$. This difference roughly corresponds to the depth of the potential if a nonrelativistic approach is used. From Eq. (4.1) the kinematically allowed region for corresponding x easily follows:

$$0.5-\Delta x \leqslant x \leqslant 0.5+\Delta x, \quad \Delta x \equiv \frac{1}{2}\sqrt{1-\left(\frac{2m}{M_D}\right)^2}. \quad (4.2)$$

In the case of partons inside the nucleon, the situation is much more delicate. The interaction among the quarks and gluons is very strong, the partons themselves are mostly in some shortly living virtual state, is it possible to speak about their mass at all? Strictly speaking, probably not. The mass in the exact sense is well defined only for free particles, whereas the partons are never free by definition. Therefore let us try to speak at least about an *effective mass*. By this term we mean the mass that a free parton would have to have to interact with the probing lepton identically as our bounded one. Intuitively, this mass should correlate to Q^2. A lower Q^2 allows more time and space for the struck parton to interact with some others, as a result the energy is transferred to a greater system than the parton itself. On the contrary, the higher Q^2 should mediate interaction with a more ''isolated'' parton.

Now let us confront the formulas from the previous section (with suggested sense of mass m) with the experimental data. In Fig. 4 a recently obtained picture of the proton structure function F_2 [12] is shown. Evidently, this figure does not exhibit any peak corresponding to Eq. (3.57) or Fig. 3. There are two extreme alternatives.

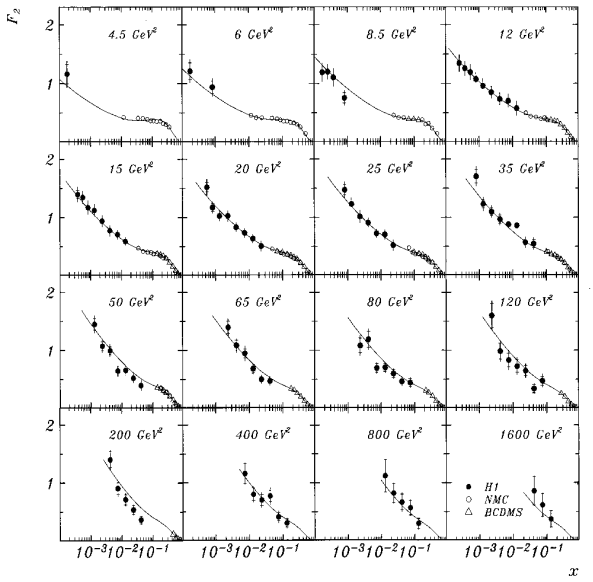

FIG. 4. The structure function $F_2(x,Q^2)$ taken from [12].

(1) The effective mass m/M of quarks can be for given Q^2, well represented by one number. Then, obviously this value should be below the experimental limit of $x \approx 10^{-3}$–10^{-4}.

(2) The concept of effective mass reflects, even for fixed Q^2, some distribution rather than a single value. Then the structure function is some superposition of curves similar to that in Fig. 2 , but with different positions of their maxima. Such superposition could be generated not only by different flavors, but also by the components commonly denoted by the term valence and sea quarks with distribution functions given, e.g., in [13]. We shall not discuss the scenario of effective mass distribution in general, but only check one extreme: the case of static partons mentioned just below Eq. (3.38). These partons exactly obey the equation $p_\alpha = xP_\alpha$. Obviously having measured F_2 from the limit $x \geqslant L$, one can estimate the mean value

$$\frac{\langle m\rangle}{M} < \frac{\int_L^1 xF(x)dx}{\int_L^1 F(x)dx} = \frac{\int_L^1 F_2(x)dx}{\int_L^1 [F_2(x)/x]dx}. \tag{4.3}$$

The numerical calculation with the function fitting the data in Fig. 4,

$$F_2(x,Q^2) = [3.07x^{0.75} + 0.14x^{-0.19}(1-2.93\sqrt{x}) \times (\ln Q^2 - 0.05\ln^2 Q^2)](1-x)^{3.65}, \tag{4.4}$$

gives the value $\langle m\rangle$ in the region of tens MeV depending on L and Q^2 very roughly as

$$\frac{\langle m\rangle}{M} < 1.8\frac{L^{0.34}}{\ln Q^2}, \quad 10^{-4} \leqslant L \leqslant 10^{-2},$$

$$20 \leqslant Q^2 \leqslant 1600 \ \text{GeV}^2. \tag{4.5}$$

Obviously, this scenario is less restrictive than the first one.

It is possible, that the real case is somewhere between the two mentioned extremes. At the same time, the Q^2 dependence in Fig. 4 could be qualitatively understood in the manner suggested above: the higher Q^2 prefers to mediate interactions with partons having less effective mass; therefore, for higher Q^2 the low-x region should be more populated. Apparently, the quantitative expression of this correspondence is a problem of dynamics.

V. SUMMARY

In the present paper we have discussed a connection between the parton distribution functions ordinarily defined in the infinite momentum frame and the analogous functions defined in the hadron rest system. Assuming spherical symmetry of the hadron and an equal effective mass m of all the partons of the considered sort we have shown the following.

(1) There exists unambiguous relation between the distribution functions defined in both reference systems.

(2) The proposed approach taking consistently parton transversal momenta into account gives the relation between the (electromagnetic) structure and the distribution function, somewhat modified in regard of the standard one. However, the standard relation is involved in that of ours as a limiting case. The approach is not connected to any preferred reference system and explicitly involves ratio m/M as a free parameter.

(3) Within our approach in the structure functions, we have identified some rather small, Q^2-dependent terms having purely kinematic origin.

(4) The resulting relations pose the constraint on the shape of structure and distribution functions, which implies, in particular, that the functions have the maximum at $x \approx m/M$ and vanish for $x < m^2/M^2$.

Further, we have compared our results with the data on proton structure function (F_2) assuming the two rather extreme scenarios.

(i) The effective mass is for a fixed Q^2 well represented by one number, then the ratio m/M is below presently reached limit of x (10^{-3}–10^{-4}).

(ii) The effective mass is at given Q^2 represented by some distribution and, moreover, the partons are static. Then the present data suggest the value $\langle m\rangle/M$ should be, at most, of order 10^{-2}.

Simultaneously, the Q^2 dependence of the structure function is qualitatively interpreted as a result of the dynamic correlation of the effective mass and Q^2.

ACKNOWLEDGMENTS

I would like to express my gratitude to J. Pišút for many inspiring discussions which as a result motivated this work. I am also indebted to J. Chýla for a critical reading of the manuscript and valuable comments.

[1] *Proceedings of the International Europhysics Conference on High Energy Physics*, Brussels 1995, edited by J. Lemonne, C. Vander Velde, and F. Verbeure (World Scientific, Singapore, 1996).
[2] J. Franklin, Phys. Rev. D **16**, 21 (1977).
[3] J. Franklin, Nucl. Phys. **B138**, 122 (1978).
[4] J. Franklin and M. Ierano, Report No. TUHE-95-82, hep-ph/9508313 (unpublished).
[5] J. Cleymans and R. L. Thews, Z. Phys. C **37**, 315 (1988).
[6] R. S. Bhalerao, Phys. Lett. B **380**, 1 (1996); **387**, 881(E) (1996).
[7] R. P. Feynman, *Photon-Hadron Interactions* (Benjamin, New York, 1972).
[8] F. E. Close, *An Introduction to Quarks and Partons* (Academic, New York, 1979).
[9] I. J. R. Aitchison and A. J. G. Hey, *Gauge Theories in Particle Physics*, 2nd ed. (Adam Hilger, Bristol, 1989).
[10] BCDMS Collaboration, A. C. Benvenuti *et al.*, Phys. Lett. B **223**, 485 (1989).
[11] W. B. Attwood, in *Proceedings of the 1979 SLAC Summer Institute on Particle Physics* (SLAC-224), edited by A. Mosher (SLAC, Stanford, 1980), Vol. 3.
[12] H1 Collaboration, T. Ahmed *et al.* Nucl. Phys. **B439**, 471 (1995).
[13] A. D. Martin, W. J. Stirling, and R. G. Roberts, Phys. Rev. D **50**, 6734 (1994).

Article copy

PHYSICAL REVIEW D VOLUME 56, NUMBER 9 1 NOVEMBER 1997

Proton spin structure in the rest frame

Petr Závada
Institute of Physics, Academy of Sciences of Czech Republic, Na Slovance 2, CZ-180 40 Prague 8, Czech Republic
(Received 15 April 1997)

It is shown that the quark-parton model in the standard infinite momentum approach overestimates the proton spin structure function $g_1(x)$ in comparison with the approach taking consistently into account the internal motion of quarks described by a spherical phase space in the proton rest frame. Particularly, it is shown the first moment of the spin structure function in the latter approach, assuming only the valence quarks contribution to the proton spin, does not contradict the experimental data. [S0556-2821(97)02821-X]

PACS number(s): 13.60.−r, 13.88.+e, 14.65.−q

I. INTRODUCTION

The proton spin problem which has attracted significant attention over the last few years was triggered by the surprising results [1] of the European Muon Collaboration (EMC), which analyzed data on polarized deep inelastic scattering (DIS). Since that time hundreds of papers have been devoted to this topic; for the present status, see, e.g., [2,3] and the comprehensive overview [4].

The essence of the problem is the following. From the very natural assumption that proton spin is created by the composition of the spins of three valence quarks being in an s state, one can estimate the value of the first moment Γ_1^p of the spin structure function $g_1^p(x)$:

$$\Gamma_1^p=\int_0^1 g_1^p(x)dx\simeq 0.17. \tag{1.1}$$

In fact, such a value was well reproduced in the SLAC experiment [5] preceding the EMC. Nevertheless, the EMC, covering also a lower x region, has convincingly shown that the first moment is considerably lower: $\Gamma_1^p=0.126\pm 0.18$. In addition the latter experiments [6,7] gave values compatible with the EMC. Such values can hardly correspond to the concept that proton spin is a simple sum of the valence spins. In fact, a global fit [8] to all available data evaluated at a common Q^2 in a consistent treatment of higher-order pertubative QCD effects suggests that the spin carried by the quarks has a value of less than one-third of the proton spin. So the question is, what is the proton spin made of?

In this paper we discuss the spin structure functions in the approach [9] based on the proton rest frame and make a comparison with the standard approach based on the infinite momentum frame (IMF). We do not attempt to account for all the details important for the complete description of the polarized proton such as, e.g., the constraints resulting from axial vector current operators, but we rather try to isolate the net effect of the oversimplified kinematics in the IMF picture. Since this paper should be read together with [9], for convenience we refer to the equations and figures in the previous paper simply with prefix P, e.g., see Eq. (P3.41).

II. SPIN STRUCTURE FUNCTIONS

In our paper [9] the master equation (P3.41) was based on the standard symmetric tensors (P3.33) and (P3.34) corresponding to the unpolarized DIS. After the introduction of the spin terms into both the tensors [see, e.g., [10], Eqs. (33.9), (33.10)] our spin equation reads

$$\begin{aligned}P_\alpha P_\beta\frac{W_2}{M^2}-g_{\alpha\beta}W_1+i\epsilon_{\alpha\beta\lambda\sigma}q^\lambda\Big[s^\sigma MG_1\\ +(Pqs^\sigma-sqP^\sigma)\frac{G_2}{M}\Big]+A(P_\alpha q_\beta+P_\beta q_\alpha)+Bq_\alpha q_\beta\\ =\frac{P_0}{M}\int\frac{G(p)}{p_0}(2p_\alpha p_\beta-g_{\alpha\beta}\,pq)\,\delta((p+q)^2-m^2)d^3p\\ +\frac{P_0}{M}\int\frac{H(p)}{p_0}i\epsilon_{\alpha\beta\lambda\sigma}q^\lambda mw^\sigma\delta((p+q)^2-m^2)d^3p,\end{aligned} \tag{2.1}$$

where G and H are related to the polarized quark distributions

$$G(p)=\sum_j e_j^2[h_j^\uparrow(p)+h_j^\downarrow(p)], \tag{2.2}$$

$$H(p)=\sum_j e_j^2[h_j^\uparrow(p)-h_j^\downarrow(p)], \tag{2.3}$$

and the spin four-vectors satisfy

$$s_\mu s^\mu=w_\mu w^\mu=-1,\quad s_\mu P^\mu=w_\mu p^\mu=0. \tag{2.4}$$

Equation (2.1) requires, for the spin terms,

$$\begin{aligned}s^\sigma MG_1+(Pqs^\sigma-sqP^\sigma)\frac{G_2}{M}\\ =\frac{m}{2M\nu}\int\frac{H(p)}{p_0}w^\sigma\delta\left(\frac{pq}{M\nu}-x\right)d^3p,\end{aligned} \tag{2.5}$$

where we use for the δ function the relation (P3.46).

Now, to be more definite, let us consider a simple scenario assuming the following.

(1) To the function H in Eq. (2.3) only the valence quarks contribute.

(2) In the proton rest frame the valence quarks are in the s state and their momenta distributions have the same (spherically symmetric) shape for the u and d quarks:

$$h_d(p)=\frac{1}{2}h_u(p)\equiv h(p). \tag{2.6}$$

(3) Both the quarks have the same effective mass $m^2=p^2$ in the sense suggested in [9]. In this way it is assumed that the effective mass of the valence quark is characterized by the one fixed value; by the end of this paper this point will obtain a more realistic form.

(4) All the three quarks contribute to the proton spin equally:

$$h_d^{\uparrow}-h_d^{\downarrow}=\frac{1}{2}(h_u^{\uparrow}-h_u^{\downarrow})\equiv\Delta h(p_0)=\frac{1}{3}h(p_0),$$

$$p_0=\sqrt{m^2+p_1^2+p_2^2+p_3^2}. \tag{2.7}$$

Since the proton and each of the three quarks have spin one half, the spin of two quarks must cancel and the spin of the third gives the proton its spin, so the last equation implies

$$3\int \Delta h(p_0)d^3p=1. \tag{2.8}$$

The combination with Eq. (2.3) gives

$$H(p_0)=2\frac{4}{9}\Delta h(p_0)+\frac{1}{9}\Delta h(p_0)=\Delta h(p_0) \tag{2.9}$$

and

$$\int H(p_0)d^3p=\frac{1}{3}. \tag{2.10}$$

Now, let us assume the proton is polarized in the direction of the collision axis (the coordinate one), then Eq. (2.4) requires, for the proton at rest,

$$s=(0,1,0,0) \tag{2.11}$$

and, for the quark with four-momentum p,

$$w=\left(\frac{p_1}{\sqrt{p_0^2-p_1^2}},\frac{p_0}{\sqrt{p_0^2-p_1^2}},0,0\right). \tag{2.12}$$

The contracting of Eq. (2.5) with P_σ and s_σ (or equivalently, simply taking $\sigma=0,1$) gives the equations

$$q_1G_2=\frac{m}{2M\nu}\int\frac{H(p_0)}{p_0}\frac{p_1}{\sqrt{p_0^2-p_1^2}}\delta\left(\frac{pq}{M\nu}-x\right)d^3p, \tag{2.13}$$

$$MG_1+\nu G_2=\frac{m}{2M\nu}\int\frac{H(p_0)}{p_0}\frac{p_0}{\sqrt{p_0^2-p_1^2}}\delta\left(\frac{pq}{M\nu}-x\right)d^3p. \tag{2.14}$$

In the next step we apply the approximations from Eqs. (P2.9) and (P2.14):

$$q_1\simeq-\nu,\quad \frac{pq}{M\nu}\simeq\frac{p_0+p_1}{M}. \tag{2.15}$$

Let us note that the negative sign in the first relation is connected with the choice of the lepton beam direction on which Eq. (P2.14) is based. The opposite choice should give

$$q_1\simeq+\nu,\quad \frac{pq}{M\nu}\simeq\frac{p_0-p_1}{M} \tag{2.16}$$

and one can check that both alternatives result in the equal pairs G_1,G_2, which read

$$2g_1(x)\equiv 2M^2\nu G_1=m\int\frac{H(p_0)}{p_0}\frac{p_0+p_1}{\sqrt{p_0^2-p_1^2}}\times\delta\left(\frac{p_0+p_1}{M}-x\right)d^3p, \tag{2.17}$$

$$2g_2(x)\equiv 2M\nu^2G_2=-m\int\frac{H(p_0)}{p_0}\frac{p_1}{\sqrt{p_0^2-p_1^2}}\times\delta\left(\frac{p_0+p_1}{M}-x\right)d^3p. \tag{2.18}$$

Let us remark that the integration of Eqs. (2.13) and (2.18) over x gives on the right-hand side (RHS) the integral

$$\int\frac{H(p_0)}{p_0}\frac{p_1}{\sqrt{p_0^2-p_1^2}}d^3p=0, \tag{2.19}$$

which is zero due to spherical symmetry. Therefore in this approach the first moment of $g_2(x)$ is zero as well. In the following we shall pay attention particularly to the function g_1, which can be rewritten

$$2g_1(x)=\frac{x_0}{3}\int h(p_0)\frac{M}{p_0}\sqrt{\frac{p_0+p_1}{p_0-p_1}}\delta\left(\frac{p_0+p_1}{M}-x\right)d^3p,$$

$$x_0=\frac{m}{M}. \tag{2.20}$$

What do our assumptions (1)–(4) mean in the language of the standard IMF approach? In [9] (end of Sec. III B) we showed that our approach is equivalent to the standard one for the static quarks described by the distribution function $h(p_0)$ sharply peaked around m. In such a case the last equation for $p_0\approx m$, $p_1\approx 0$ after combining with Eqs. (2.3) and (P3.1) gives

$$2g_1(x)=\int\sum_j e_j^2[h_j^{\uparrow}(p_0)-h_j^{\downarrow}(p_0)]\delta\left(\frac{p_0+p_1}{M}-x\right)d^3p$$

$$=\sum_j e_j^2[f_j^{\uparrow}(x)-f_j^{\downarrow}(x)], \tag{2.21}$$

where $f_j(x)$'s are corresponding distribution functions in the IMF, so in this limiting case our spin equation (2.20) is also identical to the standard one, see Eq. (33.14) in [10]. On the other hand, the last equation can be, in our simplified scenario, rewritten as

$$2g_1(x)=\frac{1}{3}\int h(p_0)\,\delta\!\left(\frac{p_0+p_1}{M}-x\right)d^3p=\frac{1}{3}f(x)=\frac{F_{2\mathrm{val}}(x)}{3x}. \tag{2.22}$$

This relation could be roughly expected in the standard IMF approach and correspondingly

$$\Gamma_{\mathrm{IMF}}\equiv\int g_1(x)dx=\frac{1}{6}\int f(x)dx=\frac{1}{6}. \tag{2.23}$$

Equations (2.20) and (2.22) are equivalent for the static quarks, but how do they differ for the nonstatic ones? In accordance with Eq. (P3.54) let us denote

$$V_j(x)\equiv\int h(p_0)\left(\frac{p_0}{M}\right)^j\delta\!\left(\frac{p_0+p_1}{M}-x\right)d^3p, \tag{2.24}$$

then Eqs. (P3.52) and (2.22) give

$$2g_1(x)=\frac{xV_{-1}(x)}{3},\quad \Gamma_{\mathrm{IMF}}=\frac{1}{6}\int xV_{-1}(x)dx. \tag{2.25}$$

Now, let us calculate the corresponding integral from our rest frame equation (2.20):

$$\Gamma_{\mathrm{lab}}=\frac{x_0}{6}\int\int h(p_0)\frac{M}{p_0}\sqrt{\frac{p_0+p_1}{p_0-p_1}}\,\delta\!\left(\frac{p_0+p_1}{M}-x\right)d^3p\,dx. \tag{2.26}$$

Due to the δ function, the square root term in the integral can be rewritten as

$$\sqrt{\frac{p_0+p_1}{p_0-p_1}}=\sqrt{\frac{Mx}{2p_0-Mx}}=\sqrt{\frac{Mx}{2p_0}}\left(1-\frac{Mx}{2p_0}\right)^{-1/2}$$
$$=\left(\frac{Mx}{2p_0}\right)^{1/2}\sum_{j=0}^{\infty}\binom{-1/2}{j}(-1)^j\left(\frac{Mx}{2p_0}\right)^j \tag{2.27}$$

and using Eq. (2.24) the integral is, correspondingly,

$$\Gamma_{\mathrm{lab}}=\frac{x_0}{6}\int\sum_{j=0}^{\infty}\binom{-1/2}{j}(-1)^jV_{-j-3/2}(x)\left(\frac{x}{2}\right)^{j+1/2}dx. \tag{2.28}$$

The integration by parts combined with the relations (P3.56) gives

$$\int V_{-j-3/2}(x)\left(\frac{x}{2}\right)^{j+1/2}dx$$
$$=\int V'_{-j-3/2}(x)\frac{2(x/2)^{j+3/2}}{j+3/2}dx$$
$$=\int V'_0(x)\left(\frac{x}{2}+\frac{x_0^2}{2x}\right)^{-j-3/2}\frac{2(x/2)^{j+3/2}}{j+3/2}dx$$
$$=\int V'_0(x)\frac{2}{j+3/2}\left(\frac{1}{1+x_0^2/x^2}\right)^{j+3/2}dx$$
$$=\int V_0(x)2\left(\frac{1}{1+x_0^2/x^2}\right)^{j+1/2}\frac{2x_0^2/x^3}{(1+x_0^2/x^2)^2}dx.$$

If we denote $t\equiv x_0^2/x^2$ and $z\equiv 1/(1+t^2)$ then Eq. (2.28) can be rewritten as

$$\Gamma_{\mathrm{lab}}=\frac{1}{6}\int V_0(x)4t^3z^{5/2}\sum_{j=0}^{\infty}\binom{-1/2}{j}(-1)^jz^j dx$$
$$=\frac{1}{6}\int V_0(x)4t^3z^2\sqrt{\frac{z}{1-z}}dx,$$

which implies

$$\Gamma_{\mathrm{lab}}=\frac{1}{6}\int_{x_0^2}^1\frac{4x_0^2/x^2}{(1+x_0^2/x^2)^2}V_0(x)dx. \tag{2.29}$$

Simultaneously, since

$$\int_{x_0^2}^1 V_0(x)dx=-\int_{x_0^2}^1 xV'_0(x)dx=-\int_{x_0^2}^1 xV'_{-1}(x)\left(\frac{x}{2}+\frac{x_0^2}{2x}\right)dx=-\int_{x_0^2}^1 V'_{-1}(x)\left(\frac{x^2}{2}+\frac{x_0^2}{2}\right)dx$$
$$=\int_{x_0^2}^1 V_{-1}(x)x\,dx,$$

the integral (2.25) can be rewritten as

$$\Gamma_{\mathrm{IMF}}=\frac{1}{6}\int_{x_0^2}^1 V_0(x)dx. \tag{2.30}$$

Let us express the last integral as

$$\int_{x_0^2}^1 V_0(x)dx=\int_{x_0^2}^{x_0} V_0(x)dx+\int_{x_0}^1 V_0(x)dx$$

and modify the first integral on the RHS using substitution $y=x_0^2/x$:

$$\int_{x_0^2}^{x_0} V_0(x)dx=\int_{x_0}^1 V_0\left(\frac{x_0^2}{y}\right)\frac{x_0^2}{y^2}dy.$$

Now let us recall the general shape of the functions (2.24) obeying Eq. (P3.24), which implies

$$V_0\left(\frac{x_0^2}{y}\right)=V_0(y),$$

therefore instead of Eq. (2.30) one can write

$$\Gamma_{\mathrm{IMF}}=\frac{1}{6}\int_{x_0}^1 V_0(x)\left(\frac{x^2+x_0^2}{x^2}\right)dx. \tag{2.31}$$

A similar modification of Eq. (2.29) gives

$$\Gamma_{\rm lab}=\frac{1}{6}\int_{x_0}^{1}V_0(x)\left(\frac{4x_0^2}{x^2+x_0^2}\right)dx. \tag{2.32}$$

Obviously, both the integrals are equal for V_0 sharply peaked around $x=x_0$, but generally, for nonstatic quarks,

$$\Gamma_{\rm lab}<\Gamma_{\rm IMF}. \tag{2.33}$$

What can our result (2.33) mean quantitatively for the more realistic scenario? In our discussion in [9] we suggested that the real structure functions could be rather some superposition of our idealized ones based on the single values of the effective mass $x_0=m/M$. This means that all the relations involving the functions $V_j(x)\equiv V_j(x,x_0)$ should be integrated over some distribution of the effective masses $\mu(x_0)$. But first, let us try to guess V_0, at least in the vicinity of x_0, which is important for the integrals (2.31) and (2.32). According to Eq. (P3.20) for $x>x_0$ one can write

$$xV_0'(x)=-\frac{M}{2}P(p_0),\quad p_0=\frac{M}{2}\left(x+\frac{x_0^2}{x}\right). \tag{2.34}$$

Now, for p_0 close to m let us parametrize the energy distribution by

$$P(p_0)=\frac{\alpha\exp(\alpha)}{m}\exp\left(-\alpha\frac{p_0}{m}\right), \tag{2.35}$$

which fulfills the normalization

$$\int_m^\infty P(p_0)dp_0=1. \tag{2.36}$$

Obviously, the distribution (2.35) means that the average quark kinetic energy equals m/α. Inserting Eq. (2.35) into Eq. (2.34) gives

$$V_0'(x)=-\frac{\alpha\exp(\alpha)}{2x_0x}\exp\left(-\frac{\alpha}{2}\left[\frac{x}{x_0}+\frac{x_0}{x}\right]\right). \tag{2.37}$$

Let us note that, for $|y|\ll 1$,

$$(1+y)^a\approx\exp(ay),$$

therefore if we substitute the exponential function in Eq. (2.37) by

$$\exp\left(-\frac{\alpha}{2}\left[\frac{x}{x_0}+\frac{x_0}{x}\right]\right)\sim\left[(1-x)\left(1-\frac{x_0^2}{x}\right)\right]^{\alpha/2x_0}\equiv f(x,x_0),\quad x_0^2\leqslant x\leqslant 1, \tag{2.38}$$

the resulting $V_0(x)$ will coincide with Eq. (2.37) in the vicinity of x_0, but moreover will obey the global kinematical constraint outlined in Fig. (P2). The ratio of integrals (2.32) and (2.31) calculated by parts with the use of Eqs. (2.37) and (2.38) gives

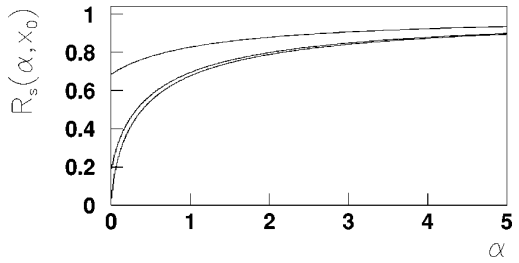

FIG. 1. Ratio R_s plotted for values $x_0=0.2$, 0.02, 0.0002, in order from top to bottom.

$$R_s(\alpha,x_0)\equiv\frac{\Gamma_{\rm lab}}{\Gamma_{\rm IMF}}=\frac{4\int_{x_0}^{1}x_0/x(\arctan[x/x_0]-\pi/4)f(x,x_0)dx}{\int_{x_0}^{1}(1-x_0^2/x^2)f(x,x_0)dx}; \tag{2.39}$$

the results of the numerical computing are plotted in Fig. 1. What do these curves mean? There are the two limiting cases.

(a) The quarks are massive and static, i.e., $\alpha\to\infty$, then $R_s\to 1$. It is the scenario in which both the approaches are equivalent.

(b) Both the quark effective mass and $\alpha\to 0$, but the quark energy $\langle E_{\rm kin}\rangle=m/\alpha>0$, then $R_s\to 0$. This is due to the fact that the massless fermions having a spin orientation always parallel to their momentum cannot contribute to the spin structure function of the system with the spherical phase space.

Obviously, the real case could be somewhere between both the extremes, i.e., α and m should be the finite, positive quantities. The combination of Eqs. (2.39) and (2.23) gives

$$\Gamma_{\rm lab}=\frac{1}{6}R_s(\alpha,x_0). \tag{2.40}$$

The comparison with the experimental value $\Gamma_{\rm exp}\simeq 0.13$ implies $R_s\simeq 0.78$, which according to Fig. 1 corresponds to $\alpha\simeq 2$. Let us note that this result depends on x_0 rather slightly, therefore, irrespective of the unknown distribution of effective masses $\mu(x_0)$ we can conclude the following. If we accept that the quarks have on average (over effective masses distribution) a mean kinetic energy roughly equal to one half of the corresponding effective mass, then within our approach, the experimental value $\Gamma_{\rm exp}$ is compatible with the assumption that the whole proton spin is carried by the valence quarks.

III. SUMMARY AND CONCLUSION

We have calculated the first moment Γ_1 of the proton spin structure function in an approach which takes consistently into account the internal motion of the quarks described by a spherical phase space. Simultaneously, we have done a com-

parison with the corresponding quantity deduced from the standard IMF approach and came to the conclusion that the latter gives a greater value Γ_1. This difference is due to the fact that the standard approach is based on the approximation (P3.36), which effectively suppresses the internal motion of quarks. On the other hand, in our approach, the total quark energy is shared between the effective mass and the kinetic energy, and correspondingly, the resulting formula correctly reflects the mass dependence of the structure function: Γ_1 continuously vanishes for massless quarks controlled by a spherical phase space. Let us note that the quark intrinsic motion has been shown to reduce Γ_1 also in some other approaches [11–15].

Finally, we came to the conclusion that our Γ_1 calculated only from the valence quarks contribution is compatible with the experimental data — provided that their kinetic energies are on average roughly equal to one half of their effective mass. The application of the constraints due to axial vector current operators on the spin contribution from different flavors can somewhat change the parameter α to achieve an agreement with the data. This question is being studied and will be discussed in a separate paper.

The corrections on Γ_1 suggested in this paper together with the corrections on the distribution functions (P3.59) should be taken into account for the interpretation of experimental data. At the same time it is obvious that the distribution of effective masses $\mu(x_0)$ is a quantity requiring further study.

ACKNOWLEDGMENTS

This work was supported by Grant Agency of the Czech Republic, Grant No. 202/95/0217.

[1] EMC Collaboration, J. Ashman *et al.*, Nucl. Phys. **B238**, 1 (1990); Phys. Lett. B **206**, 364 (1988).

[2] *Proceedings of the 12th International Symposium on High-Energy Spin Physics — SPIN96*, Amsterdam, The Netherlands, 1996 (World Scientific, Singapore, 1996).

[3] *Proceedings of the Workshop on Deep Inelastic Scattering and Related Phenomena — DIS96*, Rome, Italy, 1996, edited by G. D'Agostini and A. Nigro (World Scientific, Singapore, 1997).

[4] Hai-Yang Cheng, Int. J. Mod. Phys. A **11**, 5109 (1996).

[5] SLAC-E130 Collaboration, G. Baum *et al.*, Phys. Rev. Lett. **51**, 1135 (1983).

[6] SMC Collaboration, D. Adams *et al.*, Phys. Lett. B **329**, 399 (1994); **339**, 332(E) (1994).

[7] SLAC-E143 Collaboration, K. Abe *et al.*, Phys. Rev. Lett. **75**, 25 (1995).

[8] J. Ellis and M. Karliner, Phys. Lett. B **341**, 397 (1995).

[9] P. Zavada, Phys. Rev. D **55**, 4290 (1997).

[10] R. P. Feynman, *Photon-Hadron Interactions* (Benjamin, New York, 1972).

[11] Bo-Xiang Ma, J. Phys. G **17**, L53 (1991).

[12] Bo-Xiang Ma and Qi-Ren Zhang, Z. Phys. C **58**, 479 (1993).

[13] Bo-Xiang Ma, Phys. Lett. B **375**, 320 (1996).

[14] Bo-Xiang Ma, in *Proceedings of the 3rd Workshop on Diquarks*, Torino, Italy, 1996, edited by M. Anselmino and E. Predazzi (World Scientific, Singapore, in press).

[15] Liang Zuo-tang and R. Rittel, Mod. Phys. Lett. A **12**, 827 (1997).

Article copy

PHYSICAL REVIEW D, VOLUME 65, 054040

Spin structure functions and intrinsic motion of the constituents

Petr Závada*
Institute of Physics, Academy of Sciences of the Czech Republic, Na Slovance 2, CZ-182 21 Prague 8, Czech Republic
(Received 21 June 2001; published 20 February 2002)

The spin structure functions of the system of quasifree fermions on mass shell are studied in a consistently covariant approach. A comparison with the basic formulas following from the quark-parton model reveals the importance of the fermion motion inside the target for the correct evaluation of the spin structure functions. In particular it is shown that, regarding the moment Γ_1, both the approaches are equivalent for the static fermions but differ by a factor 1/3 in the limit of massles fermions ($m \ll p_0$, in the target rest frame). Some other sum rules are discussed as well.

DOI: 10.1103/PhysRevD.65.054040 PACS number(s): 13.60.−r, 13.88.+e, 14.65.−q

I. INTRODUCTION

Measuring the nucleon spin structure functions represents an important tool not only for better understanding of the nucleon internal structure in the language of the QCD, but also for better understanding of QCD itself. These functions contain information which is a crucial complement to the structure functions obtained in the unpolarized deep inelastic scattering (DIS) experiments.

The polarized experiments are more complex and difficult than the unpolarized ones; nevertheless the past decade has brought remarkable results also for the nucleon spin functions from the experiments at CERN [European Muon Collaboration (EMC), Spin Muon Collaboration (SMC)] and SLAC (E142,E143,E154,E155). And the new experiments are running (HERMES) or are under preparation (COMPASS). The data on polarized pp collisions are expected from the BNL Relativistic Heavy Ion Collider (RHIC). For the present status of the research in structure functions see, e.g. [1], the overview [2] and citation therein. The more formal aspects of the polarized DIS are explained in [3].

Also the interpretation and understanding of polarized structure functions seem to be more difficult. For example, until now it has not been well understood why the integral of the proton spin structure function g_1 is substantially less than expected from the very natural assumption that the nucleon spin is generated by the valence quarks. Presently, there is a tendency to explain the missing part of the nucleon spin as a contribution of the gluons. It has been also suggested that the quark orbital momentum can play some role as well [4–6].

The spin in general is a very delicate quantity, which requires correspondingly precise treatment. It has been argued, that for correct evaluation the quark contribution to the nucleon spin it is necessary to take properly into account the intrinsic quark motion [4–13]. The necessity of the covariant formulation of the quark-parton model (QPM) for the spin functions has been pointed out in [14]. These requirements are not satisfied in the standard formulation of the QPM, which is currently used for analysis and interpretation of the experimental data.

In this paper we shall attempt to demonstrate the role of the intrinsic motion for the spin structure functions, using a very simple model of the system quasifree fermions on mass shell. The basic requirement is consistently covariant formulation of the task for the system of fermions, which are not static, being characterized by some momenta distribution in the frame of their center of mass. The spin structure functions of such system are obtained in Sec. II and the sum rules following from these functions are shown in Sec. III. In Sec. IV a comparison with the formulas of the standard QPM is done. The last section is devoted to a short summary.

II. SPIN STRUCTURE FUNCTIONS IN COVARIANT APPROACH

Let us imagine a system of three quasifree charged fermions with the spin 1/2 and mass m, for which the following conditions are satisfied.

(1) The distribution of fermion momenta in the frame of their center of mass is described by some spherically symmetric function G:

$$\int G(p_0)d^3p=3; \quad p_0=\sqrt{m^2+\mathbf{p}^2}. \tag{1}$$

The free fermion states are described by the spinors

$$\psi_{p,\lambda}(x)=\frac{1}{\sqrt{\Omega}}u(p,\lambda)\exp(-ipx);$$

$$\int_\Omega \psi^\dagger_{p,\lambda}(x)\psi_{p,\lambda}(x)d^3x=1, \tag{2}$$

where Ω is the normalization volume and

$$u(p,\lambda)=\frac{1}{\sqrt{N}}\begin{pmatrix}\phi_\lambda\\ \dfrac{\mathbf{p}\sigma}{p_0+m}\phi_\lambda\end{pmatrix}; \quad N=\frac{2p_0}{p_0+m}, \quad \phi^\dagger_\lambda\phi_\lambda=1. \tag{3}$$

We assume

$$\frac{1}{2}\mathbf{n}\sigma\phi_\lambda=\lambda\phi_\lambda; \quad \lambda=\pm\frac{1}{2}, \tag{4}$$

*Email address: zavada@fzu.cz

which means that the spin projection of the fermion in its rest frame is $\pm 1/2$ in the given direction $\mathbf{n}; |\mathbf{n}|=1$.

(2) By $G_{\pm 1/2}$ we denote function, which measures the probability that the fermion is in the state $\psi_{p,\pm 1/2}$, so that

$$G(p_0)=G_{+1/2}(p_0)+G_{-1/2}(p_0) \tag{5}$$

and we assume

$$\int \Delta G(p_0)d^3p=1; \quad \Delta G(p_0)\equiv G_{+1/2}(p_0)-G_{-1/2}(p_0). \tag{6}$$

The difference ΔG consists of the corresponding contributions Δh_j from the three fermions:

$$\Delta G(p_0)=\sum_{k=1}^{3}\Delta h_k(p_0);$$

$$\Delta h_k(p_0)\equiv h_{k,+1/2}(p_0)-h_{k,-1/2}(p_0). \tag{7}$$

Later on, we shall need also the distribution

$$H(p_0)\equiv\sum_{k=1}^{3} e_k^2\Delta h_k(p_0), \tag{8}$$

where e_k are the fermion charges.

What is the resulting spin (total angular momentum) related to the whole system? Let us calculate the integral of the matrix elements

$$\langle \mathbf{nj}\rangle=\int\int_{\Omega}\sum_{\lambda} G_\lambda(p_0)(\psi^\dagger_{p,\lambda}(x)\mathbf{nj}\psi_{p,\lambda}(x))d^3xd^3p, \tag{9}$$

where the angular momentum $\mathbf{j}$ consists of the spin and orbital part

$$j_k=\Sigma_k+l_k=\frac{1}{2}\begin{pmatrix}\sigma_k & 0\\ 0 & \sigma_k\end{pmatrix}-i\varepsilon_{klm}p_l\frac{\partial}{\partial p_m}. \tag{10}$$

Since the total angular momentum $\mathbf{j}$ is a conserving quantity, which commutes with the term $\mathbf{p}\sigma$, a simple calculation gives

$$\psi^\dagger_{p,\lambda}(x)\mathbf{nj}\psi_{p,\lambda}(x)=\frac{1}{\Omega}(\lambda+\varepsilon_{klm}n_kp_lx_m). \tag{11}$$

So, after inserting to Eq. (9) and using the assumption (6) one gets

$$\begin{aligned}\langle \mathbf{nj}\rangle&=\frac{1}{\Omega}\int\int_{\Omega}[(G_{+1/2}(p_0)-G_{-1/2}(p_0))/2\\ &\quad+G(p_0)\varepsilon_{klm}n_kp_lx_m]d^3xd^3p\\ &=\frac{1}{2}\int\Delta G(p_0)d^3p=\frac{1}{2},\end{aligned} \tag{12}$$

since the term $\varepsilon_{klm}n_kp_lx_m$, due to spheric symmetry, vanishes. One can check, if $\mathbf{n}',\mathbf{n}''$ are vectors, which together with $\mathbf{n}$ generate an orthonormal base in the frame of center of mass of the three fermions, then a similar calculation gives

$$\langle \mathbf{n}'\mathbf{j}\rangle=\langle \mathbf{n}''\mathbf{j}\rangle=0. \tag{13}$$

Obviously, the simplest way is to use the base like

$$\mathbf{n}=(0,0,1), \quad \mathbf{n}'=(0,1,0), \quad \mathbf{n}''=(1,0,0). \tag{14}$$

Since we work with the probabilistic description (in terms of quantum mechanics with the statistical mixture of states) by means of the distributions G_λ, as a result we can obtain only the mean values of the total spin projections $\langle \mathbf{J}\rangle=(0,0,1/2)$. Nevertheless one could consider a more rigorous (but more complicated) approach, in which the three fermion system is not constructed as the statistical mixture of plane waves, but as the composition of the three pure states $j=1/2$, $j_z=\pm 1/2$ with the condition, that the whole system represents a pure state $J=1/2$, $J_z=1/2$. These states are represented by the relativistic spheric waves (spinors), which imply the corresponding probabilistic distributions G, G_λ, ΔG and H have spheric symmetry. In other words, if in our approach we assume the system in a pure state $J=1/2$, then its probabilistic description in terms of the plane waves will be defined by the distributions G_λ, which are spherically symmetric. In fact, that is the reason why we require spheric symmetry; deformed distributions G_λ would contradict the eigenstate $J=1/2$.

Let us point out, in the relativistic case, having one fermion state with definite projection $\mathbf{nj}$ of the total angular momentum, one cannot separate its orbital and spin part (with exception of the special case when $\mathbf{n}\|\pm\mathbf{p}$), i.e., account with the fermion orbital momentum is crucial for a consistent calculation of the resulting spin. On the other hand, a similar calculation, in which the orbital part l is ignored, gives

$$\begin{aligned}&\psi^\dagger_{p,\lambda}(x)\mathbf{n\Sigma}\psi_{p,\lambda}(x)\\ &\quad=\frac{1}{\Omega N}\left(\lambda\phi^\dagger_\lambda\phi_\lambda+\phi^\dagger_\lambda\frac{\mathbf{p}\sigma\cdot\mathbf{n}\sigma\cdot\mathbf{p}\sigma}{2(p_0+m)^2}\phi_\lambda\right)\\ &\quad=\frac{1}{\Omega N}\left(\lambda+\phi^\dagger_\lambda\frac{\mathbf{p}\sigma\cdot(-\mathbf{p}\sigma\cdot\mathbf{n}\sigma+2\mathbf{pn})}{2(p_0+m)^2}\phi_\lambda\right)\\ &\quad=\frac{1}{\Omega N}\left(\lambda-\lambda\frac{\mathbf{p}^2}{(p_0+m)^2}+\phi^\dagger_\lambda\frac{\mathbf{p}\sigma\cdot\mathbf{pn}}{(p_0+m)^2}\phi_\lambda\right).\end{aligned}$$

Since

$$\mathbf{p}\sigma\cdot\mathbf{pn}=\sum_{i=1}^{3}p_i^2\sigma_in_i+\sum_{j\neq i}p_ip_j\sigma_in_j \tag{15}$$

one can write

$$\langle \mathbf{n\Sigma}\rangle=\int\int_{\Omega}\sum_{\lambda} G_\lambda(p_0)(\psi^\dagger_{p,\lambda}(x)\mathbf{n\Sigma}\psi_{p,\lambda}(x))d^3xd^3p$$

$$= \int \sum_{\lambda} G_{\lambda}(p_0)\frac{\lambda}{N}\left(1-\frac{\mathbf{p}^2}{(p_0+m)^2} + \frac{2\mathbf{p}^2}{3(p_0+m)^2}\right)d^3p,$$

where inserting the formula (15), we take into account that due to spheric symmetry the terms $p_i p_j$ $(j\neq i)$ vanish and the terms p_i^2 can be substituted by $\mathbf{p}^2/3$. The last relation can be further simplified:

$$\langle \mathbf{n\Sigma}\rangle = \frac{1}{2}\int \Delta G(p_0)\left(\frac{1}{3}+\frac{2m}{3p_0}\right)d^3p \leqslant \frac{1}{2}. \tag{16}$$

One can observe that the correspondence with Eq. (12) takes place only for the system of *static* fermions.

For further consideration, it will be useful to substitute the vector **n**, representing the direction of the fermion polarization, by the corresponding covariant polarization vector $w^{\sigma}(\lambda)$, which satisfies

$$w^2(\lambda)=-1, \quad w(\lambda)\cdot p=0 \tag{17}$$

and

$$w(\lambda)=\frac{\lambda}{|\lambda|}(0,\mathbf{n}); \quad \lambda=\pm\frac{1}{2} \tag{18}$$

in the fermion rest frame. The explicit representation of the vectors $w(\lambda)$ will be defined hereafter.

Now, let us expose this system as a (fixed) target to the beam of polarized electrons (e.g., $helicity=+1/2$) coming with the momentum

$$k=(k_0,\sqrt{k_0^2-m_e^2},0,0) \tag{19}$$

and let us calculate the form of corresponding differential cross section. The spin dependent part of the cross section for interaction with a single fermion in one photon approximation has the form

$$d\sigma \sim -L^{\alpha\beta(A)}(q,s)T^{(A)}_{\alpha\beta}. \tag{20}$$

The antisymmetric tensor $L^{\alpha\beta(A)}$ (see e.g. [3]) related to the electron beam reads

$$L^{\alpha\beta(A)}=m_e\varepsilon_{\alpha\beta\lambda\sigma}s^{\lambda}q^{\sigma}, \tag{21}$$

where m_e is the electron mass, s denotes its polarization vector

$$s=\frac{1}{m_e}(\sqrt{k_0^2-m_e^2},k_0,0,0); \quad s^2=-1, \quad ks=0 \tag{22}$$

and $q=k-k'$ is the photon momentum. The antisymmetric tensor $T^{\alpha\beta(A)}$ related to the single fermion inside the target has a similar form:

$$T^{\alpha\beta(A)}=m\varepsilon_{\alpha\beta\lambda\sigma}q^{\lambda}w^{\sigma}(\lambda), \tag{23}$$

where m and $w(\lambda)$ denote the fermion mass and polarization vector. If one assumes that the electron scattering can be described as the incoherent sum of the interactions with the single plane waves, then the tensor $T^{\alpha\beta(A)}$ reads

$$T^{(A)}_{\alpha\beta}=\varepsilon_{\alpha\beta\lambda\sigma}q^{\lambda}m\int H(p_0)w^{\sigma}\delta((p+q)^2-m^2)\frac{d^3p}{p_0}. \tag{24}$$

Here the charge factors and the two possible signs of w^{σ} are included in the tensor through the distribution (8). By the symbol w^{σ} we mean $w^{\sigma}(\lambda=+1/2)$. Let us remark that this form of the antisymmetric part of the hadronic tensor is very similar to that used in [14]. Further, we can modify the δ-function term:

$$\delta((p+q)^2-m^2)d^3p=\delta(2pq+q^2)d^3p = \frac{1}{2\xi}\delta\left(\frac{pq}{\xi}+\frac{q^2}{2\xi}\right)d^3p, \tag{25}$$

where ξ is an arbitrary constant, which only rescales the integration variable. Now, let us imagine that our target is a part of the greater system, which is at rest with respect to the given reference frame and has the mass M, but at the same time the probing electron interacts only with the three fermions. If we put

$$\xi=Mq_0=M\nu, \tag{26}$$

then in the δ function one can identify the terms known from the formalism of deep inelastic scattering:

$$-\frac{q^2}{2M\nu}=\frac{Q^2}{2M\nu}=x, \tag{27}$$

which is the Bjorken scaling variable; its value can be directly determined using only initial and final momenta of the scattered electron. This variable is in the δ function compensated by the ratio $pq/M\nu$, which after boosting the whole target of mass M to the infinite momentum frame approximately represents ratio of dominating momenta components p'/P' of the fermion and the target.

The explicit form of the polarization vector w can be found as follows. First, let us transform the vector $w=(0,\mathbf{n})$ from the fermion rest frame to the target rest frame. After decomposition of the vector **n** to longitudinal and transversal parts with respect to the momentum fermion **p**, the corresponding Lorentz boost gives

$$(0,\mathbf{n})\rightarrow w=\left(\frac{\mathbf{pn}}{m},\mathbf{n}+\frac{\mathbf{pn}}{m(m+p_0)}\mathbf{p}\right). \tag{28}$$

Second, let us make a Lorentz boost of the whole target with mass M to some another frame, which is defined by the new components of the target momentum

$$(M,0,0,0)\rightarrow P=(P_0,\mathbf{P}); \quad P^2=M^2. \tag{29}$$

Next, if we define the covariant vector S by its components in the target rest frame as

$$S=(0,\mathbf{n}), \tag{30}$$

then the polarization vector w can be written in manifestly covariant form

$$w^\sigma = AP^\sigma + BS^\sigma + Cp^\sigma, \tag{31}$$

where A,B,C are invariant functions (scalars) of the vectors P,S,p. These three functions are fixed by two, the conditions (17) and by the constraint (28), valid in the target rest frame. A simple calculation gives

$$A=-\frac{pS}{pP+mM}, \quad B=1, \quad C=\frac{M}{m}A. \tag{32}$$

So, we have obtained the explicit covariant form of the polarization vector w entering the tensor (24), which can now in accordance with the relations (25)–(27) be rewritten

$$T^{(A)}_{\alpha\beta}=\varepsilon_{\alpha\beta\lambda\sigma}q^\lambda \frac{m}{2Pq}\int H\left(\frac{pP}{M}\right) w^\sigma \delta\left(\frac{pq}{Pq}-x\right)\frac{d^3p}{p_0}, \tag{33}$$

where we use the invariant term Pq instead of $M\nu$ and $H(pP/M)$ instead of $H(p_0)$.

On the other hand, in accordance with the general rule (see e.g. [3]), the antisymmetric tensor $T^{(A)}_{\alpha\beta}$ appearing in the formula for the cross section (20) has the form

$$T^{(A)}_{\alpha\beta}=\varepsilon_{\alpha\beta\lambda\sigma}q^\lambda\left\{MS^\sigma G_1+[(Pq)S^\sigma-(qS)P^\sigma]\frac{G_2}{M}\right\}, \tag{34}$$

where M,P,S represent the target mass, momentum, and spin polarization vector, which satisfies

$$S^2=-1, \quad PS=0. \tag{35}$$

The invariants G_1 and G_2 are the spin structure functions. In the next we shall identify the parameters M,P,S in Eq. (34) with those in the model described above and simultaneously we shall attempt to determine the spin structure functions corresponding to our target. First of all, we modify Eq. (34) by the substitution

$$G_S=MG_1+\frac{Pq}{M}G_2, \quad G_P=\frac{qS}{M}G_2, \tag{36}$$

which gives

$$T^{(A)}_{\alpha\beta}=\varepsilon_{\alpha\beta\lambda\sigma}q^\lambda\{S^\sigma G_S-P^\sigma G_P\}. \tag{37}$$

Comparison with Eq. (33) gives the equation for the structure functions:

$$\varepsilon_{\alpha\beta\lambda\sigma}q^\lambda\{S^\sigma G_S-P^\sigma G_P\} = \varepsilon_{\alpha\beta\lambda\sigma}q^\lambda\frac{m}{2Pq}\int H\left(\frac{pP}{M}\right)w^\sigma\delta\left(\frac{pq}{Pq}-x\right)\frac{d^3p}{p_0}. \tag{38}$$

Because of the antisymmetry of the tensor ε and after inserting from the relation (31) it follows that

$$S^\sigma G_S-P^\sigma G_P=\frac{m}{2Pq}\int H\left(\frac{pP}{M}\right)(AP^\sigma+BS^\sigma+Cp^\sigma) \times\delta\left(\frac{pq}{Pq}-x\right)\frac{d^3p}{p_0}+Dq^\sigma, \tag{39}$$

where D is some scalar function and the functions A,B,C are given by the relations (32). After contracting with P_σ, S_σ and q_σ one gets the equations for unknown functions G_S, G_P and D:

$$-M^2G_P=\frac{m}{2Pq}\int H\left(\frac{pP}{M}\right)(AM^2+C\cdot pP) \times\delta\left(\frac{pq}{Pq}-x\right)\frac{d^3p}{p_0}+D\cdot Pq, \tag{40}$$

$$-G_S=\frac{m}{2Pq}\int H\left(\frac{pP}{M}\right)(-B+C\cdot pS) \times\delta\left(\frac{pq}{Pq}-x\right)\frac{d^3p}{p_0}+D\cdot qS, \tag{41}$$

$$qS\cdot G_S-Pq\cdot G_P=\frac{m}{2Pq}\int H\left(\frac{pP}{M}\right)(A\cdot Pq+B\cdot qS +C\cdot pq)\delta\left(\frac{pq}{Pq}-x\right)\frac{d^3p}{p_0}+Dq^2 \tag{42}$$

and inserting G_P, G_S from the first two equations to the last one gives the condition for D:

$$\frac{m}{2Pq}\int H\left(\frac{pP}{M}\right)(C\cdot pu)\delta\left(\frac{pq}{Pq}-x\right)\frac{d^3p}{p_0}+D\cdot qu=0, \tag{43}$$

where we denote

$$u\equiv q+(qS)S-\frac{(Pq)}{M^2}P.$$

Finally, inserting D from this equation to Eqs. (40),(41) gives with the use of relations (32) the structure functions

$$G_P=\frac{m}{2Pq}\int H\left(\frac{pP}{M}\right)\frac{pS}{pP+mM}\left[1+\frac{1}{mM}\left(pP-\frac{pu}{qu}Pq\right)\right] \times\delta\left(\frac{pq}{Pq}-x\right)\frac{d^3p}{p_0}, \tag{44}$$

$$G_S=\frac{m}{2Pq}\int H\left(\frac{pP}{M}\right)\left[1+\frac{pS}{pP+mM}\frac{M}{m} \times\left(pS-\frac{pu}{qu}qS\right)\right]\delta\left(\frac{pq}{Pq}-x\right)\frac{d^3p}{p_0}. \tag{45}$$

The spin structure functions in the standard notation $g_1 = M\cdot Pq\cdot G_1$, $g_2=(Pq)^2/M\cdot G_2$ can now be obtained from Eqs. (36):

$$g_1=Pq\left(G_S-\frac{Pq}{qS}G_P\right),\quad g_2=\frac{(Pq)^2}{qS}G_P,$$

$$g_1+g_2=PqG_S, \tag{46}$$

where the functions G_S, G_P are given by relations (44),(45). Corresponding integrals, as shown in the Appendix, can be simplified to the form (A14),(A15). Let us remark that resulting functions g_1, g_2, after inserting from the relations (A14),(A15) into Eq. (46), do not depend on the variable qS despite the fact that such terms are present in the starting integrals (44),(45) in a nontrivial way. This is a consequence of spheric symmetry of the distribution H, which as we have suggested, follows from the requirement $J=1/2$.

III. SUM RULES

For the next analysis of the obtained structure functions it is convenient to express the integrals (44),(45) in the target rest frame, where $P=(M,0,0,0)$ and $S=(0,\mathbf{n})$. Detailed calculation is done in the Appendix. Now, let us assume $Q^2 \gg 4M^2x^2$; then

$$\frac{|\mathbf{q}|}{\nu}=\sqrt{1+4M^2x^2/Q^2}\to 1$$

and using the second relation (46) and Eq. (A7) one gets

$$\begin{aligned}\Gamma_2\equiv\int g_2(x)dx&=-\pi\int\int H(p_0)\left(p_1+\frac{p_1^2-p_T^2/2}{p_0+m}\right)\\&\times\delta\left(\frac{p_0+p_1}{M}-x\right)\frac{p_T dp_1 dp_T}{p_0}dx\\&=-\pi\int H(p_0)\left(p_1+\frac{p_1^2-p_T^2/2}{p_0+m}\right)\frac{p_T dp_1 dp_T}{p_0}.\end{aligned} \tag{47}$$

In the last integral, due to spheric symmetry of the distribution H, the terms proportional to p_1 and $p_1^2-p_T^2/2$ vanish, insofar as

$$\Gamma_2=0, \tag{48}$$

which is the known Burkhardt-Cottingham sum rule [15]. Similarly the third relation (46) and Eq. (A8) give

$$\int (g_1(x)+g_2(x))dx=\pi\int H(p_0)\left(m+\frac{p_T^2}{2(p_0+m)}\right)\times\frac{p_T dp_1 dp_T}{p_0}. \tag{49}$$

After the substitution

$$2\pi p_T dp_1 dp_T = d^3p \tag{50}$$

and using relation (48) one gets

$$\Gamma_1\equiv\int g_1(x)dx=\frac{1}{2}\int H(p_0)\left(m+\frac{\mathbf{p}^2}{3(p_0+m)}\right)\frac{d^3p}{p_0}. \tag{51}$$

Simple modification then gives

$$\Gamma_1=\frac{1}{2}\int H(p_0)\left(\frac{1}{3}+\frac{2m}{3p_0}\right)d^3p. \tag{52}$$

More detailed analysis of this result will be done in the next section.

The relations (A7) and (A8) can be used also for the calculation of the higher momenta. Generally, if F is a function defined as

$$F(x)=\int K(p)\,\delta\left(\frac{p_0+p_1}{M}-x\right)d^3p,$$

then

$$\begin{aligned}\int x^nF(x)dx&=\int\int K(p)x^n\delta\left(\frac{p_0+p_1}{M}-x\right)d^3p\,dx\\&=\int\int K(p)\left(\frac{p_0+p_1}{M}\right)^n\\&\times\delta\left(\frac{p_0+p_1}{M}-x\right)d^3p\,dx\\&=\int K(p)\left(\frac{p_0+p_1}{M}\right)^n d^3p.\end{aligned}$$

Application of this rule to Eqs. (A7) and (A8) gives after the substitution (50) and with the use of the second and third relation (46):

$$\int xg_2dx=-\frac{1}{6M}\int H(p_0)\left(p_0-\frac{m^2}{p_0}\right)d^3p, \tag{53}$$

$$\int x(g_1+g_2)dx=\frac{1}{6M}\int H(p_0)(p_0+2m)d^3p. \tag{54}$$

These equalities imply relation

$$\int x(g_1+2g_2)dx=\frac{1}{6M}\int H(p_0)\left(2m+\frac{m^2}{p_0}\right)d^3p, \tag{55}$$

which in the limit of the massless fermions coincides with the Efremov-Leader-Teryaev (ELT) sum rule [16]:

$$\int x(g_1+2g_2)dx=0. \tag{56}$$

IV. DISCUSSION

In the previous sections we have studied the properties of the spin structure functions related to the system of quasifree

fermions on mass shell. This system can be compared with the naive QPM, which is with embedded QCD corrections yet is the basic tool for the analysis and interpretation of polarized and unpolarized deep inelastic scattering data. What is the difference between our approach and the naive QPM, if one speaks about the proton spin structure functions? To simplify this discussion, let us assume:

(1) Spin contribution from the sea of quark-antiquark pairs and gluons can be neglected. Then the three fermions in our approach correspond to the three proton valence quarks. So, in this simplified scenario, the proton spin is generated only by the valence quarks.

(2) In an accordance with the nonrelativistic $SU(6)$ approach the spin contribution of individual valence terms is given as

$$s_u=4/3, \quad s_d=-1/3. \tag{57}$$

Let us point out, in the given context the term valence quarks means nothing else than the three fermions with defined momenta distribution, charge, mass and polarization.

Then according to the naive $SU(6)$ version of the QPM we have

$$g_1(x)=\frac{1}{2}\sum e_j^2\Delta q_j(x)=\frac{1}{2}\left(\left(\frac{2}{3}\right)^2\frac{2}{3}u_{val}(x) -\left(\frac{1}{3}\right)^2\frac{1}{3}d_{val}(x)\right), \tag{58}$$

corresponding to the two quarks with distribution $u_{val}(x)$ and the one with distribution $d_{val}(x)$, which are normalized as

$$\frac{1}{2}\int u_{val}(x)dx=\int d_{val}(x)dx=1. \tag{59}$$

It follows that

$$\Gamma_1=\int g_1(x)dx=\frac{5}{18}\doteq 0.28. \tag{60}$$

This number overestimates more than twice the experimental value. Disagreement is generally interpreted as a contradiction with the assumption that the proton spin is generated only by spins of the valence quarks.

Now let us calculate the Γ_1 in our approach. Let us denote momenta distributions of the valence quarks in the target rest frame by symbols h_u and h_d with the normalization

$$\frac{1}{2}\int h_u(p_0)d^3p=\int h_d(p_0)d^3p=1. \tag{61}$$

These distributions are connected with the $u_{val}(x)$ and $d_{val}(x)$ defined above by the relation

$$q_{val}(x)=\int h_q(p_0)\,\delta\left(\frac{p_0\nu+p_1|\mathbf{q}|}{M\nu}-x\right)d^3p. \tag{62}$$

The charge weighted distribution (8), in an $SU(6)$ picture, reads

$$H(p_0)=\sum e_j^2\Delta h_j(p_0)=\left(\left(\frac{2}{3}\right)^2\frac{2}{3}h_u(p_0)-\left(\frac{1}{3}\right)^2\frac{1}{3}h_d(p_0)\right). \tag{63}$$

Now, for simplicity let us assume the same shape of the distributions for both flavors:

$$\frac{1}{2}h_u(p_0)=h_d(p_0)\equiv h(p_0). \tag{64}$$

Then it follows

$$G(p_0)=3h(p_0), \quad \Delta G(p_0)=h(p_0), \quad H(p_0)=\frac{5}{9}h(p_0) \tag{65}$$

and the relations (16) and (52) can be rewritten:

$$\langle\mathbf{n\Sigma}\rangle=\frac{1}{2}\int h(p_0)\left(\frac{1}{3}+\frac{2m}{3p_0}\right)d^3p, \tag{66}$$

$$\Gamma_1=\frac{5}{18}\int h(p_0)\left(\frac{1}{3}+\frac{2m}{3p_0}\right)d^3p. \tag{67}$$

These relations imply the following.

(a) Because the distribution h has the defined normalization, the corresponding integrals reach their maximum in the limit, when the fermions are static ($p_0=m$). On the other hand in the limit of massless fermions ($m\ll p_0$) these integrals represent only one third of their maximal value. In particular, the Γ_1 satisfies

$$\frac{5}{18}\geqslant\Gamma_1\geqslant\frac{5}{54}. \tag{68}$$

(b) Both the integrals are (up to the factor 5/9) equal. It follows that in the case of nonstatic fermions the Γ_1 ''measures'' only the contribution from their spins, which is only part of their angular momenta; see the derivation of the relation (16). Fermions with momentum $\mathbf{p}\neq\mathbf{0}$, which is not parallel to $\pm\mathbf{n}$, necessarily contribute to the total angular momentum also by some orbital part.

Further let us notice, if we denote

$$\gamma_{ELT}\equiv\int x(g_1+2g_2)dx, \tag{69}$$

then Eq. (55) and the third relation (65) imply

$$\frac{2}{3}m\leqslant\frac{18}{5}\gamma_{ELT}\cdot M\leqslant m. \tag{70}$$

Why do these two very simple approaches for description of the target consisting of the three fermions differ so strongly regarding the prediction Γ_1? The reason is the following. The standard formulation of the QPM is closely connected with the preferred reference system—infinite momen-

tum frame (IMF). The basic relations between the distribution and structure functions such as

$$g_1(x)=\frac{1}{2}\sum e_j^2\Delta q_j(x), \quad F_2(x)=x\sum e_i^2 q_i(x) \quad (71)$$

are derived with the use of approximation

$$p_\alpha = xP_\alpha, \quad (72)$$

which seems to be plausible in the IMF. Nevertheless, in the covariant formulation this relation is equivalent to the assumption that the quarks are static with respect to the proton, since the velocities p_j/p_0 and P_j/P_0 are the same. In the proton rest frame it means $\mathbf{p}=0$. That is why both approaches are equivalent for the static quarks but differ for the quarks, which have some intrinsic motion inside the proton. In our approach we do not use assumption (72) and as a result if $p_\alpha \neq xP_\alpha$ we obtain different relations between the distribution and structure functions. In other words, the fact that the experimental value Γ_1 is substantially under the value predicted by the naive QPM in standard formulation, can be in our approach interpreted as a direct consequence of the quark intrinsic motion.

Of course, the approach discussed above concerns the simplified scenario of the quasifree fermions on mass shell. Naive QPM represents only a first approximation for a description of real nucleon, but the consistent accounting for the quark intrinsic motion as suggested in our approach can, in some aspects, improve this approximation considerably.

Nevertheless, in the realistic case of partons inside the nucleon the situation is still much more delicate. The interaction among the quarks is very strong and the partons themselves are mostly in some short-lived virtual states. Is it possible to speak about their mass at all? Strictly speaking, probably not. The mass in the exact sense is well defined only for free particles, whereas the partons are never free. However, one can assume the following. The relations obtained in the previous sections can be used as a good approximation even for the interacting quarks, but provided that the term *mass of quasifree parton* is substituted by the term *parton effective mass*. By this term we mean the mass, which a free parton would have to have to interact with the probing photon equally as the real, bounded one. Intuitively, this mass should correlate to Q^2: a lower Q^2 roughly means that the photon ''sees'' the quark surrounded by some cloud of gluons and quark-antiquark pairs as one particle, by which this photon is absorbed. And on the contrary, the higher Q^2 should mediate interaction with more ''isolated'' quark. Moreover, one should accept that the value of the effective mass can even fluctuate for a fixed Q^2. Such a phenomenological model was suggested in [13], but unfortunately calculation was based on the form of quark polarization vector which is not correct. Despite that, the general considerations in the mentioned paper can be sensible. Corresponding numerical recalculation with the correct input obtained in the present study for the invariants A,B,C,D [relations (32), (43)] should be done in a separate paper.

V. SUMMARY AND CONCLUSION

In the present paper we have studied the spin structure functions of the system of quasifree fermions on mass shell and with spherically symmetric distribution of their momenta. The main results can be summarized as follows.

(1) Using a consistently covariant description of this simple system, we have shown how the structure functions depend on the intrinsic motion of the fermions. In particular, we have suggested that the momenta Γ_1 corresponding to the two extreme scenarios, of the static (massive) fermions and massless fermions, can differ significantly: $\Gamma_1(m \ll p_0)/\Gamma_1(p_0 \approx m)=1/3$.

(2) We have shown what sum rules follow from the obtained spin structure functions. Further we have shown how these rules are related to some sum rules well known from the QPM phenomenology.

(3) We have done a comparison with the corresponding relations for the structure functions following from the standard formulation of the naive QPM. Both approaches are basically equivalent for the static quarks. Differences for quarks with intrinsic motion inside the proton are a result of the conflict with the assumption $p_\alpha = xP_\alpha$, which is crucial for derivation of the relations between structure and distribution functions in the standard QPM.

(4) The difference between the experimental value Γ_1 for the proton and the corresponding value expected from the naive QPM, or at least a part of this difference, can be interpreted as a consequence of the quark motion inside the proton.

ACKNOWLEDGMENTS

I would like to thank Anatoli Efremov and Oleg Teryaev for many useful discussions and valuable comments.

APPENDIX: CALCULATION OF THE INTEGRALS RELATED TO G_P, G_S

Integrals in the relations (44),(45) expressed in the target rest frame read

$$G_P = -\frac{m}{2M^2\nu}\int H(p_0)\frac{\mathbf{pn}}{p_0+m} \times\left[1+\frac{1}{m}\left(p_0-\frac{\mathbf{pq}-(\mathbf{pn})|\mathbf{q}|\cos\omega}{\mathbf{q}^2\sin^2\omega}\nu\right)\right] \times\delta\left(\frac{pq}{M\nu}-x\right)\frac{d^3p}{p_0}, \quad (A1)$$

$$G_S = \frac{m}{2M\nu}\int H(p_0)\left[1+\frac{\mathbf{pn}}{p_0+m}\frac{1}{m} \times\left(\mathbf{pn}-\frac{\mathbf{pq}-(\mathbf{pn})|\mathbf{q}|\cos\omega}{\mathbf{q}^2\sin^2\omega}|\mathbf{q}|\cos\omega\right)\right] \times\delta\left(\frac{pq}{M\nu}-x\right)\frac{d^3p}{p_0}, \quad (A2)$$

where $\cos\omega \equiv \mathbf{qn}/|\mathbf{q}|$. For integration we use the orthonormal system in which

$$\mathbf{p}=p_1\mathbf{e}_1+p_2\mathbf{e}_2+p_3\mathbf{e}_3;\quad \mathbf{e}_1=-\frac{\mathbf{q}}{|\mathbf{q}|},$$

$$\mathbf{e}_2=\frac{\mathbf{n}-(\mathbf{ne}_1)\mathbf{e}_1}{\sqrt{1-(\mathbf{ne}_1)^2}},\quad \mathbf{e}_3=\mathbf{e}_1\times\mathbf{e}_2, \tag{A3}$$

so one gets

$$\mathbf{pq}=-p_1|\mathbf{q}|,\quad \mathbf{pn}=-p_1\cos\omega+p_2\sin\omega,\quad \cos\omega\equiv\frac{\mathbf{qn}}{|\mathbf{q}|}. \tag{A4}$$

After the substitution $p_2=p_T\cos\varphi$, $p_3=p_T\sin\varphi$ and taking into account that the terms proportional to $\cos\varphi$ disappear, the integrals can be rewritten

$$G_P=\frac{\cos\omega}{2M^2\nu}\int H(p_0)\left(p_1+\frac{\nu}{|\mathbf{q}|}\frac{p_1^2-p_T^2\cos^2\varphi}{p_0+m}\right)\times\delta\left(\frac{p_0\nu+p_1|\mathbf{q}|}{M\nu}-x\right)\frac{p_T dp_1 dp_T d\varphi}{p_0}, \tag{A5}$$

$$G_S=\frac{m}{2M\nu}\int H(p_0)\left(1+\frac{p_T^2\cos^2\varphi}{m(p_0+m)}\right)\times\delta\left(\frac{p_0\nu+p_1|\mathbf{q}|}{M\nu}-x\right)\frac{p_T dp_1 dp_T d\varphi}{p_0}, \tag{A6}$$

where $p_0=\sqrt{m^2+p_T^2+p_1^2}$. Integration over φ gives

$$G_P=\frac{\pi\cos\omega}{M^2\nu}\int H(p_0)\left(p_1+\frac{\nu}{|\mathbf{q}|}\frac{p_1^2-p_T^2/2}{p_0+m}\right)\times\delta\left(\frac{p_0\nu+p_1|\mathbf{q}|}{M\nu}-x\right)\frac{p_T dp_1 dp_T}{p_0}, \tag{A7}$$

$$G_S=\frac{\pi m}{M\nu}\int H(p_0)\left(1+\frac{p_T^2/2}{m(p_0+m)}\right)\times\delta\left(\frac{p_0\nu+p_1|\mathbf{q}|}{M\nu}-x\right)\frac{p_T dp_1 dp_T}{p_0}. \tag{A8}$$

Further, using the relation

$$\frac{|\mathbf{q}|}{\nu}=\sqrt{1+4M^2x^2/Q^2} \tag{A9}$$

one can check that the argument of the δ function equals zero for

$$p_1=\tilde{p}_1\equiv\frac{Mx-m_T^2/Mx}{\sqrt{1+4m_T^2/Q^2}+\sqrt{1+4M^2x^2/Q^2}},\quad m_T^2\equiv m^2+p_T^2. \tag{A10}$$

This is the first root of the corresponding quadratic equation; the second one is excluded, since in the effect of the δ function this root is compatible only with negative energy p_0. The energy corresponding to the root (A10) is

$$p_0=\tilde{p}_0\equiv Mx-\frac{\tilde{p}_1|\mathbf{q}|}{\nu}=Mx-\tilde{p}_1\sqrt{1+4M^2x^2/Q^2}. \tag{A11}$$

Then in accordance with the rule

$$\delta(f(x))dx=\sum_j\frac{\delta(x-x_j)}{|f'(x_j)|}dx,\quad f(x_j)=0 \tag{A12}$$

the δ function in the integrals can be rewritten

$$\delta\left(\frac{p_0\nu+p_1|\mathbf{q}|}{M\nu}-x\right)dp_1=\frac{M\delta(p_1-\tilde{p}_1)dp_1}{\tilde{p}_1/\tilde{p}_0+\sqrt{1+4M^2x^2/Q^2}} \tag{A13}$$

and afterwards the integrals are simplified

$$G_P=\frac{\pi\cos\omega}{M\nu}\int_0^{p_{T\,\max}}H(\tilde{p}_0)\left(\tilde{p}_1+\frac{\nu}{|\mathbf{q}|}\frac{\tilde{p}_1^2-p_T^2/2}{\tilde{p}_0+m}\right)\times\frac{p_T dp_T}{\tilde{p}_1+\tilde{p}_0\sqrt{1+4M^2x^2/Q^2}}, \tag{A14}$$

$$G_S=\frac{\pi m}{\nu}\int_0^{p_{T\,\max}}H(\tilde{p}_0)\left(1+\frac{p_T^2/2}{m(\tilde{p}_0+m)}\right)\times\frac{p_T dp_T}{\tilde{p}_1+\tilde{p}_0\sqrt{1+4M^2x^2/Q^2}}, \tag{A15}$$

where $\tilde{p}_1$ and $\tilde{p}_0$ depend on p_T according to Eqs. (A10) and (A11). For the numeric calculation one should know the upper limit $p_{T\,\max}$ for given x, Q^2, and $\tilde{p}_{0\,\max}$. After inserting $\tilde{p}_1$ from Eq. (A10) into Eq. (A11) one gets the equation for m_T^2:

$$\frac{\tilde{p}_{0\,\max}-Mx}{\sqrt{1+4M^2x^2/Q^2}}=-\frac{Mx-m_T^2/Mx}{\sqrt{1+4m_T^2/Q^2}+\sqrt{1+4M^2x^2/Q^2}}. \tag{A16}$$

Instead of m_T^2 it is useful to solve this equation first for $y=\sqrt{1+4m_T^2/Q^2}$ obtaining the two roots

$$y_\pm=\frac{A\pm\sqrt{A^2+4a(\tilde{p}_{0\,\max}+a)}}{2a};\quad A\equiv\frac{\tilde{p}_{0\,\max}-Mx}{\sqrt{1+4M^2x^2/Q^2}},$$

$$a\equiv\frac{Q^2}{4Mx}. \tag{A17}$$

Since $y_- < 0$, this root is excluded. The second root y_+ after some computation implies

$$m_{T\,\max}^2 = Mx(2\tilde{p}_{0\,\max} - Mx) + \frac{(\tilde{p}_{0\,\max} - Mx)^2}{1 + Q^2/4M^2x^2},$$

$$p_{T\,\max} = \sqrt{m_{T\,\max}^2 - m^2}. \tag{A18}$$

In this way we have the recipe for how to calculate the integrals related to the structure functions G_P, G_S corresponding to the distribution $H(p_0)d^3p$.

[1] Proceedings of the 9th International Workshop on Deep Inelastic Scattering and QCD-DIS2001, Bologna, Italy, 2001.
[2] E.W. Hughes and R. Voss, Annu. Rev. Nucl. Part. Sci. **49**, 303 (1999).
[3] M. Anselmino, A. Efremov, and E. Leader, Phys. Rep. **261**, 1 (1995).
[4] S.J. Brodsky, Dae Sung Hwang, Bo-Qiang Ma, and I. Schmidt, Nucl. Phys. **B593**, 311 (2001).
[5] Bo-Qiang Ma and Ivan Schmidt, Phys. Rev. D **58**, 096008 (1998).
[6] Liang Zuo-tang and R. Rittel, Mod. Phys. Lett. A **12**, 827 (1997).
[7] Bo-Qiang Ma, J. Phys. G **17**, L53 (1991).
[8] Bo-Qiang Ma and Qi-Ren Zhang, Z. Phys. C **58**, 479 (1993).
[9] Bo-Qiang Ma, Phys. Lett. B **375**, 320 (1996).
[10] Bo-Qiang Ma, I. Schmidt, and J. Soffer, Phys. Lett. B **441**, 461 (1998).
[11] P. Zavada, Phys. Rev. D **55**, 4290 (1997).
[12] P. Zavada, Phys. Rev. D **56**, 5834 (1997).
[13] P. Zavada, Acta Phys. Slov. **49**, 273 (1999).
[14] J.D. Jackson, G.G. Ross, and R.D. Roberts, Phys. Lett. B **226**, 159 (1989).
[15] H. Burkhardt and W.N. Cottingham, Ann. Phys. (N.Y.) **56**, 453 (1970).
[16] A.V. Efremov, O.V. Teryaev, and E. Leader, Phys. Rev. D **55**, 4307 (1997).

Article copy

PHYSICAL REVIEW D **67**, 014019 (2003)

Proton spin structure and valence quarks

Petr Závada*
Institute of Physics, Academy of Sciences of the Czech Republic, Na Slovance 2, CZ-182 21 Prague 8, Czech Republic
(Received 10 October 2002; published 27 January 2003)

The spin structure of a system of quasifree fermions having a total angular momentum $J=1/2$ is studied in a consistently covariant approach. Within this model the relations between the spin functions are obtained. Their particular cases are the sum rules of Wanzura and Wilczek, Efremov, Leader, and Teryaev, and Burkhardt and Cottingham and also the expression for the Wanzura-Wilczek twist 2 term g_2^{WW}. With the use of the proton valence quark distributions as input, the corresponding spin functions are obtained. The resulting structure functions g_1 and g_2 are quite compatible with the experimental data.

DOI: 10.1103/PhysRevD.67.014019 PACS number(s): 13.60.−r, 13.88.+e, 14.65.−q

I. INTRODUCTION

The nucleon structure functions, both unpolarized and polarized, are the basic tools for understanding the nucleon internal structure in the language of QCD. Precision measurements of the polarized structure functions have been completed only in recent years [1–8]. These functions contain information which is a crucial complement to the structure functions obtained in unpolarized deep inelastic scattering (DIS) experiments. At the same time the interpretation and understanding of polarized structure functions seem to be much more difficult than in the case of unpolarized ones. Actually, it is not yet clear how the nucleon spin is generated from the spins and orbital momenta of the quarks and gluons. For the present status and perspectives of nucleon spin physics see [9] and citations therein. The more formal aspects of polarized DIS are explained in [10] and [11].

Spin in general is a very delicate quantity, which requires correspondingly precise treatment. It has been argued that for correct evaluation of the quark contribution to the nucleon spin it is necessary to take properly into account the intrinsic quark motion [12–22]. The necessity of a covariant formulation of the quark-parton model (QPM) for the spin functions has been pointed out in [23]. These requirements are not satisfied in the standard formulation of the QPM, which is currently used for analysis and interpretation of the experimental data.

In Ref. [22] we demonstrated the role of the intrinsic motion for the spin structure functions, using a simple model of a system of quasifree fermions on mass shell. The basic requirement was a consistently covariant formulation of the task for the system of fermions, which are not static, being characterized by some momentum distribution in the frame of their center of mass. In the present paper we attempt to further develop this approach. In Sec. II we introduce the spin structure functions $g_1(x), g_2(x)$, the longitudinal and transversal net spin density distributions $s_L(x), s_T(x)$, and the density of total angular momentum $j(x)$. Then in Sec. III we show how all of these functions are mutually related. Finally in Sec. IV we apply the suggested approach, with some simplified assumptions, to the description of the proton spin structure and make a comparison with the experimental data for $g_1(x)$ and $g_2(x)$. The last section is devoted to a short summary and conclusions.

II. SPIN STRUCTURE FUNCTIONS AND SPIN DISTRIBUTIONS

In a previous paper [22] we showed that the spin structure functions related to a spherically symmetric target consisting of three quasifree fermions (of spin 1/2), having resulting total angular momentum $J=1/2$, can be written as

$$g_1=\frac{1}{2}\int H(p_0)\left[m+\frac{\nu}{|\mathbf{q}|}p_1+\frac{\nu^2}{|\mathbf{q}|^2}\frac{p_1^2}{p_0+m}+\left(1-\frac{\nu^2}{|\mathbf{q}|^2}\right)\frac{p_T^2/2}{p_0+m}\right]\delta\left(\frac{p_0\nu+p_1|\mathbf{q}|}{M\nu}-x\right)\frac{d^3p}{p_0}, \quad (1)$$

$$g_2=-\frac{1}{2}\frac{\nu}{|\mathbf{q}|}\int H(p_0)\left(p_1+\frac{\nu}{|\mathbf{q}|}\frac{p_1^2-p_T^2/2}{p_0+m}\right)\times\delta\left(\frac{p_0\nu+p_1|\mathbf{q}|}{M\nu}-x\right)\frac{d^3p}{p_0}, \quad (2)$$

where $p_0=\sqrt{m^2+\mathbf{p}^2}$, $p_T^2=p_2^2+p_3^2$, and H is the charge weighted distribution

$$H(p_0)=\sum_{k=1}^{3} e_k^2\Delta G_k(p_0). \quad (3)$$

This distribution is constructed from the polarized distributions of individual fermions

$$\Delta G_k(p_0)\equiv G_{k,+1/2}(p_0)-G_{k,-1/2}(p_0), \quad (4)$$

which satisfy

$$\int G_k(p_0)d^3p=1, \quad G_k(p_0)\equiv G_{k,+1/2}(p_0)+G_{k,-1/2}(p_0), \quad (5)$$

$$\int \Delta G(p_0)d^3p=1, \quad \Delta G(p_0)=\sum_{k=1}^{3}\Delta G_k(p_0). \quad (6)$$

*Email address: zavada@fzu.cz

The distributions $G_{k,\lambda}(p_0)$ measure the probability of finding a fermion in the state

$$u(p,\lambda\mathbf{n})=\frac{1}{\sqrt{N}}\begin{pmatrix}\phi_{\lambda\mathbf{n}}\\ \dfrac{\mathbf{p}\sigma}{p_0+m}\phi_{\lambda\mathbf{n}}\end{pmatrix},\quad \frac{1}{2}n\sigma\phi_{\lambda\mathbf{n}}=\lambda\phi_{\lambda\mathbf{n}},$$

$$\lambda=\pm\frac{1}{2}, \tag{7}$$

where the direction $\mathbf{n}$ coincides with the direction of target polarization $\mathbf{J}$ and a standard normalization is used:

$$N=\frac{2p_0}{p_0+m},\quad \phi_\lambda^\dagger\phi_\lambda=1. \tag{8}$$

Now, let us try using the same system to calculate some spin distribution functions. In the first step we shall define these distributions in terms of the fermion momenta related to the target rest frame; then we shall show their representation in the variable x.

The net spin density corresponding to the projection on the direction $\mathbf{n}'$ is defined as

$$S(\mathbf{p},\mathbf{n},\mathbf{n}')=\sum_\lambda G_\lambda(p_0)u^\dagger(p,\lambda\mathbf{n})(\mathbf{n}'\boldsymbol{\Sigma})u(p,\lambda\mathbf{n}),$$

$$\boldsymbol{\Sigma}=\frac{1}{2}\begin{pmatrix}\sigma & \mathbf{0}\\ \mathbf{0} & \sigma\end{pmatrix}. \tag{9}$$

One can verify that this expression can be modified to

$$S(\mathbf{p},\mathbf{n},\mathbf{n}')=\frac{1}{N}\sum_\lambda G_\lambda(p_0)\left(\lambda\mathbf{n}\mathbf{n}'-\lambda\mathbf{n}\mathbf{n}'\frac{\mathbf{p}^2}{(p_0+m)^2}+\phi^\dagger_{\lambda\mathbf{n}}\frac{\mathbf{p}\sigma\cdot\mathbf{p}\mathbf{n}'}{(p_0+m)^2}\phi_{\lambda\mathbf{n}}\right). \tag{10}$$

We assume that the beam direction is defined by the vector $\mathbf{k}=(|\mathbf{k}|,0,0)$; then one can obtain the following particular cases of the distribution (9).

(1) Longitudinal polarization in a longitudinally polarized target, i.e., $\mathbf{n}=\mathbf{n}'=(1,0,0)$, when

$$\mathbf{p}\sigma\cdot\mathbf{p}\mathbf{n}'=\sum_{i=1}^3 p_i^2\sigma_i n_i'+\sum_{j\neq i}p_ip_j\sigma_in_j'=p_1^2\sigma_1+p_2p_1\sigma_2+p_3p_1\sigma_3 \tag{11}$$

and the relation (10) can be simplified to

$$S_L(\mathbf{p})=\frac{1}{2p_0}\Delta G(p_0)\left(m+\frac{p_1^2}{p_0+m}\right). \tag{12}$$

(2) Transverse polarization in a transversely polarized target, i.e., $\mathbf{n}=\mathbf{n}'=(0,1,0)$, then

$$\mathbf{p}\sigma\cdot\mathbf{p}\mathbf{n}=\sum_{i=1}^3 p_i^2\sigma_in_i+\sum_{j\neq i}p_ip_j\sigma_in_j=p_2^2\sigma_2+p_1p_2\sigma_1+p_3p_2\sigma_3 \tag{13}$$

and the relation (10) can be simplified to

$$S_T(\mathbf{p})=\frac{1}{2p_0}\Delta G(p_0)\left(m+\frac{p_2^2}{p_0+m}\right). \tag{14}$$

(3) In a similar way, one can also obtain the polarizations $S_L^T(\mathbf{p})$ and $S_T^L(\mathbf{p})$, which are related to the density of longitudinal polarization in a transversely polarized target, and vice versa. The density $S_L^T(\mathbf{p})$ can be obtained from the relation (10) after inserting $\mathbf{n}=(0,1,0)$, $\mathbf{n}'=(1,0,0)$, and $S_T^L(\mathbf{p})$ with $\mathbf{n}=(1,0,0),\mathbf{n}'=(0,1,0)$, correspondingly. After some calculation similar to that for obtaining the relations (12) and (14), one gets

$$S_L^T(\mathbf{p})=S_T^L(\mathbf{p})=\frac{1}{2p_0}\Delta G(p_0)\frac{p_1p_2}{p_0+m}. \tag{15}$$

(4) The density of total angular momentum can be defined as

$$J(\mathbf{p},\mathbf{n},\mathbf{n}')=\sum_\lambda G_\lambda(p_0)u^\dagger(p,\lambda\mathbf{n})(\mathbf{n}'\mathbf{j})u(p,\lambda\mathbf{n}),$$

$$j_k=\Sigma_k+l_k=\frac{1}{2}\begin{pmatrix}\sigma_k & 0\\ 0 & \sigma_k\end{pmatrix}-i\varepsilon_{klm}p_l\frac{\partial}{\partial p_m}. \tag{16}$$

One can verify that after some calculation this expression can be simplified:

$$J(\mathbf{p},\mathbf{n},\mathbf{n}')=\frac{1}{2}\mathbf{n}\mathbf{n}'\Delta G(p_0). \tag{17}$$

This result implies that J has rotational symmetry, so there is no distinction between longitudinal and transversal density:

$$J_L(\mathbf{p})=J_T(\mathbf{p})=\frac{1}{2}\Delta G(p_0)\equiv J(\mathbf{p}),\quad J_L^T(\mathbf{p})=J_T^T(\mathbf{p})=0. \tag{18}$$

Further, is it possible to express the obtained distributions as functions of x instead of p? For a simplification we shall from now on assume that

$$Q^2\gg 4M^2x^2, \tag{19}$$

which implies

$$\frac{|\mathbf{q}|}{\nu}=\sqrt{1+4M^2x^2/Q^2}\to 1. \tag{20}$$

Then the δ function term, which defines the transformation $p\to x$ in Eqs. (1),(2), will be simplified

$$\delta\left(\frac{p_0\nu+p_1|\mathbf{q}|}{M\nu}-x\right)\to\delta\left(\frac{p_0+p_1}{M}-x\right); \tag{21}$$

in this limit the coordinate p_1 defines the beam direction. The spin structure functions (1),(2) are now simplified accordingly:

$$g_1(x)=\frac{1}{2}\int H(p_0)\left(m+p_1+\frac{p_1^2}{p_0+m}\right)\delta\left(\frac{p_0+p_1}{M}-x\right)\frac{d^3p}{p_0}, \tag{22}$$

$$g_2(x)=-\frac{1}{2}\int H(p_0)\left(p_1+\frac{p_1^2-p_T^2/2}{p_0+m}\right)\delta\left(\frac{p_0+p_1}{M}-x\right)\frac{d^3p}{p_0}, \tag{23}$$

$$g_1(x)+g_2(x)=\frac{1}{2}\int H(p_0)\left(m+\frac{p_T^2/2}{p_0+m}\right)\times\delta\left(\frac{p_0+p_1}{M}-x\right)\frac{d^3p}{p_0}. \tag{24}$$

Apparently, the convolution defined by the δ function (21) also gives the rule for transformation of the spin distributions expressed in the variable p to the corresponding representation in the variable x:

$$j(x)=\int J(\mathbf{p})\delta\left(\frac{p_0+p_1}{M}-x\right)d^3p=\frac{1}{2}\int \Delta G(p_0)\delta\left(\frac{p_0+p_1}{M}-x\right)d^3p, \tag{25}$$

$$s_L(x)=\int S_L(\mathbf{p})\delta\left(\frac{p_0+p_1}{M}-x\right)d^3p=\frac{1}{2}\int \Delta G(p_0)\left(m+\frac{p_1^2}{p_0+m}\right)\delta\left(\frac{p_0+p_1}{M}-x\right)\frac{d^3p}{p_0}, \tag{26}$$

$$s_T(x)=\int S_T(\mathbf{p})\delta\left(\frac{p_0+p_1}{M}-x\right)d^3p=\frac{1}{2}\int \Delta G(p_0)\left(m+\frac{p_T^2}{2(p_0+m)}\right)\delta\left(\frac{p_0+p_1}{M}-x\right)\frac{d^3p}{p_0}. \tag{27}$$

In the last integral we could replace p_2^2 by $p_T^2/2$ because of the axial symmetry. Further, it is obvious that the densities S_L^T and S_T^L, expressed in the variable x, vanish due to the symmetry:

$$s_L^T(x)=s_T^L(x)=\frac{1}{2}\int \Delta G(p_0)\frac{p_1p_2}{p_0+m}\delta\left(\frac{p_0+p_1}{M}-x\right)\frac{d^3p}{p_0}=0. \tag{28}$$

What is the meaning of the integrals in the relations (22)–(27)? To simplify this question, let us assume the same shape of the distributions $G_k(p_0)$ for all three fermions. Then the distributions ΔG and H differ only by a constant factor, in which the charges and polarizations of individual fermions are absorbed:

$$H(p_0)=\kappa\Delta G(p_0),\quad \kappa=\sum_{k=1}^{3}e_k^2\int \Delta G_k(p_0)d^3p. \tag{29}$$

Now, in agreement with the results obtained in [22], one can observe the following. The relation (22) can be rewritten as

$$g_1(x)=\frac{\kappa}{2}\int \Delta G(p_0)\left(m+p_1+\frac{p_1^2}{p_0+m}\right)\delta\left(\frac{p_0+p_1}{M}-x\right)\frac{d^3p}{p_0} \tag{30}$$

and after integration over x one gets

$$\Gamma_1=\int g_1(x)dx=\frac{\kappa}{2}\int \Delta G(p_0)\left(\frac{1}{3}+\frac{2m}{3p_0}\right)d^3p=\kappa\langle\mathbf{n\Sigma}\rangle, \tag{31}$$

where $\mathbf{n}$ is the direction of the target polarization and $\langle\mathbf{n\Sigma}\rangle$ represents the resulting projection of the spins coming from the individual fermions. In a similar way one gets

$$\int j(x)dx=\frac{1}{2}\int \Delta G(p_0)d^3p=\frac{1}{2}, \tag{32}$$

i.e., the integral represents the resulting projection of the total angular momentum. Further, one can easily check that

$$\int s_L(x)dx=\int s_T(x)dx=\frac{1}{2}\int \Delta G(p_0)\left(\frac{1}{3}+\frac{2m}{3p_0}\right)d^3p=\frac{\Gamma_1}{\kappa}. \tag{33}$$

Moreover, the following relation is valid:

$$\kappa\cdot s_T(x)=g_1(x)+g_2(x). \tag{34}$$

Let us note that, despite our assumption that the target consists of just three fermions, the suggested approach is more general. Since the spin functions are always based on differences like Eq. (4), all the resulting relations are equally valid for any target consisting of fermions with $\Delta G_k(p_0)\neq 0$, $k=1,2,3$, which are embedded in another system with compensated spins: $\Delta G_k(p_0)=0$, $k=4,5,6,\ldots$.

Now we can summarize.

(i) The function $j(x)$ measures the contribution of the total angular momenta (spin+orbital momentum) of the constituent fermions to the target spin.

(ii) The functions $s_{L(T)}(x)$ measure the net spin contribution of the constituent fermions to the spin of the target with longitudinal (transversal) polarization. Clearly, one can calculate also the corresponding densities of the orbital momentum as

$$l_{L(T)}=j(x)-s_{L(T)}(x). \tag{35}$$

(iii) Obviously the functions $g_1(x)$, $j(x)$, $s_L(x)$, and $s_T(x)$ are equivalent in the case of static fermions, where orbital momentum does not play any role. The considered distribution functions ΔG and H have rotational symmetry in the target rest frame, which is a necessary condition for a target with spin $J=1/2$. It follows that the meaning of our function $j(x)$ suggested above *does not depend* on the orientation of the target polarization (longitudinal or transverse) with respect to the beam direction. Let us point out that the last statement can be deduced only in the framework of a relativistically covariant description, in which the rotational symmetry of the target is properly taken into account. At the same time, let us note that, in general, the function $g_1(x)$ is not equivalent to the measure of the longitudinal spin density $s_L(x)$; only their integrals over x are equal (up to a factor κ).

III. RELATIONSHIP AMONG THE SPIN FUNCTIONS

Before the next discussion we shall first prove the following proposition. The functions $V_n(x)$ defined as

$$V_n(x)=\int H(p_0)\left(\frac{p_0}{M}\right)^n \delta\left(\frac{p_0+p_1}{M}-x\right)d^3p,$$
$$p_0=\sqrt{m^2+\mathbf{p}^2} \tag{36}$$

satisfy

$$\frac{V_j'(x)}{V_k'(x)}=\left(\frac{x}{2}+\frac{x_0^2}{2x}\right)^{j-k}, \quad x_0=\frac{m}{M}, \tag{37}$$

for any powers j,k and function H for which the integral (36) exists. Proof of the last relation is given in Appendix A.

A. Spin structure functions $g_1(x)$,$g_2(x)$

With the use of the relations (36),(37), as shown in Appendix B, one can rewrite Eqs. (23) and (24) as

$$g_2(x)=-\frac{1}{2}\left[a(x)V_0(x)+\int_x^1 b(x,y)V_0(y)dy\right], \tag{38}$$

$$g_1(x)+g_2(x)=\frac{1}{2}\left[A(x)V_0(x)+\int_x^1 B(x,y)V_0(y)dy\right], \tag{39}$$

where

$$a(x)=2x\frac{x-x_0}{x^2+x_0^2},$$
$$b(x,y)=\left[\frac{3(x+x_0)^2}{(y+x_0)^4}-\frac{3x^2+2xx_0+x_0^2}{(y^2+x_0^2)^2}\right]\frac{y^2-x_0^2}{x_0}, \tag{40}$$
$$A(x)=\frac{2xx_0}{x^2+x_0^2},$$
$$B(x,y)=\left[-\frac{(x+x_0)^2}{(y+x_0)^4}+\frac{x^2-x_0^2}{(y^2+x_0^2)^2}\right]\frac{y^2-x_0^2}{x_0}. \tag{41}$$

Now, one can easily check that in the limit $x_0\to 0$ the relations (38),(39) are simplified:

$$g_2(x)=-V_0(x)+\int_x^1\left(6\frac{x^2}{y^3}-2\frac{x}{y^2}\right)V_0(y)dy, \tag{42}$$

$$g_1(x)+g_2(x)=\int_x^1\left(2\frac{x^2}{y^3}-\frac{x}{y^2}\right)V_0(y)dy. \tag{43}$$

These relations imply

$$g_1(x)=V_0(x)-\int_x^1\left(4\frac{x^2}{y^3}-\frac{x}{y^2}\right)V_0(y)dy \tag{44}$$

and

$$[g_1(x)+g_2(x)]'=\int_x^1\left(4\frac{x}{y^3}-\frac{1}{y^2}\right)V_0(y)dy-\frac{V_0(x)}{x}. \tag{45}$$

Combining the last two relations gives

$$[g_1(x)+g_2(x)]'=-\frac{g_1(x)}{x} \tag{46}$$

or

$$g_2(x)=-g_1(x)+\int_x^1\frac{g_1(y)}{y}dy, \tag{47}$$

which is the known expression for the Wanzura-Wilczek twist-2 term for the g_2 approximation [24].

Can we now obtain a similar relation for the case $x_0>0$, i.e., for massive fermions? Let us combine Eqs. (38),(39) into the form

$$g_1(x)+\left(1+\frac{A(x)}{a(x)}\right)g_2(x)$$
$$=\frac{1}{2}\int_x^1\left(B(x,y)-\frac{A(x)}{a(x)}b(x,y)\right)V_0(y)dy \tag{48}$$

and let us try to express the differentiation of right-hand side (RHS) as a combination of g_1 and g_2:

$$\left[\frac{1}{2}\int_x^1\left(B(x,y)-\frac{A(x)}{a(x)}b(x,y)\right)V_0(y)dy\right]'$$
$$=c_1(x)g_1(x)+c_2(x)g_2(x). \tag{49}$$

In Appendix C it is shown that after inserting g_1,g_2 from Eqs. (38),(39) this equation is solvable for $c_1(x),c_2(x)$, then after comparing with Eq. (48) we get

$$\left[g_1(x)+\left(1+\frac{A(x)}{a(x)}\right)g_2(x)\right]'=c_1(x)g_1(x)+c_2(x)g_2(x), \tag{50}$$

where

$$c_1(x)=-\frac{x^2+4xx_0+x_0^2}{(x^2-x_0^2)(x+2x_0)},$$

$$c_2(x)=-\frac{x_0(x^2+xx_0+4x_0^2)}{(x-x_0)(x^2-x_0^2)(x+2x_0)}. \tag{51}$$

In the same Appendix it is shown that Eq. (50) implies

$$g_2(x)=-\frac{x-x_0}{x}g_1(x)+\frac{x(x+2x_0)}{(x+x_0)^2}\int_x^1\frac{y^2-x_0^2}{y^3}g_1(y)dy, \tag{52}$$

$$g_1(x)=-\frac{x}{x-x_0}g_2(x)-\frac{x+2x_0}{x^2-x_0^2}\int_x^1 g_2(y)dy. \tag{53}$$

One can check that for $x_0\to 0$ both the last relations are equivalent to Eq. (46).

Further, in the limit $x_0\to 0$ one can also easily calculate the momenta of the spin structure functions g_1,g_2. If we define

$$\langle x^\alpha\rangle=\int_0^1 x^\alpha V_0(x)dx, \tag{54}$$

then after integrating by parts the following relation is obtained:

$$\int_0^1 x^\alpha\int_x^1\frac{V_0(y)}{y^\beta}dy=\frac{\langle x^{\alpha-\beta+1}\rangle}{\alpha+1}. \tag{55}$$

Application of this relation in Eqs. (43),(42) then gives

$$\int_0^1 x^\alpha[g_1(x)+g_2(x)]dx=\langle x^\alpha\rangle\frac{\alpha+1}{(\alpha+2)(\alpha+3)}, \tag{56}$$

$$\int_0^1 x^\alpha g_2(x)dx=-\langle x^\alpha\rangle\frac{\alpha(\alpha+1)}{(\alpha+2)(\alpha+3)} \tag{57}$$

for *any* α for which the integrals exist. The last two relations imply

$$\int_0^1 x^\alpha\left[\frac{\alpha}{\alpha+1}g_1(x)+g_2(x)\right]dx=0, \tag{58}$$

which for $\alpha=2,4,6,\ldots$ corresponds to the Wanzura-Wilczek sum rules [24]. Other special cases correspond to the Burkhardt-Cottingham ($\alpha=0$) and the Efremov-Leader-Teryaev ($\alpha=1$) sum rules [25,26].

B. Spin distributions $j(x)$, $s_L(x)$, and $s_T(x)$

Now, let us try to find the relations among the spin functions $j(x),s_L(x),s_T(x)$ and the structure functions g_1,g_2. For this purpose we only slightly change the definitions (25),(26),(27) in which we replace the function $\Delta G(p_0)$ [Eq. (6), the sum of spin contributions from individual fermions] by the function $H(p_0)$ [Eq. (3), spin contributions are weighted by the charges; see also the paragraph involving Eq. (29)]. The new relations read

$$j(x)=\frac{1}{2}\int H(p_0)\delta\left(\frac{p_0+p_1}{M}-x\right)d^3p, \tag{59}$$

$$s_L(x)=\frac{1}{2}\int H(p_0)\left(m+\frac{p_1^2}{p_0+m}\right)\delta\left(\frac{p_0+p_1}{M}-x\right)\frac{d^3p}{p_0}, \tag{60}$$

$$s_T(x)=\frac{1}{2}\int H(p_0)\left(m+\frac{p_T^2}{2(p_0+m)}\right)\delta\left(\frac{p_0+p_1}{M}-x\right)\frac{d^3p}{p_0}. \tag{61}$$

Now, using a standard notation

$$g_T(x)=g_1(x)+g_2(x), \tag{62}$$

we get from the relations (24) and (61) the equivalence

$$g_T(x)=s_T(x). \tag{63}$$

Comparison of the relations (36) and (59) implies that

$$j(x)=\frac{1}{2}V_0(x). \tag{64}$$

In Appendix D we shown that the distribution $V_0(y)$ can be extracted from the relations (38),(39), so we get

$$j(x)=\frac{x^2+x_0^2}{2x^2}g_1(x)+\frac{3x^2+2xx_0+3x_0^2}{2(x+x_0)^2}\int_x^1\frac{y^2-x_0^2}{y^3}g_1(y)dy+\int_x^1\ln\left(\frac{x(y+x_0)^2}{y(x+x_0)^2}\right)\frac{y^2-x_0^2}{y^3}g_1(y)dy, \tag{65}$$

$$j(x)=-\frac{x^2+x_0^2}{2x(x-x_0)}g_2(x)-\frac{1}{2(x^2-x_0^2)}\times\int_x^1\frac{6y^2x-2yx^2+x^2x_0+2yx_0^2-x_0^3}{y^2}g_2(y)dy. \tag{66}$$

Then for $x_0\to 0$ we have

$$j(x)=\frac{1}{2}g_1(x)+\frac{1}{2}\int_x^1\left(3+2\ln\frac{y}{x}\right)\frac{g_1(y)}{y}dy, \tag{67}$$

$$j(x)=-\frac{1}{2}g_2(x)-\frac{1}{x}\int_x^1(3y-x)\frac{g_2(y)}{y}dy. \tag{68}$$

Further, comparison of the relations (60) and (22) implies that

$$s_L(x)=g_1(x)-\frac{1}{2}\int H(p_0)p_1\delta\left(\frac{p_0+p_1}{M}-x\right)\frac{d^3p}{p_0}. \tag{69}$$

The last integral can be expressed by means of the function V_0 (see Appendix E):

$$s_L(x)=\frac{1}{2}\frac{x^2+x_0^2}{x^2}g_1(x)-\frac{x-3x_0}{2(x+x_0)}\int_x^1\frac{y^2-x_0^2}{y^3}g_1(y)dy + \int_x^1\ln\left(\frac{x(y+x_0)^2}{y(x+x_0)^2}\right)\frac{y^2-x_0^2}{y^3}g_1(y)dy. \tag{70}$$

A similar procedure gives also

$$s_L(x)=-\frac{1}{2}\frac{x^2+x_0^2}{x(x-x_0)}g_2(x) + \int_x^1\left(\frac{2y-x_0}{2y^2}-\frac{x+2x_0}{x^2-x_0^2}\right)g_2(y)dy. \tag{71}$$

One can easily check that for $x_0\to 0$ it follows that

$$s_L(x)=\frac{1}{2}g_1(x)+\int_x^1\left(\ln\frac{y}{x}-\frac{1}{2}\right)\frac{g_1(y)}{y}dy, \tag{72}$$

$$s_L(x)=-\frac{1}{2}g_2(x)+\int_x^1\left(\frac{1}{y}-\frac{1}{x}\right)g_2(y)dy. \tag{73}$$

Finally, combining the relations (52), (53), and (63) one gets

$$g_T(x)=\frac{x_0}{x}g_1(x)+\frac{x(x+2x_0)}{(x+x_0)^2}\int_x^1\frac{y^2-x_0^2}{y^3}g_1(y)dy, \tag{74}$$

$$g_T(x)=-\frac{x_0}{x-x_0}g_2(x)-\frac{x+2x_0}{x^2-x_0^2}\int_x^1 g_2(y)dy, \tag{75}$$

and for $x_0\to 0$ it follows that

$$g_T(x)=\int_x^1\frac{g_1(y)}{y}dy=-\frac{1}{x}\int_x^1 g_2(y)dy. \tag{76}$$

At the end of this section let us point out that the simple relations above, which define mutual transformations among the functions $g_1(x)$, $g_2(x)$, $j(x)$, $s_L(x)$, and $s_T(x)$, are obtained on the assumption that the fermions have some *fixed* effective mass x_0. In a more general case, for example when the structure functions are related to a system of fermions with some effective mass spectrum [21], such simple transformations do not exist.

IV. VALENCE QUARKS

Now let us try to apply the suggested approach to the description of the proton spin structure. For simplicity, as in [22], we assume the following.

(1) The spin contribution from the sea of quark-antiquark pairs and gluons can be neglected. Then the three fermions in our approach correspond to the three proton valence quarks. So, in this scenario, the proton spin is generated only by the valence quarks. Let us remark that in [22] we showed that this assumption does not contradict the experimental value Γ_1.

(2) In accordance with the nonrelativistic SU(6) approach, the spin contributions of individual valence terms are given as

$$s_u=4/3,\quad s_d=-1/3. \tag{77}$$

Let us denote the momentum distributions of the valence quarks in the target rest frame by the symbols h_u and h_d with the normalization

$$\frac{1}{2}\int h_u(p_0)d^3p=\int h_d(p_0)d^3p=1; \tag{78}$$

then the generic distribution (3) reads

$$H(p_0)=\sum e_j^2\Delta h_j(p_0)=\left(\frac{2}{3}\right)^2\frac{2}{3}h_u(p_0)-\left(\frac{1}{3}\right)^2\frac{1}{3}h_d(p_0). \tag{79}$$

In Refs. [19,21], using a similar approach, we studied also the unpolarized structure functions. In particular, we suggested that the structure function F_2 can be expressed in the limit (19) as

$$F_2(x)=x^2\int K(p_0)\frac{M}{p_0}\delta\left(\frac{p_0+p_1}{M}-x\right)d^3p,$$

$$K(p_0)=\sum_q e_q^2h_q(p_0), \tag{80}$$

where h_q are the distributions of quarks with charges e_q. For the valence quarks one can write

$$F_2(x)=\frac{4}{9}xu_V(x)+\frac{1}{9}xd_V(x); \tag{81}$$

then Eq. (80) can be split:

$$q_V(x)=x\int h_q(p_0)\frac{M}{p_0}\delta\left(\frac{p_0+p_1}{M}-x\right)d^3p,\quad q=u,d. \tag{82}$$

In accordance with the definition (36), in which h_q is inserted instead of H, one can write

$$q_V(x)=xV^q_{-1}(x), \tag{83}$$

then the relation (37) implies

$$V_0^q(x)=\frac{1}{2}\left(x+\frac{x_0^2}{x}\right)V_{-1}^q(x)+\frac{1}{2}\int_x^1\left(1-\frac{x_0^2}{y^2}\right)V_{-1}^q(x)dy, \tag{84}$$

which after inserting from Eq. (83) gives

$$V_0^q(x)=\frac{1}{2}\left[\left(1+\frac{x_0^2}{x^2}\right)q_V(x)+\int_x^1\left(1-\frac{x_0^2}{y^2}\right)\frac{q_V(y)}{y}dy\right]. \tag{85}$$

Obviously, the function $V_0(x)$ generated by the distribution (79) according to the definition (36) can be decomposed as

$$V_0(x)=\frac{8}{27}V_0^u(x)-\frac{1}{27}V_0^d(x), \tag{86}$$

and if we define

$$w_g(x)=\frac{8}{27}u_V(x)-\frac{1}{27}d_V(x) \tag{87}$$

then one can check that inserting V_0 from the relation (86) into the relations (38),(39) with the use of Eqs. (85),(87) gives

$$g_1(x)=\frac{1}{2}\left[w_g(x)-2(x+x_0)^2\int_x^1\frac{y-x_0}{(y+x_0)^3}\frac{w_g(y)}{y}dy\right], \tag{88}$$

$$g_2(x)=\frac{1}{2}\left[-\left(1-\frac{x_0}{x}\right)w_g(x)+3(x+x_0)^2\int_x^1\frac{y-x_0}{(y+x_0)^3}\frac{w_g(y)}{y}dy\right]. \tag{89}$$

Obviously, the structure functions can be split into two parts, corresponding to u and d quarks,

$$g_j(x)=\left(\frac{2}{3}\right)^2\frac{2}{3}g_j^u(x)-\left(\frac{1}{3}\right)^2\frac{1}{3}g_j^d(x),\quad j=1,2, \tag{90}$$

where the partial structure functions read

$$g_1^q(x)=\frac{1}{2}\left[q_V(x)-2(x+x_0)^2\int_x^1\frac{y-x_0}{(y+x_0)^3}\frac{q_V(y)}{y}dy\right], \tag{91}$$

$$g_2^q(x)=\frac{1}{2}\left[-\left(1-\frac{x_0}{x}\right)q_V(x)+3(x+x_0)^2\times\int_x^1\frac{y-x_0}{(y+x_0)^3}\frac{q_V(y)}{y}dy\right],\quad q=u,d. \tag{92}$$

Now we can express the corresponding contributions of different quarks to the spin distribution functions. Clearly,

$$s_T^q(x)=g_1^q(x)+g_2^q(x)=\frac{1}{2}\left[\frac{x_0}{x}q_V(x)+(x+x_0)^2\int_x^1\frac{y-x_0}{(y+x_0)^3}\frac{q_V(y)}{y}dy\right]. \tag{93}$$

Further, after inserting terms from the relations (91), (85), and (83) into Eq. (E1) one easily gets

$$s_L^q(x)=\frac{1}{4}\left[\left(1+\frac{x_0^2}{x^2}\right)q_V(x)-4(x+x_0)^2\times\int_x^1\frac{y-x_0}{(y+x_0)^3}\frac{q_V(y)}{y}dy+\int_x^1\left(1-\frac{x_0^2}{y^2}\right)\frac{q_V(y)}{y}dy\right]. \tag{94}$$

Let us remark that Eq. (E1) is obtained from the generic distribution $H(p_0)$; in its place we now have the distribution $h_q(p_0)$. Similarly, a comparison of the relations (64) and (85) gives

$$j^q(x)=\frac{1}{4}\left[\left(1+\frac{x_0^2}{x^2}\right)q_V(x)+\int_x^1\left(1-\frac{x_0^2}{y^2}\right)\frac{q_V(y)}{y}dy\right]. \tag{95}$$

Now, the net complete spin distributions can be obtained by adding individual valence terms with the weights (77), taking into account their normalization (78). If we define

$$w_s(x)=\frac{2}{3}u_V(x)-\frac{1}{3}d_V(x), \tag{96}$$

then the complete spin distributions can be obtained from the relations (93)–(95), in which the distribution q_V is replaced by w_s. Then for $x_0\to 0$ we obtain

$$g_1(x)=\frac{1}{2}\left[w_g(x)-2x^2\int_x^1\frac{w_g(y)}{y^3}dy\right], \tag{97}$$

$$g_2(x)=\frac{1}{2}\left[-w_g(x)+3x^2\int_x^1\frac{w_g(y)}{y^3}dy\right], \tag{98}$$

$$s_T(x)=\frac{1}{2}x^2\int_x^1\frac{w_s(y)}{y^3}dy, \tag{99}$$

$$s_L(x)=\frac{1}{4}\left[w_s(x)-4x^2\int_x^1\frac{w_s(y)}{y^3}dy+\int_x^1\frac{w_s(y)}{y}dy\right], \tag{100}$$

$$j(x)=\frac{1}{4}\left[w_s(x)+\int_x^1\frac{w_s(y)}{y}dy\right]. \tag{101}$$

Let us note that, if one assumes $u_V(x) \approx 2d_V(x)$, then the following substitution can be used:

$$w_g(x) \approx \frac{5}{9}\frac{F_{2val}}{x}, \quad w_s(x) \approx \frac{F_{2val}}{x}. \tag{102}$$

Further, let us make a remark about the normalization of the distributions above. To simplify this consideration, we assume the case $x_0 \to 0$. The relation (83) implies

$$\int_0^1 q_V(x)dx = \int_0^1 xV^q_{-1}(x)dx. \tag{103}$$

Since the relation (37) implies

$$V^q_{-1}(x) = \frac{2}{x}V^q_0(x) - 2\int_x^1 \frac{V^q_0(y)}{y^2}dy, \tag{104}$$

then using the relation (D7) one gets

$$\int_0^1 xV^q_{-1}(x)dx = \int_0^1 V^q_0(x)dx. \tag{105}$$

From the definition

$$V^q_0(x) = \int h_q(p_0)\delta\left(\frac{p_0+p_1}{M} - x\right)d^3p \tag{106}$$

one obtains

$$\int_0^1 V^q_0(x)dx = \int h_q(p_0)d^3p. \tag{107}$$

This relation combined with Eqs. (105) and (103) gives

$$\int_0^1 q_V(x)dx = \int h_q(p_0)d^3p, \tag{108}$$

which in accordance with the normalization (78) implies

$$\frac{1}{2}\int_0^1 u_V(x)dx = \int_0^1 d_V(x)dx = 1. \tag{109}$$

Now, one can also check the normalization of the functions (97)–(101). Taking into account that

$$\int_0^1 w_s(x)dx = 1, \quad \int_0^1 w_g(x)dx = \frac{5}{9}, \tag{110}$$

then after integration with the use of relation (D7) one gets

$$\int_0^1 j(x)dx = \frac{1}{2}, \quad \int_0^1 s_T(x)dx = \int_0^1 s_L(x)dx = \frac{1}{6}, \tag{111}$$

$$\int_0^1 g_1(x)dx = \frac{5}{54}, \quad \int_0^1 g_2(x)dx = 0. \tag{112}$$

The meaning of these integrals was discussed in Sec. II. The first integral (D7) represents the sum rule on the total proton angular momentum $J = l + s = 1/2$, which has been discussed, e.g., in [27]. The integrals over the net spin contributions s_T, s_L are correlated with Γ_1, which reaches its minimal value for $x_0 \to 0$, as we discussed in [22]; see also Eq. (31) above.

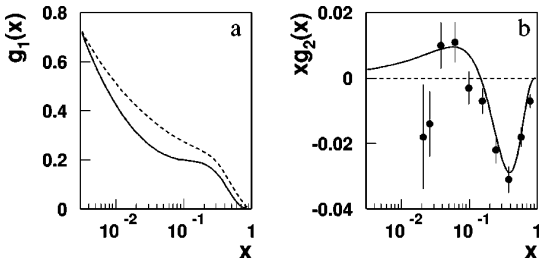

FIG. 1. Proton spin structure functions. Our calculation, which is represented by the full lines, is compared with the experimental data: dashed line (g_1) and full circles (g_2).

So the formulas obtained enable us to calculate the spin functions from input in which only the valence distributions are used. For simplicity we shall now consider only massless quarks ($x_0 \to 0$) and for the valence functions $xu_V(x)$ and $xd_V(x)$ we use the parametrization obtained (for $Q^2 = 4$ GeV$^2/c^2$) by the standard global analysis in [28]. In Fig. 1(a) we show the result of our calculation for g_1 according to Eq. (97) together with the experimental data represented by the new parametrization of the world data on g_1 [4] for $Q^2 = 4$ GeV$^2/c^2$. The calculation agrees well with the data qualitatively; however, it is apparent that the data are above our curve. This can be connected first of all with our simplification for $x_0 \to 0$, when Γ_1 is minimal. In accordance with Eq. (112) we obtain $\Gamma_1 \doteq 0.093$, but experimentally $\Gamma_1^p = 0.118 \pm 0.004(\text{stat}) \pm 0.007(\text{syst})$ at $Q^2 = 5$ GeV$^2/c^2$ [4]. Just this difference is exposed in the figure. Further, in Fig. 1(b) we show g_2 according to Eq. (98) and the precision measurement recently published by the E155 Collaboration [5]. The agreement with the data is very good and might suggest that the dependence of the function g_2 on the mass terms is rather weak. At least in our approach Γ_1 does depend on mass, but $\Gamma_2 = 0$ regardless of the mass. In Fig. 2 the corresponding spin distributions j, s_T, s_L are shown for the whole proton and also separately for u and d valence quarks

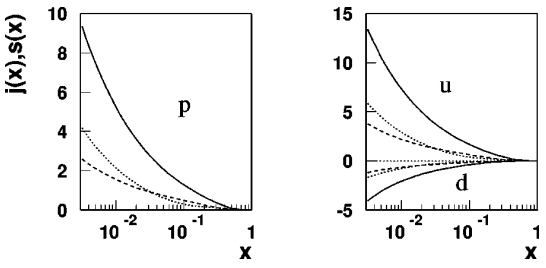

FIG. 2. Calculation of the spin densities of the valence quarks inside the proton (left) and separately the contributions from u and d quarks (right). Full lines represent the total angular momenta j, dotted and dashed lines correspond to longitudinal and transverse densities s_L and s_T.

corresponding to the assumed SU(6) symmetry, which gives the fractions (77). Figure 1(a) and the left part of Fig. 2 also demonstrate that $g_1(x)$ and $s_L(x)$ are not equivalent. The slightly different shape of the distributions on s_T and s_L is due to the variable x, in which longitudinal and transverse (in respect to the beam) quark momentum components are not involved in a symmetric way. Otherwise, for a given direction of the proton polarization, the quark spin density cannot depend on the direction from which the probing beam is coming.

Finally, let us remark that another possible effect, which can in our approach contribute to an underestimation of Γ_1, is connected with the assumption (77). For example, if one assumes full spin alignment of the u valence quarks, then

$$s_u=2, \quad s_d=-1, \tag{113}$$

and instead of the generic distribution (87) one gets

$$w_g(x)=\frac{4}{9}u_V(x)-\frac{1}{9}d_V(x), \quad \int_0^1 w_g(x)dx=\frac{7}{9}, \tag{114}$$

which implies $\Gamma_1=7/54\doteq 0.13$. Obviously, assuming isotopic symmetry, the same procedure can also be used for the neutron. For the isotopic counterparts of the compositions (77) and (113) one gets $\Gamma_1^n=0$ and $\Gamma_1^n=-1/27\doteq -0.037$, respectively. The composition (113) gives the maximum value Γ_1 for the proton and the minimum for the neutron.

V. SUMMARY AND CONCLUSION

With the use of a consistently covariant version of the naive QPM we have studied the spin structure functions together with the spin density distributions for a system of quasifree fermions having fixed effective mass $x_0=m/M$ and total spin $J=1/2$. The main results can be summarized as follows.

(1) We have shown that the corresponding spin structure functions $g_1(x)$ and $g_2(x)$ are mutually connected by a simple transformation. In the limit $x_0\to 0$ this transformation is identical to the Wanzura-Wilczek relation for the twist-2 term of the $g_2(x)$ approximation. At the same time for $x_0\to 0$ the relations for the nth momenta of the structure functions have been obtained. Their particular cases are identical to the known sum rules: the Wanzura-Wilczek sum rule ($n=2,4,6,\ldots$), the Efremov-Leader-Teryaev sum rule ($n=1$), and the Burkhardt-Cottingham sum rule ($n=0$). Further, we have shown how the structure functions are connected with the net spin densities $s_L(x), s_T(x)$ and with the density of the total angular momentum $j(x)$.

(2) The proposed approach was applied to a description of the proton spin structure with the assumption that the proton spin is generated only by the spins and orbital momenta of the valence quarks. Apart from that we assumed that the spin contributions from u and d valence quarks can be defined by the SU(6) symmetry and for the quark effective mass we used the approximation $x_0\to 0$. We suggested how one can in this approach obtain the spin functions from the valence quark distributions. Then as input we used the parametrization of the valence terms resulting from the standard global analysis. On this basis, without any other free parameter, the proton spin structure functions and related spin densities were calculated. Comparison of the obtained structure functions $g_1(x)$ and $g_2(x)$ with the experimental measurement demonstrates that the suggested approach well reproduces the basic features of the data on the proton spin structure.

To conclude, the results presented in this paper and the discussion in [22] suggest that both the proton structure functions g_1 and g_2 have a simple and natural interpretation even in terms of a naive QPM, provided that the model is based on a consistently covariant formulation, which takes into accounts spherical symmetry connected with the constraint $J=1/2$. This is not satisfied for the standard formulation of the QPM, which is based on one-dimensional kinematics related only to the preferred reference system (infinite momentum frame). As a result, there is, e.g., the known fact that the function $g_2(x)$ has no well-defined meaning in the standard naive QPM. In this case it is just a result of the simplified kinematics and not because of an absence of dynamics.

ACKNOWLEDGMENTS

I would like to thank Anatoli Efremov and Oleg Teryaev for many useful discussions and valuable comments.

APPENDIX A: PROOF OF THE RELATION (37)

The integral

$$F(x)=\int K(p_0)\,\delta\left(\frac{p_0+p_1}{M}-x\right)d^3p, \quad p_0=\sqrt{m^2+\mathbf{p}^2}, \tag{A1}$$

after the substitution

$$p_2=\sqrt{p_0^2-p_1^2-m^2}\,\sin\varphi, \quad p_3=\sqrt{p_0^2-p_1^2-m^2}\,\cos\varphi \tag{A2}$$

reads

$$F(x)=2\pi\int_m^{E_{\max}} K(p_0)p_0\left[\int_{-H}^{+H}\delta\left(\frac{p_0+p_1}{M}-x\right)dp_1\right]dp_0,$$

$$H=\sqrt{p_0^2-m^2}. \tag{A3}$$

For given x and p_0 the inner integral contributes only for

$$p_1=Mx-p_0 \tag{A4}$$

in the limits

$$-\sqrt{p_0^2-m^2}\leqslant p_1\leqslant\sqrt{p_0^2-m^2}. \tag{A5}$$

One can check that the last two conditions are compatible only for

$$p_0\geqslant\xi\equiv\frac{Mx}{2}+\frac{m^2}{2Mx}. \tag{A6}$$

It follows that Eq. (A3) can be simplified to

$$F(x)=2\pi M\int_{\xi}^{E_{\max}}K(p_0)p_0dp_0. \tag{A7}$$

According to the relation (A6) the parameter ξ is a function of x with a minimum at $x_0=m/M$, so for fixed ξ there are two roots of x,

$$x_{\pm}=\frac{\xi\pm\sqrt{\xi^2-m^2}}{M}, \tag{A8}$$

so that Eq. (A7) can be rewritten as

$$F\left(\frac{\xi\pm\sqrt{\xi^2-m^2}}{M}\right)=2\pi M\int_{\xi}^{E_{\max}}K(p_0)p_0dp_0. \tag{A9}$$

Then differentiation with respect to ξ gives

$$F'\left(\frac{\xi\pm\sqrt{\xi^2-m^2}}{M}\right)\left(\frac{1}{M}\pm\frac{\xi}{M\sqrt{\xi^2-m^2}}\right)=-2\pi MK(\xi)\xi \tag{A10}$$

and this relation can be, with the use of Eq. (A8), applied to the functions (36):

$$V_n'(x_{\pm})x_{\pm}=\mp 2\pi M^2H(\xi)\xi\sqrt{\xi^2-m^2}\left(\frac{\xi}{M}\right)^n, \tag{A11}$$

which with use of the relation (A6) implies the relation (37).

APPENDIX B: PROOF OF THE RELATIONS (38),(39)

In the relations (22)–(24) one can, due to the δ function, make the following substitutions. First,

$$p_1=Mx-p_0 \tag{B1}$$

and then from the relation

$$p_T^2=p_0^2-p_1^2-m^2 \tag{B2}$$

one gets

$$p_T^2=2Mxp_0-(M^2x^2+m^2). \tag{B3}$$

Now the relation (24) can be rewritten

$$g_1(x)+g_2(x)=\frac{1}{2}\left[x_0V_{-1}(x)+\int H(p_0)\times\left(\frac{Mxp_0-(M^2x^2+m^2)/2}{p_0(p_0+m)}\right)\times\delta\left(\frac{p_0+p_1}{M}-x\right)d^3p\right]. \tag{B4}$$

In the next step we expand the fraction

$$\frac{1}{p_0+m}=\frac{1}{p_0}\sum_{j=0}^{\infty}\left(-\frac{m}{p_0}\right)^j; \tag{B5}$$

then the relation (B4) can be expressed in terms of the functions (36) as

$$g_1(x)+g_2(x)=\frac{1}{2}\left[x_0V_{-1}(x)-\frac{x}{x_0}\sum_{j=1}^{\infty}(-x_0)^jV_{-j}(x)-\frac{x^2+x_0^2}{2x_0^2}\sum_{j=2}^{\infty}(-x_0)^jV_{-j}(x)\right] \tag{B6}$$

$$=\frac{1}{2}\left[(x+x_0)V_{-1}(x)-\frac{(x+x_0)^2}{2x_0^2}\times\sum_{j=2}^{\infty}(-x_0)^jV_{-j}(x)\right].$$

Further, from the relation (37) one obtains

$$V_{-j}(x)=-\int_x^1\left(\frac{2y}{y^2+x_0^2}\right)^jV_0'(y)dy \tag{B7}$$

and because

$$\sum_{j=2}^{\infty}\left(\frac{-2x_0y}{y^2+x_0^2}\right)^j=\frac{4x_0^2y^2}{(y+x_0)^2(y^2+x_0^2)} \tag{B8}$$

the relation (B6) can be modified

$$g_1(x)+g_2(x)=\frac{1}{2}\left[-(x+x_0)\int_x^1\frac{2y}{y^2+x_0^2}V_0'(y)dy+\frac{(x+x_0)^2}{2x_0^2}\int_x^1\frac{4x_0^2y^2}{(y+x_0)^2(y^2+x_0^2)}V_0'(y)dy\right]. \tag{B9}$$

Now, integration by parts gives

$$g_1(x)+g_2(x)=\frac{1}{2}\left[(x+x_0)\frac{2x}{x^2+x_0^2}-\frac{(x+x_0)^2}{2x_0^2}\frac{4x_0^2x^2}{(x+x_0)^2(x^2+x_0^2)}\right]V_0(x)+\frac{1}{2}\left[\int_x^1\left(-(x+x_0)\frac{2(y^2-x_0^2)}{(y^2+x_0^2)^2}+\frac{(x+x_0)^2}{2x_0^2}\frac{8x_0^2y(y^3-x_0^3)}{(y^2+x_0^2)^2(y+x_0)^3}\right)V_0(y)dy\right] \tag{B10}$$

and one can check that after some modifications the corresponding terms ahead of V_0 coincide with the functions (41).

The relation (38) can be proved by a similar procedure, so we suggest only the main steps:

$$g_2(x)=-\frac{1}{2}\Bigg[xV_{-1}(x)-V_0(x)+\int H(p_0)\times\left(\frac{p_0^2-3Mxp_0+(3M^2x^2+m^2)/2}{p_0(p_0+m)}\right)\times\delta\left(\frac{p_0+p_1}{M}-x\right)d^3p\Bigg],$$

$$g_2(x)=-\frac{1}{2}\Bigg[xV_{-1}(x)-V_0(x)+\sum_{j=0}^{\infty}(-x_0)^jV_{-j}(x)+3\frac{x}{x_0}\sum_{j=1}^{\infty}(-x_0)^jV_{-j}(x)+\frac{3x^2+x_0^2}{2x_0^2}\times\sum_{j=2}^{\infty}(-x_0)^jV_{-j}(x)\Bigg]$$

$$=-\frac{1}{2}\Bigg[-(2x+x_0)V_{-1}(x)+\frac{3(x+x_0)^2}{2x_0^2}\times\sum_{j=2}^{\infty}(-x_0)^jV_{-j}(x)\Bigg],$$

$$g_2(x)=-\frac{1}{2}\Bigg[(2x+x_0)\int_x^1\frac{2y}{y^2+x_0^2}V_0'(y)dy-\frac{3(x+x_0)^2}{2x_0^2}\int_x^1\frac{4x_0^2y^2}{(y+x_0)^2(y^2+x_0^2)}V_0'(y)dy\Bigg].$$

Then, integration by parts gives

$$g_2(x)=-\frac{1}{2}\Bigg[-(2x+x_0)\frac{2x}{x^2+x_0^2}+\frac{3(x+x_0)^2}{2x_0^2}\frac{4x_0^2x^2}{(x+x_0)^2(x^2+x_0^2)}\Bigg]V_0(x)-\frac{1}{2}\Bigg[\int_x^1\Bigg((2x+x_0)\frac{2(y^2-x_0^2)}{(y^2+x_0^2)^2}-\frac{3(x+x_0)^2}{2x_0^2}\frac{8x_0^2y(y^3-x_0^3)}{(y^2+x_0^2)^2(y+x_0)^3}\Bigg)V_0(y)dy\Bigg]$$

and one can check that the corresponding terms ahead of V_0 coincide with the functions (40).

APPENDIX C: PROOF OF THE RELATIONS (50)–(53)

First, if we define the functions

$$f_1(y)=\frac{y^2-x_0^2}{(y+x_0)^4x_0},\quad f_2(y)=\frac{y^2-x_0^2}{(y^2+x_0^2)^2x_0},\tag{C1}$$

$$f_3(x)=\frac{A(x)}{a(x)}=\frac{x_0}{x-x_0},\quad f_4(x)=A(x)+a(x)=\frac{2x^2}{x^2+x_0^2},\tag{C2}$$

then taking into account Eqs. (38)–(41), Eq. (49) can be rewritten

$$\Bigg[-(x+x_0)^2\int_x^1f_1(y)V_0(y)dy+(x^2-x_0^2)\int_x^1f_2(y)V_0(y)dy\Bigg]'+\Bigg[-f_3(x)3(x+x_0)^2\int_x^1f_1(y)V_0(y)dy+f_3(x)(3x^2+2xx_0+x_0^2)\int_x^1f_2(y)V_0(y)dy\Bigg]'$$
$$=c_1(x)f_4(x)V_0(x)+c_1(x)2(x+x_0)^2\int_x^1f_1(y)V_0(y)dy-c_1(x)2(x^2+xx_0+x_0^2)\int_x^1f_2(y)V_0(y)dy$$
$$-c_2(x)a(x)V_0(x)-c_2(x)3(x+x_0)^2\int_x^1f_1(y)V_0(y)dy+c_2(x)(3x^2+2xx_0+x_0^2)\int_x^1f_2(y)V_0(y)dy.\tag{C3}$$

After differentiating the LHS one gets

$$
\begin{aligned}
&-2(x+x_0)\int_x^1 f_1(y)V_0(y)dy+2x\int_x^1 f_2(y)V_0(y)dy\\
&-3x_0\frac{x^2-2xx_0-3x_0^2}{(x-x_0)^2}\int_x^1 f_1(y)V_0(y)dy+3x_0\frac{x^2-2xx_0-x_0^2}{(x-x_0)^2}\int_x^1 f_2(y)V_0(y)dy\\
&+[(x+x_0)^2f_1(x)-(x^2-x_0^2)f_2(x)+f_3(x)3(x+x_0)^2f_1(x)-f_3(x)(3x^2+2xx_0+x_0^2)f_2(x)]V_0(x)\\
&=c_1(x)\frac{2x^2}{x^2+x_0^2}V_0(x)+c_1(x)2(x+x_0)^2\int_x^1 f_1(y)V_0(y)dy-c_1(x)2(x^2+xx_0+x_0^2)\int_x^1 f_2(y)V_0(y)dy\\
&-c_2(x)2x\frac{x-x_0}{x^2+x_0^2}V_0(x)-c_2(x)3(x+x_0)^2\int_x^1 f_1(y)V_0(y)dy+c_2(x)(3x^2+2xx_0+x_0^2)\int_x^1 f_2(y)V_0(y)dy.
\end{aligned}
\tag{C4}
$$

This equality contains the three linearly independent terms

$$
V_0(x),\quad \int_x^1 f_1(y)V_0(y)dy,\quad \int_x^1 f_2(y)V_0(y)dy,
\tag{C5}
$$

and comparison of these terms on both the sides gives the equations

$$
c_1(x)x-c_2(x)(x-x_0)=-\frac{x+2x_0}{x+x_0},
\tag{C6}
$$

$$
2c_1(x)-3c_2(x)=-\frac{2x^2-xx_0-7x_0^2}{(x+x_0)(x-x_0)^2},
\tag{C7}
$$

$$
\begin{aligned}
&2c_1(x)(x^2+xx_0+x_0^2)-c_2(x)(3x^2+2xx_0+x_0^2)\\
&\quad=-\frac{2x^3-x^2x_0-4xx_0^2-3x_0^3}{(x-x_0)^2}.
\end{aligned}
\tag{C8}
$$

One can check that these three equations with the two unknowns c_1,c_2 are dependent and solvable, giving the solution (51).

Now, we can solve the differential equation (50) for g_1 or g_2. Its homogeneous version for g_1 reads

$$
g_1'(x)+\frac{x^2+4xx_0+x_0^2}{(x^2-x_0^2)(x+2x_0)}g_1(x)=0,
\tag{C9}
$$

which has the solution

$$
g_1(x)=C\frac{x+2x_0}{x^2-x_0^2}.
\tag{C10}
$$

The nonhomogeneous term [the part of Eq. (50) involving g_2] gives the equation for the function $C(x)$

$$
\begin{aligned}
C'(x)\frac{x+2x_0}{x^2-x_0^2}&=-\frac{x_0(x^2+xx_0+4x_0^2)}{(x-x_0)(x^2-x_0^2)(x+2x_0)}g_2(x)\\
&\quad-\left(\frac{x}{x-x_0}g_2(x)\right)',
\end{aligned}
\tag{C11}
$$

which has the solution

$$
C(x)=-x\frac{x+x_0}{x+2x_0}g_2(x)-\int_x^1 g_2(y)dy.
\tag{C12}
$$

After inserting this into Eq. (C10) one gets the relation (53). The inverse relation (52) can be proved in a similar way.

APPENDIX D: PROOF OF THE RELATIONS (65),(66)

The relations (38) and (39)

$$
\begin{aligned}
g_2(x)=-\Bigg[&x\frac{x-x_0}{x^2+x_0^2}V_0(x)+\int_x^1\Bigg(\frac{3(x+x_0)^2}{(y+x_0)^4}\\
&-\frac{3x^2+2xx_0+x_0^2}{(y^2+x_0^2)^2}\Bigg)\frac{y^2-x_0^2}{2x_0}V_0(y)dy\Bigg],
\end{aligned}
$$

$$
\begin{aligned}
g_1(x)+g_2(x)=\Bigg[&\frac{xx_0}{x^2+x_0^2}V_0(x)+\int_x^1\Bigg(-\frac{(x+x_0)^2}{(y+x_0)^4}\\
&+\frac{x^2-x_0^2}{(y^2+x_0^2)^2}\Bigg)\frac{y^2-x_0^2}{2x_0}V_0(y)dy\Bigg]
\end{aligned}
$$

can be combined in such a way that the second terms in the integrals cancel:

$$(3x^2+2xx_0+x_0^2)g_1(x)+2(x^2+xx_0+x_0^2)g_2(x)$$
$$=(x+2x_0)xV_0(x)-(x+2x_0)(x+x_0)^2$$
$$\times\int_x^1\frac{y^2-x_0^2}{(y+x_0)^4}V_0(y)dy. \quad \text{(D1)}$$

Further, this equation can be modified to

$$\frac{x}{(x+x_0)^2}V_0(x)-\int_x^1\frac{y^2-x_0^2}{(y+x_0)^4}V_0(y)dy$$
$$=\frac{3x^2+2xx_0+x_0^2}{(x+2x_0)(x+x_0)^2}g_1(x)+\frac{2(x^2+xx_0+x_0^2)}{(x+2x_0)(x+x_0)^2}g_2(x),$$

which implies a differential equation for $V_0(x)$:

$$\left(\frac{x}{(x+x_0)^2}V_0(x)\right)'+\frac{x^2-x_0^2}{(x+x_0)^4}V_0(x)$$
$$=\left(\frac{3x^2+2xx_0+x_0^2}{(x+2x_0)(x+x_0)^2}g_1(x)\right.$$
$$\left.+\frac{2(x^2+xx_0+x_0^2)}{(x+2x_0)(x+x_0)^2}g_2(x)\right)'. \quad \text{(D2)}$$

The corresponding homogeneous equation

$$\frac{x}{(x+x_0)^2}V_0'(x)=0 \quad \text{(D3)}$$

gives the solution

$$V_0(x)=C \quad \text{(D4)}$$

and for $C(x)$ we have the equation

$$\frac{x}{(x+x_0)^2}C'(x)=\left(\frac{3x^2+2xx_0+x_0^2}{(x+2x_0)(x+x_0)^2}g_1(x)\right.$$
$$\left.+\frac{2(x^2+xx_0+x_0^2)}{(x+2x_0)(x+x_0)^2}g_2(x)\right)'. \quad \text{(D5)}$$

The solution reads

$$V_0(x)=C(x)=\frac{3x^2+2xx_0+x_0^2}{(x+2x_0)x}g_1(x)$$
$$+\frac{2(x^2+xx_0+x_0^2)}{(x+2x_0)x}g_2(x)$$
$$+\int_x^1\frac{(3y^2+2yx_0+x_0^2)(y-x_0)}{(y+x_0)(y+2x_0)y^2}g_1(y)dy$$
$$+\int_x^1\frac{2(y^2+yx_0+x_0^2)(y-x_0)}{(y+x_0)(y+2x_0)y^2}g_2(y)dy. \quad \text{(D6)}$$

After inserting terms from Eq. (52) one gets

$$V_0(x)=\frac{3x^2+2xx_0+x_0^2}{(x+2x_0)x}g_1(x)+\frac{2(x^2+xx_0+x_0^2)}{(x+2x_0)x}\left(-\frac{x-x_0}{x}g_1(x)+\frac{x(x+2x_0)}{(x+x_0)^2}\int_x^1\frac{y^2-x_0^2}{y^3}g_1(y)dy\right)$$
$$+\int_x^1\frac{(3y^2+2yx_0+x_0^2)(y-x_0)}{(y+x_0)(y+2x_0)y^2}g_1(y)dy+\int_x^1\frac{2(y^2+yx_0+x_0^2)(y-x_0)}{(y+x_0)(y+2x_0)y^2}\left(-\frac{y-x_0}{y}g_1(y)\right.$$
$$\left.+\frac{y(y+2x_0)}{(y+x_0)^2}\int_y^1\frac{z^2-x_0^2}{z^3}g_1(z)dz\right)dy.$$

The double integral is calculated according to the formula

$$\int_x^1 a(y)\left(\int_y^1 b(z)dz\right)dy=\int_x^1(A(y)-A(x))b(y)dy,$$

$$A'(x)=a(x); \quad \text{(D7)}$$

then after collecting the corresponding terms with g_1 we obtain with the use of Eq. (64) the relation (65). A similar procedure with inserting terms from Eq. (53) into Eq. (D6) gives the relation (66).

APPENDIX E: PROOF OF THE RELATIONS (70),(71)

In the relation (69) one can, due to the δ function, make the substitution $p_1=Mx-p_0$. Then, using the definition (36), one obtains

$$s_L(x)=g_1(x)+\frac{1}{2}V_0(x)-\frac{1}{2}xV_{-1}(x). \quad \text{(E1)}$$

Further, the relation (37) implies that

$$V_{-1}(x)=\frac{2x}{x^2+x_0^2}V_0(x)-2\int_x^1\frac{y^2-x_0^2}{(y^2+x_0^2)^2}V_0(y)dy, \tag{E2}$$

which after inserting into Eq. (E1) gives

$$s_L(x)=g_1(x)-\frac{x^2-x_0^2}{2(x^2+x_0^2)}V_0(x)+x\int_x^1\frac{y^2-x_0^2}{(y^2+x_0^2)^2}V_0(y)dy. \tag{E3}$$

After inserting $V_0=2j(x)$ and using the relation (65) we obtain

$$\begin{aligned}s_L(x)=&\frac{1}{2}\frac{x^2+x_0^2}{x^2}g_1(x)-\frac{x^2-x_0^2}{2(x^2+x_0^2)}\frac{3x^2+2xx_0+3x_0^2}{(x+x_0)^2}\int_x^1\frac{y^2-x_0^2}{y^3}g_1(y)dy-\frac{x^2-x_0^2}{(x^2+x_0^2)}\int_x^1\ln\left(\frac{x(y+x_0)^2}{y(x+x_0)^2}\right)\frac{y^2-x_0^2}{y^3}g_1(y)dy\\&+x\int_x^1\frac{y^2-x_0^2}{(y^2+x_0^2)y^2}g_1(y)dy+x\int_x^1\frac{y^2-x_0^2}{(y^2+x_0^2)^2}\frac{3y^2+2yx_0+3x_0^2}{(y+x_0)^2}\int_y^1\frac{z^2-x_0^2}{z^3}g_1(z)dzdy\\&+2x\int_x^1\frac{y^2-x_0^2}{(y^2+x_0^2)^2}\int_y^1\ln\left(\frac{y(z+x_0)^2}{z(y+x_0)^2}\right)\frac{z^2-x_0^2}{z^3}g_1(z)dzdy.\end{aligned}$$

Then calculation of the double integrals with the use of the relation (D7) and collecting the corresponding terms with g_1 give the relation (70).

Further, one can insert g_1 from the relation (53) into the relation (70); then a similar procedure with double integrals gives the relation (71).

[1] E142 Collaboration, P. L. Anthony *et al.*, Phys. Rev. D **54**, 6620 (1996).
[2] E143 Collaboration, K. Abe *et al.*, Phys. Rev. D **58**, 112003 (1998).
[3] E154 Collaboration, K. Abe *et al.*, Phys. Rev. Lett. **79**, 26 (1997).
[4] E155 Collaboration, P. Anthony *et al.*, Phys. Lett. B **493**, 19 (2000).
[5] E155 Collaboration, P. Anthony *et al.*, hep-ex/0204028.
[6] Spin Muon Collaboration, B. Adeva *et al.*, Phys. Rev. D **58**, 112001 (1998).
[7] HERMES Collaboration, K. Ackerstaff *et al.*, Phys. Lett. B **404**, 383 (1997).
[8] HERMES Collaboration, A. Airapetian *et al.*, Phys. Lett. B **442**, 484 (1998).
[9] U. Stösslein, in *Proceedings of the X International Workshop on Deep Inelastic Scattering—DIS2002, Cracow, Poland* [Acta Phys. Pol. B **33**, 2813 (2002)].
[10] M. Anselmino, A. Efremov, and E. Leader, Phys. Rep. **261**, 1 (1995).
[11] V. Barone, A. Drago, and P. G. Ratcliffe, Phys. Rep. **359**, 1 (2002).
[12] S. J. Brodsky, Dae Sung Hwang, Bo-Qiang Ma, and I. Schmidt, Nucl. Phys. **B593**, 311 (2001).
[13] Bo-Qiang Ma and Ivan Schmidt, Phys. Rev. D **58**, 096008 (1998).
[14] Liang Zuo-tang and R. Rittel, Mod. Phys. Lett. A **12**, 827 (1997).
[15] Bo-Qiang Ma, J. Phys. G **17**, L53 (1991).
[16] Bo-Qiang Ma and Qi-Ren Zhang, Z. Phys. C **58**, 479 (1993).
[17] Bo-Qiang Ma, Phys. Lett. B **375**, 320 (1996).
[18] Bo-Qiang Ma, I. Schmidt, and J. Soffer, Phys. Lett. B **441**, 461 (1998).
[19] P. Zavada, Phys. Rev. D **55**, 4290 (1997).
[20] P. Zavada, Phys. Rev. D **56**, 5834 (1997).
[21] P. Zavada, Acta Phys. Slov. **49**, 273 (1999); updated version hep-ph/9810540.
[22] P. Zavada, Phys. Rev. D **65**, 054040 (2002).
[23] J. D. Jackson, G. G. Ross, and R. D. Roberts, Phys. Lett. B **226**, 159 (1989).
[24] S. Wanzura and W. Wilczek, Phys. Lett. **72B**, 195 (1977).
[25] H. Burkhardt and W. N. Cottingham, Ann. Phys. (N.Y.) **56**, 453 (1970).
[26] A. V. Efremov, O. V. Teryaev, and E. Leader, Phys. Rev. D **55**, 4307 (1997).
[27] O. Teryaev, B. Pire, and J. Soffer, hep-ph/9806502.
[28] A. D. Martin, W. J. Stirling, and R. G. Roberts, Phys. Rev. D **50**, 6734 (1994).

Eur. Phys. J. C 52, 121–131 (2007)
DOI 10.1140/epjc/s10052-007-0360-1

Article copy
THE EUROPEAN PHYSICAL JOURNAL C

Regular Article – Theoretical Physics

Parton distribution functions and quark orbital motion

P. Závada[a]

Institute of Physics, Academy of Sciences of the Czech Republic, Na Slovance 2, 182 21 Prague 8, Czech Republic

Received: 12 April 2007 / Revised version: 8 June 2007 /
Published online: 21 July 2007 – © Springer-Verlag / Società Italiana di Fisica 2007

Abstract. A covariant version of the quark–parton model is studied. The dependence of the structure functions and parton distributions on the 3D intrinsic motion of the quarks is discussed. The important role of the orbital momentum of the quark, which is a particular case of intrinsic motion, appears as a direct consequence of the covariant description. The effect of the orbital motion is substantial, especially for polarized structure functions. At the same time, the procedure for obtaining the momentum distributions of polarized quarks from the combination of polarized and unpolarized structure functions is suggested.

PACS. 13.60.-r; 13.88.+e; 14.65.-q

1 Introduction

The nucleon structure functions are a basic tool for understanding the internal structure of the nucleon in the language of QCD. At the same time, measurement and analysis of the structure functions represent an important experimental test of this theory. Unpolarized nucleon structure functions are known with high accuracy in a very broad kinematical region, but in recent years also some precision measurements on the polarized structure functions have been completed [1–8]. For the present status of the spin structure of the nucleon, see e.g. [9] and references therein. The more formal aspects of the structure functions of the nucleon are explained in [10]. In fact, only the complete set of the four electromagnetic unpolarized and polarized structure functions F_1, F_2, g_1 and g_2 can give a consistent picture of the nucleon. However, this picture is usually drawn in terms of the distribution functions, which are connected with the structure functions in some model-dependent way. Distribution functions are not directly accessible from experiment, and the model that is normally applied for their extraction from the structure functions is the well known quark–parton model (QPM). Application of this model to analysis and interpretation of the unpolarized data does not create any contradiction. On the other hand, the situation is much less clear in the case of the spin functions g_1 and g_2.

In our previous study [12, 13] we have suggested that a reasonable explanation of the experimentally measured spin functions g_1 and g_2 is possible in terms of a generalized covariant QPM in which the intrinsic motion of the quarks (i.e. 3D motion with respect to the nucleon rest frame) is consistently taken into account. Therefore the transversal momentum of the quarks appears in this approach on the same level as the longitudinal one. The quarks are represented by free Dirac spinors, which allows one to obtain an exact and covariant solution for the relations between the quark momentum distribution functions and the structure functions accessible from experiment. In this way the model (in its present LO version) contains no dynamics but only the "exact" kinematics of the quarks, so it can be an effective tool for analysis and interpretation of the experimental data on the structure functions, particularly for separating the effects of the dynamics (QCD) from the effects of the kinematics. This point of view is well supported by our previous results.

In the cited papers we showed that the model simply implies the well known sum rules (due to Wanzura–Wilczek, Efremov–Leader–Teryaev and Burkhardt–Cottingham) for the spin functions g_1, g_2. Simultaneously, we showed that the same set of assumptions implies a rather substantial dependence of the first moment Γ_1 of the function g_1 on the kinematical effects. Further, we showed that the model allows one to calculate the functions g_1 and g_2 from the unpolarized valence quark distributions, and the result is quite compatible with the experimental data. In [14] we showed that the model allows one to relate the transversity distribution to some other structure functions.

These results cannot be obtained from the standard versions of the QPM (naive or QCD improved), which are currently used for the analysis of experimental data on the structure functions. The reason is that the standard QPM is based on the simplified and non-covariant kinematics in the infinite momentum frame (IMF), which does not allow

[a] e-mail: zavada@fzu.cz

one to properly take into account the intrinsic or orbital motion of the quarks.

The subject of our previous study was the question: what is the dependence of the structure functions on the intrinsic motion of the quarks? The aim of the present paper is a discussion of related problems: how can one extract information about the intrinsic motion of the quarks from the experimentally measured structure functions? What is the role of the orbital momentum of the quarks, which is a particular case of the intrinsic motion?

The paper is organized as follows. In the first part of Sect. 2 the basic formulas, which follow from the generalized QPM, are presented. The general covariant relations are compared with their limiting case, which is represented by the standard formulation of the QPM in the IMF. In the next part of the section we calculate the 3D momentum distributions of the quarks and the structure functions are used as the input. The momentum distributions of positively and negatively polarized quarks are separately obtained from the combination of the structure functions F_2 and g_1 or the corresponding parton distributions $q(x)$ and $\Delta q(x)$. A particular form of intrinsic motion of the quarks is the orbital momentum. In Sect. 3 the role of the orbital momentum of the quark in covariant description is discussed, and it is shown why its contribution to the total angular momentum of the quark can be quite substantial. It is demonstrated that the orbital motion is an inseparable part of the covariant approach. The last section is devoted to a short summary and to our conclusions. In fact, this paper is inspired by many previous papers, see e.g. [15–27], in which the problem of the orbital momentum of the quarks in the context of nucleon spin was recognized and studied.

2 Structure functions and intrinsic quark motion

In our previous study [11–13] of the proton structure functions we showed how these functions depend on the intrinsic motion of the quarks. The quarks in the suggested model are represented by free fermions, which are in the rest frame of the nucleon described by a set of distribution functions with spheric symmetry, $G_k^{\pm}(p_0)\,\mathrm{d}^3p$, where $p_0=\sqrt{m^2+\mathbf{p}^2}$, and the symbol k represents the quark and antiquark flavors. These distributions measure the probability to find a quark of given flavor in the state

$$u(\mathbf{p},\lambda\mathbf{n})=\frac{1}{\sqrt{N}}\begin{pmatrix}\phi_{\lambda\mathbf{n}}\\ \frac{\mathbf{p}\sigma}{p_0+m}\phi_{\lambda\mathbf{n}}\end{pmatrix};$$
$$\frac{1}{2}\mathbf{n}\sigma\phi_{\lambda\mathbf{n}}=\lambda\phi_{\lambda\mathbf{n}}\,,\qquad N=\frac{2p_0}{p_0+m}\,, \tag{1}$$

where m and p are the quark mass and momentum, $\lambda=\pm1/2$, $\phi^\dagger_{\lambda\mathbf{n}}\phi_{\lambda\mathbf{n}}=1$ and $\mathbf{n}$ coincides with the direction of the polarization of the nucleon. The distributions together with the corresponding quark (and antiquark) charges e_k allow one to define the generic functions G and ΔG[1]:

$$G(p_0)=\sum_k e_k^2 G_k(p_0)\,,\qquad G_k(p_0)\equiv G_k^+(p_0)+G_k^-(p_0)\,, \tag{2}$$

$$\Delta G(p_0)=\sum_k e_k^2\Delta G_k(p_0)\,,\quad \Delta G_k(p_0)\equiv G_k^+(p_0)-G_k^-(p_0)\,, \tag{3}$$

from which the structure functions can be obtained. If q is the momentum of the photon absorbed by the nucleon of momentum P and mass M, in which the phase space of the quarks is controlled by the distributions $G_k^{\pm}(p_0)\,\mathrm{d}^3p$, then there are the following representations of the corresponding LO structure functions.

Manifestly covariant representation

First we have the unpolarized structure functions:

$$F_1(x)=\frac{M}{2}\left(A+\frac{B}{\gamma}\right),\quad F_2(x)=\frac{Pq}{2M\gamma}\left(A+\frac{3B}{\gamma}\right), \tag{4}$$

where

$$A=\frac{1}{Pq}\int G\left(\frac{Pp}{M}\right)[pq-m^2]\delta\left(\frac{pq}{Pq}-x\right)\frac{\mathrm{d}^3p}{p_0}\,, \tag{5}$$

$$B=\frac{1}{Pq}\int G\left(\frac{pP}{M}\right)\left[\left(\frac{Pp}{M}\right)^2+\frac{(Pp)(Pq)}{M^2}-\frac{pq}{2}\right]\times\delta\left(\frac{pq}{Pq}-x\right)\frac{\mathrm{d}^3p}{p_0} \tag{6}$$

and

$$\gamma=1-\left(\frac{Pq}{Mq}\right)^2. \tag{7}$$

The functions $F_1=MW_1$ and $F_2=(Pq/M)W_2$ follow from the tensor equation

$$\left(-g_{\alpha\beta}+\frac{q_\alpha q_\beta}{q^2}\right)W_1+\left(P_\alpha-\frac{Pq}{q^2}q_\alpha\right)\left(P_\beta-\frac{Pq}{q^2}q_\beta\right)\frac{W_2}{M^2}$$
$$=\int G\left(\frac{pP}{M}\right)[2p_\alpha p_\beta+p_\alpha q_\beta+q_\alpha p_\beta-g_{\alpha\beta}pq]\times\delta\left((p+q)^2-m^2\right)\frac{\mathrm{d}^3p}{p_0}\,. \tag{8}$$

[1] In [12, 13] we used a different notation for the distributions defined by (2) and (3): $G_k^{\pm}$, ΔG_k and ΔG were denoted $h_{k\pm}$, Δh_k and H. Apart from that we assumed for simplicity that only three (valence) quarks contribute to the sums (2) and (3). In the present paper we assume contributions of all the quarks and antiquarks, but apparently the general form of relations (4)–(7) and (10)–(12) is in the LO approach independent of the chosen set of quarks.

The modification of the delta function term

$$\begin{aligned}\delta((p+q)^2-m^2) &= \delta(2pq+q^2)\\ &= \delta\left(2Pq\left(\frac{pq}{Pq}-\frac{Q^2}{2Pq}\right)\right)\\ &= \frac{1}{2Pq}\delta\left(\frac{pq}{Pq}-x\right),\\ q^2=-Q^2,\qquad x&=\frac{Q^2}{2Pq}\,, \end{aligned} \tag{9}$$

introduces the dependence on the Bjorken variable x. Then contracting with the tensors $g_{\alpha\beta}$ and $P_\alpha P_\beta$ gives the set of two equations, which determine the functions F_1 and F_2 in accordance with (4)–(7).

Next, we treat the polarized structure functions. As follows from [12] the corresponding spin functions in covariant form read

$$g_1 = Pq\left(G_S-\frac{Pq}{qS}G_P\right),\quad g_2=\frac{(Pq)^2}{qS}G_P\,, \tag{10}$$

where S is the spin polarization vector of the nucleon, and the functions G_P and G_S are defined by

$$\begin{aligned}G_P = \frac{m}{2Pq}\int &\Delta G\left(\frac{pP}{M}\right)\frac{pS}{pP+mM}\\ &\times\left[1+\frac{1}{mM}\left(pP-\frac{pu}{qu}Pq\right)\right]\delta\left(\frac{pq}{Pq}-x\right)\frac{\mathrm{d}^3p}{p_0}\,,\end{aligned} \tag{11}$$

$$\begin{aligned}G_S = \frac{m}{2Pq}\int &\Delta G\left(\frac{pP}{M}\right)\left[1+\frac{pS}{pP+mM}\frac{M}{m}\left(pS-\frac{pu}{qu}qS\right)\right]\\ &\times\delta\left(\frac{pq}{Pq}-x\right)\frac{\mathrm{d}^3p}{p_0}\,,\end{aligned} \tag{12}$$

$$u = q+(qS)S-\frac{(Pq)}{M^2}P\,.$$

Rest frame representation

We now come to the rest frame representation for $Q^2 \gg 4M^2x^2$. As follows from the appendix in [12], if $Q^2 \gg 4M^2x^2$ and the above integrals are expressed in terms of the rest frame variables of the nucleon, then one can substitute

$$\frac{pq}{Pq}\to\frac{p_0+p_1}{M}\,,$$

and the structure functions are simplified as follows:

$$F_1(x) = \frac{Mx}{2}\int G(p_0)\delta\left(\frac{p_0+p_1}{M}-x\right)\frac{\mathrm{d}^3p}{p_0}\,, \tag{13}$$

$$F_2(x) = Mx^2\int G(p_0)\delta\left(\frac{p_0+p_1}{M}-x\right)\frac{\mathrm{d}^3p}{p_0}\,, \tag{14}$$

$$\begin{aligned}g_1(x) = \frac{1}{2}\int &\Delta G(p_0)\left(m+p_1+\frac{p_1^2}{p_0+m}\right)\\ &\times\delta\left(\frac{p_0+p_1}{M}-x\right)\frac{\mathrm{d}^3p}{p_0}\,,\end{aligned} \tag{15}$$

$$\begin{aligned}g_2(x) = -\frac{1}{2}\int &\Delta G(p_0)\left(p_1+\frac{p_1^2-p_\mathrm{T}^2/2}{p_0+m}\right)\\ &\times\delta\left(\frac{p_0+p_1}{M}-x\right)\frac{\mathrm{d}^3p}{p_0}\,,\end{aligned} \tag{16}$$

where p_1 and p_T are the longitudinal and transversal momentum components of the quark. These structure functions consist of terms like

$$q(x) = Mx\int G_q(p_0)\delta\left(\frac{p_0+p_1}{M}-x\right)\frac{\mathrm{d}^3p}{p_0}\,, \tag{17}$$

$$\begin{aligned}\Delta q(x) = \int &\Delta G_q(p_0)\left(m+p_1+\frac{p_1^2}{p_0+m}\right)\\ &\times\delta\left(\frac{p_0+p_1}{M}-x\right)\frac{\mathrm{d}^3p}{p_0}\,,\end{aligned} \tag{18}$$

which correspond to the contributions from different quark flavors, $q = u, \bar{u}, d, \bar{d}, s, \bar{s}, \ldots$ Let us remark, in the limit of the IMF approach (see next paragraph), that these functions represent probabilistic distributions of the quark momentum in terms of the fraction x of the momentum of the nucleon, $p = xP$. However, the content and interpretation of the functions (17) and (18) depending on the Bjorken variable x is more complex; their form reflects in a nontrivial way the intrinsic 3D motion of quarks.

Standard IMF representation

On the standard IMF representation we remark the following. The usual formulation of the QPM gives the known relations between the structure functions and the parton distribution functions [10]:

$$F_1(x) = \frac{1}{2}\sum_q e_q^2 q(x)\,,\qquad F_2(x) = x\sum_q e_q^2 q(x)\,, \tag{19}$$

$$g_1(x) = \frac{1}{2}\sum_q e_q^2\Delta q(x),\quad g_2(x) = 0\,, \tag{20}$$

where the functions

$$q(x) = q^+(x)+q^-(x)\,,\quad \Delta q(x) = q^+(x)-q^-(x) \tag{21}$$

represent probabilistic distributions of the momentum fraction x of the quark in the IMF. In Appendix A we have proved that these relations represent the particular, limit case of the covariant relations (4) and (10).

The three versions of the relations between the structure functions and the quark distributions can be compared. If we skip the function g_2 in the IMF representation, then the relations (19) and (20) practically represent the identity between the structure functions and distributions of the quark momentum fraction. Such simple relations are valid only for the IMF approach based on the approximation (A.1), which means that the intrinsic motion of the quarks is suppressed. In the more general versions (the covariant and the rest frame representation), where the intrinsic motion is allowed, the relations

are more complex. The intrinsic motion strongly modifies also the g_2. In the standard IMF representation one has $g_2(x)=0$, but $g_2(x)\neq 0$ in the covariant and the rest frame representations.

The rest frame representation allows one to easily calculate the dependence of the first moment Γ_1 on the rate of intrinsic motion. A more detailed discussion follows in the next section. The same approach implies that the functions g_1 and g_2 for massless quarks satisfy a relation equivalent to the Wanzura–Wilczek term and obey some well known sum rules, as is shown in [12].

The functions F_1 and F_2 exactly satisfy the Callan–Gross relation $F_2(x)/F_1(x)=2x$ in the rest frame and the IMF representations, but this relation is satisfied only approximately in the manifestly covariant representation: $F_2(x)/F_1(x)\approx 2x+O(4M^2x^2/Q^2)$.

The task which was solved in the different approximations above can be formulated as follows: how can one obtain the structure functions F_1, F_2 and g_1, g_2 from the probabilistic distributions G and ΔG defined by (2) and (3)? But now we will study the inverse problem; the aim is to find a rule for obtaining the distribution functions G and ΔG from the structure functions. In the present paper we consider the functions F_2 and g_1 represented by (14) and (15). As follows from Appendix A in [13], the function

$$V_n(x)=\int K(p_0)\left(\frac{p_0}{M}\right)^n\delta\left(\frac{p_0+p_1}{M}-x\right)\mathrm{d}^3p \qquad (22)$$

satisfies

$$V_n'(x_\pm)x_\pm=\mp 2\pi MK(\xi)\xi\sqrt{\xi^2-m^2}\left(\frac{\xi}{M}\right)^n;$$
$$x_\pm=\frac{\xi\pm\sqrt{\xi^2-m^2}}{M}. \qquad (23)$$

In this section we consider only the case $m\to 0$; then we have

$$V_n'(x)x=-2\pi MK(\xi)\xi^2\left(\frac{\xi}{M}\right)^n;\quad x=\frac{2\xi}{M}. \qquad (24)$$

As we shall see below, with the use of this relation one can obtain the probabilistic distributions $G(p)$ and $\Delta G(p)$ from the experimentally measured structure functions. The same procedure will be applied to get $G_q(p)$ and $\Delta G_q(p)$ from the usual parton distributions $q(x)$ and $\Delta q(x)$, defined by (19) and (20).

Let us remark that in the present stage QCD evolution is not included into the model. However, this fact does not represent any restriction for the present purpose: to obtain information about the distributions of the quarks at some scale Q^2 from the structure functions measured at the same Q^2. The distribution of the gluons is another part of the nucleon picture. But since our present discussion is directed to the relation between the structure functions and the corresponding distributions of the quarks at a given scale, the gluon distribution is left aside.

2.1 Momentum distribution from structure function F_2

In accordance with the definition (22), in which the distribution $K(p_0)$ is substituted for by $G(p_0)$, the structure function (14) can be written in the form

$$F_2(x)=x^2V_{-1}(x). \qquad (25)$$

Then, with the use of (24), one gets

$$G(p)=-\frac{1}{\pi M^3}\left(\frac{F_2(x)}{x^2}\right)'=\frac{1}{\pi M^3x^2}\left(\frac{2F_2(x)}{x}-F_2'(x)\right);$$
$$x=\frac{2p}{M},\qquad p\equiv\sqrt{\mathbf{p}^2}=p_0, \qquad (26)$$

which in terms of the quark distributions means

$$G_q(p)=-\frac{1}{\pi M^3}\left(\frac{q(x)}{x}\right)'=\frac{1}{\pi M^3x^2}(q(x)-xq'(x)). \qquad (27)$$

The probability distribution G_q measures the number of quarks of flavor q in the element d^3p. Since $\mathrm{d}^3p=4\pi p^2\,\mathrm{d}p$, the distribution measuring the number of quarks in the element $\mathrm{d}p/M$ reads

$$P_q(p)=4\pi p^2MG_q(p)=-x^2\left(\frac{q(x)}{x}\right)'=q(x)-xq'(x). \qquad (28)$$

The probability distribution $G_q(p)$ is positive, so the last relation implies

$$\left(\frac{q(x)}{x}\right)'\le 0. \qquad (29)$$

Let us note that the maximum value of the momentum of the quark is $p_{\max}=M/2$, which is a consequence of the kinematics in the nucleon rest frame, where the single quark momentum must be compensated by the momentum of the other partons.

Another quantity that can be obtained is the distribution of the transversal momentum of the quarks. Obviously the integral

$$\frac{\mathrm{d}N_q}{\mathrm{d}p_\mathrm{T}^2}=\int G_q(p)\delta\left(p_2^2+p_3^2-p_\mathrm{T}^2\right)\mathrm{d}^3p, \qquad (30)$$

which represents the number of quarks in the element $\mathrm{d}p_\mathrm{T}^2$, can be modified as

$$\frac{\mathrm{d}N_q}{\mathrm{d}p_\mathrm{T}^2}=2\pi\int_0^{\sqrt{p_{\max}^2-p_\mathrm{T}^2}}G_q\left(\sqrt{p_1^2+p_\mathrm{T}^2}\right)\mathrm{d}p_1. \qquad (31)$$

It follows that the distribution corresponding to the number of quarks in the element $\mathrm{d}p_\mathrm{T}/M$ reads

$$P_q(p_\mathrm{T})=M\frac{\mathrm{d}N_q}{\mathrm{d}p_\mathrm{T}}=4\pi p_\mathrm{T}M\int_0^{\sqrt{p_{\max}^2-p_\mathrm{T}^2}}G_q\left(\sqrt{p_1^2+p_\mathrm{T}^2}\right)\mathrm{d}p_1. \qquad (32)$$

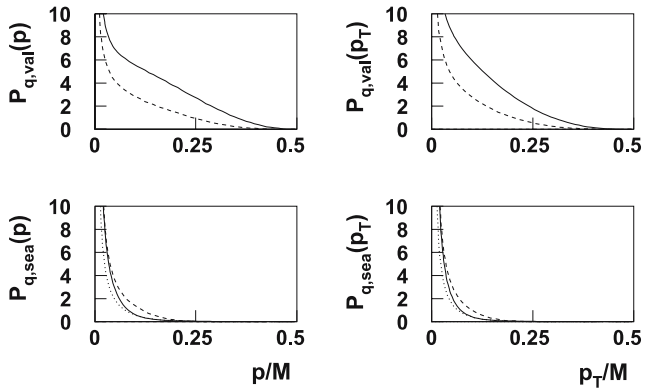

Fig. 1. The quark momentum distributions in the rest frame of the proton: the p and p_{T} distributions for valence quarks $P_{q,\mathrm{val}} = P_q - P_{\bar{q}}$ and sea quarks $P_{\bar{q}}$ at $Q^2 = 4\,\mathrm{GeV}^2$. Notation: $u, \bar{u}$ is indicated by a *solid line*, $d, \bar{d}$ by a *dashed line* and $\bar{s}$ by a *dotted line*

Then, with the use of (28), one gets the distribution

$$P_q(p_{\mathrm{T}}) = \frac{4p_{\mathrm{T}}}{M^2}\int_0^{\sqrt{p_{\max}^2 - p_{\mathrm{T}}^2}} \frac{1}{x^2}(q(x) - xq'(x))\,\mathrm{d}p_1\,,$$
$$x = \frac{2\sqrt{p_1^2 + p_{\mathrm{T}}^2}}{M}\,. \tag{33}$$

In Fig. 1 the distributions (28) and (33) are displayed for the valence and sea quarks. As input we used the standard parameterization [28] of the parton distribution functions $q(x)$ and $\bar{q}(x)$ (LO at the scale $4\,\mathrm{GeV}^2$). The resulting distributions P_q and $P_{\bar{q}}$ are positive, and this means that the input distributions q and $\bar{q}$ satisfy the constraint (29).

Using (27) one can calculate the mean values

$$\langle p\rangle_q = \frac{\int pG_q(p)\,\mathrm{d}^3p}{\int G_q(p)\,\mathrm{d}^3p} = \frac{M}{2}\frac{\int_0^1 x(q(x) - xq'(x))\,\mathrm{d}x}{\int_0^1 (q(x) - xq'(x))\,\mathrm{d}x}\,. \tag{34}$$

In the case of sea quarks extrapolation of the distribution functions for $x \to 0$ gives a divergent integral in the denominator, and it follows that $\langle p\rangle_{\mathrm{sea}} \to 0$. For the valence quarks $q_{\mathrm{val}} = q - \bar{q}$ this integral converges and integration by parts gives

$$\langle p\rangle_{q,\mathrm{val}} = \frac{3M}{4}\frac{\int_0^1 xq_{\mathrm{val}}(x)\,\mathrm{d}x}{\int_0^1 q_{\mathrm{val}}(x)\,\mathrm{d}x}\,. \tag{35}$$

Calculation of $\langle p\rangle_{q,\mathrm{val}}$ gives roughly $0.11\,\mathrm{GeV}/c$ for u and $0.083\,\mathrm{GeV}/c$ for d quarks. Since $G_q(p)$ has rotational symmetry, the average transversal momentum can be calculated to be $\langle p_{\mathrm{T}}\rangle = \pi/4 \cdot \langle p\rangle$.

2.2 Momentum distribution from structure function g_1

In (44) of [13] we proved that

$$g_1(x) = V_0(x) - \int_x^1 \left(4\frac{x^2}{y^3} - \frac{x}{y^2}\right)V_0(y)\,\mathrm{d}y\,, \tag{36}$$

where the function V_0 is defined by (22) for $n = 0$ and $K(p) = \Delta G(p)$. In Appendix B it is shown that the last relation can be modified to:

$$V_{-1}(x) = \frac{2}{x}\left(g_1(x) + 2\int_x^1 \frac{g_1(y)}{y}\,\mathrm{d}y\right). \tag{37}$$

Then, in an accordance with (24), we obtain

$$V'_{-1}(x) = -\pi M^3 \Delta G(p)\,, \quad x = \frac{2p}{M}\,, \tag{38}$$

$$\Delta G(p) = -\frac{2}{\pi M^3}\left[\frac{1}{x}\left(g_1(x) + 2\int_x^1 \frac{g_1(y)}{y}\,\mathrm{d}y\right)\right]' \tag{39}$$

or

$$\Delta G(p) = \frac{2}{\pi M^3 x^2}\left(3g_1(x) + 2\int_x^1 \frac{g_1(y)}{y}\,\mathrm{d}y - xg'_1(x)\right). \tag{40}$$

Now we substitute

$$\Delta q(x) = 2g_1(x)\,,$$
$$g_1(x) + g_2(x) = \int_x^1 \frac{g_1(y)}{y}\,\mathrm{d}y = \Delta q_{\mathrm{T}}(x)/2 \tag{41}$$

and next we shall consider the flavors separately. The second equality represents the Wanzura–Wilczek relation for the twist-2 approximation of g_2, which is valid for the present approach, as proved in [13]. Now (40) in terms of the quark distributions reads

$$\Delta G_q(p) = \frac{1}{\pi M^3 x^2}\left(3\Delta q(x) + 2\int_x^1 \frac{\Delta q(y)}{y}\,\mathrm{d}y - x\Delta q'(x)\right), \tag{42}$$

or, equivalently, with the use of (39) and (41),

$$\Delta G_q(p) = -\frac{1}{\pi M^3}\left(\frac{\Delta q(x) + 2\Delta q_{\mathrm{T}}(x)}{x}\right)'; \quad x = \frac{2p}{M}\,. \tag{43}$$

Obviously the distribution ΔG_q together with the distribution (27) allows one to obtain the polarized distributions $G_q^{\pm}$ as follows:

$$G_q^{\pm}(p) = \frac{1}{2}(G_q(p) \pm \Delta G_q(p))\,. \tag{44}$$

The distributions ΔG_q and $G_q^{\pm}$ measure the number of quarks in the element d^3p. They can be replaced, similarly as the distribution G_q in (28), by the distributions ΔP_q and $P_q^{\pm}$, measuring the number of quarks in the element $\mathrm{d}p/M$:

$$\Delta P_q(p) = 3\Delta q(x) + 2\int_x^1 \frac{\Delta q(y)}{y}\,\mathrm{d}y - x\Delta q'(x)\,, \tag{45}$$

$$P_q^{\pm}(p) = \frac{1}{2}(q(x) - xq'(x)) \pm \left(\frac{3}{2}\Delta q(x) + \int_x^1 \frac{\Delta q(y)}{y}\,\mathrm{d}y - \frac{x}{2}\Delta q'(x)\right). \tag{46}$$

Obviously the probability distributions should satisfy

$$|\Delta G_q(p)| \le G_q(p)\,, \tag{47}$$

which after inserting the results from (43) and (27) implies

$$\left|\left(\frac{\Delta q(x)+2\Delta q_{\rm T}(x)}{x}\right)'\right| \le -\left(\frac{q(x)}{x}\right)', \tag{48}$$

where positivity of the right hand side was required in (29). Another self-consistency test of the approach is represented by the inequality

$$|\Delta q(x)| \le q(x)\,, \tag{49}$$

which is proved in Appendix C.

With the use of (17) one can formally calculate the partial structure functions corresponding to the subsets of positively and negatively polarized quarks:

$$f_q^{\pm}(x) = Mx\int G_q^{\pm}(p)\delta\left(\frac{p_0+p_1}{M}-x\right)\frac{{\rm d}^3p}{p_0}\,. \tag{50}$$

Apparently the following equation holds:

$$f_q(x) \equiv f_q^+(x)+f_q^-(x) = q(x)\,, \tag{51}$$

and one can also define

$$\Delta f_q(x) = f_q^+(x)-f_q^-(x)\,, \tag{52}$$

or, equivalently,

$$\Delta f_q(x) = Mx\int \Delta G_q(p)\delta\left(\frac{p_0+p_1}{M}-x\right)\frac{{\rm d}^3p}{p_0}\,. \tag{53}$$

Obviously we have

$$f_q^{\pm}(x) = \frac{1}{2}(f_q(x)\pm\Delta f_q(x))\,, \tag{54}$$

and (47) implies

$$|\Delta f_q(x)| \le q(x)\,. \tag{55}$$

Let us note that $f_q^+ + f_q^- = q$, but $f_q^+ - f_q^- \ne \Delta q$ in the sense of (17) and (18). The last inequality is replaced by equality only in the limit of the IMF approach. The relation (53) can be written

$$\Delta f_q(x) = xV_{q,-1}(x)\,, \tag{56}$$

where

$$V_{q,-1}(x) = M\int \Delta G_q(p)\delta\left(\frac{p_0+p_1}{M}-x\right)\frac{{\rm d}^3p}{p_0}\,. \tag{57}$$

At the same time (37) can be replaced by

$$V_{q,-1}(x) = \frac{1}{x}\left(\Delta q(x)+2\int_x^1\frac{\Delta q(y)}{y}\,{\rm d}y\right), \tag{58}$$

which, after inserting the result from (56), gives

$$\Delta f_q(x) = \Delta q(x)+2\int_x^1\frac{\Delta q(y)}{y}\,{\rm d}y. \tag{59}$$

This equality together with (55) gives

$$\left|\Delta q(x)+2\int_x^1\frac{\Delta q(y)}{y}\,{\rm d}y\right| \le q(x)\,, \tag{60}$$

or, equivalently,

$$|\Delta q(x)+2\Delta q_{\rm T}(x)| \le q(x)\,. \tag{61}$$

Now, using the input on $q(x)$ [28] and $\Delta q(x)$ [29] (LO at the scale $4\,{\rm GeV}^2$) one can calculate the distributions ΔP_q, P_q and $P_q^{\pm}$ and the related structure functions Δf_q, f_q and $f_q^{\pm}$. The result is displayed in Fig. 2 and one can observe the following.

Positivity of the distributions $P_q^{\pm}$ and $f_q^{\pm}$ implies that the self-consistency tests (47) and (55) and their equivalents (48) and (60) are satisfied with the exception of a small negative disturbance in $G_u^-(P_u^-)$ and f_u^-. A possible reason is that the results of the two different procedures for fitting $q(x)$ and $\Delta q(x)$ are combined and some uncertainty is unavoidable.

The mean value of the distribution ΔG_q can be estimated to be

$$\langle p\rangle_q = \frac{\int p\Delta G_q(p)\,{\rm d}^3p}{\int \Delta G_q(p)\,{\rm d}^3p} = \frac{M}{2}\frac{\int_0^1 x\Delta q(x)\,{\rm d}x}{\int_0^1\Delta q(x)\,{\rm d}x}\,. \tag{62}$$

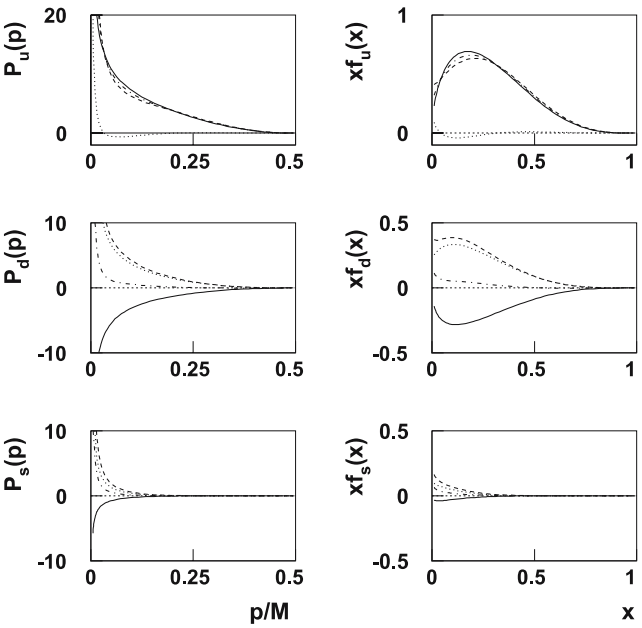

Fig. 2. The probability distributions ΔP_q, P_q, P_q^+ and P_q^- of the u, d, s quarks, and the related structure functions Δf_q, f_q, f_q^+ and f_q^- are represented by the *solid*, *dashed*, *dash-and-dot* and *dotted lines*

The proof of this relation is given in Appendix D. The numerical calculation gives $0.090\,\mathrm{GeV}/c$ for the u and $0.070\,\mathrm{GeV}/c$ for the d quarks. These numbers are well comparable with those calculated from (35), which correspond to the valence quarks. Also the shape of the distributions $x\Delta f_u(x)$ and $x\Delta f_d(x)$ is very similar to that of the valence terms. In other words, the results confirm that the spin contribution of the quarks comes dominantly from the valence region.

Due to the input values with $\Delta u(x) > 0$ and $\Delta d(x) < 0$ one can expect that $P_u^+ \geq P_u^-$, $P_d^- \geq P_d^+$, $f_u^+ \geq f_u^-$ and $f_d^- \geq f_d^+$. Besides, the curves in the figure show that P_u^-, P_d^+, f_u^- and f_d^+ are close to zero, at least in the valence region.

3 Intrinsic quark motion and orbital momentum

The rules of quantum mechanics say that angular momentum consists of an orbital and a spin part, $\mathbf{j} = \mathbf{l} + \mathbf{s}$, and that in the relativistic case the quantities $\mathbf{l}$ and $\mathbf{s}$ are not conserved separately, but only the total angular momentum $\mathbf{j}$ is conserved. This simple fact was in the context of quarks inside the nucleon pointed out in [30]. It means that only j^2 and j_z are well-defined quantum numbers and the corresponding states of the particle with spin $1/2$ are represented by the bispinor spherical waves [31]

$$\psi_{kjlj_z}(\mathbf{p}) = \frac{\delta(p-k)}{p\sqrt{2p_0}} \begin{pmatrix} \mathrm{i}^{-l}\sqrt{p_0+m}\,\Omega_{jlj_z}(\omega) \\ \mathrm{i}^{-\lambda}\sqrt{p_0-m}\,\Omega_{j\lambda j_z}(\omega) \end{pmatrix}, \qquad (63)$$

where $\omega = \mathbf{p}/p$, $l = j \pm \frac{1}{2}$, $\lambda = 2j - l$ (l defines the parity) and

$$\Omega_{j,l,j_z}(\omega) = \begin{pmatrix} \sqrt{\frac{j+j_z}{2j}}\,Y_{l,j_z-1/2}(\omega) \\ \sqrt{\frac{j-j_z}{2j}}\,Y_{l,j_z+1/2}(\omega) \end{pmatrix}; \qquad l = j - \frac{1}{2},$$

$$\Omega_{j,l,j_z}(\omega) = \begin{pmatrix} -\sqrt{\frac{j-j_z+1}{2j+2}}\,Y_{l,j_z-1/2}(\omega) \\ \sqrt{\frac{j+j_z+1}{2j+2}}\,Y_{l,j_z+1/2}(\omega) \end{pmatrix}; \quad l = j + \frac{1}{2}.$$

The states are normalized by

$$\int \psi^\dagger_{k'j'l'j'_z}(\mathbf{p})\psi_{kjlj_z}(\mathbf{p})\,\mathrm{d}^3p = \delta(k-k')\delta_{jj'}\delta_{ll'}\delta_{j_zj'_z}. \quad (64)$$

The wavefunction (63) is simplified for $j = j_z = 1/2$ and $l = 0$. Taking into account that

$$Y_{00} = \frac{1}{\sqrt{4\pi}}, \qquad Y_{10} = \mathrm{i}\sqrt{\frac{3}{4\pi}}\cos\theta,$$
$$Y_{11} = -\mathrm{i}\sqrt{\frac{3}{8\pi}}\sin\theta\exp(\mathrm{i}\varphi),$$

one gets

$$\psi_{kjlj_z}(\mathbf{p}) = \frac{\delta(p-k)}{p\sqrt{8\pi p_0}} \begin{pmatrix} \sqrt{p_0+m}\begin{pmatrix}1\\0\end{pmatrix} \\ -\sqrt{p_0-m}\begin{pmatrix}\cos\theta \\ \sin\theta\exp(\mathrm{i}\varphi)\end{pmatrix} \end{pmatrix}. \qquad (65)$$

Let us note that $j = 1/2$ is the minimum angular momentum for a particle with spin $1/2$. If one considers the quark state as a superposition,

$$\Psi(\mathbf{p}) = \int a_k\psi_{kjlj_z}(\mathbf{p})\,\mathrm{d}k, \quad \int a_k^\star a_k\,\mathrm{d}k = 1, \qquad (66)$$

then its average spin contribution to the total angular momentum reads

$$\langle s\rangle = \int \Psi^\dagger(\mathbf{p})\Sigma_z\Psi(\mathbf{p})\,\mathrm{d}^3p, \quad \Sigma_z = \frac{1}{2}\begin{pmatrix}\sigma_z & \cdot \\ \cdot & \sigma_z\end{pmatrix}. \quad (67)$$

After inserting (65) and (66) into (67) one gets

$$\langle s\rangle = \int a_p^\star a_p \frac{(p_0+m)+(p_0-m)(\cos^2\theta-\sin^2\theta)}{16\pi p^2 p_0}\,\mathrm{d}^3p$$
$$= \frac{1}{2}\int a_p^\star a_p\left(\frac{1}{3}+\frac{2m}{3p_0}\right)\mathrm{d}p. \qquad (68)$$

Since $j = 1/2$, the last relation implies for the orbital momentum of the quark that

$$\langle l\rangle = \frac{1}{3}\int a_p^\star a_p\left(1-\frac{m}{p_0}\right)\mathrm{d}p. \qquad (69)$$

This means that for quarks in the state $j = j_z = 1/2$ there are the following extreme scenarios.

Either one has massive and static quarks ($p_0 = m$), which implies that $\langle s\rangle = j = 1/2$ and $\langle l\rangle = 0$. This is evident, since without kinetic energy no orbital momentum can be generated.

But another possibility is that one has massless quarks ($m \ll p_0$), which implies that $\langle s\rangle = 1/6$ and $\langle l\rangle = 1/3$.

Generally, for $p_0 \geq m$, one gets $1/3 \leq \langle s\rangle/j \leq 1$. In other words, for the states with $p_0 > m$, part of the total angular momentum $j = 1/2$ is necessarily generated by the orbital momentum. This is a consequence of quantum mechanics, and not a consequence of the particular model. If one assumes the effective mass of the quark to be of the order of thousandths and the intrinsic momentum to be of the order of tenths of GeV, which is a quite realistic assumption, then the second scenario is clearly preferred. Further, the mean kinetic energy corresponding to the superposition (66) reads

$$\langle E_{\mathrm{kin}}\rangle = \int a_p^\star a_p E_{\mathrm{kin}}\,\mathrm{d}p; \quad E_{\mathrm{kin}} = p_0 - m, \qquad (70)$$

and at the same time (69) can be rewritten

$$\langle l\rangle = \frac{1}{3}\int a_p^\star a_p\frac{E_{\mathrm{kin}}}{p_0}\,\mathrm{d}p. \qquad (71)$$

It is evident that for fixed $j = 1/2$ both quantities are almost equivalent in the nucleon rest frame: more kinetic energy generates more orbital momentum and vice versa.

Further, the average spin part $\langle s \rangle$ of the total angular momentum $j = 1/2$ related to a single quark according to (68) can be compared to the integral

$$\Gamma_1 = \int_0^1 g_1(x)\,\mathrm{d}x\,, \tag{72}$$

which measures the total quark spin contribution to the spin of the nucleon. For g_1 in (15) this integral reads

$$\Gamma_1 = \frac{1}{2}\int \Delta G(p_0)\left(\frac{1}{3}+\frac{2m}{3p_0}\right)\mathrm{d}^3p\,. \tag{73}$$

The dependence of the integrals (68) and (73) on the intrinsic motion is controlled by the same term $(1/3 + 2m/3p_0)$, which in both cases has its origin in the covariant kinematics of the particle with $s = 1/2$. In fact, the procedures for the calculation of these integrals are based on the two different representations of the solutions of the Dirac equation: plane waves (1) and spherical waves (65). It is apparent that for the scenario of massless quarks ($m \ll p_0$), due to the necessary presence of the orbital motion, both numbers Γ_1 and $\langle s \rangle$ are roughly three times less than for the scenario of massive and static quarks ($m \simeq p_0$). What is the underlying physics behind the interplay between the spin and orbital momentum? Actually, speaking about the spin of the particle represented by the state (1), one should take into account the following.

The definite projection of the spin in the direction $\mathbf{n}$ is a well-defined quantum number only for the particle at rest ($p = 0$) or for the particle moving in the direction $\mathbf{n}$, i.e. $\mathbf{p}/p = \pm\mathbf{n}$. In these cases we have

$$s = u^\dagger(\mathbf{p}, \lambda\mathbf{n})\mathbf{n}\boldsymbol{\Sigma}u(\mathbf{p}, \lambda\mathbf{n}) = \pm 1/2\,. \tag{74}$$

But in other cases, as shown in Appendix E, only the inequality

$$\langle s \rangle = |u^\dagger(\mathbf{p}, \lambda\mathbf{n})\mathbf{n}\boldsymbol{\Sigma}u(\mathbf{p}, \lambda\mathbf{n})| < 1/2 \tag{75}$$

is satisfied. Roughly speaking, the result of measuring the spin of a quark depends on its momentum in the given reference frame (the rest frame of the nucleon). This obvious effect acts also in the states that are represented by the superposition of plane waves (1) with different momenta $\mathbf{p}$ and resulting in $\langle \mathbf{p} \rangle = 0$, but with $\langle \mathbf{p}^2 \rangle > 0$. In [12] we showed that averaging of the spin projection (75) over the spherical momentum distribution gives the result equivalent to (73). The state (66) can also be decomposed into plane waves having a spherical momentum distribution and the spin mean value given by (68). The well-defined quantum numbers $j = j_z = 1/2$ imply that the spin reduction due to an increasing intrinsic kinetic energy is compensated by an increasing orbital momentum.

Now, what does the preferred scenario of massless quarks ($\langle m/p_0 \rangle \ll 1$) imply for the spin structure of the whole nucleon, and what are the integral quark spin and orbital contributions to the spin of the nucleon? Obviously, using some input on the total quark longitudinal polarization $\Delta\Sigma$, one can estimate the relative quark spin and orbital contributions to be

$$S = \Delta\Sigma\,, \quad L = 2\Delta\Sigma\,, \quad \Delta\Sigma = \sum_q \int_0^1 \Delta q(x)\,\mathrm{d}x\,. \tag{76}$$

At the same time our approach can be compared with the calculation based on the chiral quark soliton model (CQSM) [24, 25], in which a significant role for the orbital momentum of the quark is assumed as well. In Table 1 some results of both models are shown. In spite of some similarity between the two sets of numbers, there are substantial differences between both approaches. Let us mention at least the two that seem to be most evident.

Table 1. Relative integral contributions of the quark spins (S), orbital momenta (L) and their sum (J) to the total spin of the nucleon. Results are shown of our calculation (*right*) and the prediction of the CQSM model (*left*)

	CQSM		Present paper	
	$Q^2 = 0.3\,\mathrm{GeV}^2$	$Q^2 = 4\,\mathrm{GeV}^2$	$\Delta\Sigma = 0.2$	$\Delta\Sigma = 0.3$
S [%]	35.0	31.8	20.0	30.0
L [%]	65.0	35.8	40.0	60.0
J [%]	100.0	67.6	60.0	90.0

First, the presence of a significant fraction of the orbital momentum in the CQSM apparently follows from the dynamics inherent in the model. On the other hand, in our approach the important role of the orbital momentum follows from the kinematics, so it should not be too sensitive to the details of the inherent dynamics. Actually the effect takes place in LO when quarks interacting with the probing photon can be effectively described as free fermions in states like (66) with a sufficiently low effective ratio $\langle m/p_0 \rangle$, which controls the fraction of orbital momentum (69). Of course, the value of this ratio itself is a question of the dynamics.

Second, in the CQSM antiquarks are predicted to have opposite signs for the spin and orbital contributions. In our approach the two contributions are proportional and have the same signs regardless of flavor or antiflavor.

A last comment concerns the total angular momentum of the quarks, J, by which room for the gluon contribution J_g is defined. Results in Table 1 related to the CQSM suggest that a higher Q^2 implies a greater gluon contribution. Our results suggest that the gluon contribution can be rather sensitive to the longitudinal polarization: for $\Delta\Sigma \simeq 1/3$, 0.3 and 0.2 the gluon contribution can represent $\simeq 0$, 10 and 40%, respectively. So the value empirically known [25],

$$\Delta\Sigma \simeq 0.2\text{–}0.35\,, \tag{77}$$

does not exclude any of these possibilities.

4 Summary and conclusion

We studied a covariant version of the QPM with spherically symmetric distributions of the quark momentum in the rest frame of the nucleon. The main results obtained in this paper can be summarized as follows.

The relations between the distribution functions $q(x)$, $\Delta q(x)$ and the corresponding 3D momentum distributions $G_q^{\pm}(p) = G_q(p) \pm \Delta G_q(p)$ of the quarks are obtained. In this way the momentum distributions of the positively and negatively polarized quarks $G_q^{\pm}(p)$ are calculated from the experimentally measured structure functions F_2 and g_1. At the same time these relations, due to positivity of the probabilistic distributions G_q and $G_q^{\pm}$, imply some inequalities for $q(x)$ and $\Delta q(x)$. We proved that these constraints, serving as self-consistency tests of the approach, are satisfied.

Next, we showed that an important role of the orbital momentum of the quark emerges as a direct consequence of a covariant description. Since in the relativistic case only the total angular momentum $\mathbf{j} = \mathbf{l} + \mathbf{s}$ is a well-defined quantum number, there arises some interplay between its spin and orbital parts. For the quark in the state, $j_z = 1/2$, as a result of this interplay its spin part is reduced in favor of the orbital one. The role of the orbital motion increases with the rate of the intrinsic motion of the quark; for $\langle m/p_0 \rangle \ll 1$ its fraction reaches $\langle l_z \rangle = 2/6$, whereas $\langle s_z \rangle = 1/6$ only. Simultaneously this effect is truly reproduced also in the formalism of structure functions, and in this connection some implications for the global spin structure of the nucleon were suggested.

Acknowledgements. This work was supported by the project AV0Z10100502 of the Academy of Sciences of the Czech Republic. I am grateful to Anatoli Efremov and Oleg Teryaev for many useful discussions and valuable comments.

Appendix A: Structure functions in the approach of the infinite momentum frame

The necessary condition for obtaining the equalities (19) and (20) is the covariant relation

$$p_\alpha = yP_\alpha \,, \tag{A.1}$$

which implies

$$m = yM \,, \tag{A.2}$$

and $\mathbf{p} = 0$ in the rest frame of the nucleon and $p_{\mathrm{T}} = 0$ in the IMF.

For the calculation of the integrals (5) and (6) in the IMF approach one can substitute p by yP, and d^3p/p_0 by $\pi\,\mathrm{d}p_{\mathrm{T}}^2\,\mathrm{d}y/y$. Then, after some algebra the structure functions (4) read

$$\begin{aligned} F_1(x) &= \frac{1}{2}Mx \int G(yM)\delta(y-x)\pi\,\mathrm{d}p_{\mathrm{T}}^2 \frac{\mathrm{d}y}{y} \,, \\ F_2(x) &= Mx^2 \int G(yM)\delta(y-x)\pi\,\mathrm{d}p_{\mathrm{T}}^2 \frac{\mathrm{d}y}{y} \,. \end{aligned} \tag{A.3}$$

Since the approximation (A.1) implies a sharply peaked distribution at $p_{\mathrm{T}}^2 \to 0$, one can identify

$$MG_q(yM)\pi\,\mathrm{d}p_{\mathrm{T}}^2 = q(y) \,, \tag{A.4}$$

and then (19) and (A.3) after integrating are equivalent.

In the same way the equalities (10)–(12) can be modified. Taking into account that $pS \to yPS = 0$, one obtains

$$g_1(x) = \frac{m}{2} \int \Delta G(yM)\delta(y-x)\pi\,\mathrm{d}p_{\mathrm{T}}^2 \frac{\mathrm{d}y}{y} \,, \quad g_2(x) = 0 \,. \tag{A.5}$$

If we put

$$M\Delta G_q(yM)\pi\,\mathrm{d}p_{\mathrm{T}}^2 = \Delta q(y) \tag{A.6}$$

and take into account (A.2), then it is obvious that (20) and (A.5) are equivalent.

Appendix B: Proof of (37)

In [13] we proved the relation

$$\frac{V_j'(x)}{V_k'(x)} = \left(\frac{x}{2} + \frac{x_0^2}{2x}\right)^{j-k} \,; \quad x_0 = \frac{m}{M} \,, \tag{B.1}$$

which for $m \to 0$ implies

$$V_0(x) = \frac{1}{2}\left(xV_{-1}(x) + \int_0^x V_{-1}(y)\,\mathrm{d}y\right) . \tag{B.2}$$

After inserting V_0 from this relation into (36) one gets

$$\begin{aligned} g_1(x) = {} & \frac{1}{2}\left(xV_{-1}(x) + \int_0^x V_{-1}(y)\,\mathrm{d}y\right) \\ & - 2x^2\left(\int_x^1 \frac{V_{-1}(y)}{y^2}\,\mathrm{d}y + \int_x^1 \frac{1}{y^3}\int_y^1 V_{-1}(z)\,\mathrm{d}z\,\mathrm{d}y\right) \\ & + \frac{1}{2}x\left(\int_x^1 \frac{V_{-1}(y)}{y}\,\mathrm{d}y + \int_x^1 \frac{1}{y^2}\int_y^1 V_{-1}(z)\,\mathrm{d}z\,\mathrm{d}y\right) . \end{aligned} \tag{B.3}$$

The double integrals can be reduced by integration by parts with the use of

$$\begin{aligned} \int_x^1 a(y)\left(\int_y^1 b(z)\,\mathrm{d}z\right)\mathrm{d}y &= \int_x^1 (A(y) - A(x))b(y)\,\mathrm{d}y \,, \\ A'(x) &= a(x) \,, \end{aligned} \tag{B.4}$$

and then (B.3) is simplified:

$$g_1(x) = \frac{1}{2}xV_{-1}(x) - x^2\int_x^1 \frac{V_{-1}(y)}{y^2}\,\mathrm{d}y\,. \tag{B.5}$$

In the next step we extract V_{-1} from this relation. After the substitution $V(x) = V_{-1}(x)/x$, the relation reads

$$\frac{g_1(x)}{x^2} = \frac{1}{2}V(x) - \int_x^1 \frac{V(y)}{y}\,\mathrm{d}y\,, \tag{B.6}$$

which implies the differential equation for $V(x)$:

$$\frac{1}{2}V'(x) + \frac{V(x)}{x} = \left(\frac{g_1(x)}{x^2}\right)'. \tag{B.7}$$

The corresponding homogeneous equation

$$\frac{1}{2}V'(x) + \frac{V(x)}{x} = 0 \tag{B.8}$$

gives the solution

$$V(x) = \frac{C}{x^2}\,, \tag{B.9}$$

which after inserting into (B.7) gives

$$C'(x) = 2x^2\left(\frac{g_1(x)}{x^2}\right)'. \tag{B.10}$$

After integration one easily gets the relation inverse to (B.5):

$$V_{-1}(x) = \frac{2}{x}\left(g_1(x) + 2\int_x^1 \frac{g_1(y)}{y}\,\mathrm{d}y\right), \tag{B.11}$$

which coincides with (37).

Appendix C: Proof of (49)

The relations (17) and (18) imply that the inequality (49) is satisfied if

$$p_0 + p_1 \geq \left|m + p_1 + \frac{p_1^2}{p_0+m}\right| = \left|p_0 + p_1 - \frac{p_\mathrm{T}^2}{p_0+m}\right|. \tag{C.1}$$

There are two cases.

First, $p_0 + p_1 - p_\mathrm{T}^2/(p_0+m) \geq 0$; then instead of (C.1) one can write

$$p_0 + p_1 \geq p_0 + p_1 - \frac{p_\mathrm{T}^2}{p_0+m}\,, \tag{C.2}$$

which is always satisfied.

Second, $p_0 + p_1 - p_\mathrm{T}^2/(p_0+m) < 0$; then (C.1) is equivalent to

$$p_0 + p_1 \geq -p_0 - p_1 + \frac{p_\mathrm{T}^2}{p_0+m} \Leftrightarrow 2(p_0+p_1) \geq \frac{p_\mathrm{T}^2}{p_0+m}\,. \tag{C.3}$$

Since

$$\begin{aligned} 2p_0 \geq p_0 - p_1 &\Rightarrow 2(p_0+m) \geq p_0 - p_1 \\ &\Rightarrow 2(p_0+m)(p_0+p_1) \geq (p_0-p_1)(p_0+p_1) \\ &\Rightarrow 2(p_0+m)(p_0+p_1) \geq p_\mathrm{T}^2 \\ &\Rightarrow 2(p_0+p_1) \geq \frac{p_\mathrm{T}^2}{p_0+m}\,, \end{aligned}$$

(C.3) is always satisfied. In this way (C.1) and (49) are proved.

Appendix D: Proof of (62)

The relation (40) implies

$$\int \Delta G_q(p)\,\mathrm{d}^3p = \frac{1}{2}\int_0^1 \left(3\Delta q(x) + 2\int_x^1 \frac{\Delta q(y)}{y}\,\mathrm{d}y - x\Delta q'(x)\right)\mathrm{d}x \tag{D.1}$$

and

$$\int p\Delta G_q(p)\,\mathrm{d}^3p = \frac{M}{4}\int_0^1 \left(3x\Delta q(x) + 2x\int_x^1 \frac{\Delta q(y)}{y}\,\mathrm{d}y - x^2\Delta q'(x)\right)\mathrm{d}x\,. \tag{D.2}$$

If one denotes

$$\Gamma_1^q = \int_0^1 \Delta q(x)\,\mathrm{d}x\,, \quad \Gamma_2^q = \int_0^1 x\Delta q(x)\,\mathrm{d}x\,, \tag{D.3}$$

then integration by parts gives

$$\int_0^1\int_x^1 \frac{\Delta q(y)}{y}\,\mathrm{d}y\,\mathrm{d}x = \Gamma_1^q\,, \quad \int_0^1 x\Delta q'(x)\,\mathrm{d}x = -\Gamma_1^q \tag{D.4}$$

and

$$\int_0^1 2x\int_x^1 \frac{\Delta q(y)}{y}\,\mathrm{d}y\,\mathrm{d}x = \Gamma_2^q\,, \quad \int_0^1 x^2\Delta q'(x)\,\mathrm{d}x = -2\Gamma_2^q\,. \tag{D.5}$$

Now, one can easily express the ratio:

$$\frac{\int p\Delta G_q(p)\,\mathrm{d}^3p}{\int \Delta G_q(p)\,\mathrm{d}^3p} = \frac{M}{2}\frac{\Gamma_2^q}{\Gamma_1^q}\,, \tag{D.6}$$

and in this way (62) is proved.

Appendix E: Proof of (75)

With the use of the rule

$$\mathbf{p}\sigma\cdot\mathbf{n}\sigma+\mathbf{n}\sigma\cdot\mathbf{p}\sigma=2\mathbf{pn} \tag{E.1}$$

the term in (75) can be modified as follows:

$$\begin{aligned}
&u^\dagger(\mathbf{p},\lambda\mathbf{n})\mathbf{n}\boldsymbol{\Sigma}u(\mathbf{p},\lambda\mathbf{n})\\
&=\frac{1}{2N}\phi^\dagger_{\lambda\mathbf{n}}\left(\mathbf{n}\sigma+\frac{\mathbf{p}\sigma\cdot\mathbf{n}\sigma\cdot\mathbf{p}\sigma}{(p_0+m)^2}\right)\phi_{\lambda\mathbf{n}}\\
&=\frac{1}{2N}\phi^\dagger_{\lambda\mathbf{n}}\left(\mathbf{n}\sigma+\frac{\mathbf{p}\sigma\cdot(-\mathbf{p}\sigma\cdot\mathbf{n}\sigma+2\mathbf{pn})}{(p_0+m)^2}\right)\phi_{\lambda\mathbf{n}}\\
&=\frac{1}{2N}\phi^\dagger_{\lambda\mathbf{n}}\left(\mathbf{n}\sigma\left(\mathbf{1}-\frac{\mathbf{p}^2}{(p_0+m)^2}\right)+\frac{2\mathbf{pn}\cdot\mathbf{p}\sigma}{(p_0+m)^2}\right)\phi_{\lambda\mathbf{n}}\\
&=\frac{1}{2p_0}\phi^\dagger_{\lambda\mathbf{n}}\left(m\cdot\mathbf{n}\boldsymbol{\Sigma}+\frac{\mathbf{pn}\cdot\mathbf{p}\sigma}{p_0+m}\right)\phi_{\lambda\mathbf{n}}\,.
\end{aligned}\tag{E.2}$$

Since

$$\left|\phi^\dagger_{\lambda\mathbf{n}}\mathbf{n}\sigma\phi_{\lambda\mathbf{n}}\right|=1\,,\quad \left|\phi^\dagger_{\lambda\mathbf{n}}\mathbf{p}\sigma\phi_{\lambda\mathbf{n}}\right|\le p\,,\quad \mathbf{pn}=p\cos\alpha\,, \tag{E.3}$$

it follows that

$$|u^\dagger(\mathbf{p},\lambda\mathbf{n})\mathbf{n}\boldsymbol{\Sigma}u(\mathbf{p},\lambda\mathbf{n})|\le\frac{1}{2p_0}\left(m+\frac{p^2}{p_0+m}\right)=\frac{1}{2}\,. \tag{E.4}$$

Obviously

$$|u^\dagger(\mathbf{p},\lambda\mathbf{n})\mathbf{n}\boldsymbol{\Sigma}u(\mathbf{p},\lambda\mathbf{n})|=\frac{1}{2} \tag{E.5}$$

only for $\mathbf{p}/p=\pm\mathbf{n}$ or $p=0$.

References

1. E142 Collaboration, P.L. Anthony et al., Phys. Rev. D **54**, 6620 (1996)
2. E154 Collaboration, K. Abe et al., Phys. Rev. Lett. **79**, 26 (1997)
3. HERMES Collaboration, K. Ackerstaff et al., Phys. Lett. B **404**, 383 (1997)
4. HERMES Collaboration, A. Airapetian et al., Phys. Lett. B **442**, 484 (1998)
5. Spin Muon Collaboration, B. Adeva et al., Phys. Rev. D **58**, 112001 (1998)
6. E143 Collaboration, K. Abe et al., Phys. Rev. D **58**, 112003 (1998)
7. E155 Collaboration, P. Anthony et al., Phys. Lett. B **493**, 19 (2000)
8. E155 Collaboration, P. Anthony et al., Phys. Lett. B **553**, 18 (2003)
9. K. Imai et al., (Eds.), Proc. 17th International Spin Physics Symposium – SPIN 2006, Kyoto, Japan, 2–7 October 2006 (American Institute of Physics, New York, 2007)
10. M. Anselmino, A.V. Efremov, E. Leader, Phys. Rep. **261**, 1 (1995)
11. P. Zavada, Phys. Rev. D **55**, 4290 (1997)
12. P. Zavada, Phys. Rev. D **65**, 0054040 (2002)
13. P. Zavada, Phys. Rev. D **67**, 014019 (2003)
14. A.V. Efremov, O.V. Teryaev, P. Zavada, Phys. Rev. D **70**, 054018 (2004) [hep-ph/0512034]
15. L.M. Sehgal, Phys. Rev. D **10**, 1663 (1974)
16. L.M. Sehgal, Phys. Rev. D **10**, 2016 (1974) [Erratum]
17. P.G. Ratcliffe, Phys. Lett. B **192**, 180 (1987)
18. A. Abbas, J. Phys. G **16**, L21 (1990)
19. A. Abbas, J. Phys. G **15**, L73 (1989)
20. J. Keppler, H.M. Hofmann, Phys. Rev. D **51**, 3936 (1995)
21. M. Casu, L.M. Sehgal, Phys. Rev. D **55**, 2644 (1996)
22. B.-Q. Ma, I. Schmidt, Phys. Rev. D **58**, 096008 (1998)
23. S.J. Brodsky, D.S. Hwang, B.-Q. Ma, I. Schmidt, Nucl. Phys. B **593**, 311 (2001)
24. M. Wakamatsu, T. Watabe, Phys. Rev. D **62**, 054009 (2000)
25. M. Wakamatsu, Y. Nakakoji, Phys. Rev. D **74**, 054006 (2006)
26. X. Song, Int. J. Mod. Phys. A **16**, 3673 (2001)
27. X. Ji, J.-P. Ma, F. Yuan, Nucl. Phys. B **652**, 383 (2003)
28. A.D. Martin, R.G. Roberts, W.J. Stirling, R.S. Thorne, hep-ph/0411040
29. E. Leader, A.V. Sidorov, D.B. Stamenov, Phys. Rev. D **73**, 034023 (2006)
30. Z. Liang, T. Meng, Z. Phys. A **344**, 171 (1992)
31. L.D. Landau, E.M. Lifshitz et al., Quantum Electrodynamics, Course of Theoretical Physics, vol. 4 (Elsevier Butterworth Heinemann, Oxford, 1982)

3.2 Nepolarizované strukturní funkce

Nejprve porovnáme nepolarizované funkce, které vyplývají z nekovariantní a kovariantní formulace QPM. Vyjdeme přitom z následující tabulky:

	nekovariantní QPM	kovariantní QPM
distribuční funkce	$q(x)$	$G_q\left(\frac{pP}{M}\right)$
forma strukturní funkce F_2 :	$x\sum_q e_q^2 q(x)$	$Mx^2\sum_q e_q^2 \int G_q(p_0)$ $\times\delta\left(\frac{p_0+p_1}{M}-x\right)\frac{d^3p}{p_0}$
Callan-Gross: $F_2/F_1=2x$	ano	ano
nepolarizované TMDs	ne	ano

Nekovariantní formulace

Jednoduchý vztah mezi strukturními a distribučními funkcemi vede k tomu, že se oba pojmy často zaměňují. Distribuční funkce $q(x)$ reprezentují pravděpodobnost, že podíl impulsu daného kvarku na impulsu nukleonu je roven x. Jak ovšem bylo řečeno v komentáři ke vztahu (1.7), jedná se fakticky o zjednodušení kinematiky kvarku do jedné dimenze. Přesto se toto zjednodušení v případě analýzy nepolarizovaných strukturních funkcí osvědčuje. Velmi důležitou vlastnost funkce F_2, tzv. „narušení škálování“ (viz část 2.2) lze v případě nekovariantního QPM velmi dobře reprodukovat zavedením korekcí z pQCD. V tomto přiblížení lze na základě znalosti distribučních funkcí $q(x,Q^2)$ při dané škále Q_0^2 vypočítat jejich průběh při jiné hodnotě Q^2. Tento postup dává konzistentní výsledky ve velmi široké oblasti x, Q^2, v níž jsou dnes strukturní funkce $F_2(x,Q^2)$ s vysokou přesností změřeny. Šíře této oblasti je patrná z obrázku 2.3.

Kovariantní formulace

Výchozí distribuční funkce $G_q(\mathbf{p})d^3p$ reprezentuje pravděpodobnostní 3D rozdělení hybností kvarků. Současně se předpokládá sférická symetrie tohoto rozdělení v klidové soustavě nukleonu, tento předpoklad má i hlubší teoretické zdůvodnění. V klidové soustavě se tedy pracuje s distribuční funkcí $G_q(p_0)d^3p$, která charakterizuje vnitřní pohyb kvarků. V libovolné vztažné soustavě distribuční funkce závisí na invariantní proměnné pP/M, v klidové soustavě se tento výraz redukuje na p_0. Od odpovídající kovariantní strukturní funkce lze k jejímu nekovariantnímu protějšku (vlevo) dospět limitním přechodem, při němž je vnitřní pohyb kvarků potlačen. Distribuční a strukturní funkce v kovariantní verzi rovněž obecně závisí na proměnné Q^2, avšak alespoň v současnosti algoritmus pro výpočet evoluce (analog k ‘DGLAP evolution equations’) nemáme k dispozici. Za přednosti kovariantního přístupu pro nepolarizované funkce lze však zatím považovat:

1) Ze strukturní funkce změřené v experimentu lze v daném přiblížení zrekonstruovat 3D rozdělení hybností kvarků v klidové (nebo jakékoli jiné) referenční soustavě. Příznivou okolností je přitom skutečnost, že příslušný integrál lze analyticky invertovat [A9], viz část 3.1.5.

2) 'Transverse momentum dependent parton distributions' (TMDs) jsou funkce obsahující informaci o vnitřním pohybu kvarků uvnitř nukleonu. Zájem o jejich studium značně vzrůstá v posledních několika letech. V naší zcela nedávné práci [A10], viz část 3.5.1, jsme mimo jiné ukázali, že kovariantní model nabízí pro jejich studium zvláště příznivý rámec. Dalším výsledkem jsou pravidla, která ukazují vztah mezi 1D a 3D distribučními funkcemi [A13], viz část 3.5.4. Na druhé straně nekovariantní model, ve kterém jsou příčné hybnosti kvarků zcela potlačeny, stěží může být vhodným rámcem pro studium TMDs.

3) Z formálního hlediska je třeba kovariantní přístup vždy upřednostnit, k jeho dalším praktickým přednostem se dostaneme v dalším při diskusi o polarizovaných funkcích.

Společnou vlastností kovariantního i nekovariantního přístupu je obecná vazba mezi strukturními funkcemi F_2, F_1 vyjádřená relací Callan-Grosse [A9], viz část 3.1.5. Tato relace však pro reálné strukturní funkce platí jen přibližně, je to důsledek zjednodušených předpokladů QPM. Důvody pro pouze přibližné splnění této relace jsou podobné důvodům narušení škálování. Obojí souvisí s tím, že kvarky při interakci s fotonem nejsou volné, ale jejich chování je ovlivněno interakcí s ostatními kvarky prostřednictvím gluonů. Avšak jako první přiblížení QPM funguje velmi dobře.

3.3 Polarizované strukturní funkce

Distribuční funkce $G_q = G_q^+ + G_q^-$, které jsme zavedli pro kovariantní popis nepolarizovaného DIS jsou pro polarizovaný případ nahrazeny funkcemi $\Delta G_q = G_q^+ - G_q^-$, kde $G_q^\pm$ jsou odpovídající rozdělení kvarků s polarizací $\pm$ vzhledem k polarizaci protonu. Pro porovnání s nekovariantním přístupem nyní vyjdeme z tabulky 3.1.

V případě nekovariantního popisu je rovněž vypracovaná metoda pro výpočet evoluce Q^2 v rámci pQCD, viz např. [49]. Již na počátku této kapitoly jsme se zmínili, že nekovariantní model se v případě polarizovaných funkcí střetává s některými vážnými problémy. Jako první příklad lze uvést skutečnost, že výrazy vycházející v tomto přiblížení pro strukturní funkci g_2 nedávají rozumný smysl. Na druhé straně výraz, který pro g_2 vychází v kovariantním přístupu, je zcela korektní a smysluplný. Svědčí o tom i následující pravidla, do nichž tato funkce vstupuje. Wanzura-Wilczekova relace (WW) byla původně odvozena v rámci zcela jiného formalismu (OPE). Je podstatné, že dnes existující experimentální data k oběma strukturním funkcím g_1, g_2 potvrzují, že relace WW je v rámci stávajících chyb splněna. Podobný závěr lze učinit i o pravidlech *Burkhardt-Cottingham* (BC) a *Efremov-Leader-Teryaev* (ELT). V rámci kovariantního modelu lze odvodit obecné pravidlo momentů pro libovolnou (i neceločíselnou) hodnotu parametru α pro níž má integrál smysl, předchozí dvě pravidla odpovídají hodnotám $\alpha = 0, 1$. Pro hodnoty $\alpha = 2, 4, 6, ...$ relace představuje již dříve známá Wanzura-Wilczekova sumační pravidla. Doplňme, že uvedená pravidla (počínaje WW) byla v rámci kovariantního modelu odvozena pro nehmotné kvarky, $m \to 0$, pro hmotné kvarky je struktura pravidel

	nekovariantní QPM	kovariantní QPM
distribuční funkce	$\Delta q(x)$	$\Delta G_q\left(\frac{pP}{M}\right)$
strukturní funkce g_1 :	$\frac{1}{2}\sum_q e_q^2 \Delta q(x)$	$\frac{1}{2}\sum_q e_q^2 \int \Delta G_q(p_0) \times\left(m+p_1+\frac{p_1^2}{p_0+m}\right) \times\delta\left(\frac{p_0+p_1}{M}-x\right)\frac{d^3p}{p_0}$
strukturní funkce g_2 :	ne	$-\frac{1}{2}\sum_q e_q^2 \int \Delta G_q(p_0) \times\left(p_1+\frac{p_1^2-p_T^2/2}{p_0+m}\right) \times\delta\left(\frac{p_0+p_1}{M}-x\right)\frac{d^3p}{p_0}$
Wanzura-Wilczek $g_2(x)=-g_1(x)+\int_x^1 \frac{g_1(y)dy}{y}$	ne	ano
Burkhardt-Cottingham $\int_0^1 g_2(x)dx=0$	ne	ano
ELT $\int_0^1 x\left(\frac{1}{2}g_1+g_2\right)dx=0$	ne	ano
obecné α $\int_0^1 x^\alpha\left(\frac{\alpha}{\alpha+1}g_1+g_2\right)dx=0$	ne	ano
polarizované TMDs	ne	ano
připouští orbitální moment	ne	ano

Tabulka 3.1:

složitější [A8], viz část 3.1.4. Výjimku tvoří pravidlo BC, které lze v daném tvaru odvodit bez předpokladu o hmotnosti kvarku, v tomto smyslu má toto pravidlo „silnější“ povahu.

Další předností kovariantního přístupu je možnost opět do schématu přirozeně zahrnout TMDs. Přitom zde platí přesně totéž, co bylo řečeno v bodě 2) na konci předchozího paragrafu 3.2.

3.4 Orbitální moment kvarků a spin protonu

Tato část je komentářem k našemu studiu otázky orbitálního momentu v článku [A9], viz část 3.1.5. Jde o téma, kterému je v souvislosti se spinovou strukturou protonu věnována v současnosti značná pozornost. Různé přístupy k otázce orbitálního momentu kvarků jsou diskutovány například v pracech [38]− [48]. Obecně kvarky ke spinu nukleonu přispívají svým celkovým úhlovým momentem $\mathbf{j}$, který se skládá z orbitálního momentu a spinu kvarku, $\mathbf{j}=\mathbf{l}+\mathbf{s}$. Před diskusí o skládání spinů kvarků je vhodné si

připomenout podobnou, ale přitom jednodušší a známější situaci se skládáním spinů a orbitálních momentů elektronů v atomovém obalu nebo nukleonů v atomovém jádře. Zdůrazněme na tomto místě, že orbitální moment v naší diskusi je vždy vztažen ke *klidové soustavě* odpovídajícího objektu: atom, jádro, nukleon. V této soustavě srovnejme uvedené úrovně:

a) atomový obal − elektrony

Elektrony v jednotlivých slupkách mají přesně definovaný spin i orbitální moment. Stav každého atomu se vyjadřuje symbolem $^{2S+1}L_J$, kde S, L, J jsou výsledné hodnoty spinu, orbitálního momentu a celkového úhlového momentu dané skládáním odpovídajících hodnot jednotlivých elektronů. Například atom Cl v základním stavu je charakterizován symbolem $^2P_{3/2}$ (namísto $L = 1, 2, 3...$ se užívá konvence $L = S, P, D...$). Hodnoty v symbolu lze přesně odvodit z počtu elektronů daného atomu, kterými se postupně zaplňují slupky v základním stavu, viz on-line tabulku [18]. Poznamenejme současně, že elektrony v atomech lze v rozumné aproximaci popsat nerelativisticky. Protože rozměr atomu je v řádu 10^{-10} m, relace neurčitosti implikuje hybnost elektronu v řádu 10^{-3} MeV, což znamená odpovídající rychlost $\beta \approx 0.002$.

b) atomové jádro − nukleony

Stav atomového jádra se standardně vyjadřuje symbolem J^π, kde J je celkový úhlový moment jádra a $\pi = \pm$ je odpovídající parita. Výsledný moment J představuje spin jádra. Například základní stav stabilního izotopu $^{17}_{8}$O je $5/2^+$, viz interaktivní tabulku [24]. Z rozměru jádra v řádu 10^{-15} m lze odvodit hybnost řádu 10^2 MeV a odpovídající rychlost $\beta \approx 0.1$.

c) nukleon − kvarky

Oblast pohybu kvarků v nukleonu je také omezena rozměrem 10^{-15} m, jejich hybnost je proto rovněž řádu 10^2 MeV. I když se jedná o hrubý odhad, poznamenejme, že tato velikost hybnosti velmi dobře souhlasí i s výsledky analýz strukturních funkcí nukleonů provedených v rámci některých modelových přístupů. Dále, přijmeme-li předpoklad, že hmotnosti kvarků jsou malé ve srovnání s jejich energií, kterou se na celkové energii nukleonu podílejí (tzv. *current quark masses* v řádu několika MeV tento předpoklad splňují), pak je evidentní, že vnitřní pohyb kvarků má relativistický rozměr, $\beta \to 1$. Připomeňme nyní, že v relativistickém případě jsou kvantově-mechanická pravidla pro kombinaci spinu a orbitálního momentu odlišná od pravidel platících v nerelativistických podmínkách. V relativistických podmínkách totiž platí, že zachovávající se veličinou je pouze celkový úhlový moment $\mathbf{j} = \mathbf{l} + \mathbf{s}$ a nikoliv jeho orbitální a spinová část odděleně, jak tomu je např. v případě elektronů v poli jádra. Jinými slovy, přípustné jsou pouze vlastní stavy operátorů j^2 a j_z, které jsou reprezentovány sférickými bispinory. Tato skutečnost má velmi důležité důsledky. Lze je ilustrovat na stavu kvarku $j = j_z = 1/2$, pro nějž platí:

$$j_z = \langle s_z \rangle + \langle l_z \rangle = \frac{1}{2}, \tag{3.2}$$

t.j. i když daný stav není vlastním stavem operátorů spinové a orbitální projekce,

součet jejich středních hodnot musí dát 1/2. Podrobnější analýza této „souhry“ ukazuje, že rozdělení hybností je v tomto stavu sféricky symetrické, přímý výpočet pak vede k integrálu

$$\langle s_z\rangle = \frac{1}{2}\int a_p^* a_p \left(\frac{1}{3}+\frac{2m}{3p_0}\right) d^3p, \tag{3.3}$$

v němž se integruje přes absolutní hybnosti kvarků (a_p je amplituda pravděpodobnosti stavu s $p = |\mathbf{p}|$ a $j = j_z = 1/2$). Z tohoto výrazu plyne, že $\langle s_z\rangle \leq 1/2$. Rovnost nastane pro stav, kdy vnitřní pohyb je zcela potlačen, t.j. kdy se jedná o nerelativistický případ a platí $s_z = 1/2, \quad l_z = 0$. Míru vnitřního pohybu lze charakterizovat např. středními hodnotami kinetické energie $E_{kin} = \langle p_0 - m\rangle$, v našem případě je výhodné užít bezrozměrný faktor $\mu = \langle m/p_0\rangle = \left\langle\sqrt{1-\beta^2}\right\rangle$. V limitě nehmotných kvarků ze vztahu (3.3) dostaneme $\langle s_z\rangle = 1/6$, t.j. pouze *třetinu* klidové hodnoty. Mezní hodnoty spinové a odpovídající orbitální projekce závisející na μ shrnuje tabulka:

1	$\geq \mu \geq$	0
0	$\leq \langle l_z\rangle \leq$	1/3
1/2	$\geq \langle s_z\rangle \geq$	1/6

a obecně platí

$$\langle l_z\rangle = 2\frac{1-\mu}{1+2\mu}\langle s_z\rangle . \tag{3.4}$$

Tento vztah platí i v obecnějším případě, když daný stav $j = 1/2$ je současně vlastním stavem projekce do jiného směru než osy z. Efekt tedy spočívá v tom, že (relativistický) vnitřní pohyb redukuje příspěvek spinu a současně generuje orbitální moment. Vztah (3.2) tak reprezentuje souhru veličiny z prostoru vnitřních symetrií s veličinou odrážející symetrii v časoprostoru.

Tento efekt by se měl projevit při analýze strukturní funkce g_1, jejímž cílem je stanovení příspěvku kvarků k celkovému spinu protonu. Na základě našeho studia lze v tomto kontextu uvést následující.

1) Spinový příspěvek kvarků

Příspěvek spinů kvarků ke spinu protonu lze stanovit z integrálu

$$\Gamma_1 = \int_0^1 g_1(x)dx, \tag{3.5}$$

který lze určit z experimentálně změřené funkce g_1. V *kovariantní verzi QPM* tento integrál vede k výrazu

$$\Gamma_1 = \frac{1}{2}\int \Delta G(p_0)\left(\frac{1}{3}+\frac{2m}{3p_0}\right) d^3p; \qquad \Delta G(p_0) = \sum_q e_q^2 \Delta G_q(p_0), \tag{3.6}$$

jehož hodnota rovněž závisí na μ:

1	$\geq \mu \geq$	0
$\Gamma_{1\,\max}$	$\geq \Gamma_1 \geq$	$\Gamma_{1\,\max}/3$

Obě veličiny $\langle s_z \rangle$ a Γ_1 jsou měřítkem (projekce) spinu kvarků v protonu, první se vztahuje k jednotlivému kvarku, druhá k souboru kvarků v protonu. Výsledek, že obě tyto veličiny jsou v relativistickém případě ($\mu \to 0$) redukovány stejně, na jednu třetinu své nerelativistické hodnoty ($\mu \to 1$), je potvrzením správnosti našich výpočtů. Jde o výpočty provedené v rámci odlišných formalismů, které však mají společný základ v relativistické, kovariantní kinematice, v jejímž rámci lze korektně zacházet s oběma veličinami − se spinem a orbitálním momentem částic. Do integrálu Γ_1 vstupují kvarkové distribuční funkce s vahami danými kvadráty odpovídajících nábojů, nicméně s použitím dalších metod (standard QCD analysis) lze z hodnot Γ_1 stanovit absolutní spinový příspěvek kvarků $\Delta\Sigma$.

2) Srovnání s experimentem

Bylo by přirozené očekávat, že spin protonu bude výslednicí spinů kvarků, podobně jako je jeho náboj součtem nábojů kvarků. Tomuto očekávání by odpovídala hodnota $\Delta\Sigma \approx 1$. Značné překvapení nastalo, když experiment EMC (jednalo se o tentýž tým, kterým byl několik let předtím objeven EMC efekt) naměřil integrál Γ_1, z kterého vyplývalo, že $\Delta\Sigma$ je podstatně menší [50]. Malé hodnoty Γ_1 a $\Delta\Sigma$ byly jednoznačně potvrzeny i v řadě experimentů, které následovaly a dávaly výsledky v rozmezí $\Delta\Sigma \simeq 0.2 - 0.35$. Tyto výsledky byly v nedávné době podstatně zpřesněny v experimentech HERMES a COMPASS:

$\Delta\Sigma$	experiment
$0.30 \pm 0.010(stat.) \pm 0.02(evol.)$	COMPASS [51]
$0.33 \pm 0.025(exp.) \pm 0.011(theo.) \pm 0.028(evol.)$	HERMES [52]

Tyto hodnoty znamenají, že spiny kvarků generují pouze zhruba jednu třetinu spinu protonu. Odkud se však bere ta větší zbývající část spinu protonu, $(1 - \Delta\Sigma)$? Pro vysvětlení byla navržena řada hypotéz, zde uveďme alespoň dvě, které lze v současnosti považovat za nejpravděpodobnější.

Jednou z nich je příspěvek gluonů. Víme totiž, že proton kromě kvarků obsahuje i gluony o nichž je známo, že mohou být zodpovědné za zhruba polovinu hmotnosti protonu, proč by srovnatelnou měrou nemohly přispívat i k jeho spinu? Taková možnost by měla silnou podporu i v rámci pQCD [55]− [57]. Experimentálně lze polarizaci gluonů různými metodami rovněž testovat, je však třeba konstatovat, že existující data naznačují gluonový příspěvek spíše malý [53, 54]. Z existujících dat na obrázku 3.1 fakticky není ani zřejmo, jaké znaménko by gluonový příspěvek měl mít.

Druhou, v současnosti zvláště sledovanou alternativou pro doplnění spinu kvarků je korektní započtení jejich orbitálního momentu. Veličiny Γ_1 a $\Delta\Sigma$ jsou měřítkem sumární projekce spinů kvarků v protonu, nicméně kvarky ke spinu protonu přispívají

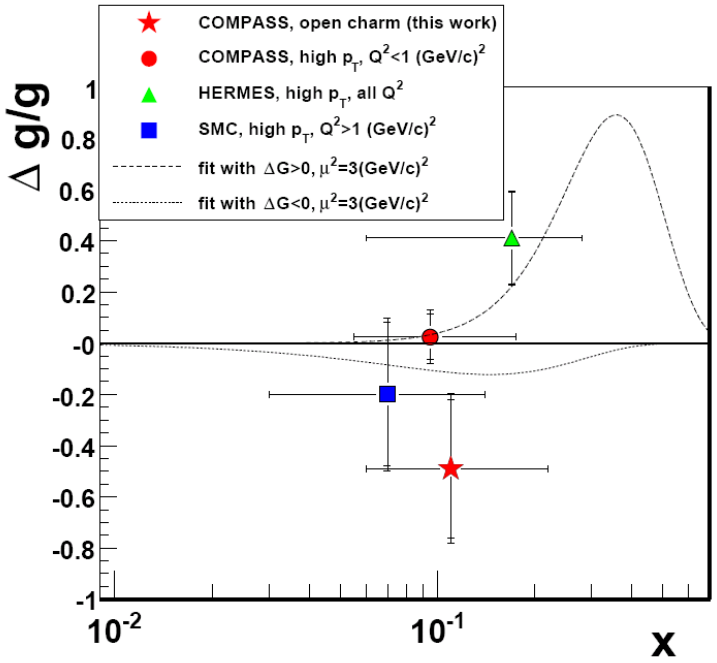

Obrázek 3.1: Polarizace gluonů změřená v různých experimentech, obrázek je převzat z nedávné práce experimentu COMPASS [53].

svým celkovým úhlovým momentem, tj. nejen spinem ale i orbitálním momentem. Jak velký může být celkový orbitální příspěvek?

V rámci nekovariantního QPM odpověď nelze hledat především z těchto důvodů:

i) Jak jsme se již zmínili v paragrafu 3.2, v nekovariantním QPM je kinematika kvarků redukována do jedné dimenze, v níž lze stěží korektně definovat operátor orbitálního momentu.

ii) Protože naše úvaha se týká orbitálního momentu, který přispívá ke spinu protonu, musí být tento orbitální moment vztažen ke klidovému systému protonu. To je ovšem požadavek opět těžko slučitelný s nekovariantním QPM, jehož filosofie je neoddělitelná od 'infinite momentum frame'.

V kovariantním QPM tyto potíže nenastávají. Celkový příspěvek kvarků se skládá ze spinové a orbitální části

$$J_q = \frac{1}{2}\Delta\Sigma + L, \tag{3.7}$$

kde pro celkový orbitální moment platí tatáž úměra (3.4) jako pro jednotlivé kvarky

$$L = \frac{1-\mu}{1+2\mu}\Delta\Sigma. \tag{3.8}$$

Vezmeme-li v úvahu, že spin protonu je tvořen celkovými úhlovými momenty kvarků a gluonů, potom platí

$$J_q + J_g = \frac{1}{2}, \tag{3.9}$$

což po dosazení ze vztahů (3.7) a (3.8) dává podmínku konzistence

$$\frac{3}{1+2\mu}\Delta\Sigma + 2J_g = 1, \tag{3.10}$$

z níž plyne vztah mezi celkovým příspěvkem gluonů a spinovým příspěvkem kvarků, který zahrnuje všechny možné scénáře pohybu kvarků mezi nerelativistickým ($\mu = 1$)

$$J_g = \frac{1}{2}\left(1 - \Delta\Sigma\right) \tag{3.11}$$

a relativistickým případem ($\mu = 0$)

$$J_g = \frac{1}{2}\left(1 - 3\Delta\Sigma\right). \tag{3.12}$$

Ve druhém případě jsou slučitelné i hodnoty $\Delta\Sigma = 1/3$ a $J_g = 0$, které nejsou v rozporu s experimentálními daty prezentovanými v tabulce a na obrázku výše.

3.5 Další predikce a variace kovariantního QPM

Dosavadní úvahy se týkaly modelu, jehož konstrukce byla založena pouze na požadavcích relativistické kovariance a sférické symetrie nukleonu. Jsou to velmi obecné požadavky, jejichž platnost lze stěží zpochybňovat a vážně je proto třeba brát i jejich důsledky, například vztahy mezi funkcemi g_1 a g_2 nebo i významnou roli orbitálního momentu. V tomto rámci lze například ze strukturních funkcí určit rozdělení hybností kvarků v klidovém systému protonu [A9], viz část 3.1.5. A tyto naše výsledky (pro valentní kvarky) nejsou v rozporu ani s odhadem v bodě *c)* paragrafu 3.3, ale ani s predikcemi získanými v rámci různých variant statistického modelu nukleonu [58]− [60].

Detailnější obraz o vnitřním pohybu kvarků je zprostředkován distribučními funkcemi, které poskytují 3D obrazy rozdělení hybností kvarků, jde o již zmiňované *transverse momentum dependent parton distributions* − TMDs, kterými jsme se zabývali v našich zcela nedávných pracech [A10, A13], viz části 3.5.1, 3.5.4.

Do obecné modelové konstrukce lze však vkládat i další předpoklady, které mohou vést k dalším vztahům mezi strukturními a distribučními funkcemi. Například s využitím předpokladu o symetrii SU(6) jsme získali vztahy mezi polarizovanými strukturními funkcemi g_1, g_2 a nepolarizovanými distribučními funkcemi valentních kvarků $q_{val}(x)$ [A8], viz část 3.1.4. Takto získané funkce g_1, g_2 velmi dobře souhlasí i s experimentálními daty. Shoda je zajímavá a důležitá především tím, že náš výpočet provedený v limitě nehmotných kvarků neobsahuje žádné volné parametry, vychází pouze ze znalosti nepolarizovaných distribučních funkcí a z předpokladu symetrie SU(6), který definuje relativní příspěvky kvarků u a d k celkovému spinu. Jiné dodatečné předpoklady umožnily do modelu zahrnout další distribuční funkce: transversity [A11], viz část 3.5.2, pretzelosity [A12], viz část 3.5.3 a některé další typy TMDs. S dalšími distribučními funkcemi se objevují i další vztahy a pravidla, která například umožňují odhadnout některé dosud nezměřené typy distribučních funkcí na základě již známých. V tom asi spočívá i hlavní potenciál navrženého modelu.

Article copy

PHYSICAL REVIEW D **80,** 014021 (2009)

Transverse momentum dependent distribution functions in a covariant parton model approach with quark orbital motion

A. V. Efremov,[1] P. Schweitzer,[2] O. V. Teryaev,[1] and P. Zavada[3]

[1]*Bogoliubov Laboratory of Theoretical Physics, JINR, 141980 Dubna, Russia*
[2]*Department of Physics, University of Connecticut, Storrs, Connecticut 06269, USA*
[3]*Institute of Physics, Academy of Sciences of the Czech Republic, Na Slovance 2, CZ-182 21 Prague 8, Czech Republic*

(Received 7 May 2009; published 29 July 2009)

Transverse parton momentum dependent distribution functions (TMDs) of the nucleon are studied in a covariant model, which describes the intrinsic motion of partons in terms of a covariant momentum distribution. The consistency of the approach is demonstrated, and *model relations* among TMDs are studied. As a by-product it is shown how the approach allows to formulate the nonrelativistic limit.

DOI: 10.1103/PhysRevD.80.014021 PACS numbers: 13.88.+e, 13.60.−r, 13.85.Ni, 13.85.Qk

I. INTRODUCTION

Studies of hard scattering processes such as inclusive deep-inelastic lepton-nucleon scattering (DIS) have given rise to a good understanding of parton distribution functions, which tell us how the parton momenta parallel to the nucleon momentum are distributed. One way to gain insights into the partonic quark-gluon substructure of the nucleon beyond this one-dimensional picture is to consider transverse momentum dependent ('unintegrated') parton distributions (TMDs) [1]. These objects can be accessed by observing transverse momenta of, e.g., hadrons produced in semi-inclusive DIS (SIDIS) or dileptons produced in the Drell-Yan process [2–10] thanks to factorization [11–14]. Much theoretical progress was made [15–26], and first data [27–45] give rise to phenomenological insights [46–62].

Nevertheless, presently model studies [63–78] play an important role. It is worth to recall that important insights concerning the very existence [9] or universality [16] of effects were made on the basis of model studies, see [79] for a review. Moreover, model results help to sharpen our physical intuition on these novel objects, and can be used to make estimates for planned experiments. Another aspect is that, thanks to the far simpler dynamics as compared to QCD, one may find relations among the different TMDs in some [63–67] though not all [68,69] models. As all TMDs are *a priori* independent structures, any such *model relations* among TMDs are not expected to hold in QCD.

It is interesting to ask, however, whether such relations could nevertheless be satisfied in nature at least approximately. Recalling that the nucleon is characterized by 8 leading-twist [7] and 16 subleading-twist [23] TMDs, such approximate relations could be valuable, for the interpretation of first data, or for estimates for new experiments [25].

In order to judge to which extent a particular *model relation* among TMDs might be respected by nature, till we know the answer from experiment, it is helpful to understand under which general conditions in a model this relation holds. For example, suppose a model relation relies on the SU(6) spin-flavor symmetry of the nucleon wave-function. We know from experiment that the SU(6) symmetry concept is useful—within certain limitations [78,80]. This implies that model relations based on SU(6) symmetry are respected in nature, if at all, at best within similar limitations. It happens that all model relations among TMDs observed so far have been found in models based on SU(6) symmetry [63–65].

The purpose of this work is to study TMDs in the covariant model of the nucleon proposed in Ref. [81] which makes *no use* of SU(6) spin-flavor symmetry. Some of the results presented here were discussed previously in [66]. In this model the intrinsic motion of partons inside the nucleon is described in terms of a covariant momentum distribution. The model was applied to the study of unpolarized and polarized parton distribution functions accessible in DIS $f_1^a(x)$, $g_1^a(x)$ and $g_T^a(x)$, and extended to compute the transversity distribution $h_1^a(x)$ [82–86].

In this work we generalize the approach [81–86] to the description of TMDs. In particular, we focus on the so-called T-even, leading-twist TMDs, and pay particular attention to the demonstration of the consistency of the approach. We shall see that certain model relations among TMDs hold *even without* invoking SU(6) symmetry. For earlier studies of the parton transverse momenta contribution to the transverse spin in the parton model framework we refer to [87,88].

This note is organized as follows. In Sec. II we briefly introduce TMDs. In Sec. III we introduce the model, and review previous works. In Sec. IV we generalize the approach to the description of TMDs, and in Sec. V we demonstrate its consistency. In Sec. VI we discuss the model relations among the polarized T-even TMDs. In Sec. VII we apply the approach to a study of TMDs in the nonrelativistic limit, before we summarize and conclude in Sec. VIII. The Appendices contain details of the calculations, and supplementary results.

II. TMDS

In this Section we introduce and define briefly TMDs. With the use of light-cone coordinates, $a^{\pm} = (a^0 \pm a^1)/\sqrt{2}$, TMDs are defined in terms of light-front correlators as

$$\phi(x, \vec{p}_T)_{ij} = \int \frac{dz^- d^2\vec{z}_T}{(2\pi)^3} e^{ipz} \langle N(P,S)|\bar{\psi}_j(0)\mathcal{W}(0,z,\text{path}) \times \psi_i(z)|N(P,S)\rangle|_{z^+=0,p^+=xP^+}. \quad (1)$$

In SIDIS the singled-out space-direction is along the momentum of the hard virtual photon $q^\mu = (q^0, q^1, 0, 0)$, and transverse vectors like $\vec{p}_T$ are perpendicular to it. The path of the Wilson-link $\mathcal{W}$ depends on the process [10,19]. In the nucleon rest frame the polarization vector is $S = (0, -S_L, \vec{S}_T)$ with $S_L^2 + \vec{S}_T^2 = 1$. The negative sign in front of S_L is because by convention [24] the nucleon has positive helicity, i.e. $S_L > 0$, if it moves towards the virtual photon.

The information content of the correlator (1) is summarized by eight leading-twist TMDs [7], that can be projected out from the correlator (1) as follows (for convenience we will often suppress flavor indices)

$$\frac{1}{2}\,\text{tr}[\gamma^+\phi(x,\vec{p}_T)] = f_1 - \frac{\varepsilon^{jk} p_T^j S_T^k}{M_N} f_{1T}^\perp \quad (2)$$

$$\frac{1}{2}\,\text{tr}[\gamma^+\gamma_5\phi(x,\vec{p}_T)] = S_L g_1 + \frac{\vec{p}_T\cdot\vec{S}_T}{M_N} g_{1T}^\perp \quad (3)$$

$$\frac{1}{2}\,\text{tr}[i\sigma^{j+}\gamma_5\phi(x,\vec{p}_T)] = S_T^j h_1 + S_L\frac{p_T^j}{M_N} h_{1L}^\perp + \frac{(p_T^j p_T^k - \frac{1}{2}\vec{p}_T^{\,2}\delta^{jk})S_T^k}{M_N^2} h_{1T}^\perp + \frac{\varepsilon^{jk}p_T^k}{M_N} h_1^\perp, \quad (4)$$

where the space-indices j, k refer to the plane transverse with respect to the light-cone, and $\varepsilon^{32} = -\varepsilon^{23} = 1$ and zero else (which is consistent with $\varepsilon^{0123} = 1$). Integrating out transverse momenta in the correlator (1) leads to the three 'usual' parton distributions known from collinear kinematics $j_1^a(x) = \int d^2\vec{p}_T j_1^a(x,\vec{p}_T^{\,2})$ with $j = f,\ g,\ h$ [89,90]. Dirac-structures other than that in Eqs. (2)–(4) lead to subleading-twist terms [23,24].

III. THE COVARIANT MODEL OF THE NUCLEON, AND ITS APPLICABILITY

In this section we first briefly introduce the model, and sketch the calculation of the 'collinear' parton distribution functions done so far, namely $f_1^a(x)$, $g_1^a(x)$, $g_T^a(x)$ and $h_1^a(x)$. Then we discuss the applicability of the approach to the calculation of TMDs which will be done in Sec. IV.

The starting point for the calculation of the chirally even functions accessible in DIS, $f_1^a(x)$, $g_1^a(x)$, and $g_T^a(x)$ [81–83], is the hadronic tensor. The latter is evaluated in the Bjorken-limit, i.e. in the limit that the four-momentum transfer q^μ from the lepton beam to the nucleon with momentum P is such that $Q^2 = -q^2$ and $Pq \to \infty$ while $x = Q^2/(2Pq)$ is fixed. In the model it is assumed that unpolarized DIS can be described as the incoherent sum of the scattering of electrons off noninteracting quarks, whose momentum distributions inside the nucleon are given in terms of the scalar function $G(pP/M)$. Here p and P are the momenta of the quark and nucleon, and M is the nucleon mass. Though all expressions can always be formulated in a manifestly covariant way, it is convenient to work in the nucleon rest-frame, where the momentum distribution becomes $G(p^0)$ with $p^0 = \sqrt{\vec{p}^2 + m^2}$. Here m denotes the quark mass. Clearly, the distribution of the quark momenta in the nucleon rest frame is rotationally symmetric.

Applying these ideas to the description of the symmetric part of the hadronic tensor has shown that in the model the Callan-Gross relation among the unpolarized structure functions holds exactly, and the unpolarized parton distribution function is given by [81] (notice that $G(p^0)$ depends on flavor, which we suppress for brevity)

$$f_1^q(x) = \int \frac{d^3p}{p^0} G(p^0)\delta\left(\frac{p^0 - p^1}{M} - x\right)(p^0 - p^1). \quad (5)$$

Next we review the calculation of $g_1^q(x)$ and $g_T^q(x)$ appearing in the antisymmetric part of the hadronic tensor. For a single quark the latter would be given by $W_{\alpha\beta}^{A,q} = m\epsilon_{\alpha\beta\mu\nu}q^\mu w^\nu$, where q^μ is the momentum transfer from the electron in DIS, and w^ν denotes the polarization vector of the quark. In the model—assuming the covariant distribution of polarized quarks to be given by $H(pP/M)$—the antisymmetric part of the hadronic tensor of the nucleon is given by

$$W_{\alpha\beta}^A = \int \frac{d^3p}{Pp/M} H(pP/M)\delta((p+q)^2 - m^2) W_{\alpha\beta}^{A,q} \overset{\text{Bj}}{=} \frac{m}{2Pq}\epsilon_{\alpha\beta\mu\nu}q^\mu \int \frac{d^3p}{p^0} H(p^0)\delta\left(\frac{p^0 - p^1}{M} - x\right)w^\nu. \quad (6)$$

The second expression in (6) is given in the nucleon rest frame choosing $q^\mu = (q^0, q^1, 0, 0)$ and holds in the Bjorken limit (more precisely: here and in the following for the steps marked by 'Bj' the condition $Q^2 \gg 4M^2x^2$ is essential).

Notice that the covariant distribution of polarized quarks can be expressed as $H(p^0) = G^+(p^0) - G^-(p^0)$, where the indices $(\pm)$ refer to the respective quark polarizations which are parallel $(+)$ or antiparallel $(-)$ to the nucleon spin. In this notation the covariant distribution of unpolarized quarks in (5) is $G(p^0) = G^+(p^0) + G^-(p^0)$.

The most general expression for the covariant quark polarization vector [82] is given by

$$w^\mu = -\frac{pS}{pP+mM}P^\mu + S^\mu - \frac{M}{m}\frac{pS}{pP+mM}p^\mu, \quad (7)$$

where S^μ denotes the nucleon polarization vector given in the nucleon rest frame by $S^\mu = (0,\vec{S})$ with $|\vec{S}| = 1$. The evaluation of Eqs. (6) and (7) and comparison to the general Lorentz-decomposition of $W^A_{\alpha\beta}$, namely

$$W^A_{\alpha\beta} = \epsilon_{\alpha\beta\mu\nu}q^\mu\left(\frac{S^\nu}{Pq}g_1 + \frac{(Pq)S^\nu - (Sq)P^\nu}{(Pq)^2}g_2\right), \quad (8)$$

yield the following results for $g_1^q(x)$ and $g_T^q(x) = g_1^q(x) + g_2^q(x)$ [82,83]

$$g_1^q(x) = \int\frac{d^3p}{p^0}H(p^0)\delta\left(\frac{p^0-p^1}{M}-x\right) \times\left[p^0 - p^1 - \frac{\vec{p}_T^{\,2}}{p^0+m}\right], \quad (9)$$

$$g_T^q(x) = \int\frac{d^3p}{p^0}H(p^0)\delta\left(\frac{p^0-p^1}{M}-x\right)\left[m + \frac{\vec{p}_T^{\,2}}{2(p^0+m)}\right]. \quad (10)$$

In the model the Burkhardt-Cottingham sum rule [91] is satisfied. When neglecting terms proportional to m also the Efremov-Leader-Teryaev sum rule [92] holds, while $g_T^q(x)$ is given by the Wandzura-Wilczek (WW) approximation [93]

$$g_T^q(x) \overset{\text{WW}}{=} \int_x^1\frac{dy}{y}g_1^q(y) + \mathcal{O}\left(\frac{m}{M}\right) \quad (11)$$

as was proven in [82,83]. Notice that in QCD what is neglected are not only mass terms but also pure twist-3 terms [93]. That in the model such pure twist-3 ('interaction dependent') terms in $g_T(x)$ are absent, is *consistent* because in our approach the quarks are assumed to be free. (We remark that the approximation $g_T^q(x) \approx \int_x^1\frac{dy}{y}g_1^q(y)$ is supported by data [94] and theoretical approaches [95]. Further discussions of WW- and WW-type approximations in related and other contexts can be found in Refs. [25,26,96].)

The chirally odd transversity distribution function cannot be accessed through the hadronic tensor and DIS. For theoretical purposes, however, one may consider the auxiliary polarized process described by the interference of a vector and a scalar current. On the quark level this interference is described by $T_\mu^q = \epsilon_{\alpha\beta\lambda\nu}p^\beta q^\lambda w^\nu$ from which one obtains for the nucleon—in analogy to the procedure in Eq. (6)—the following expression

$$T_\alpha = \int\frac{d^3p}{Pp/M}H(pP/M)\delta((p+q)^2-m^2)T_\alpha^q \overset{\text{Bj}}{=} \frac{1}{2Pq}\epsilon_{\alpha\beta\lambda\nu}q^\lambda\int\frac{d^3p}{p^0}H(p^0)\delta\left(\frac{p^0-p^1}{M}-x\right)p^\beta w^\nu. \quad (12)$$

The general Lorentz-decomposition in this case reads ($j = 2, 3$ is a 'transverse index' with respect to q and P)

$$2MT_\alpha\epsilon^{\alpha j} = S_T^j h_1^q(x) \quad (13)$$

one obtains after evaluating (12) with (7) the following result for the transversity distribution function [84]

$$h_1(x) = \int\frac{d^3p}{p^0}H(p^0)\delta\left(\frac{p^0-p^1}{M}-x\right) \times\left[p^0 - p^1 - \frac{\vec{p}_T^{\,2}}{2(p^0+m)}\right]. \quad (14)$$

We remark that in Eqs. (9), (10), and (14) we did not distinguish momentum distributions in differently polarized nucleons. In general one might suspect the covariant distributions to be different. In QCD, if nothing else, different evolution properties clearly distinguish chirally even vs odd, and twist-2 vs twist-3 distribution functions. In the model, however, it is natural to assume the distributions in longitudinally and transversely polarized nucleons to be equal. In order to understand that this assumption is indeed natural, we recall that the approach is covariant. Therefore one may go to the nucleon rest frame, where it certainly makes no difference whether the quarks in the nucleon are polarized longitudinally or transversely (with respect to the space component of the four-vector q in DIS or SIDIS).[1] Since in this model the quarks are noninteracting, it does not matter how they are polarized—because, for example, there are also no spin-orbit- or spin-spin-interactions. (Sec. VI A will show that the covariant distribution in various polarized TMDs must be equal, in order to comply with QCD.)

However, this by no means implies that the parton distributions describing longitudinally and transversely polarized quarks, $g_1(x)$ and $h_1(x)$, are equal. They are, in fact, rather different even if described in terms of the same covariant momentum distribution $H(p^0)$ [84]. By introducing adequate normalizations (as dictated, e.g., by SU(6) symmetry) one could furthermore relate the polarized covariant distribution function $H(p^0)$ to the unpolarized one $G(p^0)$. This is, however, a severe restriction and simplification of the model, which we do not need in general.

When extending the approach below to the description of TMDs it is important to keep in mind the following point. The QCD definition of a parton distribution function

[1] Since q^μ is spacelike $q^2 < 0$, its space-component $\vec{q}$ is nonzero in any frame, and always provides an axis for the quantization of the nucleon spin.

includes a Wilson line, which in DIS describes the interaction of the struck nucleon with the target remnant. It is possible to find a gauge in which the Wilson line drops out, and the partons seem 'noninteracting'—an idea eventually underlying the parton model in general, and the approach of Refs. [82–86] in particular. When dealing with TMDs, however, the Wilson line cannot be 'gauged away' [9,10,19].

In the present framework we have no tool to include the effects of the Wilson line, and therefore the description of the so-called 'naively T-odd' parton distribution functions, the Sivers function $f_{1T}^{\perp}$ and the Boer-Mulders function $h_1^{\perp}$, is beyond the scope of the approach. These TMDs crucially rely on the initial- and final-state-interactions encoded in the Wilson line [9,10], and are expected to be absent in our framework.

Finally, we remark that the model is 'opposite' to the Gaussian ansatz for TMDs in the following sense. In the Gaussian ansatz one assumes the extreme situation that distribution of longitudinal momentum (i.e. x-dependence) and the distribution of p_T are decoupled. For example, one has $f_1(x, p_T^2) = f_1(x)\exp(-p_T^2/\langle p_T^2\rangle)/(\pi\langle p_T^2\rangle)$. It is even possible to "switch off" p_T-effects: in the limit $\langle p_T^2\rangle \to 0$ one has $f_1(x, p_T^2) = f_1(x)\delta^{(2)}(\vec{p}_T)$. In contrast to this in the present model the longitudinal and transverse motions are coupled "maximally". It is not possible to "switch off" p_T-effects. As a consequence one has, e.g., interesting implications for the quark orbital motion [86].

IV. EXTENSION OF THE APPROACH TO TMDS

In this section we extend the approach to the description of TMDs. Since none of the new TMDs in Eqs. (2)–(4) is accessible directly via the hadronic tensor in DIS or via the auxiliary process explored for the calculation of $h_1^q(x)$, we need to establish a more general relation in the model to the correlators (2)–(4). For that we observe that the model expressions for the antisymmetric part of the hadronic tensor (6) or the auxiliary current (12) include integration over $d^3p = dp^1 d^2p_T$ with $d^2p_T \equiv dp_2 dp_3$. In the following we will explore the consequences of what happens if one *does not integrate out* transverse momenta in these expressions, and demonstrate the consistency of this approach.

The 'integrated' symmetric part of the hadronic tensor, to which f_1^q is related, was studied in Ref. [81]. The study of its 'unintegrated' version would give model results for f_1^q and the T-odd $f_{1T}^{\perp q}$, as revealed by the correlator in Eq. (2). However, the description of the Sivers function is beyond the scope of our approach, see Sec. III, and we therefore start with the more interesting case of the correlator (2) which describes $g_1^q(x, p_T)$ and the T-even TMD $g_{1T}^q(x, p_T)$. (We shall come back to f_1^q at the end of the next section.)

In order to access the information contained in the correlator (3) we consider the transverse space components $(j, k = 2, 3)$ of the 'unintegrated' antisymmetric part of the hadronic tensor in Eq. (6). We work in the nucleon rest frame with the nucleon polarization vector as introduced in the sequence of Eq. (1) and choose $q^\mu = (q^0, q^1, 0, 0)$. Then, using (7) we obtain in the Bjorken-limit

$$2MW_{jk}^A(x, \vec{p}_T) \overset{\text{Bj}}{=} \epsilon_{jk}\int \frac{dp^1}{p^0} H(p^0)\delta\Big(\frac{p^0 - p^1}{M} - x\Big) \times \Big\{-S_L\Big(p^0 - p^1 - \frac{\vec{p}^2}{p^0 + m}\Big) - \frac{\vec{p}_T\vec{S}_T}{2}\,\frac{p^0 - p^1}{p^0 + m}\Big\}. \tag{15}$$

We recognize two contributions in (15), one proportional to the longitudinal nucleon spin component S_L and one proportional to the projection of the nucleon spin on the transverse parton momentum. These contributions coincide exactly with the decomposition of the correlator in Eq. (3). Thus, from the comparison of the coefficients we obtain

$$g_1^q(x, p_T) = \int \frac{dp^1}{p^0} H(p^0)\delta\Big(\frac{p^0 - p^1}{M} - x\Big) \times \Big[p^0 - p^1 - \frac{\vec{p}_T^{\,2}}{p^0 + m}\Big], \tag{16}$$

$$g_{1T}^{\perp q}(x, p_T) = \int \frac{dp^1}{p^0} H(p^0)\delta\Big(\frac{p^0 - p^1}{M} - x\Big) \times \Big[M\,\frac{p^0 - p^1 + m}{p^0 + m}\Big]. \tag{17}$$

Notice that there is no arbitrariness concerning an overall prefactor, because in the integrated case we reproduce $2MW_{jk}^A(x) = -\epsilon_{jk}S_L g_1^q(x)$ in agreement with the general Lorentz-decomposition for the transverse components of the antisymmetric part of the hadronic tensor. The other components of $W_{\mu\nu}^A$ describe subleading-twist structures, for example $g_T^q(x)$ in the integrated case, which we do not consider in this work.

Now we wish to access the information content described in the chirally odd correlator (4). For that we consider the 'unintegrated' version of the auxiliary current T_α in Eq. (12). For $T_\alpha(x, \vec{p}_T)$ contracted with $\epsilon^{j\alpha}$ we obtain:

$$2MT_\alpha(x, \vec{p}_T)\varepsilon^{\alpha j} = \int \frac{dp^1}{p^0} H(p^0)\delta\Big(\frac{p^0 - p^1}{M} - x\Big) \times \Big\{S_T^j(p^0 - p^1) - S_L p_T^j\,\frac{p^0 - p^1 + m}{p^0 + m} - p_T^j\,\frac{\vec{S}_T\vec{p}_T}{p^0 + m}\Big\}. \tag{18}$$

In order to easier compare to (4) we rewrite the decomposition of that correlator as often done [6,7] as follows

$$\frac{1}{2}\,\mathrm{tr}[i\sigma^{j+}\gamma_5\phi(x,\vec{p}_T)] = S_T^j\underbrace{\left(h_1^q - \frac{\vec{p}_T^{\,2}}{2M_N^2}h_{1T}^{\perp q}\right)}_{h_{1T}^q} - S_L\frac{p_T^j}{M_N}h_{1L}^{\perp q} + \frac{p_T^j(\vec{p}_T\vec{S}_T)}{M_N^2}h_{1T}^{\perp} + \frac{\varepsilon^{jk}p_T^k}{M_N}h_1^{\perp q}, \tag{19}$$

where we suppressed the arguments x, p_T of the TMDs for brevity. By comparing the coefficients in Eqs. (18) and (19) we read off the following results:

$$h_{1T}^q(x,p_T) = \int\frac{dp^1}{p^0}H(p^0)\delta\left(\frac{p^0-p^1}{M}-x\right)[p^0-p^1] \tag{20}$$

$$h_{1L}^{\perp q}(x,p_T) = \int\frac{dp^1}{p^0}H(p^0)\delta\left(\frac{p^0-p^1}{M}-x\right)\times\left[-M\left(1-\frac{p^1}{p^0+m}\right)\right] \tag{21}$$

$$h_{1T}^{\perp q}(x,p_T) = \int\frac{dp^1}{p^0}H(p^0)\delta\left(\frac{p^0-p^1}{M}-x\right)\left[-\frac{M^2}{p^0+m}\right] \tag{22}$$

$$h_1^{\perp q}(x,p_T) = 0. \tag{23}$$

V. CONSISTENCY OF THE APPROACH

It is necessary to demonstrate the consistency of our approach. For that we remark first that by integrating the expression for $g_1^q(x,p_T)$ in Eq. (16) over transverse momenta we recover the model result for $g_1^q(x)$ derived in [82] and quoted in Eq. (9). Next, by exploring the connection of transversity to the functions $h_{1T}(x,p_T)$ and $h_{1T}^{\perp}(x,p_T)$ [6,7]

$$h_1(x,p_T) = h_{1T}(x,p_T) + \frac{\vec{p}_T^{\,2}}{2M^2}h_{1T}^{\perp}(x,p_T) = \int\frac{dp^1}{p^0}H(p^0)\delta\left(\frac{p^0-p^1}{M}-x\right)\times\left[p^0-p^1-\frac{\vec{p}_T^{\,2}}{2(p^0+m)}\right] \tag{24}$$

and integrating over transverse momenta we recover the correct result for transversity derived in [84] and quoted above in Eq. (14). This means that the Lorentz-decomposition of the structure (18) in the model is consistent with the Lorentz-decomposition of the correlator in Eqs. (4) and (19). Since the model is covariant, this is an expected feature. We finally notice that there is no polarization-independent term in (18) meaning the absence of the Boer-Mulders function—as expected in the present framework, see Sec. III.

We observe that the results for $g_1^q(x,p_T)$ and $h_1^q(x,p_T)$ derived here could have been simply 'guessed' from the results for the integrated functions $g_1^q(x)$ and $h_1^q(x)$ by 'skipping' the integration over d^2p_T. This is by no means trivial, because in the respective TMDs there could have been structures—e.g., of the type $F(p^0,p^1)(p_2^2-p_3^2)$ with some function $F(p^0,p^1)$ making the integrals converging—which would drop out in the expression for the integrated functions due to rotational symmetry in the transverse plane. On the other hand, in the present approach described by a free Hamiltonian (that commutes with the momentum operator) the model expressions for TMDs could be written as nucleon expectation values of certain polynomials of the momentum operator. Then it is clear that such 'multipol-terms' in TMDs are forbidden by the Wigner-Eckart theorem. After these considerations we conclude that the model expression for the unintegrated unpolarized distribution function is given by

$$f_1^q(x,p_T) = \int\frac{dp^1}{p^0}G(p^0)\delta\left(\frac{p^0-p^1}{M}-x\right)(p^0-p^1). \tag{25}$$

As a next important consistency check let us test whether the model results satisfy positivity constraints, and for that we need the expression for the unpolarized distribution function (25), since the inequalities for TMDs we wish to verify read [15]

$$|h_1^q(x,p_T)| \le \frac{1}{2}[f_1^q(x,p_T)+g_1^q(x,p_T)] \tag{26}$$

$$|h_{1T}^{\perp(1)q}(x,p_T)| \le \frac{1}{2}[f_1^q(x,p_T)-g_1^q(x,p_T)] \tag{27}$$

$$g_{1T}^{\perp(1)q}(x,p_T)^2 + f_{1T}^{\perp(1)q}(x,p_T)^2 \le \frac{\vec{p}_T^{\,2}}{4M^2}[f_1^q(x,p_T)^2 - g_1^q(x,p_T)^2] \tag{28}$$

$$h_{1L}^{\perp(1)q}(x,p_T)^2 + h_1^{\perp(1)q}(x,p_T)^2 \le \frac{\vec{p}_T^{\,2}}{4M^2}[f_1^q(x,p_T)^2 - g_1^q(x,p_T)^2], \tag{29}$$

where the 'unintegrated' transverse moment of a TMD is defined as

$$j_1^{(1)}(x,p_T) = \frac{\vec{p}_T^{\,2}}{2M^2}j_1(x,p_T). \tag{30}$$

Notice that the T-odd functions $f_{1T}^{\perp(1)q}(x,p_T)$ and $h_1^{\perp(1)q}(x,p_T)$ are absent in our approach. A direct test of the inequalities is actually difficult because different covariant functions $G(p^0)$, $H(p^0)$ appear in the TMDs. One way to proceed is to assume SU(6) spin-flavor symmetry of

the nucleon wave function. If one assumes SU(6) symmetry, the inequalities (26)–(29) are manifestly satisfied in our framework, see Appendix A. If one does not, the positivity conditions (26)–(29) are 'translated' into certain constraints among the covariant momentum distributions $G(p^0)$ and $H(p^0)$, see Ref. [84], where the p_T-integrated version of (26) known as Soffer bound [97] was discussed in this way.

We conclude this section with the observation that so far our approach satisfied all imposed consistency checks. Further consistency tests will be provided in the next Section, where we shall see that our approach satisfies certain *exact relations* as well as *model relations* among different TMDs found also in other relativistic quark models.

VI. RELATIONS IN THE MODEL AMONG TMDS

It has to be stressed that in QCD all TMDs are independent structures, and it is not possible to find exact relations among them that would allow to express one TMD in terms of other TMDs. However, especially in models without gauge-field degrees of freedom [63–65], it might be possible to find relations among different (T-even) TMDs. Such model relations are of interest by themselves, and might be supported by data within certain 'model accuracies'. It would be interesting to know the general conditions a quark-model must satisfy in order to fulfill such relations.

In order to recognize more easily the relations among the different T-even TMDs let us introduce the following compact notation for the measures

$$\{d\tilde{p}^1\} \equiv \frac{dp^1}{p^0}\,\frac{G(p^0)}{p^0+m}\,\delta\!\left(\frac{p^0-p^1}{M}-x\right) \tag{31}$$

$$\{dp^1\} \equiv \frac{dp^1}{p^0}\,\frac{H(p^0)}{p^0+m}\,\delta\!\left(\frac{p^0-p^1}{M}-x\right). \tag{32}$$

The measure (31) is positive definite, while the sign of the measure (32) depends on the sign of $H(p^0)$. Then the various TMDs can be written as follows

$$f_1^q(x,p_T) = \int\{d\tilde{p}^1\}[(p^0+m)xM] \tag{33}$$

$$g_1^q(x,p_T) = \int\{dp^1\}[(p^0+m)xM-\vec{p}_T^{\,2}] \tag{34}$$

$$\begin{aligned} h_1^q(x,p_T) &= \int\{dp^1\}\left[(p^0+m)xM-\frac{1}{2}\vec{p}_T^{\,2}\right] \\ &= \int\{dp^1\}\left[\frac{1}{2}(xM+m)^2\right] \end{aligned} \tag{35}$$

$$g_{1T}^{\perp q}(x,p_T) = \int\{dp^1\}[+M(xM+m)] \tag{36}$$

$$h_{1L}^{\perp q}(x,p_T) = \int\{dp^1\}[-M(xM+m)] \tag{37}$$

$$h_{1T}^{\perp q}(x,p_T) = \int\{dp^1\}[-M^2], \tag{38}$$

where we remind that $p^0=\sqrt{p_1^2+\vec{p}_T^{\,2}+m^2}$ and $p^0-p^1=xM$ due to the delta-function in the measures. When deriving the second equality in (35) one may make use of the identity $\vec{p}_T^{\,2}=xM(p^0+p^1)-m^2$ valid due to the delta function. From the expressions (34)–(38) we can read off numerous *model* relations among polarized TMDs, which we shall discuss in the following.

Notice that none of the relations discussed in the following involves the unpolarized parton distribution function. Such relations are *impossible* in our approach, simply because there is in general no way to connect the different covariant distributions $G(p^0)$ and $H(p^0)$. If (and only if) one makes an additional model assumption, namely, assumes the SU(6) spin-flavor symmetry, then we obtain relations including $f_1^q(x,p_T)$ and other TMDs, see Appendix. B.

A. An exact relation in QCD, and its consistent realization in the model

Let us first discuss an *exact* relation which is valid in the model and which involves $g_T^q(x)$. (Later we shall discuss also several *approximate* relations involving this twist-3 parton distribution function.) For that we introduce the measure $\{d^3p\}=\{dp^1\}d^2p_T$ which allows us to rewrite the model expression (10) as

$$g_T^q(x) = \int\{d^3p\}\left[m(p^0+m)+\frac{1}{2}\vec{p}_T^{\,2}\right]. \tag{39}$$

From Eqs. (35), (36), and (39) we find that the following QCD relation [24] is satisfied consequently in the model

$$xg_T^q(x) = g_{1T}^{\perp(1)q}(x) + \frac{m}{M}h_1^q(x) + \underbrace{x\tilde{g}_T^q(x)}_{=0,\ \text{here!}}. \tag{40}$$

This further demonstrates the consistency of our approach, although $\tilde{g}_T^q(x)\neq 0$ in general, because in our model such pure twist-3 terms (quark-gluon-correlations) are consequently absent. We learn two further important lessons.

First, the relation (40) crucially relies on the fact that g_T^q, $h_1^q(x)$, $g_{1T}^{\perp q}$ are described in terms of the *same* covariant distribution function $H(p^0)$. In other words, to be consistent with QCD, we actually have no choice but must work with the same covariant distribution function $H(p^0)$ for all polarized functions (c.f. the discussion in Sec. III). Second, we clearly see that the model parameter m is really to be identified with the current quark mass in QCD.

Let us remark that in QCD the relation (40) is valid also in 'unintegrated version', i.e. with the TMDs not integrated over p_T. Here we confine ourselves to the 'integrated

relation' (40), as we have not derived the model expression for $g_T^q(x, p_T)$ (though, in view of the experience with g_1^q and h_1^q, presumably it is given by (10) and (39) with p_T-integration omitted and the 'unintegrated version' of (40) is valid, too).

B. Exact relations among leading-twist TMDs in the model

Next we focus on a class of relations among leading-twist TMDs which are exact in our approach, and can hold in models only. By comparing the expressions in Eqs. (36) and (37) we observe the following *exact* relation in our model

$$g_{1T}^{\perp q}(x, p_T) = -h_{1L}^{\perp q}(x, p_T). \tag{41}$$

This relation was observed previously in the spectator model of Ref. [63] and the constituent model [65].

Next, by comparing Eqs. (34), (35), and (38) we see that the model results satisfy the relation

$$g_1^q(x, p_T) - h_1^q(x, p_T) = h_{1T}^{\perp(1)q}(x, p_T). \tag{42}$$

This relation was first observed in the bag model [64] and it is also valid in the spectator model of Ref. [63]. It was argued [64] that (42) could be valid in a larger class of *relativistic* models. It is thus gratifying to observe that subsequently (42) was confirmed in the relativistic constituent quark model [65] and now also in our approach. Interestingly, the relation (42) is not supported in the spectator model version of Ref. [68].

Both quark-model relations, Eqs. (41) and (42), are not supported in models with gauge-field degrees of freedom [69]. This observation is in line with the expectation that even if the relations (41) and (42) were valid in QCD at some scale (which, of course, does not need to be the case) they would be spoiled at any different scale by evolution effects that clearly discriminate chirally even and odd functions.

Finally, from Eqs. (20)–(22) we find the following remarkable exact relation

$$\frac{1}{2}[h_{1L}^{\perp q}(x, p_T)]^2 = -h_1^q(x, p_T) h_{1T}^{\perp q}(x, p_T), \tag{43}$$

that was not observed before in literature to best of our knowledge and connects only chirally odd TMDs—in contrast to (41) and (42). This nonlinear relation is obeyed in the spectator model [63]. Combining (41) and (43) we find

$$\frac{1}{2}[g_{1T}^{\perp q}(x, p_T)]^2 = -h_1^q(x, p_T) h_{1T}^{\perp q}(x, p_T), \tag{44}$$

which again mixes chirally odd and even TMDs (though the product of two chirally odd objects 'conserves' chirality).

From Eqs. (34) and (35) we find also relations among the signs of TMDs, for example:

$$\text{sign}\,(h_1^q) = \text{sign}(g_1^q), \tag{45}$$

$$\text{sign}\,(h_1^q) = -\text{sign}(h_{1T}^{\perp q}). \tag{46}$$

Notice that (46) could be concluded as a corollary from the result (43). Also from Eqs. (34) and (35), or from combining (45) and (42), we find

$$|h_1^q(x, p_T)| > |g_1^q(x, p_T)| \quad \text{for } p_T > 0, \tag{47}$$

i.e. the modulus of the transversity distribution function is larger than that of the helicity distribution function. This inequality survives integration over p_T and x, and we obtain for $g_T^q = \int dx h_1^q(x)$ and $g_A^q = \int dx g_1^q(x)$, the tensor and axial charges, the relation

$$|g_T^q| > |g_A^q|, \tag{48}$$

which was also observed in [84], in many other models [98–100], and in lattice QCD [101].

Although some of these results have been obtained before in literature, it is remarkable that in our approach all these relations follow *without* assuming SU(6) spin-flavor symmetry.

C. Relations in the model in the chiral limit

From Eqs. (35)–(38) one can find further relations by observing that h_1^q, $g_{1T}^{\perp q}$, $h_{1L}^{\perp q}$, $h_{1T}^{\perp q}$ are functions of the type const $\times (xM + m)^n \times \int\{dp^1\}$, which looks 'so trivial' only due to the compact notation introduced in Eq. (32). Recall that m is to be identified with the QCD current quark mass, see Sec. VI A, whose effects are expected to be negligible in deeply inelastic reactions. We can formulate those relations in the chiral limit, and obtain

$$2h_1^q(x, p_T) + x^2 h_{1T}^{\perp q}(x, p_T) = \mathcal{O}\left(\frac{m}{M}\right), \tag{49}$$

$$2h_1^q(x, p_T) + x h_{1L}^{\perp q}(x, p_T) = \mathcal{O}\left(\frac{m}{M}\right), \tag{50}$$

$$h_{1L}^{\perp q}(x, p_T) - x h_{1T}^{\perp q}(x, p_T) = \mathcal{O}\left(\frac{m}{M}\right). \tag{51}$$

Upon the use of (41) one obtains relations similar to (50) and (51) but with $h_{1L}^{\perp q}$ replaced by $(-g_{1T}^{\perp q})$.

Remarkably, in the model it is possible to relate the transverse moments of the chirally odd TMDs $h_{1L}^{\perp q}$ and $h_{1T}^{\perp q}$ to the chirally even twist-3 parton distribution function $g_T^q(x)$ as follows

$$h_{1L}^{\perp(1)q}(x) + x g_T^q(x) = \mathcal{O}\left(\frac{m}{M}\right), \tag{52}$$

$$h_{1T}^{\perp(1)}(x) + g_T(x) = \mathcal{O}\left(\frac{m}{M}\right). \tag{53}$$

Notice that (52) follows also from combining (40) and (41) .

D. Wandzura-Wilczek (type) approximations

We already mentioned the Wandzura-Wilczek approximation [93] which allows to connect the twist-3 distribution function $g_T^q(x)$ and the twist-2 distribution function $g_1^q(x)$, see Eq. (11). In the model this approximation requires the neglect of quark-mass terms. In QCD one has to neglect in addition pure twist-3 terms.

An important practical application is that Eqs. (11) and (53) allow to express the unknown $h_{1T}^{\perp(1)q}(x)$ in terms of the well-known $g_1^q(x)$. In [66] we made use of this relation in order to estimate the transverse moment of pretzelosity, and used the results for predictions of SSAs in SIDIS.

In a similar way, i.e. upon the neglect of pure twist-3 and quark-mass terms, one obtains further 'Wandzura-Wilczek-type approximations' [25], namely

$$g_{1T}^{\perp(1)q}(x) \approx x\int_x^1 \frac{dy}{y} g_1^q(y), \tag{54}$$

$$h_{1L}^{\perp(1)q}(x) \approx -x^2\int_x^1 \frac{dy}{y^2} h_1^q(y). \tag{55}$$

Both Wandzura-Wilczek-type approximations are valid in our approach upon the neglect of quark-mass terms. The validity of (54) follows directly from Eqs. (11) and (40). The proof of the Wandzura-Wilczek-type approximation (55) is given in App. C.

E. Transverse momentum dependence

The probably most exciting thing about TMDs is, of course, their p_T-dependence. The power of the covariant approach with rotationally symmetric momentum distributions of quarks in the nucleon rest frame is based on the fact that this symmetry ultimately connects the distributions of transverse and longitudinal momenta. Some exciting consequences of this symmetry in the context of the spin content were discussed in [86], and a detailed study of the effects of this symmetry in the context of TMDs is in preparation.

However, a couple of simple but already interesting conclusions on the 'mean transverse momenta' of TMDs can be drawn without modelling the covariant momentum distribution $H(p^0)$. Notice that all p_T-integrals given below are well-defined in our approach.

Let us introduce the notion of mean transverse momenta moments of a TMD j_1 as follows

$$\langle \vec{p}_T^{\,2}, j_1\rangle = \frac{\int dx \int d^2p_T \vec{p}_T^{\,2} j_1(x, p_T)}{\int dx \int d^2p_T j_1(x, p_T)}, \tag{56}$$

and the n-th moment p-moment ($p = |\vec{p}|$) of the covariant distribution function is defined as follows

$$\langle\langle p^n\rangle\rangle = \int d^3p\, p^n H(p^0). \tag{57}$$

Then we obtain the following relations valid in the chiral limit

$$\lim_{m\to 0}\langle \vec{p}_T^{\,2}, g_1^q\rangle = \lim_{m\to 0}\langle \vec{p}_T^{\,2}, h_1^q\rangle = \frac{2}{3}\frac{\langle\langle p^2\rangle\rangle}{\langle\langle 1\rangle\rangle} \tag{58}$$

$$\lim_{m\to 0}\langle \vec{p}_T^{\,2}, g_{1T}^{\perp q}\rangle = \lim_{m\to 0}\langle \vec{p}_T^{\,2}, h_{1L}^{\perp q}\rangle = \frac{2}{3}\frac{\langle\langle p\rangle\rangle}{\langle\langle p^{-1}\rangle\rangle} \tag{59}$$

$$\lim_{m\to 0}\langle \vec{p}_T^{\,2}, h_{1T}^{\perp q}\rangle = \frac{2}{3}\frac{\langle\langle 1\rangle\rangle}{\langle\langle p^{-2}\rangle\rangle}. \tag{60}$$

It is instructive to learn that, although $g_1(x)$ and $h_1(x)$ are very different in the model [84], their mean transverse momenta coincide in the chiral limit.

VII. NON-RELATIVISTIC LIMIT

The assumption of a nonrelativistic dynamics of light quarks in the nucleon is not realistic. Nevertheless certain conclusions from this limit are very popular—like, for example, the relation $h_1(x) = g_1(x)$ which has often been used in literature to obtain order of magnitude estimates for effects of transversity. It is therefore worth to study how this limit can be formulated in our framework. This will yield nonrelativistic limit results for TMDs.

In the strict nonrelativistic limit, we have particle conservation and the nucleon consists of exactly 3 (valence) quarks. Then we deal with the dynamics of constituent ('valence') quarks, whose momenta become negligible with respect to m, and whose binding energy becomes negligible with respect to the nucleon mass such that $M = 3m$ up to relativistic corrections. The heavy constituent quarks obey spin-flavor symmetry which is introduced in the context of TMDs in Appendix A in Eq. (A1).

The nonrelativistic limit makes the following predictions for the collinear parton distribution functions

$$\begin{aligned}\lim_{\text{non-rel}} f_1^q(x) &= N_q\delta\Big(x-\frac{1}{3}\Big),\\ \lim_{\text{non-rel}} g_1^q(x) &= \lim_{\text{non-rel}} h_1^q(x) = P_q\delta\Big(x-\frac{1}{3}\Big).\end{aligned} \tag{61}$$

If the momenta of quarks are not negligible with respect to their mass m, the δ-functions in Eq. (61) are spread out. The normalizations N_q and P_q in Eq. (61) dictated by SU(6) spin-flavor symmetry are given in Eq. (A1) in Appendix A. One can check that all sum rules are correctly reproduced:

$$\int dx f_1^q(x) = N_q \qquad \text{('normalization')}, \qquad \sum_q \int dx x f_1^q(x) = 1 \qquad \text{(momentum sum rule)},$$

$$\sum_q \int dx g_1^q(x) = \sum_q \int dx h_1^q(x) = g_A^{(0)} = g_T^{(0)} = 1 \qquad \text{('spin sum rule'/isoscalar tensor charge)},$$

$$\int dx(g_1^u(x) - g_1^d(x)) = \int dx(h_1^u(x) - h_1^q(x)) = g_A^{(3)} = g_T^{(3)} = \frac{5}{3} \qquad \text{(Bjorken sum rule/isovector tensor charge)}. \tag{62}$$

The model is formulated in a covariant way, which means that it also can be applied to the situation when the motion of quarks is assumed to be nonrelativistic, i.e. when $|\vec{p}| \ll m$ and $p_0 = m\{1 + \mathcal{O}(\vec{p}^2/m^2)\}$. In order to formulate the nonrelativistic limit in our model, we assume SU(6) symmetry and set the covariant momentum distributions in unpolarized or polarized nucleons equal, i.e. we assume $G(p^0) \to N_q J(\vec{p})$ and $H(p^0) \to P_q J(\vec{p})$ with $\int d^3\vec{p} J(\vec{p}) = 1$. Of course, $J(\vec{p})$ strictly speaking depends only on the modulus $|\vec{p}|$ (or $p^0 = \sqrt{m^2 + |\vec{p}|^2}$) due to the rotational symmetry in the nucleon rest frame, but this notation is more convenient for the following.

In the nonrelativistic limit one expects only small momenta $\vec{p} \to 0$ to be relevant in the integral over $d^3\vec{p}$. Thus, it is natural to assume

$$\lim_{\text{non-rel}} J(\vec{p}) \to \delta^{(3)}(\vec{p}) \tag{63}$$

This is in some sense an 'axiom', and we have to verify that it yields to consistent results. For that we insert (63) in Eq. (5), and obtain (notice that $p^0 \to m$ for $|\vec{p}| \ll m$)

$$\lim_{\text{non-rel}} f_1^q(x) = N_q x M \int \frac{d^3\vec{p}}{p^0} \delta^{(3)}(\vec{p}) \delta\left(\frac{p^0 + p^1}{M} - x\right) = N_q \underbrace{\frac{xM}{m}}_{=1} \delta\left(\frac{m}{M} - x\right) = N_q \delta\left(x - \frac{1}{3}\right). \tag{64}$$

Thus, our prescription (63) gives the correct nonrelativistic result. What do we obtain for the collinear polarized distribution functions? Let us insert (63) in Eqs. (9), (10), and (14). We obtain

$$\lim_{\text{non-rel}} g_1^q(x) = \lim_{\text{non-rel}} g_T^q(x) = \lim_{\text{non-rel}} h_1^q(x) = P_q \delta\left(x - \frac{1}{3}\right). \tag{65}$$

Thus, the polarized distributions $g_1^q(x)$, $g_T^q(x)$, $h_1^q(x)$ become equal and correctly reproduce the nonrelativistic result (61). Thus, we see that our formulation of the nonrelativistic limit also yields correct results for the polarized parton distribution functions.

Let us now apply the nonrelativistic limit to the description of TMDs. We obtain

$$\lim_{\text{non-rel}} f_1^q(x, p_T) = N_q \delta\left(x - \frac{1}{N_c}\right) \delta^{(2)}(\vec{p}_T), \tag{66}$$

$$\lim_{\text{non-rel}} g_1^q(x, p_T) = P_q \delta\left(x - \frac{1}{N_c}\right) \delta^{(2)}(\vec{p}_T), \tag{67}$$

$$\lim_{\text{non-rel}} h_1^q(x, p_T) = P_q \delta\left(x - \frac{1}{N_c}\right) \delta^{(2)}(\vec{p}_T), \tag{68}$$

$$\lim_{\text{non-rel}} g_{1T}^{\perp q}(x, p_T) = N_c P_q \delta\left(x - \frac{1}{N_c}\right) \delta^{(2)}(\vec{p}_T), \tag{69}$$

$$\lim_{\text{non-rel}} h_{1L}^{\perp q}(x, p_T) = -N_c P_q \delta\left(x - \frac{1}{N_c}\right) \delta^{(2)}(\vec{p}_T), \tag{70}$$

$$\lim_{\text{non-rel}} h_{1T}^{\perp q}(x, p_T) = -\frac{N_c^2}{2} P_q \delta\left(x - \frac{1}{N_c}\right) \delta^{(2)}(\vec{p}_T). \tag{71}$$

In $g_{1T}^{\perp q}(x, p_T)$ and $h_{1L}^{\perp q}(x, p_T)$ the factors $\frac{M}{m} = N_c$ appear, while in $h_{1T}^{\perp q}(x, p_T)$ the factor $\frac{M^2}{2m^2} = \frac{N_c^2}{2}$ appears with $N_c = 3$ colors. These factors appear here somehow artificially because the nucleon mass was chosen in the Lorentz-decomposition of the correlators (2)–(4) to compensate the dimension of transverse momentum. Nevertheless, once one introduces the nucleon mass in this context (and sets the according 'units to measure' TMDs), the integrated functions $g_{1T}^{\perp q}(x)$, $h_{1L}^{\perp q}(x)$, $h_{1T}^{\perp q}(x)$ are larger then the parton distributions $g_1^q(x)$ and $h_1^q(x)$. It even happens that $|h_{1T}^{\perp q}(x)| > f_1^q(x)$ as also observed in other models [64,65]. This is not in contradiction with positivity which constrains only the transverse moments of TMDs, see Eqs. (27)–(29).

From Eqs. (66)–(71) we see that the transverse moments of all TMDs vanish. In particular, $h_{1T}^{\perp(1)q}(x)$ vanishes. This is consistent from the point of view of the relation between helicity, transversity and (the transverse moment of) pretzelosity, $h_{1T}^{\perp(1)q}$ Eq. (42), since in the nonrelativistic limit, helicity and transversity distributions become equal (65).

Thus, a nonzero transverse moment of pretzelosity [64] or any other TMD (as we learn here) can be considered to be a 'measure of relativistic' effects in the nucleon. Clearly, any effect of TMDs would disappear from a cross section (or spin asymmetry). However, the TMDs themselves are all nonzero in the nonrelativistic limit, see Eqs. (66)–(71).

VIII. CONCLUSIONS

We have generalized the covariant model developed in Refs. [81–86] to the description of T-even leading-twist TMDs in the nucleon. We have paid particular attention to the demonstration of the consistency of the extended approach. For example, we have shown that it gives the familiar results for the 'integrated' functions known from studies of collinear parton distributions [81–86], proven that it satisfies inequalities among TMDs, and discussed that it yields results consistent with the large-N_c limit, lattice QCD, and many other models.

In particular, we have also shown that in the approach a relation, which is derived from the QCD equations of motion and connects several TMDs and a pure twist-3 ('tilde') function, is consequently satisfied in the model. In our covariant approach with free partons 'consequently' means that the 'tilde'-function is absent.

We have rederived several known quark-model relations among polarized leading-twist TMDs [63–65], and found several new relations so far not observed in models, *without* assuming SU(6) spin-flavor symmetry. In our approach these relations refer to a scale of several GeV^2. Whenever previously such relations were observed, the corresponding model explicitly made use of the SU(6) symmetry and the results referred to low hadronic scales [63–65]. Not all quark models support these relations [68], and by including gauge-field degrees of freedom [69] such relations are definitely spoiled which one expects to be the case also in QCD. However, it remains to be seen whether in nature some of these relations could at least be approximately satisfied.

We have also shown that the Wandzura-Wilczek-type approximation, which allow to approximate the transverse moments of $g_{1T}^{\perp q}$ and $h_{1L}^{\perp q}$ in terms of respectively $g_1^q(x)$ and $h_1^q(x)$ are valid in the model upon the neglect of quark-mass terms. In QCD these relations are valid if one in addition neglects also pure twist-3 terms [25].

As an interesting digression, we have discussed how the covariant model framework can be used to formulate the nonrelativistic limit for TMDs, and derived the nonrelativistic limit results for all leading-twist T-even TMDs. In the nonrelativistic limit all these TMDs are nonzero, however, their transverse moments vanish. Interestingly the nonrelativistic approach is consistent with the basic features of the relativistic model calculations.

In this work we focussed on the general aspects of TMDs in the model. Further consequences for TMDs due to the parton intrinsic motion, as well as phenomenological applications (see [66] for first results) will be discussed elsewhere.

ACKNOWLEDGMENTS

A. E. and O. T. are supported by the Grants RFBR 09-02-01149 and 07-02-91557, RF MSE 2.1.1/2512 (MIREA) and by the Heisenberg-Landau and (also P. Z.) Votruba-Blokhitsev Programs of JINR. P. Z. is supported by the project AV0Z10100502 of the Academy of Sciences of the Czech Republic.

APPENDIX A: PROOF OF INEQUALITIES

In this Appendix we prove that the inequalities (27)–(29) are satisfied, if one assumes SU(6) symmetry and if one assumes all TMDs to be described in terms of the same covariant distribution $J(p^0)$ normalized as $\int d^3pJ(p^0) = 1$. Then, in SU(6) with $N_c = 3$ denoting the number of colors [102], the TMDs of definite flavor are given by

$$f_1^q(x) = N_q f_1(x), \qquad N_u = \frac{N_c+1}{2}, \qquad N_d = \frac{N_c-1}{2}$$
$$g_1^q(x) = P_q g_1(x), \qquad P_u = \frac{N_c+5}{6},$$
$$P_d = -\frac{N_c-1}{6}, \text{ and analog } g_{1T}^{\perp}, h_1, h_{1L}^{\perp}, h_{1T}^{\perp}. \tag{A1}$$

The 'flavorless' functions introduced in (A1) are given, respectively, by Eq. (33) with $G(p^0)$ replaced by $J(p^0)$, and by Eqs. (34)–(38) with $H(p^0)$ replaced by $J(p^0)$. We immediately see that $g_1(x, p_T) \le f_1(x, p_T)$ and $h_1(x, p_T) \le f_1(x, p_T)$. Since $|P_q| < N_q$, this means that the 'trivial' inequalities $|g_1^q(x, p_T)| \le f_1^q(x, p_T)$ and $|h_1^q(x, p_T)| \le f_1^q(x, p_T)$ hold.

Using the notation of the 'unintegrated' transverse moment of a TMD introduced in (30) we obtain the following *equalities* among the 'bare' (flavorless) functions

$$f_1(x, p_T) + g_1(x, p_T) = 2h_1(x, p_T) \tag{A2}$$

$$f_1(x, p_T) - g_1(x, p_T) = -2h_{1T}^{\perp(1)}(x, p_T) \tag{A3}$$

$$g_{1T}^{\perp(1)}(x, p_T)^2 = h_{1L}^{\perp(1)}(x, p_T)^2 = \frac{\vec{p}_T^{\,2}}{4M^2}(f_1(x, p_T)^2 - g_1(x, p_T)^2). \tag{A4}$$

The relations (A2) and (A3) among the bare distributions were discussed previously in various models [64,65]. It is important to notice that even if one assumes SU(6) symmetry, the relations (A2) and (A3) among bare distributions do not need to imply relations among TMDs of definite flavor, though it is the case in the bag and constituent-quark models [64,65]. But the spectator model of Ref. [63] provides a counterexample: there the bare TMDs satisfy (A2) and (A3), but the flavored TMDs constructed from them do not.

The equalities (A2)–(A4) do not mean that the inequalities (26)–(29) are saturated. That would be the case, in SU(6), only for TMDs of s-quarks in Λ^0 where $N_s = P_s = 1$, see [98] where the Soffer bound [97] was discussed. For the nucleon in SU(6) we have $|P_q| < N_q$, and the equalities (A2)–(A4) lead to real (never saturated) inequalities

(26)–(29). (We recall that T-odd distributions are absent in our approach.)

Thus, we conclude that the inequalities are manifestly satisfied in our approach—if one assumes SU(6) symmetry. If one does not, the positivity conditions (26)–(29) 'translate' into certain constraints among the covariant momentum distributions $G(p^0)$ and $H(p^0)$, see Ref. [84].

APPENDIX B: RELATIONS AMONG TMDS IN SU(6)

In this Appendix we discuss relations among TMDs that are obtained in our approach under the assumptions of SU(6) symmetry and that at all TMDs are characterized in terms of the same covariant momentum distribution $J(p^0)$, see Appendix A. From Eqs. (A1)–(A4) we obtain the following relations among TMDs with definite flavor

$$\frac{P_q}{N_q} f_1^q(x, p_T) + g_1^q(x, p_T) = 2h_1^q(x, p_T) \tag{B1}$$

$$\frac{P_q}{N_q} f_1^q(x, p_T) - g_1^q(x, p_T) = -2h_{1T}^{\perp(1)q}(x, p_T) \tag{B2}$$

$$g_{1T}^{\perp(1)q}(x, p_T)^2 = h_{1L}^{\perp(1)q}(x, p_T)^2 = \frac{\vec{p}_T^{\,2}}{4M^2}\left(\frac{P_q^2}{N_q^2} f_1^q(x, p_T)^2 - g_1^q(x, p_T)^2\right) \tag{B3}$$

We remark that the relations (B1) and (B2) hold in the bag [64] and constituent-quark [65] model, but not in spectator models [63,68]. Integrated versions of (B1) were discussed previously in [90,98,99].

The assumption of SU(6) symmetry by itself is a phenomenologically well-motivated concept especially in the valence-x region, see [78] for a recent discussion in the context of TMDs. However, in our approach this is not yet a sufficient condition for the relations (B1)–(B3) to be valid. *In addition* to SU(6) symmetry, we have to assume here that the covariant momentum distribution $J(p^0)$ appears in all TMDs.

This fully supports the observation [64], that SU(6) symmetry in a quark model *alone* is not a sufficient condition for this kind of relations to hold. Another SU(6) symmetric model, which in general does not support (B1)–(B3), is the spectator model of [63]—though upon an additional assumption (large-N_c limit) they hold there, too [64].

APPENDIX C: PROOF OF THE WW-TYPE RELATION EQ. (55)

In this Appendix we present two independent proofs of Eq. (55). For the first proof, we use the notation of Eq. (22) in [86] to write the model expressions (35) and (37) as

$$h_{1L}^{\perp(1)}(x) = -x^2 V_{-1}(x) + \frac{x^3}{2} V_{-2}(x) + \mathcal{O}\left(\frac{m}{M}\right),$$
$$h_1(x) = \frac{x^2}{2} V_{-2}(x) + \mathcal{O}\left(\frac{m}{M}\right). \tag{C1}$$

Then, exploring the identity $V'_{-1}(x) = \frac{x}{2} V'_{-2}(x)$ derived Eq. (24) of [86], we obtain

$$\left(\frac{h_{1L}^{\perp(1)}(x)}{x^2}\right)' - \frac{h_1(x)}{x^2} = -V'_{-1}(x) + \frac{x}{2} V'_{-2}(x) + \mathcal{O}\left(\frac{m}{M}\right) = \mathcal{O}\left(\frac{m}{M}\right), \tag{C2}$$

which is equivalent to Eq. (55).

For the second proof we show that $h_{1L}^{\perp(1)q}(x)$ and $-x^2 \int_x^1 \frac{dy}{y^2} h_1^q(y)$ have the same Mellin moments. Notice that in the model all TMDs $j^q(x)$ are well-behaving functions without singularities, have no support outside the region $x \in [0, 1]$, and have well-defined Mellin moments $\int_0^1 dx x^N j^q(x) \;\; \forall\; N = 0, 1, 2, \ldots$ Therefore Eq. (55) is equivalent to

$$A_N \equiv \int_0^1 dx \left(x^N h_{1L}^{\perp(1)q}(x) + \frac{x^{N+1}}{N+3} h_1^q(x)\right) = \mathcal{O}\left(\frac{m}{M}\right). \tag{C3}$$

Introducing the notation $[dp^3] \equiv \frac{d^3p}{p^0} \frac{H(p^0)}{p^0+m}$ we write the expressions (35) and (37) for $h_1^q(x)$ and $h_{1L}^{\perp(1)q}(x)$ as

$$h_{1L}^{\perp(1)q}(x) = -\frac{M^2}{2} \int [dp^3] \delta\left(\frac{p^0 - p^1}{M} - x\right) x^2 \frac{p^0 + p^1}{M} + \mathcal{O}\left(\frac{m}{M}\right), \tag{C4}$$

$$h_1^q(x) = \frac{M^2}{2} \int [dp^3] \delta\left(\frac{p^0 - p^1}{M} - x\right) x^2 + \mathcal{O}\left(\frac{m}{M}\right), \tag{C5}$$

where $p^0 = |\vec{p}|$ (recall we neglect m). We insert the expressions (C4) and (C5) into Eq. (C3), interchange the order of the integrations over x and p, introduce spherical coordinates such that $p^1 = |\vec{p}| \cos\theta$, and obtain

$$A_N = \frac{1}{2M^{N+1}} \int \{d^3p\} |\vec{p}|^{N+2} \left(-(1 - \cos\theta)^{N+2}(1 + \cos\theta) + \frac{(1 - \cos\theta)^{N+3}}{N+3}\right) + \mathcal{O}\left(\frac{m}{M}\right). \tag{C6}$$

Now, our proof is completed because in (C6) the integral over $z \equiv \cos\theta$ is

$$\int_{-1}^1 dz \left(-(1 - z)^{N+2}(1 + z) + \frac{(1 - z)^{N+3}}{N+3}\right) = \int_{-1}^1 dz \frac{d}{dz}\left(\frac{(1 - z)^{N+3}(1 + z)}{N+3}\right) = 0. \tag{C7}$$

[1] J. C. Collins, Acta Phys. Pol. B **34**, 3103 (2003); J. C. Collins, T. C. Rogers, and A. M. Stasto, Phys. Rev. D **77**, 085009 (2008); J. C. Collins and F. Hautmann, Phys. Lett. B **472**, 129 (2000); J. High Energy Phys. 03 (2001) 016; F. Hautmann, Phys. Lett. B **655**, 26 (2007).

[2] R. N. Cahn, Phys. Lett. B **78**, 269 (1978).

[3] D. W. Sivers, Phys. Rev. D **41**, 83 (1990); **43**, 261 (1991).

[4] A. V. Efremov, L. Mankiewicz, and N. A. Tornqvist, Phys. Lett. B **284**, 394 (1992); J. C. Collins, Nucl. Phys. **B396**, 161 (1993); J. C. Collins, S. F. Heppelmann, and G. A. Ladinsky, Nucl. Phys. **B420**, 565 (1994).

[5] A. Kotzinian, Nucl. Phys. **B441**, 234 (1995); A. M. Kotzinian and P. J. Mulders, Phys. Rev. D **54**, 1229 (1996).

[6] P. J. Mulders and R. D. Tangerman, Nucl. Phys. **B461**, 197 (1996); **B484**, 538(E) (1997).

[7] D. Boer and P. J. Mulders, Phys. Rev. D **57**, 5780 (1998).

[8] D. Boer, Phys. Rev. D **60**, 014012 (1999).

[9] S. J. Brodsky, D. S. Hwang, and I. Schmidt, Phys. Lett. B **530**, 99 (2002); Nucl. Phys. **B642**, 344 (2002).

[10] J. C. Collins, Phys. Lett. B **536**, 43 (2002).

[11] A. V. Efremov and A. V. Radyushkin, JINR Report No. E2-11726, 1978; Teor. Mat. Fiz. **44**, 157 (1980) [Theor. Math. Phys. **44**, 664 (1980)]; D. Amati, R. Petronzio, and G. Veneziano, Nucl. Phys. **B140**, 54 (1978); S. B. Libby and G. Sterman, Phys. Rev. D **18**, 3552 (1978

[12] J. C. Collins and D. E. Soper, Nucl. Phys. **B193**, 381 (1981); **B213**, 545(E) (1983).

[13] X. D. Ji, J. P. Ma, and F. Yuan, Phys. Rev. D **71**, 034005 (2005); Phys. Lett. B **597**, 299 (2004).

[14] J. C. Collins and A. Metz, Phys. Rev. Lett. **93**, 252001 (2004).

[15] A. Bacchetta, M. Boglione, A. Henneman, and P. J. Mulders, Phys. Rev. Lett. **85**, 712 (2000).

[16] A. Metz, Phys. Lett. B **549**, 139 (2002).

[17] P. V. Pobylitsa, arXiv:hep-ph/0301236.

[18] S. J. Brodsky and F. Yuan, Phys. Rev. D **74**, 094018 (2006).

[19] A. V. Belitsky, X. Ji, and F. Yuan, Nucl. Phys. **B656**, 165 (2003); X. D. Ji and F. Yuan, Phys. Lett. B **543**, 66 (2002); D. Boer, P. J. Mulders, and F. Pijlman, Nucl. Phys. **B667**, 201 (2003); I. O. Cherednikov and N. G. Stefanis, Phys. Rev. D **77**, 094001 (2008); Nucl. Phys. **B802**, 146 (2008).

[20] H. Avakian, S. J. Brodsky, A. Deur, and F. Yuan, Phys. Rev. Lett. **99**, 082001 (2007).

[21] G. A. Miller, Phys. Rev. C **76**, 065209 (2007).

[22] M. Burkardt, arXiv:0709.2966; arXiv:0810.3589; arXiv:0902.0163.

[23] K. Goeke, A. Metz, and M. Schlegel, Phys. Lett. B **618**, 90 (2005).

[24] A. Bacchetta, M. Diehl, K. Goeke, A. Metz, P. J. Mulders, and M. Schlegel, J. High Energy Phys. 02 (2007) 093.

[25] H. Avakian, A. V. Efremov, K. Goeke, A. Metz, P. Schweitzer, and T. Teckentrup, Phys. Rev. D **77**, 014023 (2008).

[26] A. Metz, P. Schweitzer, and T. Teckentrup, arXiv:0810.5212.

[27] M. Arneodo *et al.* (European Muon Collaboration), Z. Phys. C **34**, 277 (1987).

[28] A. Airapetian *et al.* (HERMES Collaboration), Phys. Rev. Lett. **84**, 4047 (2000); H. Avakian (HERMES Collaboration), Nucl. Phys. B, Proc. Suppl. **79**, 523 (1999).

[29] A. Airapetian *et al.* (HERMES Collaboration), Phys. Rev. D **64**, 097101 (2001).

[30] A. Airapetian *et al.* (HERMES Collaboration), Phys. Lett. B **562**, 182 (2003).

[31] H. Avakian *et al.* (CLAS Collaboration), Phys. Rev. D **69**, 112004 (2004).

[32] A. Airapetian *et al.* (HERMES Collaboration), Phys. Rev. Lett. **94**, 012002 (2005).

[33] V. Y. Alexakhin *et al.* (COMPASS Collaboration), Phys. Rev. Lett. **94**, 202002 (2005).

[34] M. Diefenthaler, AIP Conf. Proc. **792**, 933 (2005).

[35] I. M. Gregor (HERMES Collaboration), Acta Phys. Pol. B **36**, 209 (2005).

[36] E. S. Ageev *et al.* (COMPASS Collaboration), Nucl. Phys. **B765**, 31 (2007).

[37] H. Avakian, P. Bosted, V. Burkert, and L. Elouadrhiri (CLAS Collaboration), AIP Conf. Proc. **792**, 945 (2005).

[38] A. Airapetian *et al.* (HERMES Collaboration), Phys. Lett. B **622**, 14 (2005).

[39] A. Airapetian *et al.* (HERMES Collaboration), Phys. Lett. B **648**, 164 (2007).

[40] K. Abe *et al.* (Belle Collaboration), Phys. Rev. Lett. **96**, 232002 (2006).

[41] A. Ogawa, M. Grosse-Perdekamp, R. Seidl, and K. Hasuko, arXiv:hep-ex/0607014.

[42] A. Martin (COMPASS Collaboration), Czech. J. Phys. **56**, 33 (2006).

[43] M. Diefenthaler (HERMES Collaboration), arXiv:0706.2242; AIP Conf. Proc. **915**, 509 (2007).

[44] A. Kotzinian (on behalf of the COMPASS collaboration), arXiv:0705.2402.

[45] R. Seidl, M. Grosse-Perdekamp, and A. Ogawa (Belle Collaboration), Phys. Rev. D **78**, 032011 (2008).

[46] E. De Sanctis, W. D. Nowak, and K. A. Oganessian, Phys. Lett. B **483**, 69 (2000); K. A. Oganessian, N. Bianchi, E. De Sanctis, and W. D. Nowak, Nucl. Phys. **A689**, 784 (2001).

[47] M. Anselmino and F. Murgia, Phys. Lett. B **483**, 74 (2000).

[48] A. V. Efremov, K. Goeke, and P. Schweitzer, Phys. Lett. B **522**, 37 (2001); **544**, 389(E) (2002).

[49] A. V. Efremov, K. Goeke, and P. Schweitzer, Eur. Phys. J. C **24**, 407 (2002); Phys. Lett. B **568**, 63 (2003); Phys. Rev. D **67**, 114014 (2003).

[50] B. Q. Ma, I. Schmidt, and J. J. Yang, Phys. Rev. D **66**, 094001 (2002).

[51] A. V. Efremov, K. Goeke, and P. Schweitzer, Eur. Phys. J. C **32**, 337 (2003).

[52] U. D'Alesio and F. Murgia, Phys. Rev. D **70**, 074009 (2004).

[53] M. Anselmino, M. Boglione, U. D'Alesio, A. Kotzinian, F. Murgia, and A. Prokudin, Phys. Rev. D **71**, 074006 (2005).

[54] A. V. Efremov, K. Goeke, S. Menzel, A. Metz, and P. Schweitzer, Phys. Lett. B **612**, 233 (2005).

[55] J. C. Collins, A. V. Efremov, K. Goeke, S. Menzel, A. Metz, and P. Schweitzer, Phys. Rev. D **73**, 014021 (2006).

[56] J. C. Collins *et al.*, Phys. Rev. D **73**, 094023 (2006).

[57] W. Vogelsang and F. Yuan, Phys. Rev. D **72**, 054028 (2005).

[58] A. V. Efremov, K. Goeke, and P. Schweitzer, Phys. Rev. D

73, 094025 (2006).
[59] M. Anselmino, M. Boglione, U. D'Alesio, A. Kotzinian, F. Murgia, A. Prokudin, and C. Turk, Phys. Rev. D **75**, 054032 (2007).
[60] S. Arnold, A. V. Efremov, K. Goeke, M. Schlegel, and P. Schweitzer, arXiv:0805.2137.
[61] M. Anselmino *et al.*, Eur. Phys. J. A **39**, 89 (2009).
[62] A. Kotzinian, B. Parsamyan, and A. Prokudin, Phys. Rev. D **73**, 114017 (2006).
[63] R. Jakob, P. J. Mulders, and J. Rodrigues, Nucl. Phys. **A626**, 937 (1997); arXiv:hep-ph/9707340.
[64] H. Avakian, A. V. Efremov, P. Schweitzer, and F. Yuan, Phys. Rev. D **78**, 114024 (2008).
[65] B. Pasquini, S. Cazzaniga, and S. Boffi, Phys. Rev. D **78**, 034025 (2008).
[66] A. V. Efremov, P. Schweitzer, O. V. Teryaev, and P. Zavada, arXiv:0812.3246.
[67] J. She, J. Zhu, and B. Q. Ma, Phys. Rev. D **79**, 054008 (2009).
[68] A. Bacchetta, F. Conti, and M. Radici, Phys. Rev. D **78**, 074010 (2008).
[69] S. Meissner, A. Metz, and K. Goeke, Phys. Rev. D **76**, 034002 (2007).
[70] A. Bacchetta, R. Kundu, A. Metz, and P. J. Mulders, Phys. Rev. D **65**, 094021 (2002).
[71] A. V. Efremov and P. Schweitzer, J. High Energy Phys. 08 (2003) 006; P. Schweitzer, Phys. Rev. D **67**, 114010 (2003).
[72] L. P. Gamberg, G. R. Goldstein, and K. A. Oganessyan, Phys. Rev. D **67**, 071504 (2003).
[73] F. Yuan, Phys. Lett. B **575**, 45 (2003).
[74] Z. Lu and B. Q. Ma, Nucl. Phys. **A741**, 200 (2004); Phys. Rev. D **70**, 094044 (2004); Z. Lu and I. Schmidt, Phys. Rev. D **75**, 073008 (2007).
[75] M. Burkardt and B. Hannafious, Phys. Lett. B **658**, 130 (2008).
[76] L. P. Gamberg, G. R. Goldstein, and M. Schlegel, Phys. Rev. D **77**, 094016 (2008).
[77] A. Courtoy, F. Fratini, S. Scopetta, and V. Vento, Phys. Rev. D **78**, 034002 (2008); Phys. Rev. D **79**, 074001 (2009).
[78] S. Boffi, A. V. Efremov, B. Pasquini, and P. Schweitzer, Phys. Rev. D **79**, 094012 (2009).
[79] A. Metz and M. Schlegel, Ann. Phys. (Leipzig) **13**, 699 (2004).
[80] F. E. Close and A. W. Thomas, Phys. Lett. B **212**, 227 (1988).
[81] P. Zavada, Phys. Rev. D **55**, 4290 (1997).
[82] P. Zavada, Phys. Rev. D **65**, 054040 (2002).
[83] P. Zavada, Phys. Rev. D **67**, 014019 (2003).
[84] A. V. Efremov, O. V. Teryaev, and P. Zavada, Phys. Rev. D **70**, 054018 (2004); arXiv:hep-ph/0512034.
[85] P. Zavada, arXiv:hep-ph/0609027; arXiv:hep-ph/0511142; arXiv:hep-ph/0412206; arXiv:hep-ph/0408182.
[86] P. Zavada, Eur. Phys. J. C **52**, 121 (2007).
[87] R. G. Roberts and G. G. Ross, Phys. Lett. B **373**, 235 (1996).
[88] J. D. Jackson, G. G. Ross, and R. G. Roberts, Phys. Lett. B **226**, 159 (1989).
[89] J. P. Ralston and D. E. Soper, Nucl. Phys. **B152**, 109 (1979).
[90] R. L. Jaffe and X. D. Ji, Nucl. Phys. **B375**, 527 (1992).
[91] H. Burkhardt and W. N. Cottingham, Ann. Phys. (N.Y.) **56**, 453 (1970).
[92] A. V. Efremov, O. V. Teryaev, and E. Leader, Phys. Rev. D **55**, 4307 (1997).
[93] S. Wandzura and F. Wilczek, Phys. Lett. B **72**, 195 (1977).
[94] X. Zheng *et al.* (Jefferson Lab Hall A Collaboration), Phys. Rev. C **70**, 065207 (2004); M. Amarian *et al.* (Jefferson Lab E94-010 Collaboration), Phys. Rev. Lett. **92**, 022301 (2004); P. L. Anthony *et al.* (E155 Collaboration), Phys. Lett. B **553**, 18 (2003).
[95] J. Balla, M. V. Polyakov, and C. Weiss, Nucl. Phys. **B510**, 327 (1998); M. Gockeler *et al.*, Phys. Rev. D **63**, 074506 (2001); **72**, 054507 (2005).
[96] I. V. Anikin and O. V. Teryaev, Phys. Lett. B **509**, 95 (2001); A. V. Radyushkin and C. Weiss, Phys. Rev. D **63**, 114012 (2001); N. Kivel, M. V. Polyakov, A. Schäfer, and O. V. Teryaev, Phys. Lett. B **497**, 73 (2001); B. Dressler and M. V. Polyakov, Phys. Rev. D **61**, 097501 (2000); J. Blümlein and A. Tkabladze, Nucl. Phys. **B553**, 427 (1999); J. Blümlein and N. Kochelev, Nucl. Phys. **B498**, 285 (1997); O. V. Teryaev, in *Proceedings of "Prospects of Spin Physics at HERA, Zeuthen, Germany, 1995"*, edited by J. Blümlein and W.-D. Nowak (DESY DESY-95-200, Hamburg, Germany, 1995), pp. 132; P. Ball and V. M. Braun, Phys. Rev. D **54**, 2182 (1996).
[97] J. Soffer, Phys. Rev. Lett. **74**, 1292 (1995); X. Artru, M. Elchikh, J. M. Richard, J. Soffer, and O. V. Teryaev, Phys. Rep. **470**, 1 (2009).
[98] V. Barone, A. Drago, and P. G. Ratcliffe, Phys. Rep. **359**, 1 (2002).
[99] B. Pasquini, M. Pincetti, and S. Boffi, Phys. Rev. D **72**, 094029 (2005); **76**, 034020 (2007); S. Boffi and B. Pasquini, Riv. Nuovo Cimento Soc. Ital. Fis. **30**, 387 (2007).
[100] P. Schweitzer, D. Urbano, M. V. Polyakov, C. Weiss, P. V. Pobylitsa, and K. Goeke, Phys. Rev. D **64**, 034013 (2001); K. Goeke *et al.*, Acta Phys. Pol. B **32**, 1201 (2001); M. Wakamatsu and T. Kubota, Phys. Rev. D **60**, 034020 (1999).
[101] M. Gockeler *et al.* (QCDSF and UKQCD Collaborations), Phys. Rev. Lett. **98**, 222001 (2007).
[102] G. Karl and J. E. Paton, Phys. Rev. D **30**, 238 (1984).

Article copy

PHYSICAL REVIEW D, VOLUME 70, 054018

Transversity and intrinsic motion of the constituents

A.V. Efremov,[1] O.V. Teryaev,[1] and P. Závada[2]

[1]*Bogoliubov Laboratory of Theoretical Physics, JINR, 141980, Dubna, Russia*

[2]*Institute of Physics, Academy of Sciences of the Czech Republic, Na Slovance 2, CZ-182 21 Prague 8*

(Received 25 May 2004; published 17 September 2004)

The probabilistic model of parton distributions, previously developed by one of the authors, is generalized to include the transversity distribution. When interference effects are attributed to quark level only, the intrinsic quark motion produces the transversity, which is about twice as large as the usual polarized distribution. The applicability of such a picture is considered and possible corrections, accounting for interference effects at the parton-hadron transition stage are discussed.

DOI: 10.1103/PhysRevD.70.054018 PACS numbers: 13.60.–r, 12.39.Ki, 13.88.+e, 14.65.–q

I. INTRODUCTION

Nucleon spin functions represent a sensitive tool for understanding the nucleon internal structure in the language of QCD. Up to this day we have accumulated a very good knowledge of the nucleon spin functions g_1 and g_2, which were measured in deep-inelastic scattering [1–8]. A further important and interesting quark spin distribution function is the transversity, the third, nondiagonal, element of the quark spin density matrix. Transversity is not accessible from the measuring of deep-inelastic scattering, since it corresponds to the helicity flip amplitude. Its measuring is more complicated and that is the reason why some more accurate and complete experimental data on the transversity are still missing. However, the recent and/or future data from the experiments HERMES (DESY-Hamburg), CLAS (JLab), COMPASS (CERN-Geneva), and RHIC (Brookhaven National Laboratory) could be interpreted also in terms of the transversity [9–11]. For the present status of research in both theory and experiment, see, e.g., [12] and overview [13].

In Refs. [14,15], the probabilistic, covariant quark-parton model (QPM), in which intrinsic quark motion with spheric symmetry is consistently taken into account, was developed by one of us (P. Z.). It was shown that such a model nicely reproduces some well-known sum rules and gives a very reasonable agreement with experimental data on the spin structure functions g_1 and g_2. Assuming SU(6) symmetry, a calculation was done from the input on unpolarized valence quark distributions q_V. The aim of this paper is to extend this model also for description and calculation of the transversity distribution.

II. TRANSVERSITY

First, let us shortly summarize how the spin structure functions g_1, g_2 were calculated in the paper [14]. The antisymmetric part of the tensor related to the photon absorption by a single quark reads:

$$t_{\alpha\beta} = m\varepsilon_{\alpha\beta\lambda\sigma}q^\lambda w^\sigma, \tag{1}$$

where q, m, w are the photon momentum, quark mass, and polarization vector; the corresponding handbag diagram is in Fig. 1(a). Then it was shown that the corresponding tensor related to the target (proton) consisting of quasi-free quarks can be written as

$$T^{(A)}_{\alpha\beta} = \varepsilon_{\alpha\beta\lambda\sigma}q^\lambda \frac{m}{2Pq}\int H\left(\frac{pP}{M}\right)w^\sigma \delta\left(\frac{pq}{Pq} - x\right)\frac{d^3p}{p_0}; \qquad x = \frac{Q^2}{2Pq}, \tag{2}$$

where M is the proton mass, p and P are the quark and proton momenta. The distribution H is the difference of the quark distributions with opposite spin projections. In the proton rest frame one can write

$$H(p_0) = G_+(p_0) - G_-(p_0). \tag{3}$$

For the time being, if not stated otherwise, we consider that quark charge equals unity. Further, we showed that the covariant form of the quark polarization vector reads

$$w^\sigma = AP^\sigma + BS^\sigma + Cp^\sigma, \tag{4}$$

where S is the proton polarization vector and

$$A = -\frac{pS}{pP + mM}, \qquad B = 1, \qquad C = \frac{M}{m}A. \tag{5}$$

Finally, in the last step the functions g_1, g_2 were extracted from the tensor (2). In the approximation

$$Q^2 \gg 4M^2x^2 \tag{6}$$

and, identifying the beam direction with coordinate 1 in the proton rest frame, we obtain

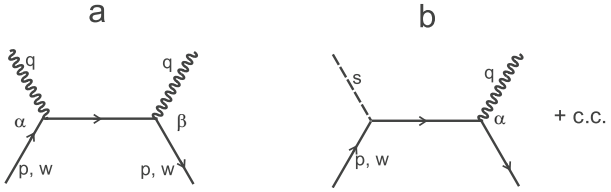

FIG. 1. Diagram related to deep-inelastic scattering (a) and the transversity (b); see text.

$$g_1(x) = \frac{1}{2}\int H(p_0)\Big(m + p_1 + \frac{p_1^2}{p_0+m}\Big) \times\delta\Big(\frac{p_0+p_1}{M} - x\Big)\frac{d^3p}{p_0}, \tag{7}$$

$$g_2(x) = -\frac{1}{2}\int H(p_0)\Big(p_1 + \frac{p_1^2 - p_T^2/2}{p_0+m}\Big) \times\delta\Big(\frac{p_0+p_1}{M} - x\Big)\frac{d^3p}{p_0}, \tag{8}$$

which implies

$$g_T(x) = g_1(x) + g_2(x) = \frac{1}{2}\int H(p_0)\Big(m + \frac{p_T^2/2}{p_0+m}\Big)\delta\Big(\frac{p_0+p_1}{M} - x\Big)\frac{d^3p}{p_0}. \tag{9}$$

Since

$$\begin{aligned} m + p_1 + \frac{p_1^2}{p_0+m} &= m - p_0 + p_0 + p_1 + \frac{p_1^2}{p_0+m} \\ &= p_0 + p_1 - \frac{(p_0-m)(p_0+m) - p_1^2}{p_0+m} \\ &= p_0 + p_1 - \frac{\mathbf{p}^2 - p_1^2}{p_0+m} \\ &= p_0 + p_1 - \frac{p_T^2}{p_0+m}, \end{aligned}$$

the $\delta-$ function allows a useful alternative representation of g_1:

$$g_1(x) = \frac{1}{2}\int H(p_0)\Big(Mx - \frac{p_T^2}{p_0+m}\Big)\delta\Big(\frac{p_0+p_1}{M} - x\Big)\frac{d^3p}{p_0}. \tag{10}$$

Let us also remark that in the paper [16] we showed that a similar approach for the corresponding symmetric part of the proton tensor gives the unpolarized structure function

$$f_1(x) = \frac{F_2(x)}{x} = Mx\int[G_+(p_0) + G_-(p_0)]\delta\Big(\frac{p_0+p_1}{M} - x\Big)\frac{d^3p}{p_0}. \tag{11}$$

Now, if one assumes the same spheric shape of the distributions $G_\pm$ for both opposite polarizations, then the corresponding probabilities can be parameterized as

$$G_+ = G(p_0)\cos^2(\eta/2), \qquad G_- = G(p_0)\sin^2(\eta/2), \qquad 0 \le \eta \le \pi, \tag{12}$$

so for $\eta = 0(\pi)$ we have a pure state with the polarization $+(-)$. For example, in the case of SU(6) we have $\cos\eta = 2/3(-1/3)$ for $u(d)$ quarks. The last relations imply

$$\begin{aligned} G_+(p_0) + G_-(p_0) &= G(p_0), \\ G_+(p_0) - G_-(p_0) &= G(p_0)\cos\eta, \end{aligned} \tag{13}$$

so the relations (8)–(12) can be rewritten as

$$g_1(x) = \frac{1}{2}\cos\eta\int G(p_0)\Big(Mx - \frac{p_T^2}{p_0+m}\Big) \times\delta\Big(\frac{p_0+p_1}{M} - x\Big)\frac{d^3p}{p_0}, \tag{14}$$

$$g_2(x) = -\frac{1}{2}\cos\eta\int G(p_0)\Big(p_1 + \frac{p_1^2 - p_T^2/2}{p_0+m}\Big) \times\delta\Big(\frac{p_0+p_1}{M} - x\Big)\frac{d^3p}{p_0}, \tag{15}$$

$$g_T(x) = \frac{1}{2}\cos\eta\int G(p_0)\Big(m + \frac{p_T^2/2}{p_0+m}\Big) \times\delta\Big(\frac{p_0+p_1}{M} - x\Big)\frac{d^3p}{p_0}, \tag{16}$$

$$f_1(x) = Mx\int G(p_0)\delta\Big(\frac{p_0+p_1}{M} - x\Big)\frac{d^3p}{p_0}. \tag{17}$$

Here, in the same approach, we shall try to calculate the transversity. Generally, transversity may be related to the auxiliary polarized process described by the interference of vector and scalar currents [17,18], so that the respective quark tensor carries only one Lorentz index. The simplest handbag diagram in Fig. 1(b) corresponds to the expression

$$\tau_\alpha = \varepsilon_{\alpha\beta\lambda\sigma}p^\beta q^\lambda w^\sigma, \tag{18}$$

which will be used instead of the tensor (1). In the next step we integrate this vector equally as the tensor in (2). Here we assume for the time being, that due to rotational symmetry in the proton rest frame, the transversity distribution is generated by the same function H as that in the case of the longitudinal one:

$$T_\alpha = \varepsilon_{\alpha\beta\lambda\sigma}q^\lambda\frac{1}{2Pq}\int H\Big(\frac{pP}{M}\Big)p^\beta w^\sigma\delta\Big(\frac{pq}{Pq} - x\Big)\frac{d^3p}{p_0}. \tag{19}$$

Obviously, only the terms S^σ, P^σ from the vector (4) contribute here, i.e.,

$$T_\alpha = \varepsilon_{\alpha\beta\lambda\sigma}q^\lambda\frac{1}{2Pq}\int H\Big(\frac{pP}{M}\Big)\Big(S^\sigma - \frac{pS}{pP+mM}P^\sigma\Big)p^\beta\delta\Big(\frac{pq}{Pq} - x\Big)\frac{d^3p}{p_0}. \tag{20}$$

Now we take the proton rest frame and assume

$$S = (0, 0, 1, 0), \tag{21}$$

$$q = (\nu, |\mathbf{q}|, 0, 0), \tag{22}$$

$$P = (M, 0, 0, 0). \tag{23}$$

Then one can check that only $T_3 \neq 0$,

$$T_3 = \frac{1}{2M\nu}\int H(p_0)\Big(p_0|\mathbf{q}| - p_1\nu - |\mathbf{q}|\frac{p_2^2}{p_0+m}\Big)\delta\Big(\frac{p_0\nu - p_1|\mathbf{q}|}{M\nu} - x\Big)\frac{d^3p}{p_0}. \tag{24}$$

Further, if we again assume approximation (6), then

$$\frac{|\mathbf{q}|}{\nu} = \sqrt{1 + 4M^2x^2/Q^2} \to 1 \tag{25}$$

and

$$\begin{aligned} T_3 &= \frac{1}{2}\int H(p_0)\Big(\frac{p_0 - p_1}{M} - \frac{p_2^2}{M(p_0+m)}\Big) \\ &\quad\times\delta\Big(\frac{p_0 - p_1}{M} - x\Big)\frac{d^3p}{p_0} \\ &= \frac{1}{2}\int H(p_0)\Big(x - \frac{p_T^2/2}{M(p_0+m)}\Big)\delta\Big(\frac{p_0 - p_1}{M} - x\Big)\frac{d^3p}{p_0} \\ &= \frac{1}{2}\cos\eta\int G(p_0)\Big(x - \frac{p_T^2/2}{M(p_0+m)}\Big) \\ &\quad\times\delta\Big(\frac{p_0 + p_1}{M} - x\Big)\frac{d^3p}{p_0}. \end{aligned} \tag{26}$$

So now we shall try to identify the transversity with the dimensionless function

$$\delta q(x) = \cos\eta\int G(p_0)\Big(Mx - \frac{p_T^2/2}{p_0+m}\Big)\times\delta\Big(\frac{p_0 + p_1}{M} - x\Big)\frac{d^3p}{p_0}. \tag{27}$$

If we use the alternative notation

$$q(x) = f_1(x), \qquad \Delta q(x) = 2g_1(x), \qquad \Delta q_T(x) = 2g_T(x), \tag{28}$$

then combination of the relations (14) and (16) assuming $m \to 0$ gives

$$\delta q(x) = \Delta q(x) + \Delta q_T(x). \tag{29}$$

Note that for the first moments, assuming the validity of the Burkhardt-Cottingham sum rule, this implies

$$\int_0^1 \delta q(x)dx = 2\int_0^1 \Delta q(x)dx. \tag{30}$$

Further, using the Wanzura-Wilczek [19] relation, which was proved for our g_1, g_2 in [15],

$$g_1(x) + g_2(x) = \int_x^1 \frac{g_1(y)}{y}dy, \tag{31}$$

the rule (29) can be represented as

$$\delta q(x) = \Delta q(x) + \int_x^1 \frac{\Delta q(y)}{y}dy. \tag{32}$$

Moreover, in the same paper we suggested the relations between the spin functions and valence quark distributions:

$$\begin{aligned} g_1^q(x) &= \frac{\cos\eta_q}{2}\Big[q_V(x) - 2x^2\int_x^1 \frac{q_V(y)}{y^3}dy\Big], \\ g_2^q(x) &= \frac{\cos\eta_q}{2}\Big[-q_V(x) + 3x^2\int_x^1 \frac{q_V(y)}{y^3}dy\Big]; \\ q &= u, d, \end{aligned} \tag{33}$$

which imply

$$\delta q(x) = \cos\eta_q\Big[q_V(x) - x^2\int_x^1 \frac{q_V(y)}{y^3}dy\Big]. \tag{34}$$

So now one can calculate δq either using experimental input on Δq or from some fit on the valence distribution q_V. In Fig. 2 we show transversities calculated with the use of formulas (32) and (34). The spin functions Δu and Δd are extracted here from the parametrization of the world data on the proton spin function g_1 [4] assuming the SU(6) approach,

$$\begin{aligned} \Delta u(x){:}\Delta d(x) &= \frac{4}{3}{:}\Big(-\frac{1}{3}\Big); \\ g_1(x) &= \frac{1}{2}\Big[\frac{4}{9}\Delta u(x) + \frac{1}{9}\Delta d(x)\Big]. \end{aligned} \tag{35}$$

For the valence functions $xu_V(x)$ and $xd_V(x)$ we use the parametrization obtained by the standard global analysis in [20]. All the parametrizations are taken for $Q^2 = 4\ \mathrm{GeV}^2/c^2$. The reason why in this figure the curves based on the experimental input on g_1 (dashed lines) are above the curves calculated from fitted q_V (solid lines) can be the same as those discussed in [15] for the g_1.

Now we check if the obtained transversities satisfy the Soffer inequality [21]:

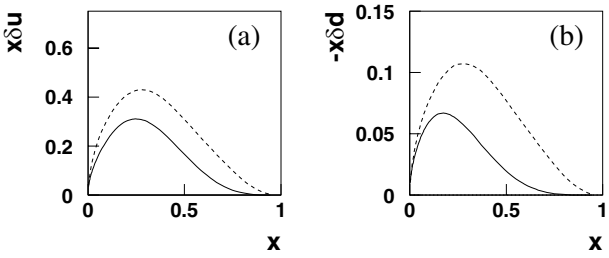

FIG. 2. Transversities of the u (a) and d (b) valence quarks calculated from the valence distributions (solid lines) and extracted from the experimental data on proton spin function g_1 (dashed lines)—the first approach; see text.

$$|\delta q(x)| \le \frac{1}{2}[q(x) + \Delta q(x)] = q^+(x). \tag{36}$$

After inserting $\delta q, f_1, g_1$ from the relations (27), (17), and (14) we get

$$\left|\cos\eta_q \int G(p_0)\Big(Mx - \frac{p_T^2/2}{p_0+m}\Big)\delta\Big(\frac{p_0+p_1}{M} - x\Big)\frac{d^3p}{p_0}\right| \le \frac{1}{2}\int\Big[MxG(p_0) + \cos\eta_q MxG(p_0) - \cos\eta_q \frac{p_T^2}{p_0+m}\Big]\delta\Big(\frac{p_0+p_1}{M} - x\Big)\frac{d^3p}{p_0} \tag{37}$$

and after rearranging the right-hand side one obtains

$$\left|\cos\eta_q \int G(p_0)\Big(Mx - \frac{p_T^2/2}{p_0+m}\Big)\delta\Big(\frac{p_0+p_1}{M} - x\Big)\frac{d^3p}{p_0}\right| \le \frac{1}{2}Mx(1-\cos\eta_q)\int G(p_0)\delta\Big(\frac{p_0+p_1}{M} - x\Big)\frac{d^3p}{p_0} + \cos\eta_q \int G(p_0)\Big(Mx - \frac{p_T^2/2}{p_0+m}\Big)\delta\Big(\frac{p_0+p_1}{M} - x\Big)\frac{d^3p}{p_0}, \tag{38}$$

which means that

$$|\delta q(x)| - \delta q(x) \le Mx\sin^2(\eta_q/2)\int G(p_0)\delta\Big(\frac{p_0+p_1}{M} - x\Big)\frac{d^3p}{p_0}, \tag{39}$$

which is apparently correct for $\delta q(x) \ge 0$. Further, since

$$Mx - \frac{p_T^2/2}{p_0+m} = \frac{2Mxp_0 + 2Mxm - (p_0^2 - m^2) + p_1^2}{2(p_0+m)} = \frac{2Mxp_0 + 2Mxm - (p_0^2-m^2) + M^2x^2 - 2Mxp_0 + p_0^2}{2(p_0+m)} = \frac{(m+Mx)^2}{2(p_0+m)} > 0,$$

we have also

$$\int G(p_0)\Big(Mx - \frac{p_T^2/2}{p_0+m}\Big)\delta\Big(\frac{p_0+p_1}{M} - x\Big)\frac{d^3p}{p_0} = \int G(p_0)\frac{(m+Mx)^2}{2(p_0+m)}\delta\Big(\frac{p_0+p_1}{M} - x\Big)\frac{d^3p}{p_0} > 0, \tag{40}$$

which means that the transversity sign is controlled only by the sign of $\cos\eta$, which is determined by the sign of $G_+(p_0) - G_-(p_0)$. So in our SU(6) approach the inequality (39) is safely satisfied for u quarks. Now let us consider negative δq, for d quarks in the SU(6) approach, when $\cos\eta = -1/3$ and $\sin^2(\eta/2) = 2/3$. Then the combination of Eq. (27) and relation (39) gives

$$\int G(p_0)\Big(Mx - \frac{p_T^2/2}{p_0+m}\Big)\delta\Big(\frac{p_0+p_1}{M} - x\Big)\frac{d^3p}{p_0} \le Mx\int G(p_0)\delta\Big(\frac{p_0+p_1}{M} - x\Big)\frac{d^3p}{p_0},$$

which is obviously valid. So in the SU(6) approach the Soffer inequality is satisfied for both u and d quarks. However, let us now consider a rather extreme case when $\cos\eta \to -1$. Relation (39) for the angle $\eta = \pi$ reads

$$2\int G(p_0)\Big(Mx - \frac{p_T^2/2}{p_0+m}\Big)\delta\Big(\frac{p_0+p_1}{M} - x\Big)\frac{d^3p}{p_0} \le 0, \tag{41}$$

which contradicts the inequality (40), so in this limit also, the transversity (27) contradicts the Soffer inequality. Why?

The reason is in the assumption that transversity is generated by the same function $H = G\cos\eta$ as the spin functions g_1 and g_2. The resulting transversity contradicts the Soffer inequality in the case of large negative quark polarization. Indeed, inequality (36) means that $|\delta q(x)|$ cannot exceed $q^+(x)$. At the same time, large negative polarization takes place for $\cos\eta \to -1$; then $q^+(x)$ becomes small, while $\delta q(x)$ is large (and negative). Below we shall modify the transversity definition as follows. The structure functions are proportional (see, e.g., [17]) to the combinations of amplitudes:

$$f_1 \propto \sum_X [a^*_{++}(X)a_{++}(X) + a^*_{+-}(X)a_{+-}(X)] \tag{42}$$

$$g_1 \propto \sum_X [a^*_{++}(X)a_{++}(X) - a^*_{+-}(X)a_{+-}(X)] \tag{43}$$

$$\delta q \propto \sum_X [a^*_{++}(X)a_{--}(X) + a^*_{--}(X)a_{++}(X)]. \quad (44)$$

Now, in our approach we identify

$$\sum_X a^*_{++}(X)a_{++}(X) = G_+(p_0),$$
$$\sum_X a^*_{+-}(X)a_{+-}(X) = G_-(p_0), \quad (45)$$

where $G_+ \pm G_-$ are the distributions in relations (13) from which the structure functions g_1, g_2, g_T and f_1 are constructed in Eqs. (14)–(17). But what about the remaining interference function

$$G_T(p_0) \equiv \sum_X [a^*_{++}(X)a_{--}(X) + a^*_{--}(X)a_{++}(X)], \quad (46)$$

which we are going to insert into Eq. (27) instead of $G_+ - G_- = G\cos\eta$? The G_T is a new function, which has no definite relation to the functions $G_\pm$. However, as a consequence of

$$\sum_X \|a_{++}(X) \pm a_{--}(X)\|^2 \geq 0, \quad (47)$$

one gets

$$|G_T(p_0)| \leq G_+(p_0) = G(p_0)\cos^2(\eta/2). \quad (48)$$

So in the first step we check the Soffer inequality for both corresponding extremes $\pm\delta q_{\max}(x)$;

$$\delta q_{\max}(x) = \cos^2(\eta_q/2) \int G(p_0)\Big(Mx - \frac{p_T^2/2}{p_0 + m}\Big)\delta\Big(\frac{p_0 + p_1}{M} - x\Big)\frac{d^3p}{p_0}. \quad (49)$$

After inserting into the Soffer inequality[1] one gets for both extremes

$$0 \leq \sin^2(\eta_q/2) \int G(p_0)\frac{p_T^2/2}{p_0 + m}\delta\Big(\frac{p_0 + p_1}{M} - x\Big)\frac{d^3p}{p_0}, \quad (50)$$

so the inequality is satisfied for any transversity $\delta q(x)$ in the band $\pm\delta q_{\max}(x)$ given by Eq. (49) with *any* η_q. In fact, two inequalities are now satisfied:

$$|\delta q(x)| \leq \delta q_{\max}(x) \leq \frac{1}{2}[q(x) + \Delta q(x)] \quad (51)$$

and in this way we have shown that taking into account the interference nature of the transversity at the stage of parton-hadron transition is quite substantial for general compliance with the Soffer inequality.

Obviously, nothing can be said about saturation of the inequality

$$|\delta q(x)| \leq \delta q_{\max}(x) \quad (52)$$

within this simple approach. Concerning the sign of the transversity δq, let us note that now there is no simple correspondence with the sign of Δq.

Since the relations (27) and (49) differ only in the η-dependent factor ahead of the integral, the relations (29), (32), and (34) imply for the second approach

$$\delta q_{\max}(x) = \kappa \cdot [\Delta q(x) + \Delta q_T(x)] = \kappa \cdot \Big[\Delta q(x) + \int_x^1 \frac{\Delta q(y)}{y}dy\Big]; \quad (53)$$
$$\kappa = \frac{\cos^2(\eta_q/2)}{\cos\eta_q},$$

$$\delta q_{\max}(x) = \cos^2(\eta_q/2)\Big[q_V(x) - x^2\int_x^1 \frac{q_V(y)}{y^3}dy\Big]. \quad (54)$$

This approach for the transversity is compared with the previous one in Fig. 3, again assuming SU(6) approximation for contributions from u and d valence quarks. However, one should point out that curves corresponding to the second approach represent only upper limits $\delta q_{\max}$ for transversities, in the sense of the relation (51). Part (a) of the figure shows results for u quarks. The relations (53) (dashed lines) and (54) (solid lines) are compared with those in Fig. 2, calculated from Eqs. (32) and (34). It follows that curves of the second approach are enhanced by the factor $\cos^2(\eta_u/2)/\cos\eta_u = 5/4$ with respect to the first one. Part (b) of the figure demonstrates similar curves for d quarks, but since $\cos^2(\eta_d/2) = -\cos\eta_d = 1/3$, both the corresponding pairs of curves are equal up to sign. So only the second pair is displayed. The dotted lines in both parts represent tranversities calculated in Ref. [22] in the LO and evolved from the initial scale

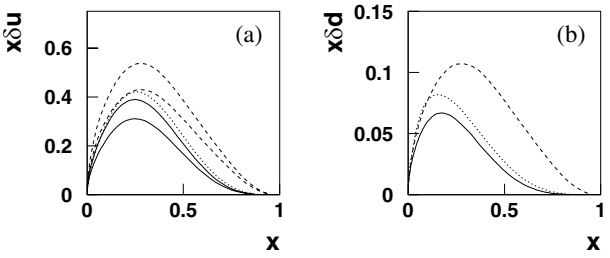

FIG. 3. Transversities of the u valence quarks (a) calculated from the valence distributions (solid lines) and extracted from the experimental data on proton spin function g_1 (dashed lines). Lower curves correspond to the first approach from Fig. 2; upper curves represent the second approach given by $\delta q_{\max}$ calculated from Eqs. (53) and (54). The corresponding transversities $\delta q_{\max}$ of the second approach for the d valence quarks (b) coincide, up to sign, with the first approach from Fig. 2. The dotted lines represent the calculation [22], with opposite sign for d quarks.

[1]One can start from relation (38), where on the l.h.s. $\cos\eta_q$ is substituted by $\cos^2(\eta_q/2)$.

0.6 GeV$^2/c^2$ to 4 GeV$^2/c^2$. Obviously, our results are well compatible with them.

Further, let us analyze the relation

$$\delta q_{\max}(x) \leq \frac{1}{2}[q(x) + \Delta q(x)] = q^+(x). \qquad (55)$$

Obviously, its saturation is equivalent to the equality in relation (50), which takes place either for $\eta = 0$ (pure state of the quark with polarization +) or for static quarks ($p_T^2 = 0$). On the other hand, in the limit $m \to 0$ and with the use of Eq. (33), one can write

$$q^+(x) = \frac{1}{2}\left\{q_V(x) + \cos\eta_q\left[q_V(x) - 2x^2\int_x^1 \frac{q_V(y)}{y^3}dy\right]\right\}$$
$$= \cos^2(\eta_q/2)\cdot q_V(x) - x^2\cos\eta_q\int_x^1 \frac{q_V(y)}{y^3}dy. \qquad (56)$$

In this way, both sides of relation (55) are displayed in Fig. 4. It is seen that particularly the transversity of d quarks is considerably more constrained in this approach than by the Soffer bound q^+. The relationship between both bounds depends on $\cos\eta_q$. One can check that

$$\frac{\int_0^1 \delta q_{\max}(x)dx}{\int_0^1 q^+(x)dx} = \frac{2 + 2\cos\eta_q}{3 + \cos\eta_q}, \qquad (57)$$

which in the SU(6) approach gives fractions $10/11$ and $1/2$ for u and d quarks.

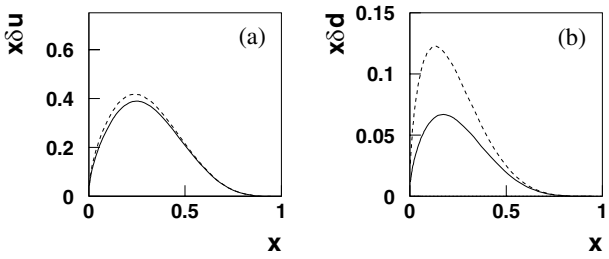

FIG. 4. Bounds on the transversities of the u (a) and d (b) valence quarks: $\delta q_{\max}$ (solid lines) and q^+ (dashed lines).

III. SUMMARY

The covariant QPM, which takes into account intrinsic quark motion, was generalized to involve the transversity distribution. Two ways of generalization were considered:

1) The interference effects were assumed on a quark level only (interference of vector and scalar currents produce the quark trace with one Lorentz index), and the generic quark polarized distribution $H = G_+ - G_-$ was assumed the same as that for the structure functions g_1 and g_2. We derived the relation between the transversity δq and the usual polarized distribution Δq, which implies that the resulting transversity is roughly twice as large as the usual distribution function. We discussed the compatibility of the obtained transversity with the Soffer inequality, and we have found that the inequality is violated in the case of large negative quark polarization.

2) In the second approach we accounted also for interference effects at the quark-hadron transition stage, which is formally represented by the interference sum (46). In this approach, assuming the validity of Soffer inequality at the stage of parton-hadron transition (48), we obtained a new bound on the transversity, rather than the transversity in itself. This bound is more strict than the Soffer one. Roughly speaking, the new bound is more restrictive for quarks with a greater proportion of intrinsic motion and/or smaller (or negative) portion in the resulting polarization.

For both approaches, with the use of the obtained sum rules, we have done the numeric calculations in which either experimentally measured spin function $g_1(x)$ or the valence quark distributions $q_V(x)$ were used as an input. To conclude, in general our calculations suggest that the quark intrinsic motion plays an important role for the spin functions—including the transversity.

ACKNOWLEDGMENTS

We thank P. Schweitzer for discussion and for help in comparison of models. This work was supported by the Votruba-Blokhitsev Programme of JINR. A. E. and O. T. are also supported by Grant Nos. INTAS 00/587 and RFBR 03-02-16816.

[1] E142 Collaboration, P. L. Anthony *et al.*, Phys. Rev. D **54**, 6620 (1996).
[2] E143 Collaboration, K. Abe *et al.*, Phys. Rev. D **58**, 112003 (1998).
[3] E154 Collaboration, K. Abe *et al.*, Phys. Rev. Lett. **79**, 26 (1997).
[4] E155 Collaboration, P. Anthony *et al.*, Phys. Lett. B **493**, 19 (2000).
[5] E155 Collaboration, P. Anthony *et al.*, Phys. Lett. B **553**, 18 (2003).
[6] Spin Muon Collaboration, B. Adeva *et al.*, Phys. Rev. D **58**, 112001 (1998).
[7] HERMES Collaboration, K. Ackerstaff *et al.*, Phys. Lett. B **404**, 383 (1997).
[8] HERMES Collaboration, A. Airapetian *et al.*, Phys. Lett. B **442**, 484 (1998).

[9] E. De Sanctis, W. D. Nowak, and K. A. Oganesian, Phys. Lett. B **483**, 69 (2000).
[10] Bo-Qiang Ma, Ivan Schmidt, and J. J. Yang, Phys. Rev. D **66**, 094001 (2002).
[11] A.V. Efremov, K. Goeke, and P. Schweitzer, Phys. Lett. B **522**, 37 (2001); **544**, 389 (2002).
[12] E. M. Kabuss, Proceedings of the XII. International Workshop on Deep Inelastic Scattering, DIS2004, Štrbské pleso, Slovakia, April 14–18, 2004 (in preparation).
[13] V. Barone, A. Drago, and P. G. Ratcliffe, Phys. Rep. **359**, 1 (2002).
[14] P. Zavada, Phys. Rev. D **65**, 054040 (2002).
[15] P. Zavada, Phys. Rev. D **67**, 014019 (2003).
[16] P. Zavada, Phys. Rev. D **55**, 4290 (1997).
[17] G. R. Goldstein, R. L. Jaffe, and X. Ji, Phys. Rev. D **52**, 5006 (1995).
[18] B. L. Ioffe and A. Khodjamirian, Phys. Rev. D **51**, 3373 (1995).
[19] S. Wanzura and W. Wilczek, Phys. Lett. B **72**, 195 (1977).
[20] A. D. Martin, W. J. Stirling, and R. G. Roberts, Phys. Rev. D **50**, 6734 (1994).
[21] J. Soffer, Phys. Rev. Lett. **74**, 1292 (1995).
[22] P. Schweitzer, D. Urbano, M.V. Polyakov, C. Weiss, P.V. Pobylitsa, and K. Goeke, Phys. Rev. D **64**, 034013 (2001).

Article copy

The Pretzelosity Distribution Function and Intrinsic Motion of the Constituents in Nucleon

A. V. Efremov*, P. Schweitzer†, O. V. Teryaev* and P. Závada**

*Bogoliubov Laboratory of Theoretical Physics, JINR, 141980 Dubna, Russia
†Department of Physics, University of Connecticut, Storrs, CT 06269, USA
**Institute of Physics, Academy of Sciences of the Czech Republic, Na Slovance 2, CZ-182 21 Prague 8, Czech Republic

Abstract. The pretzelosity distribution function $h_{1T}^{\perp}$ is studied in a covariant quark-parton model which describes the structure of the nucleon in terms of 3D quark intrinsic motion. This relativistic model framework supports the relation between helicity, transversity and pretzelosity observed in other relativistic models *without* assuming SU(6) spin-flavor symmetry. Numerical results and predictions for SIDIS experiments are presented.

Keywords: transverse momentum dependent distribution function, single spin asymmetry (SSA)
PACS: 13.88.+e, 13.85.Ni, 13.60.-r, 13.85.Qk

1. INTRODUCTION

Transverse parton momentum dependent parton distribution (TMDs) and fragmentation functions [1–6] offer the access to novel information on the nucleon structure [7]. TMDs can be accessed in processes like semi-inclusive deep-inelastic lepton nucleon scattering (SIDIS) [8]. Data on such reactions [9–14] provide first insights [18–24]. However, model calculations play an important role for the understanding of the novel functions [25–37].

An important question in this context is whether it is possible to relate unknown TMDs with possibly better known ones. Such relations cannot be exact, since all TMDs are independent. Approximations motivated partly by data were discussed in [38]. The ideal playground to motivate and test any such relations among TMDs are models.

An interesting relation between pretzelosity $h_{1T}^{\perp q}$, transversity h_1^q and helicity g_1^q was observed in bag model [26]. The name pretzelosity reflects that this function 'measures' an appropriately defined deviation of the nucleon from spherical shape which could look like a pretzel [7]. This relation holds also in the spectator model [25], and was subsequently confirmed in the constituent quark model [27] but not in the model of [28].

The purpose of this work is to study pretzelosity, and its possible relations, in the covariant model of the nucleon of Ref. [30]. In this model the intrinsic motion of partons inside the nucleon is described in terms of a covariant momentum distribution. The model was applied to the study of unpolarized and polarized structure functions accessible in DIS $f_1^a(x)$, $g_1^a(x)$ and $g_T^a(x)$ [30, 31] and extended to compute transversity $h_1^a(x)$ [32]. In this work we will generalize the approach to the description of TMDs, focusing on chiral-odd TMDs accessible with transverse nucleon polarization.

CP1149, *Spin Physics, 18th International Spin Physics Symposium*
edited by D. G. Crabb, D. B. Day, S. Liuti, X. Zheng, M. Poelker, and Y. Prok

2. CHIRAL-ODD TMDS WITH TRANSVERSE POLARIZATION

We focus on chiral-odd TMDs in a nucleon polarized transversely, e.g. in SIDIS, with respect to the hard virtual photon $q^\mu = (q^0, |\vec{q}|, 0, 0)$. The light-front quark-correlator with the process-dependent Wilson-link $\mathscr{W}$ [6] where $z^\pm = (z^0 \pm z^1)/\sqrt{2}$ etc.,

$$\phi(x, \vec{p}_T, \vec{S}_T)_{ij} = \int \frac{\mathrm{d}z^- \mathrm{d}^2\vec{z}_T}{(2\pi)^3} e^{ipz} \langle P, \vec{S}_T | \bar{\psi}_j(0) \mathscr{W}(0, z, \mathrm{path}) \psi_i(z) | P, \vec{S}_T \rangle \Big|_{z^+=0, p^+=xP^+}, \quad (1)$$

allows to define (3 out of the 4) chiral-odd TMDs in the nucleon as follows

$$\frac{1}{2} \mathrm{tr}\left[i\sigma^{j+}\gamma_5 \, \phi(x, \vec{p}_T, \vec{S}_T) \right] = S_T^j h_1 + \frac{(p_T^j p_T^k - \frac{1}{2}\vec{p}_T^{\,2}\delta^{jk}) S_T^k}{M_N^2} h_{1T}^\perp + \frac{\varepsilon^{jk} p_T^k}{M_N} h_1^\perp , \quad (2)$$

where $\varepsilon^{32} = -\varepsilon^{23} = 1$ and zero else. The only structure surviving the $\vec{p}_T$-integration in (1) is transversity $h_1^a(x)$. Nucleon polarizations and Dirac-structures other than that in Eqs. (1, 2) lead to further leading- and subleading-twist TMDs [3, 4, 16].

3. THE COVARIANT MODEL OF THE NUCLEON AND TMDS

The starting point for the calculation of the chiral-even functions accessible in DIS, $f_1^a(x)$, $g_1^a(x)$, $g_T^a(x)$, is the hadronic tensor [30, 31]. In the model it is assumed that DIS can be described as the incoherent sum of the scattering of electrons off non-interacting quarks, whose momentum distributions inside the nucleon are given in terms of the scalar functions: $G = G^\uparrow + G^\downarrow$ for unpolarized and $H = G^\uparrow - G^\downarrow$ for polarized quarks.

$G^i(pP/M)$ denotes the distribution of quarks of some (not indicated) flavour that are polarized parallel (antiparallel) $\uparrow(\downarrow)$ to the i-axis, where p is the quark momentum and M the nucleon mass. Though all expressions can be formulated in a manifestly covariant way, it is convenient to work in the nucleon rest-frame, where the G^i become functions of $p^0 = \sqrt{\vec{p}^{\,2} + m^2}$ with m the quark mass, and the distributions are rotationally symmetric.

The chiral-odd $h_1^q(x)$ cannot be accessed in DIS through the hadronic tensor. However, for theoretical purposes one may consider the auxiliary process described by the interference of a vector and a scalar current, described on the quark level by $T_\alpha^q = \varepsilon_{\alpha\beta\lambda\nu} p^\beta q^\lambda w^\nu$ where w^ν is the quark polarization vector. The nucleon current follows from convoluting T_α^q with the momentum distribution of polarized quarks $H(p^0)$ and reads

$$T_\alpha(x) = \frac{1}{2Pq} \varepsilon_{\alpha\beta\lambda\nu} q^\lambda \int \frac{\mathrm{d}^3 p}{p^0} H(p^0) \delta\left(\frac{p^0 - p^1}{M} - x \right) p^\beta w^\nu . \quad (3)$$

The auxiliary current is related to transversity as

$$2M T_\alpha(x) \varepsilon^{\alpha j} = S_T^j h_1^q(x) . \quad (4)$$

Before attempting to extend the approach to TMDs, let us stress that the QCD definition of TMDs includes a Wilson line absent in our model with no gauge boson degrees

of freedom. In such an approach time-reversal (T) odd TMDs, such as the Boer-Mulders function $h_1^\perp$ in (2), vanish [5, 6].

Now we turn to the question how to extend the approach to describe of TMDs, focusing here on chiral-odd ones in a transversely polarized nucleon. For that we observe that the expression for the auxiliary current (3) is of the type: $T_\alpha(x) = \int \mathrm{d}^2 p_T T_\alpha(x, \vec{p}_T)$. In the following we explore the consequences of what happens if one *does not integrate out* transverse momenta in this expression.

With S^μ denoting the nucleon polarization vector (here $S^\mu = (0, 0, \vec{S}_T)$ with $|\vec{S}_T| = 1$) the most general expression [31] for the covariant quark polarization vector w^μ reads

$$w^\mu = -\frac{pS}{pP+mM} P^\mu + S^\mu - \frac{M}{m}\frac{pS}{pP+mM} p^\mu \,. \tag{5}$$

From (5) we obtain for the 'unintegrated' auxiliary current contracted with $\varepsilon^{\alpha j}$ the result

$$2M T_\alpha(x, \vec{p}_T)\, \varepsilon^{\alpha j} = \int \frac{\mathrm{d}p^1}{p^0} H(p^0)\, \delta\left(\frac{p^0 - p^1}{M} - x\right) \left\{ S_T^j (p^0 - p^1) - p_T^j \frac{\vec{S}_T \vec{p}_T}{p^0 + m} \right\}. \tag{6}$$

By comparing to (2) we read off the following results:

$$h_1^q(x, p_T) = \int \frac{\mathrm{d}p^1}{p^0} H(p^0)\, \delta\left(\frac{p^0 - p^1}{M} - x\right) \left[p^0 - p^1 - \frac{\vec{p}_T^{\,2}}{2(p^0+m)} \right], \tag{7}$$

$$h_{1T}^{\perp q}(x, p_T) = \int \frac{\mathrm{d}p^1}{p^0} H(p^0)\, \delta\left(\frac{p^0 - p^1}{M} - x\right) \left[-\frac{M^2}{p^0+m} \right], \tag{8}$$

and $h_1^{\perp q}(x, p_T) = 0$. Several comments are in order. First, in our approach the vanishing of the T-odd $h_1^{\perp q}$ is consistent. Second, integrating in Eq. (7) over $\vec{p}_T$ yields the model expression for $h_1^q(x) \equiv \delta q(x)$ from [32]. Third, $h_{1T}^{\perp q} \neq 0$ implies non-sphericity in the nucleon in the sense of [7] inspite of a spherically symmetric $H(p_0)$. Forth, adding $h_1^q(x)$ and $h_{1T}^{\perp (1) q}(x) = \int \mathrm{d}^2 p_T \frac{\vec{p}_T^{\,2}}{2M^2} h_{1T}^{\perp q}(x, p_T)$ yields the model expression for $g_1^q(x) \equiv \Delta q(x)$ derived in [31], i.e. we recover the remarkable relation [26]:

$$g_1^q(x) - h_1^q(x) = h_{1T}^{\perp (1) q}(x) \,. \tag{9}$$

This relation is satisfied in several [25–27] though not all [28] quark models. Remarkably, it follows in our approach *without* assuming SU(6) spin-flavour symmetry of the nucleon wave function as was done in [25–27]. This is an important observation: SU(6) is not a necessary condition for the relation (9) to be satisfied in a *quark model*. What is a necessary condition is the absence of gluon degrees of freedom [29].

Finally, we remark that in the chiral limit $m \to 0$ it is possible to relate the transverse moment of pretzelosity to the twist-3 parton distribution function $g_T^q(x)$ [31] as follows

$$h_{1T}^{\perp (1) q}(x) + g_T^q(x) = \mathscr{O}\left(\frac{m}{M}\right) . \tag{10}$$

Since in the model the WW-relation holds, $g_T^q(x) = \int_x^1 \mathrm{d}y\, g_1^q(y)/y + \mathscr{O}(\frac{m}{M})$ [31], this offers a possibility to *estimate* pretzelosity numerically in the model framework.

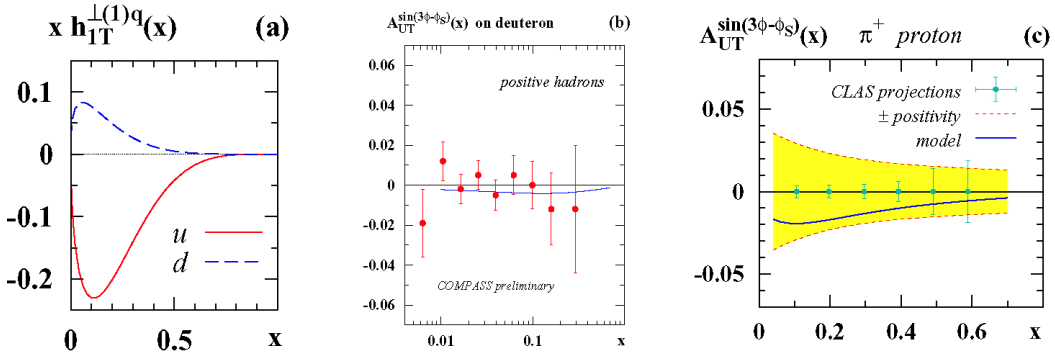

FIGURE 1. (a) $x\,h_{1T}^{\perp(1)q}(x)$ vs. x from the present approach. (b) $A_{UT}^{\sin(3\phi-\phi_S)}$ as function of x computed with pretzelosity from Fig. 1a for positive hadrons from a deuterium target at COMPASS in comparison to preliminary data [14]. (c) The same as Fig. 1b but for π^+ from proton target at CLAS. The shaded area is the region allowed by positivity [26], the error projections are from [40].

4. RESULTS AND PHENOMENOLOGY

We estimate $h_{1T}^{\perp(1)q}(x)$ in our approach using (10) and the WW-approximation for $g_T^q(x)$ with $g_1^q(x)$ at a scale of $2.5\,\mathrm{GeV}^2$ from [39]. We obtain the results shown in Fig. 1a.

The azimuthal SSA from transversely polarized targets, $A_{UT}^{\sin(3\phi-\phi_S)} \propto \sum_a e_a^2 h_{1T}^{\perp(1)a} H_1^{\perp a}$, allows to access pretzelosity in SIDIS due to the Collins effect [2], see [3, 26] for details. We use the information on $H_1^\perp$ from [20–22]. Figure 1b shows that the model results for the SSA are compatible with preliminary COMPASS deuteron target data [14]. Figure 1c shows estimates for the SSA in the kinematics of the CLAS 12 GeV beam experiment. The error projections from [40] included in the plot demonstrate that CLAS will be able to measure effects of pretzelosity of the size predicted by the model.

5. CONCLUSIONS

A generalization of the covariant model [30–32] to the description of TMDs was suggested, and applied to compute the pretzelosity distribution function $h_{1T}^\perp$. In particular, it was shown that the relation between helicity, transversity and pretzelosity [26] is satisfied in this model — remarkably, without assuming SU(6) symmetry.

A numerical estimate of $h_{1T}^{\perp(1)q}$ was presented, and used to compute $A_{UT}^{\sin(3\phi-\phi_S)}$, the leading-twist SSA in SIDIS due to Collins effect and pretetzelosity. The model results are compatible with the preliminary deuteron target data from COMPASS [14]. Predictions of this observable in the kinematics of the CLAS experiment with upgraded 12 GeV beam suggest that information on pretzelosity is accessible at Jefferson Lab [40].

ACKNOWLEDGMENTS

A. E. and O. T. are supported by the Grants RFBR 06-02-16215 and 07-02-91557, RF MSE RNP.2.2.2.2.6546 (MIREA) and by the Heisenberg-Landau and (also P.Z.) Votruba-Blokhitsev Programs of JINR. P. Z. is supported by the project AV0Z10100502 of the Academy of Sciences of the Czech Republic.

REFERENCES

1. J. C. Collins, *Acta Phys. Polon. B* **34**, 3103 (2003) [arXiv:hep-ph/0304122].
2. J. C. Collins, *Nucl. Phys. B* **396**, 161 (1993) [arXiv:hep-ph/9208213].
3. P. J. Mulders and R. D. Tangerman, *Nucl. Phys. B* **461** (1996) 197 and **484** (1997) 538E.
4. D. Boer and P. J. Mulders, *Phys. Rev. D* **57**, 5780 (1998) [arXiv:hep-ph/9711485].
5. S. J. Brodsky, D. S. Hwang and I. Schmidt, *Phys. Lett. B* **530**, 99; *Nucl. Phys. B* **642**, 344 (2002).
6. J. C. Collins, *Phys. Lett. B* **536**, 43 (2002) [arXiv:hep-ph/0204004].
7. G. A. Miller, arXiv:0708.2297 [nucl-th]. M. Burkardt, arXiv:0709.2966 [hep-ph].
8. X. D. Ji, J. P. Ma and F. Yuan, *Phys. Rev. D* **71**, 034005 (2005); *Phys. Lett. B* **597**, 299 (2004). J. C. Collins and A. Metz, *Phys. Rev. Lett.* **93**, 252001 (2004) [arXiv:hep-ph/0408249].
9. M. Arneodo et al. [European Muon Collaboration], *Z. Phys. C* **34** (1987) 277.
10. A. Airapetian et al. [HERMES], *Phys. Rev. Lett.* **84**, 4047 (2000); *Phys. Rev. D* **64**, 097101 (2001); *Phys. Lett. B* **562**, 182 (2003); *Phys. Lett. B* **622**, 14 (2005); *Phys. Lett. B* **648** (2007) 164.
11. H. Avakian et al. [CLAS], *Phys. Rev. D* **69**, 112004 (2004); *AIP Conf. Proc.* **792** (2005) 945.
12. A. Airapetian et al. [HERMES], *Phys. Rev. Lett.* **94**, 012002 (2005) [arXiv:hep-ex/0408013].
13. V. Alexakhin et al. [COMPASS], *Phys. Rev. Lett.* **94**, 202002 (2005); *Nucl. Phys. B* **765** (2007) 31.
14. A. Kotzinian [on behalf of the COMPASS collaboration], arXiv:0705.2402 [hep-ex].
15. K. Abe et al. [Belle Collaboration], *Phys. Rev. Lett.* **96**, 232002 (2006); arXiv:hep-ex/0607014; arXiv:0805.2975 [hep-ex].
16. A. Bacchetta, M. Diehl, K. Goeke, A. Metz, P. J. Mulders and M. Schlegel, *JHEP* **0702** (2007) 093.
17. A. Bacchetta, M. Boglione, A. Henneman and P. J. Mulders, *Phys. Rev. Lett.* **85**, 712 (2000).
18. A. V. Efremov et al., *Phys. Rev. D* **67**, 114014 (2003) *Eur. Phys. J. C* **32** (2003) 337.
19. A. V. Efremov et al., *Phys. Lett. B* **612**, 233 (2005) [arXiv:hep-ph/0412353].
20. W. Vogelsang and F. Yuan, *Phys. Rev. D* **72** (2005) 054028 [arXiv:hep-ph/0507266].
21. A. V. Efremov, K. Goeke and P. Schweitzer, *Phys. Rev. D* **73**, 094025 (2006).
22. M. Anselmino et al., *Phys. Rev. D* **75**, 054032 (2007) [arXiv:hep-ph/0701006].
23. S. Arnold et al., arXiv:0805.2137 [hep-ph]. M. Anselmino et al., arXiv:0805.2677 [hep-ph].
24. B. Zhang, Z. Lu, B. Q. Ma and I. Schmidt, *Phys. Rev. D* **77**, 054011 (2008).
25. R. Jakob, P. J. Mulders and J. Rodrigues, *Nucl. Phys. A* **626**, 937 (1997) [arXiv:hep-ph/9704335].
26. H. Avakian, A. V. Efremov, P. Schweitzer and F. Yuan, arXiv:0805.3355 [hep-ph].
27. B. Pasquini, S. Cazzaniga and S. Boffi, arXiv:0806.2298 [hep-ph].
28. A. Bacchetta, F. Conti and M. Radici, arXiv:0807.0323 [hep-ph].
29. S. Meissner, A. Metz and K. Goeke, *Phys. Rev. D* **76**, 034002 (2007) [arXiv:hep-ph/0703176].
30. P. Závada, *Phys. Rev. D* **55**, 4290 (1997) [arXiv:hep-ph/9609372].
31. P. Závada, *Phys. Rev. D* **65**, 054040 (2002); *ibid.* **67**, 014019 (2003); *Eur. Phys. J. C* **52**, 121 (2007).
32. A. V. Efremov, O. V. Teryaev and P. Závada, *Phys. Rev. D* **70**, 054018 (2004).
33. P. Závada, hep-ph/0609027; hep-ph/0511142; hep-ph/0412206; hep-ph/0408182.
34. P. Schweitzer et al., *Phys. Rev. D* **64**, 034013. K. Goeke et al., *Acta Phys. Polon. B* **32**, 1201 (2001).
35. F. Yuan, *Phys. Lett. B* **575**, 45 (2003) [arXiv:hep-ph/0308157].
36. L. P. Gamberg, G. R. Goldstein and M. Schlegel, arXiv:0708.2580, arXiv:0708.0324.
37. B. Pasquini et al.,*Phys. Rev. D* **72**, 094029 (2005); *Phys. Rev. D* **76**, 034020 (2007).
38. H. Avakian et al., *Phys. Rev. D* **77**, 014023 (2008). A. Metz, P. Schweitzer and T. Teckentrup, arXiv:0810.5212 [hep-ph].
39. M. Glück, E. Reya, M. Stratmann and W. Vogelsang, *Phys. Rev. D* **63**, 094005 (2001).
40. H. Avakian et al., JLab LOI 12-06-108 (2008).

Joint Institute for Nuclear Research *Article copy*

XIII Advanced Research Workshop on High Energy Spin Physics

(DSPIN-09)

Dubna, September 1–5, 2009

Proceedings

Edited by *A.V. Efremov* and *S.V. Goloskokov*

Dubna 2010

QUARK INTRINSIC MOTION AND THE LINK BETWEEN TMDs AND PDFs IN COVARIANT APPROACH

A. V. Efremov[1], P. Schweitzer[2], O. V. Teryaev[1] and P. Zavada[3]

(1) *Bogoliubov Laboratory of Theoretical Physics, JINR, 141980 Dubna, Russia*
(2) *Department of Physics, University of Connecticut, Storrs, CT 06269, USA*
(3) *Institute of Physics of the AS CR, Na Slovance 2, CZ-182 21 Prague 8, Czech Republic*

Abstract

The relations between TMDs and PDFs are obtained from the symmetry requirement: relativistic covariance combined with rotationally symmetric parton motion in the nucleon rest frame. This requirement is applied in the covariant parton model. Using the usual PDFs as an input, we are obtaining predictions for some polarized and unpolarized TMDs.

The transverse momentum dependent parton distribution functions (TMDs) [1,2] open the new way to more complete understanding of the quark-gluon structure of the nucleon. We studied this topic in our recent papers [3–5]. We have shown, that requirements of symmetry (relativistic covariance combined with rotationally symmetric parton motion in the nucleon rest frame) applied in the covariant parton model imply the relation between integrated unpolarized distribution function and its unintegrated counterpart. Obtained results are shortly discussed in the first part. Second part is devoted to the discussion of analogous relation valid for polarized distribution functions.

Unpolarized distribution function. In the covariant parton model we showed [6], that the parton distribution function $f_1^q(x)$ generated by the 3D distribution G_q of quarks reads:

$$f_1^q(x) = Mx \int G_q(p_0)\delta\left(\frac{p_0+p_1}{M} - x\right)\frac{dp_1 d^2\mathbf{p}_T}{p_0} \tag{1}$$

and that this integral can be inverted

$$G_q\left(\frac{M}{2}x\right) = -\frac{1}{\pi M^3}\left(\frac{f_1^q(x)}{x}\right)'. \tag{2}$$

Further, due to rotational symmetry of the distribution G_q in the nucleon rest frame, the following relations for unintegrated distribution were obtained [5]:

$$f_1^q(x,\mathbf{p}_T) = MG_q\left(\frac{M}{2}\xi\right). \tag{3}$$

After inserting from Eq. (2) we get relation between unintegrated distribution and its integrated counterpart:

$$f_1^q(x,\mathbf{p}_T) = -\frac{1}{\pi M^2}\left(\frac{f_1^q(\xi)}{\xi}\right)'; \qquad \xi = x\left(1+\left(\frac{p_T}{Mx}\right)^2\right). \tag{4}$$

Now, using some input distributions $f_1^q(x)$ one can calculate transverse momentum distribution functions $f_1^q(x, \mathbf{p}_T)$. As the input we used the standard PDF parameterization [8] (LO at the scale $4GeV^2$). The pictures of this distributions for u and $d-$quarks can be found in paper [5]. A part of this figures, but in different scale, is shown again in Fig 1. One can observe the following:

i) For fixed x the corresponding p_T- distributions are very close to the Gaussian distributions

$$f_1^q(x, p_T) \propto \exp\left(-\frac{p_T^2}{\langle p_T^2\rangle}\right). \qquad (5)$$

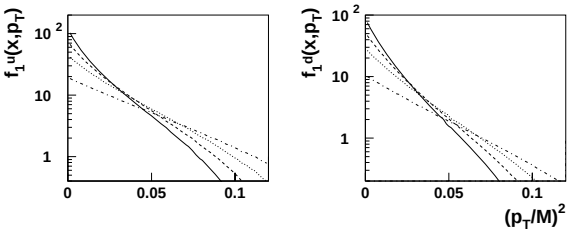

Figure 1: Transverse momentum dependent unpolarized distribution functions for u and $d-$quarks. Dependence on $(p_T/M)^2$ for $x = 0.15, 0.18, 0.22, 0.30$ is indicated by solid, dash, dotted and dash-dot curves.

ii) The width $\langle p_T^2\rangle = \langle p_T^2(x)\rangle$ depends on x. This result corresponds to the fact, that in our approach, due to rotational symmetry, the parameters x and p_T are not independent.

iii) Figures suggest the typical values of transversal momenta, $\langle p_T^2\rangle \approx 0.01GeV^2$ or $\langle p_T\rangle \approx 0.1GeV$. These values correspond to the estimates based the analysis of the experimental data on structure function $F_2(x, Q^2)$ [5]. They are substantially lower, than the values $\langle p_T^2\rangle \approx 0.25GeV^2$ or $\langle p_T\rangle \approx 0.44GeV$ following e.g. from the analysis of data on the Cahn effect [9] or HERMES data [10]. At the same time the fact, that the shape of obtained p_T- distributions (for fixed x) is close to the Gaussian, is remarkable. In fact, the Gaussian shape is supported by phenomenology.

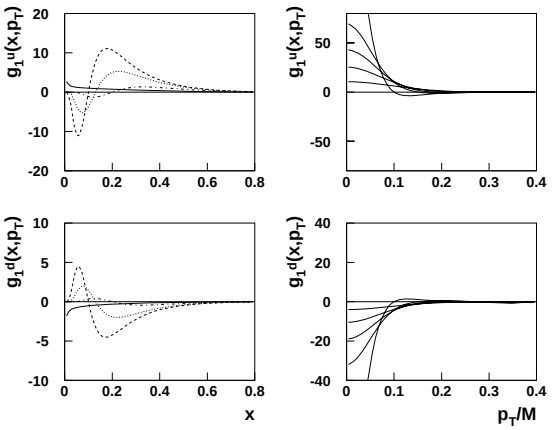

Figure 2: Transverse momentum dependent polarized distribution functions for u (*upper figures*) and $d-$quarks (*lower figures*). **Left part**: dependence on x for $p_T/M = 0.10, 0.13, 0.20$ is indicated by dash, dotted and dash-dot curves; solid curve correspods to the integrated distribution $g_1^q(x)$. **Right part**: dependence on p_T/M for $x = 0.10, 0.15, 0.18, 0.22, 0.30$ from top to down for $u-$quarks, and symmetrically for $d-$quarks.

Polarized distribution functions. Relation between the distribution $g_1^q(x)$ and its unintegrated counterpart can be obtained in a similar way, however in general the calculation with polarized structure functions is slightly more complicated. First let us remind procedure for obtaining structure functions g_1, g_2 from starting distribution functions $G^{\pm}$ defined in [6], Sec. 2, see also the footnote there. In fact the auxiliary functions G_P, G_S are obtained in appendix of the paper [7]. If we assume that $Q^2 \gg 4M^2x^2$, then the approximations $|\mathbf{q}| \approx \nu$, $\frac{pq}{Pq} \approx \frac{p_0+p_1}{M}$ are valid and the equations (A1),(A2) can be with the use of (A3),(A4) rewritten as

$$G_X = \int \Delta G\,(p_0)\, w_X \delta\left(\frac{p_0+p_1}{M} - x\right) \frac{dp_1 d^2\mathbf{p}_T}{p_0}, \quad X = P, S \qquad (6)$$

where

$$w_P = -\frac{m}{2M^2\nu}\frac{-p_1\cos\omega + p_T\cos\varphi\sin\omega}{p_0+m} \times\left(1+\frac{1}{m}\left(p_0-\frac{-p_1-(-p_1\cos\omega+p_T\cos\varphi\sin\omega)\cos\omega}{\sin^2\omega}\right)\right), \tag{7}$$

$$w_S = \frac{m}{2M\nu}\left(1+\frac{-p_1\cos\omega+p_T\cos\varphi\sin\omega}{p_0+m}\frac{1}{m} \times\left(-p_1\cos\omega+p_T\cos\varphi\sin\omega-\frac{-p_1-(-p_1\cos\omega+p_T\cos\varphi\sin\omega)\cos\omega}{\sin^2\omega}\cos\omega\right)\right). \tag{8}$$

Let us remark, that using the notation defined in [3] we can identify

$$-\cos\omega = S_L, \qquad \sin\omega = S_T, \qquad p_T\sin\omega\cos\varphi = \mathbf{p}_T\mathbf{S}_T, \tag{9}$$

which appear in definition of the TMDs [2]:

$$\frac{1}{2}\mathrm{tr}\left[\gamma^+\gamma_5\phi^q(x,\mathbf{p}_T)\right] = S_L g_1^q(x,p_T) + \frac{\mathbf{p}_T\mathbf{S}_T}{M}g_{1T}^{\perp q}(x,p_T). \tag{10}$$

The expressions (7),(8) can be reordered in terms of powers of $\cos\varphi$:

$$w_P = -\frac{\cos\omega}{2M^2\nu}\left(\frac{p_T^2}{m+p_0}\cos^2\varphi+(p_T\tan\omega + \frac{p_T}{m+p_0}p_1(\tan\omega-\cot\omega)\right)\cos\varphi - p_1\left(\frac{p_1}{m+p_0}+1\right)\Bigg), \tag{11}$$

$$w_S = \frac{1}{2M\nu}\left(\frac{p_T^2}{m+p_0}\cos^2\varphi - \frac{p_1p_T\cot\omega}{m+p_0}\cos\varphi + m\right). \tag{12}$$

Now, in analogy with Eq.(46) in [7] we define (note that $Pq/qS = -M/\cos\omega$):

$$w_1 = M\nu\cdot w_S + \frac{M^2\nu}{\cos\omega}\cdot w_P, \qquad w_2 = -\frac{M^2\nu}{\cos\omega}\cdot w_P, \tag{13}$$

which implies

$$g_k^q = \int \Delta G\,(p_0)\,w_k\delta\left(\frac{p_0+p_1}{M}-x\right)\frac{dp_1d^2\mathbf{p}_T}{p_0}, \qquad k=1,2. \tag{14}$$

After inserting from Eqs. (11),(12) definition (13) implies

$$w_1 = \frac{1}{2}\left(m+p_1\left(1+\frac{p_1}{m+p_0}\right)-p_T\tan\omega\left(1+\frac{p_1}{m+p_0}\right)\cos\varphi\right), \tag{15}$$

$$w_2 = \frac{1}{2}\left(\frac{p_T^2}{m+p_0}\cos^2\varphi+(p_T\tan\omega + \frac{p_T}{m+p_0}p_1(\tan\omega-\cot\omega)\right)\cos\varphi - p_1\left(\frac{p_1}{m+p_0}+1\right)\Bigg), \tag{16}$$

$$w_1 + w_2 = \frac{1}{2}\left(\frac{p_T^2}{m+p_0}\cos^2\varphi - \frac{p_1 p_T \cot\omega}{m+p_0}\cos\varphi + m\right). \tag{17}$$

Apparently, the terms proportional to $\cos\varphi$ disappear in the integrals (14) and the remaining terms give structure functions g_1, g_2 defined by Eqs. (15),(16) in [6].

Now, the integration over p_1 and further procedure can be done in a similar way as for unpolarized distribution. First, to simplify calculation, we assume $m \to 0$. For w_1 we get

$$g_1^q(x) = \frac{1}{2}\int \Delta G_q(p_0)\left(1+\frac{p_1}{p_0}\right)(p_1 - p_T\tan\omega\cos\varphi)\,\delta\left(\frac{p_0+p_1}{M} - x\right)\frac{dp_1 d^2\mathbf{p}_T}{p_0}. \tag{18}$$

The $\delta-$function is modified as

$$\delta\left(\frac{p_0+p_1}{M} - x\right)dp_1 = \frac{\delta\left(p_1 - \tilde{p}_1\right)dp_1}{x/\tilde{p}_0}, \tag{19}$$

where

$$\tilde{p}_1 = \frac{Mx}{2}\left(1 - \left(\frac{p_T}{Mx}\right)^2\right), \qquad \tilde{p}_0 = \frac{Mx}{2}\left(1 + \left(\frac{p_T}{Mx}\right)^2\right). \tag{20}$$

Modified $\delta-$function allows to simplify the integral

$$g_1^q(x) = \frac{1}{2}\int \Delta G_q(\tilde{p}_0)\left(M\left(2x-\xi\right) - 2p_T\tan\omega\cos\varphi\right)\frac{d^2\mathbf{p}_T}{\xi}, \tag{21}$$

where

$$\xi = x\left(1 + \left(\frac{p_T}{Mx}\right)^2\right). \tag{22}$$

Now we define

$$\Delta q(x,\mathbf{p}_T) = \frac{1}{2}\Delta G_q\left(\frac{M\xi}{2}\right)\left(M\left(2x-\xi\right) - 2p_T\tan\omega\cos\varphi\right)\frac{1}{\xi}. \tag{23}$$

According to Eq. (40) in [6] we have

$$\Delta G_q\left(\frac{M\xi}{2}\right) = \frac{2}{\pi M^3\xi^2}\left(3g_1^q(\xi) + 2\int_\xi^1 \frac{g_1^q(y)}{y}dy - \xi\frac{d}{d\xi}g_1^q(\xi)\right). \tag{24}$$

After inserting to Eq. (23) one gets:

$$\begin{aligned}\Delta q(x,\mathbf{p}_T) \;=\; & \frac{1}{\pi M^2\xi^3}\left(3g_1^q(\xi) + 2\int_\xi^1 \frac{g_1^q(y)}{y}dy - \xi\frac{d}{d\xi}g_1^q(\xi)\right) \\ & \times\left(2x - \xi - 2\frac{p_T}{M}\tan\omega\cos\varphi\right).\end{aligned} \tag{25}$$

This relation allows us to calculate the distribution $\Delta q(x,\mathbf{p}_T)$ from a known input on $g_1^q(x)$. Further, it can be shown, that using the notation defined in Eqs. (9),(10), our result reads

$$-\cos\omega\cdot\Delta q(x,\mathbf{p}_T) = S_L g_1^q(x,p_T) + \frac{\mathbf{p}_T\mathbf{S}_T}{M}g_{1T}^{\perp q}(x,p_T), \tag{26}$$

where

$$g_1^q(x,p_T) = \frac{2x-\xi}{\pi M^2 \xi^3}\left(3g_1^q(\xi) + 2\int_\xi^1 \frac{g_1^q(y)}{y}dy - \xi\frac{d}{d\xi}g_1^q(\xi)\right), \tag{27}$$

$$g_{1T}^{\perp q}(x,p_T) = \frac{2}{\pi M^2 \xi^3}\left(3g_1^q(\xi) + 2\int_\xi^1 \frac{g_1^q(y)}{y}dy - \xi\frac{d}{d\xi}g_1^q(\xi)\right). \tag{28}$$

Apparently, both functions are related in our approach:

$$\frac{g_1^q(x,p_T)}{g_{1T}^{\perp q}(x,p_T)} = \frac{x}{2}\left(1-\left(\frac{p_T}{Mx}\right)^2\right) = \tilde{p}_1/M. \tag{29}$$

Finally, with the use of standard input [11] on $g_1^q(x) = \Delta q(x)/2$ we can obtain the curves $g_1^q(x,p_T)$ displayed in Fig. 2. Let us remark, that the curves change the sign at the point $p_T = Mx$. This change is due to the term

$$2x-\xi = x\left(1-\left(\frac{p_T}{Mx}\right)^2\right) = 2\tilde{p}_1/M \tag{30}$$

in relation (27). This term is proportional to the quark longitudinal momentum $\tilde{p}_1$ in the proton rest frame, which is defined by given x and p_T. It means, that sign of the $g_1^q(x,p_T)$ is controlled by sign of $\tilde{p}_1$. On the other hand, the function $g_{1T}^{\perp q}(x,p_T)$ does not involve term, which changes the sign. The shape of both functions should be checked by experiment.

To conclude, we presented our recent results on relations between TMDs and PDFs. The study is in progress, further results will be published later.

Acknowledgements. A. E. and O. T. are supported by the Grants RFBR 09-02-01149 and 07-02-91557, RF MSE RNP 2.1.1/2512(MIREA) and (also P.Z.) Votruba-Blokhitsev Programs of JINR. P. Z. is supported by the project AV0Z10100502 of the Academy of Sciences of the Czech Republic. The work was supported in part by DOE contract DE-AC05-06OR23177.

References

[1] J. C. Collins, Acta Phys. Polon. B **34**, 3103 (2003); J. C. Collins, T. C. Rogers and A. M. Stasto, Phys. Rev. D **77**, 085009 (2008) ; J. C. Collins and F. Hautmann, Phys. Let. B **472**, 129 (2000); J. High Energy Phys. 03 (2001) 016; F. Hautmann, Phys. Let. B **655**, 26 (2007).

[2] P. J. Mulders and R. D. Tangerman, Nucl. Phys. B **461**, 197 (1996) [Erratum-ibid. B **484**, 538 (1997)] [arXiv:hep-ph/9510301].

[3] A. V. Efremov, P. Schweitzer, O. V. Teryaev and P. Zavada, Phys. Rev. D **80**, 014021 (2009) [arXiv:0903.3490 [hep-ph]].

[4] H. Avakian, A. V. Efremov, P. Schweitzer, O. V. Teryaev, F. Yuan and P. Zavada, arXiv:0910.3181 [hep-ph].

[5] P. Zavada, arXiv:0908.2316 [hep-ph].

[6] P. Zavada, Eur. Phys. J. C **52**, 121 (2007) [arXiv:0706.2988 [hep-ph]].

[7] P. Zavada, Phys. Rev. D **65**, 0054040 (2002).

[8] A. D. Martin, R. G. Roberts, W. J. Stirling and R. S. Thorne, Eur. Phys. J. C **39**, 155 (2005) [arXiv:hep-ph/0411040].

[9] M. Anselmino, M. Boglione, U. D'Alesio, A. Kotzinian, F. Murgia and A. Prokudin, Phys. Rev. D **71**, 074006 (2005).

[10] J. C. Collins, A. V. Efremov, K. Goeke, S. Menzel, A. Metz and P. Schweitzer, Phys. Rev. D **73,** (2006) 014021 [arXiv:hep-ph/0509076].

[11] E. Leader, A.V. Sidorov, and D.B. Stamenov, Phys. Rev. D **73**, (2006) 034023.

Kapitola 4

Shrnutí a závěr

Předložená dizertační práce je věnována studiu strukturních a distribučních funkcí nukleonů a částečně i jader. Prvá část práce je experimentální a týká se zejména metodického zpracování a fyzikální analýzy výsledků experimentu BCDMS. Experimentální data byla získána při několika energiích mionového svazku urychlovače SPS v CERN v intervalu $100-280$ GeV, tento rozsah energií umožnil měření nepolarizovaných strukturních funkcí F_2, F_1 v kinematické oblasti

$$0.06 \leq x \leq 0.80, \qquad 7 \text{ GeV}^2 \leq Q^2 \leq 260 \text{ GeV}^2.$$

Za nejdůležitější výsledky prvé části práce je třeba považovat získání velmi přesných hodnot strukturních funkcí protonu a deuteronu v uvedené kinematické oblasti. V dalším kroku byly pro oba terče získané strukturní funkce $F_2(x, Q^2)$ analyzovány z hlediska narušení škálování. Z obou strukturních funkcí byly nezávisle získány hodnoty QCD parametru Λ_{QCD}, které jsou ve velmi dobré vzájemné shodě. Výsledky experimentu BCDMS, společně s výsledky jiných experimentů, v nichž byly rovněž měřeny strukturní funkce nukleonů, jsou spolehlivým potvrzením předpovědí pQCD.

Dalším velmi důležitým výsledkem experimentu BCDMS je přesné změření poměru strukturních funkcí

$$F_2^{Fe}(x, Q^2)/F_2^D(x, Q^2).$$

Závislost tohoto poměru na proměnné x je podstatou tzv. EMC efektu. Experiment BCDMS významně přispěl k potvrzení a k dalšímu kvantitativnímu zpřesnění tohoto efektu. Současně je však třeba konstatovat, že v chápání EMC efektu dosud přetrvávají některé nejasnosti. Proto tento efekt i nadále zůstává aktuálním tématem pro další teoretický i experimentální výzkum.

V druhé části práce, která je zaměřena teoreticky, je navržena a analyzována kovariantní verze QPM. Současně je provedeno srovnání se standardním, tj. nekovariantním QPM. Výchozí filosofie obou přístupů jsou v obecné rovině podobné, v kovariantní verzi jsou však navíc uplatňovány požadavky symetrie:

A. Relativistická kovariance

Tato vlastnost umožňuje strukturu protonu, zahrnující i vnitřní pohyb kvarků, transformovat do různých souřadných systémů prostřednictvím obecných Lorentzových transformací. Mezi nimi zaujímá zvláštní místo klidová soustava protonu, mimo jiné proto, že orbitální moment kvarků vztažený k této (a právě k této) soustavě může představovat důležitou komponentu výsledného spinu protonu. Požadavek kovariance tak vytváří podstatný rozdíl od nekovariantního QPM, jehož formulace je striktně vázána na preferovaný souřadný systém, IMF. I z formálního hlediska je třeba dát vyšší prioritu kovariantnímu přístupu, u kterého je zabezpečen soulad s teorií relativity.

B. Sférická symetrie

Tento předpoklad, který se vztahuje k rozdělení hybností kvarků v klidové soustavě protonu, má rovněž hlubší teoretické opodstatnění. Jeho uplatnění pak znamená, že podélné a příčné komponenty hybností kvarků (vztaženo k hybnosti leptonu či fotonu vstupujícího do DIS) vystupují na téže úrovni a z protonu činí realistický 3D objekt. Tím je umožněno i konsistentní zavedení orbitálního momentu. I tento předpoklad je v protikladu s nekovariantním QPM, u nějž je vnitřní pohyb efektivně potlačen a kinematika v IMF je zjednodušena do jedné dimenze.

Přestože požadavek uvedených symetrií je velmi obecný, jeho uplatnění generuje řadu vztahů a pravidel mezi strukturními či distribučními funkcemi i pravidel zahrnujících orbitální moment. Z fenomenologického hlediska je důležité a zajímavé, že tato pravidla lze experimentálně prověřovat. Z těchto důvodů může být navržený model efektivním doplňkem k standardní verzi QPM a k rigorózní, ale značně komplikované a dosud neúplné teorii nukleonu založené na QCD.

Literatura

[A] **Publikace, které jsou podkladem disertační práce**

i) Experimentální výsledky

[A1] **A High Statistics Measurement of the Proton Structure Functions $F_2(x,Q^2)$ and R from Deep Inelastic Muon Scattering at High Q^2**
A. C. Benvenuti,...P. Zavada,.... *et al.* [BCDMS Collaboration]
Phys. Lett. B **223**, 485 (1989).

[A2] **Test of QCD and a Measurement of Lambda from Scaling Violations in the Proton Structure Function $F_2(x,Q^2)$ at High Q^2**
A. C. Benvenuti,...P. Zavada,.... *et al.* [BCDMS Collaboration]
Phys. Lett. B **223**, 490 (1989).

[A3] **A High Statistics Measurement of the Deuteron Structure Functions $F_2(x,Q^2)$ and R from Deep Inelastic Muon Scattering at High Q^2**
A. C. Benvenuti,...P. Zavada,.... *et al.* [BCDMS Collaboration]
Phys. Lett. B **237**, 592 (1990).

[A4] **Nuclear Effects in Deep Inelastic Muon Scattering on Deuterium and Iron Targets**
A. C. Benvenuti,...P. Zavada,.... *et al.* [BCDMS Collaboration]
Phys. Lett. B **189**, 483 (1987).

ii) Teorie

[A5] **The structure functions and parton momenta distribution in the hadron rest system**
P. Zavada, Phys. Rev. D **55**, 4290 (1997) [arXiv:hep-ph/9609372]

[A6] **Proton spin structure in the rest frame**
P. Zavada, Phys. Rev. D **56**, 5834 (1997) [arXiv:hep-ph/9704320]

[A7] **Spin structure functions and intrinsic motion of the constituents**
P. Zavada, Phys. Rev. D **65**, 054040 (2002) [arXiv:hep-ph/0106215]

[A8] **Proton spin structure and valence quarks**
P. Zavada, Phys. Rev. D **67**, 014019 (2003) [arXiv:hep-ph/0210141]

[A9] **Parton distribution functions and quark orbital motion**
P. Zavada, Eur. Phys. J. C **52**, 121 (2007) [arXiv:0706.2988 [hep-ph]]

[A10] **Transverse momentum dependent distribution functions in a covariant parton model approach with quark orbital motion**
A. V. Efremov, P. Schweitzer, O. V. Teryaev and P. Zavada
Phys. Rev. D **80**, 014021 (2009) [arXiv:0903.3490 [hep-ph]]

[A11] **Transversity and intrinsic motion of the constituents**
A. V. Efremov, O. V. Teryaev and P. Zavada
Phys. Rev. D **70**, 054018 (2004) [arXiv:hep-ph/0405225]

[A12] **The pretzelosity distribution function and intrinsic motion of the constituents in nucleon**
A. V. Efremov, P. Schweitzer, O. V. Teryaev and P. Zavada
AIP Conf. Proc. **1149**, 547 (2009) [arXiv:0812.3246 [hep-ph]] *Proceedings of 18th International Spin Physics Symposium (SPIN 2008), Charlottesville, Virginia, 6–11 Oct 2008.*

[A13] **Quark intrinsic motion and the link between TMDs and PDFs in covariant approach**
A. V. Efremov, P. Schweitzer, O. V. Teryaev and P. Zavada
Proceedings of XIII Advanced Research Workshop on High Energy Spin Physics (DSPIN-09), pp 159-164, JINR Dubna, Russia, September 1–5, 2009, arXiv:0912.3380[hep-ph].

[B] **Publikace, které s disertační prací souvisejí**

[B1] **The Tracking, Calorimeter and Muon Detectors of the H1 Experiment at HERA**
I. Abt, ...P. Zavada, ... *et al.* [H1 Collaboration],
Nucl. Instrum. Meth. A **386**, 348 (1997).

[B2] **The H1 Detector at HERA**
I. Abt, ...P. Zavada, ... *et al.* [H1 Collaboration],
Nucl. Instrum. Meth. A **386**, 310 (1997).

[B3] **Scaling Violations of the Proton Structure Function F_2 at Small x**
I. Abt, ...P. Zavada, ... *et al.* [H1 Collaboration],
Phys. Lett. B **321**, 161 (1994).

[B4] **A Measurement of Multi-jet Rates in Deep Inelastic Scattering at HERA**
I. Abt, ...P. Zavada, ... *et al.* [H1 Collaboration],
Z. Phys. C **61**, 59 (1994).

[B5] **Measurement of the Proton Structure Function $F_2(x, Q^2)$ in the Low x Region at HERA**
I. Abt, ...P. Zavada, ... *et al.* [H1 Collaboration],
Nucl. Phys. B **407**, 515 (1993)

[B6] **Measurement of Inclusive Jet Cross-sections in Photoproduction at HERA**
I. Abt, ...P. Zavada, ... *et al.* [H1 Collaboration], Phys. Lett. B **314**, 436 (1993).

[B7] **The H1 Liquid Argon Calorimeter System**
B. Andrieu, ...P. Zavada, ... *et al.* [H1 Calorimeter Group],
Nucl. Instrum. Meth. A **336**, 460 (1993).

[B8] **A Search for Leptoquarks, Leptogluons and Excited Leptons in H1 at HERA**
I. Abt, ...P. Zavada, ... *et al.* [H1 Collaboration],
Nucl. Phys. B **396**, 3 (1993).

[B9] **Observation Of Deep Inelastic Scattering At Low x**
T. Ahmed, ...P. Zavada, ... *et al.* [H1 Collaboration],
Phys. Lett. B **299**, 385 (1993).

[B10] **Measurement of the Hadronic Final State in Deep Inelastic Scattering at HERA**
T. Ahmed, ...P. Zavada, ... *et al.* [H1 Collaboration],
Phys. Lett. B **298**, 469 (1993).

[B11] **Total Photoproduction Cross-section Measurement at HERA Energies**
T. Ahmed, ...P. Zavada, ... *et al.* [H1 Collaboration],
Phys. Lett. B **299**, 374 (1993).

[B12] **Hard Scattering in Gamma p Interactions**
T. Ahmed, ...P. Zavada, ... *et al.* [H1 Collaboration],
Phys. Lett. B **297**, 205 (1992).

[B13] **Manufacture of Readout Boards for a Liquid Argon Calorimeter**
J. Antos, ...P. Zavada, ... *et al.*,
Nucl. Instrum. Meth. A **302**, 277 (1991).

[B14] **Proton spin structure and quark-parton model**
P. Zavada, Acta Phys. Slov. **49**, 273 (1999) [arXiv:hep-ph/9810540].

[B15] **Insights on non-perturbative aspects of TMDs from models**
H. Avakian, A. V. Efremov, P. Schweitzer, O. V. Teryaev, F. Yuan and P. Zavada,
Mod. Phys. Lett. A **24**, 2995 (2009) [arXiv:0910.3181 [hep-ph]].

[B16] **Generalized Cahn effect and parton 3D motion in covariant approach**
P. Zavada, *Presented at the Workshop on Transverse Partonic Structure of Hadrons (TPSH 2009), Yerevan, Armenia, 21–26 Jun 2009*, arXiv:0908.2316 [hep-ph]

[C] Ostatní literatura

[1] R.P.Feynman, *Photon-Hadron Interactions* (W.A.Benjamin, Inc. 1972).

[2] F.E.Close, *An Introduction to Quarks and Partons* (Academic, New York, 1979).

[3] I.J.R.Aitchison, A.J.G.Hey, *Gauge Theories in Particle Physics*, 2nd edition (Adam Hilger, Bristol, 1989).

[4] J. Chýla, *Quarks, Partons and Quantum Chromodynamics*, http://www-hep2.fzu.cz/Theory/notes/text.pdf

[5] http://nobelprize.org/nobel_prizes/physics/laureates/1990/

[6] M. Anselmino, A. Efremov and E. Leader, Phys. Rept. **261**, 1 (1995) [Erratum-ibid. **281**, 399 (1997)]

[7] Claudia Glasman and Juan Terron [editors]: *Proc. of XVII Int. Workshop on Deep-Inelastic Scattering and Related Topics*, Madrid, Spain, April 2009.

[8] Donald G. Crabb *et al.* [editors]: *The 18th International Spin Physics Symposium*, Charlottesville, Virginia 6-11 October 2008, AIP Conference Procceedings 1149.

[9] A. Airapetian *et al.* [HERMES Collaboration], Phys. Rev. Lett. **84**, 4047 (2000).

[10] A. Airapetian *et al.* [HERMES Collaboration], Phys. Rev. D **64**, 097101 (2001).

[11] A. Airapetian *et al.* [HERMES Collaboration], Phys. Rev. Lett. **94**, 012002 (2005).

[12] D. L. Adams *et al.* [E581 Collaboration and E704 Collaboration], Phys. Lett. B **261**, 201 (1991).

[13] D. L. Adams *et al.* [FNAL-E704 Collaboration], Phys. Lett. B **264**, 462 (1991).

[14] A. Bravar *et al.* [Fermilab E704 Collaboration], Phys. Rev. Lett. **77**, 2626 (1996).

[15] J. Adams *et al.* [STAR Collaboration], Phys. Rev. Lett. **92**, 171801 (2004).

[16] C. Amsler et al. (Particle Data Group), *Review of Particle Physics*, Phys. Lett. **B667**, 1 (2008) and 2009 partial update for the 2010 edition [on-line: http://pdg.lbl.gov/]

[17] D. Bollini *et al.* [BCDMS Collaboration], Nucl. Instrum. Methods **204** (1983) 333; A.C. Benvenuti *et al.* [BCDMS Collaboration], Nucl. Instrum. Methods **226** (1984) 330.

[18] http://pdg.lbl.gov/2009/reviews/rpp2009-rev-elements-electronic-struct.pdf

[19] C. Adloff *et al.,* Eur. Phys. J. C **21**, 33 (2001); Eur. Phys. J. C **30**, 1 (2003).

[20] S. Chekanov *et al.,* Eur. Phys. J. C **21**, 443 (2001); Phys. Rev. D **70**, 052001 (2004).

[21] M.R. Adams *et al.,* Phys. Rev. D **54**, 3006 (1996).

[22] M. Arneodo *et al.,* Nucl. Phys. B **483**, 3 (1997).

[23] L.W. Whitlow *et al.,* Phys. Lett. B **282**, 475 (1992).

[24] http://www.nndc.bnl.gov/chart/

[25] J. J. Aubert *et al.* [European Muon Collaboration], Phys. Lett. B **123**, 275 (1983).

[26] J. Ashman *et al.* [European Muon Collaboration], Z. Phys. C **57**, 211 (1993).

[27] J. Gomez *et al.,* Phys. Rev. D **49,** 4348 (1994).

[28] J. Seely *et al.*, Phys. Rev. Lett. **103**, 202301 (2009).

[29] Y. Zhang, L. Shao and B. Q. Ma, Nucl. Phys. A **828**, 390 (2009).

[30] B. Lu and B. Q. Ma, Phys. Rev. C **74**, 055202 (2006).
[31] E142 Collaboration, P.L. Anthony *et. al.*, Phys. Rev. D **54**, 6620 (1996).
[32] E154 Collaboration, K. Abe *et. al.*, Phys. Rev. Lett. **79**, 26 (1997).
[33] HERMES Collaboration, K. Ackerstaff *et. al.*, Phys. Lett. B **404**, 383 (1997).
[34] HERMES Collaboration, A. Airapetian *et. al.*, Phys. Lett. B **442**, 484 (1998).
[35] Spin Muon Collaboration, B. Adeva *et. al.*, Phys. Rev. D **58**, 112001 (1998).
[36] E143 Collaboration, K. Abe *et. al.*, Phys. Rev. D **58**, 112003 (1998).
[37] E155 Collaboration, P. Anthony *et al.*, Phys. Lett. B **493**, 19 (2000); Phys. Lett. B **553**, 18 (2003).
[38] L.M. Sehgal, Phys. Rev. D **10**, 1663 (1974); D **10**, 2016 (E) (1974).
[39] P.G. Ratcliffe, Phys. Lett. B **192**, 180 (1987).
[40] A. Abbas, J.Phys. G, Nucl. Part. Phys. **16**, L21-L26 (1990); **15**, L73-L77 (1989).
[41] J. Keppler and H.M. Hofmann, Phys. Rev. D **51**, 3936 (1995).
[42] M. Casu and L.M. Sehgal, Phys. Rev. D **55**, 2644 (1996).
[43] B.-Q. Ma and I. Schmidt, Phys. Rev. D **58**, 096008 (1998).
[44] S. J. Brodsky, Dae Sung Hwang, B.-Q. Ma and I. Schmidt, Nucl.Phys.B **593,** 311 (2001).
[45] M. Wakamatsu and T. Watabe, Phys. Rev. D **62**, 054009 (2000).
[46] M. Wakamatsu and Y. Nakakoji, Phys. Rev. D **74** 054006 (2006).
[47] X. Song, Int. J. Mod. Phys. A **16**, 3673 (2001).
[48] X. Ji, J.-P. Ma and F. Yuan, Nucl. Phys. B **652**, 383 (2003).
[49] E. Leader, A.V. Sidorov, and D.B. Stamenov, Phys. Rev. D **73**, 034023.
[50] J. Ashman *et al.* [European Muon Collaboration], Phys. Lett. B **206**, 364 (1988).
[51] V. Y. Alexakhin *et al.* [COMPASS Collaboration], Phys. Lett. B **647**, 8 (2007).
[52] A. Airapetian *et al.* [HERMES Collaboration], Phys. Rev. D **75**, 012007 (2007).
[53] M. Alekseev *et al.* [COMPASS Collaboration], Phys. Lett. B **676**, 31 (2009).
[54] F. Ellinghaus, AIP Conf. Proc. **1149** (2009) 259.
[55] A. V. Efremov and O. V. Teryaev, Report JINR-E2-88-287 (1988).
[56] G. Altarelli and G. G. Ross, Phys. Lett. B **212**, 391 (1988).
[57] R. D. Carlitz, J. C. Collins and A. H. Mueller, Phys. Lett. B **214**, 229 (1988).
[58] R. S. Bhalerao, N. G. Kelkar and B. Ram, Phys. Lett. B **476**, 285 (2000).
[59] J. Cleymans and R. L. Thews, Z. Phys. C **37**, 315 (1988).
[60] C. Bourrely, J. Soffer and F. Buccella, Eur. Phys. J. C **23**, 487 (2002); Mod. Phys. Lett. A **18**, 771 (2003); Eur. Phys. J. C **41**, 327 (2005); Mod. Phys. Lett. A **21**, 143 (2006); Phys. Lett. B **648**, 39 (2007).
[61] A. D. Martin, R. G. Roberts, W. J. Stirling and R. S. Thorne, Eur. Phys. J. C **39**, 155 (2005).

RESUME

This thesis is devoted to the study of structure and distribution functions of nucleons and some nuclei. The first, experimental part concerns analysis of experimental data obtained in the BCDMS experiment ('BCDMS Collaboration' – Labs: Bologna, CERN, Dubna, Mnichov, Saclay). The data were collected at the muon beam of the SPS accelerator at CERN in the energy range $100 - 280$ GeV. As a result, the unpolarized structure functions F_2, F_1 have been obtained in the kinematical region

$$0.06 \leq x \leq 0.80, \qquad 7 \text{ GeV}^2 \leq Q^2 \leq 260 \text{ GeV}^2.$$

The precise measurement of the *proton* and *deuteron* structure functions represent most important results of this part of thesis. In a next step, both the structure functions have been analyzed from the viewpoint of scaling violation. We proved, that values of the QCD parameter Λ_{QCD} obtained from the two structure functions well agree. Results of the BCDMS experiment, together with the results of other experiments on structure functions, reliably demonstrate the relevance and validity of pertubative QCD.

Further very important BCDMS result is the precise measurement of the ratio of functions

$$F_2^{Fe}(x, Q^2)/F_2^D(x, Q^2).$$

Dependence of this ratio on the parameter x is a basis of the EMC effect. The BCDMS experiment has significantly contributed to the measurement and study of this effect. At the same time, one has to say, that until now this effect is not completely explained. In fact it still represents a very interesting topic for further theoretical and experimental research.

In the second, theoretical part of this thesis, the covariant version of quark-parton model (QPM) is proposed and analyzed. At the same time, a comparison with the standard, non-covariant QPM is performed. In fact, the starting general philosophy is rather similar for the both approaches, but our covariant approach insists on two additional symmetry requirements:

A. Relativistic covariance

This condition allows to transform the proton structure from one reference frame to the another by means of the Lorentz boosts. The special case is the proton rest frame, in which among others, the quark orbital momentum can represent an important component of the resulting proton spin. This is the crucial distinction from the standard,

non-covariant QPM, which is strictly formulated in the preferred frame (IMF=Infinite Momentum Frame). The covariant approach should be preferred also from the formal point of view, because of compatibility with the theory of relativity.

B. Rotational symmetry

This requirement is related to the quark momentum distribution in the proton rest frame and has a deeper theoretical justification. Its application means, that the quark longitudinal and transversal momenta (related to the direction of the momentum of photon mediating lepton-quark interaction) are equally important for description of the proton − as a realistic 3D object. Rotational symmetry also allows to consistently introduce the orbital momentum. These consequences contrast to the non-covariant QPM, in which intrinsic motion is effectively suppressed and the kinematics of the IMF is reduced to one dimension.

In spite of the fact, that both the requirements are rather general, they imply a set of relations holding for structure and distribution functions and rules related the quark orbital momentum. From phenomenological point of view it is important and interesting, that these rules can be experimentally tested. That is the main reason, why proposed model can serve as an effective complement to the standard version of the QPM and to rigorous, but rather complicated and still incomplete theory of the nucleon based on the QCD.